University of Southampton

Faculty of Environmental and Life Sciences

Biological Science

Modelling organophosphate intoxication in *C. elegans*: a framework for new treatments vistas

by

Patricia Gonzalez Izquierdo

ORCID ID 0000-0002-5491-0048

Thesis for the degree of Doctor of Philosophy

January 2021

University of Southampton

Abstract

Faculty of Environmental and Life Sciences

Biological Science

Thesis for the degree of Doctor of Philosophy

Modelling organophosphate intoxication in *C. elegans*: a framework for new treatments vistas

Patricia Gonzalez Izquierdo

Organophosphates are potent neurotoxins that bind to acetylcholinesterase and inhibit its function. The inhibited enzyme fails to hydrolyse acetylcholine at the synaptic cleft and neuromuscular junctions which leads to accumulate. The excess of neurotransmitter reflects prolonged activation of both nicotinic and muscarinic types of receptors triggering varying levels of toxicity in humans. Asphyxia is the main cause of death and arises due to the paralysis of the breathing musculature aggravated by the disruption of the respiratory centres in the brain.

The evolutionary conservation of acetylcholinesterase has led to the wide use of organophosphates as pesticides. Despite their known toxicity, a large volume of organophosphates is still in use for this purpose. In addition, organophosphates are used as nerve agents for chemical warfare and terrorism. The limited efficiency of the current therapy urges the necessity of developing alternative strategies to treat organophosphate poisoning. These strategies frequently emerge from investigations using mammalian model organisms.

Here, I exploit the free-living nematode *C. elegans* as suitable model to achieve this goal. This nematode exhibits a set of well-characterized behaviours that rely on the proper signalling of acetylcholine at its neuromuscular junctions. Behavioural and biochemical studies highlighted the pharyngeal pumping on food as the most suitable phenotype to research organophosphate intoxication, recovery and antidotes. Further investigations indicated that the profound organophosphate-induced inhibition of pumping is actually triggered by overstimulation of the body wall muscle nerve transmission. This raises the idea of an inter-tissue communication happened in this stress condition.

Systematic investigation of pharyngeal and body wall cholinergic transmission revealed an unexpected organophosphate-induced plasticity in which prolonged incubation in presence of organophosphates sees a mitigation against toxicity. A methodical screening of strains deficient in cholinergic transmission identified that the integrity of the levamisole-sensitive acetylcholine receptor at the body wall muscle is central to the organophosphate-induced plasticity.

Importantly, two auxiliary proteins these receptors involved in the synaptic homeostasis during poisoning (OIG-4 and RSU-1) have been identified to modulate the severity of the drug-induced plasticity. In addition, key receptor subunit alleles (UNC-29 P284S and LEV-1 G461E) and the positive allosteric modulator MOLO-1 were identified as determinants underpinning the level of mitigating plasticity. I take these results to provoke the idea of using nicotinic receptors and/or the auxiliary proteins involved in their function as drug targets to develop new antidotes against organophosphate poisoning. Overall, the outcome of this thesis highlights a novel whole organism quantitative approach capable of revealing new insights into the mechanism and mitigation of this important class of neurotoxins.

List of contents

List of figures

List of tables

Abbreviations

CNS: central nervous system

PNS: peripheral nervous system

NMJ: neuromuscular junction

PLC: phospholipase C

ER: endoplasmic reticulum

GC: Golgi complex

AChE: acetylcholinesterase

BChE: butyrylcholinesterase

AChR: acetylcholine receptor

OP(s): organophosphate(s)

GFP: green fluorescent protein

NGM: nematode grow media

DFP: diisopropylfluorophosphate

Declaration of Authorship

Print name: Patricia Gonzalez Izquierdo

Title of thesis: Modelling organophosphate intoxication in *C. elegans*: a framework for new treatments vistas.

I declare that this thesis and the work presented in it are my own and has been generated by me as the result of my own original research.

I confirm that:

1. This work was done wholly or mainly while in candidature for a research degree at this University;

2. Where any part of this thesis has previously been submitted for a degree or any other qualification at this University or any other institution, this has been clearly stated;

3. Where I have consulted the published work of others, this is always clearly attributed;

4. Where I have quoted from the work of others, the source is always given. With the exception of such quotations, this thesis is entirely my own work;

5. I have acknowledged all main sources of help;

6. Where the thesis is based on work done by myself jointly with others, I have made clear exactly what was done by others and what I have contributed myself;

7. Parts of this work have been published as:

Izquierdo, P. G., O'Connor, V., Green, A. C., Holden-Dye, L., and Tattersall, J. E. H. (2020) *C. elegans* pharyngeal pumping provides a whole organism bio-assay to investigate anti-cholinesterase intoxication and antidotes. Neurotoxicology 82, 50-62. 10.1016/j.neuro.2020.11.001.

8. Parts of this work have been deposited as:

Izquierdo, P. G., T. Thisainathan, J. H. Atkins, C. J. Lewis, J. E. H. Tattersall, A. C. Green, L. Holden-Dye and V. O'Connor (2021) Cholinergic signalling at the body wall neuromuscular junction couples to distal inhibition of feeding in *C. elegans*. BioRxiv. 10.1101/2021.02.12.430967. Submitted to Journal of Biological Chemistry (JBC).

Izquierdo, P. G., Charvet, C. L., Neveu, C., Green, A. C., Tattersall, J. E., Holden-Dye, L., & O'Connor, V. (2021). Organophosphate intoxication in C. elegans reveals a new route to mitigate poisoning through the modulation of determinants responsible for nicotinic acetylcholine receptor function. BioRxiv. 10.1101/2021.05.01.442241.

Signed:.....

Date:.....

Acknowledgments

I would like to thank all the present and past people that have been involved in the progression of this thesis and myself as scientist. First to my supervisors Professor Vincent O'Connor, Professor Lindy Holden-Dye, Dr Christopher Green and Dr John Tattersall without which none of this would have been possible. Thank you for your invaluable advice, continuous support and patience during this project.

I am also grateful to University of Southampton, Dstl Porton Down and Gerald Kerkut Trust for financial support.

A huge thank to Dr Cedric Neveu and Dr Claude Charvet at French National Institute for Agriculture, Food, and Environment (INRAE) for their precious input in the last chapter of this thesis.

I would also like to thank Professor Robert Walker and Dr Katrin Deinhardt for their support and guidance. I would like to extend my gratitude to Dr James Kearn for his assistance at Dstl Porton Down.

The friendship and commitments of the master's students James Atkins, Thibana Thisainathan and Christian Lewis has been important for the development of this project.

I am extremely grateful to all WormLab past and present members for their friendship and assistance in the daily work, in special to Dr Fernando Calahorro, Helena Rawsthorne-Manning and Yogendra Gaihre. Friends that I will last beyond this step.

My love and gratitude go to my family who has supported me in this and many other adventures. Your advices have been the most valuable lessons I have learned in my life. To my father who taught me to be stubborn and to follow my dreams. To my mother who taught me that every single problem has a solution and that I am capable of find it. To my uncle, for teaching me that the only way to achieve goals in life in working on them without waiting for being lucky. And to my grandmother who taught me to do things right no matter how long it takes. Thank you for always believing in me.

Spanish translation: Quiero mandar a mi familia todo mi cariño y gratitud. Muchas gracias por apoyarme siempre en esta y otras muchas aventuras. Vuestros consejos han sido las lecciones mas importantes que he aprendido en mi vida. A mi padre, que me enseño a ser cabezona y a perseguir mis metas: "vista larga, paso corto y mala leche". A mi madre, que me enseño a buscar alternativas y a ser resolutiva ante cualquier situacion: "tu, hija mia, no te veas aturdida ante ninguna situacion". A mi tio, por enseñarme que las cosas se consiguen con trabajo: "tu confia en tu trabajo y no en la suerte". Y a mi abuela, que me enseño a hacer las cosas bien sin importar el tiempo que tome: "el tiempo no lo ve nadie". Muchas gracias por creer en mi siempre.

My last acknowledgment goes to my husband for always being there to get my back when things are wrong and celebrate with me when things are right. Thanks for sharing every dream with me and for pushing together to make all of them possible.

Chapter 1

Introduction

1.1. Organophosphates

Organophosphate is the standard name used to define 12 subcategories of chemical compounds characterized as esters, amides or thiol derivatives of the phosphoric acid (**Error! Reference source not found.** and Table 1.1.1).

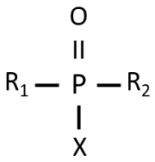

Figure 1.1. General chemical structure of organophosphates

1.1.1. Types of organophosphates

The side chains R1 and R2 in Figure 1.1 are either aryl or alkyl groups that can be bound to the phosphorous atom (phosphinates). Alternatively, the link can be more complex and involve oxygen (phosphates), sulphur (phosphothioates) or amino (phosphoramidates) linkers. Frequently, R1 is directly bound to the phosphorus atom while R2 is bound to an oxygen (phosphonates) or a sulphur (thiophosphonates). The X group, known as "leaving group", can be halogen, aliphatic, aromatic or heterocyclic groups. This is linked to the phosphorous atom by a labile group, usually oxygen of sulphur (Table 1.1.1). This property is critical for the mode of action and toxicity of organophosphates exerted by the binding to and subsequent inhibition of the enzyme acetylcholinesterase [1] (section 1.1.5.4).

1.1.2. Uses of organophosphates

Organophosphates were originally synthesised for the use as pesticides in the 1930s to replace organochlorine compounds as they had reduced accumulation in the environment. More than 60 tons of organophosphates were used in the UK and more than 11,000 were employed worldwide in 2017 according to the Food and Agriculture Organization of the United Nations [2]. Some of the most commonly used organophosphates pesticides are paraoxon, parathion, malathion, chlorpyrifos, diazinon or dichlorvos (Table 1.1.1).

Table 1.1. Classification of organophosphate compounds, chemical structure and examples.

Chemical structure and classification	Examples
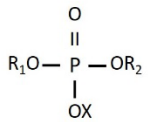 Phosphates	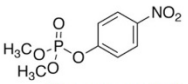 Paraoxon-methyl 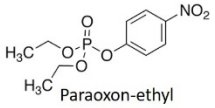 Paraoxon-ethyl 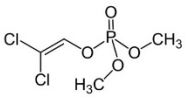 Dichlorvos
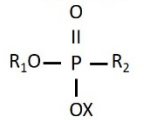 Phosphonates	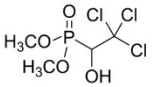 Trichlorfon
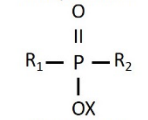 Phosphinates	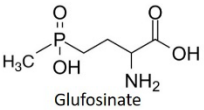 Glufosinate
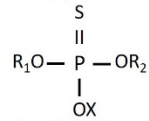 Phosphorothioates	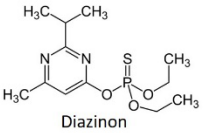 Diazinon 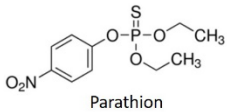 Parathion
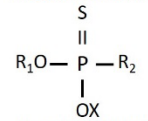 Phosphonothioates	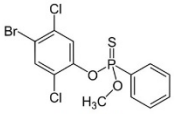 Leptophos
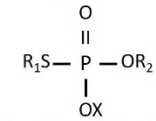 Phosphorothioates (S-substituted)	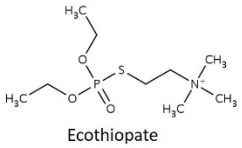 Ecothiopate
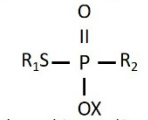 Phosphonothioates (S-substituted)	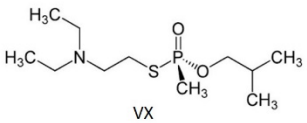 VX
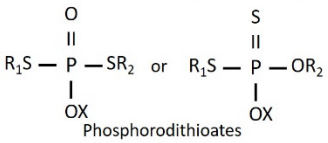 Phosphorodithioates	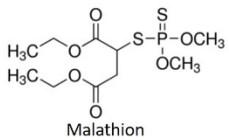 Malathion 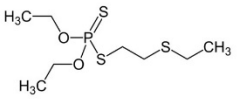 Disulfoton
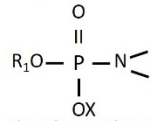 Phosphoramidates	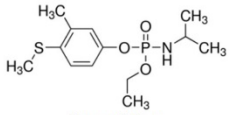 Fenamiphos
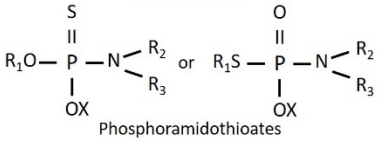 Phosphoramidothioates	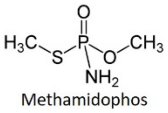 Methamidophos 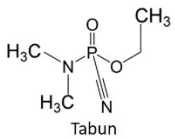 Tabun
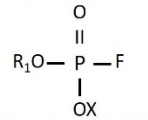 Phosphorofluoridates	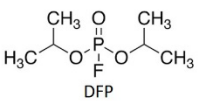 DFP
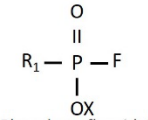 Phosphonofluoridates	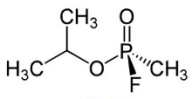 Sarin 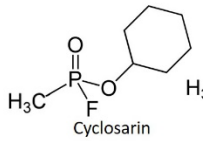 Cyclosarin 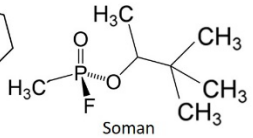 Soman

The discovery of organophosphate pesticides led to the development of nerve agents, that have been used for chemical warfare and terrorism [3]. The classification of organophosphates within the pesticide or the nerve agent group is based on their toxicity, nerve agents being the most toxic of these chemicals. These agents are classified into four types: the G-series, the V-series, the GV-series [4] and the Novichok-series [5]. The G-series, named as such because they were developed by a German research program, were discovered in 1936 and include GA (tabun), GB (sarin), GD (soman) and GF (cyclosarin) compounds (Table 1.1.1). The V-series, where V stands for venomous, were mainly developed in 1950s and include VE, VG, VM and VX (Table 1.1.1). Generally, V-series compounds are more toxic than G-series of chemicals. The GV-series which have combined properties of both G- and V-series chemicals. The Novichok-series, also known as A agents, were created by a Soviet chemical warfare development program in 1989 and include A230, A232, A234, Novichok-5 and Novichok-7 [6]. The chemical structure and physicochemical properties of these series of compounds is still unclear [5,6].

Some organophosphates have been approved as therapeutic agents in human medicine. Trichlorfon (Table 1.1.1) was introduced as a drug for the treatment of schistosomiasis during the 1960s. This organophosphate was investigated as therapy for Alzheimer's Diseases due to the beneficial effects in memory and learning [7-9]. Ecothiopate and DFP were approved for the treatment of chronic glaucoma. However, the use of these drugs is limited due to severe side effects [10].

1.1.3. Global impact of organophosphate use

The use of organophosphates as pesticides in agriculture and as self-poisoning agent in suicides causes at least two million of intoxications per year that results in an estimated 200,000 deaths annually worldwide [11-13].

Although the use of organophosphate nerve agents for chemical warfare was prohibited by the Geneva Protocol and The Organisation for the Prohibition of Chemical Weapons in 1987 some incidents in different conflicts and terrorist attacks have been reported in the past years [14]. In 1994 and 1995, a Japanese terrorist group carried out attacks with sarin both in the subway of Tokyo and in residential areas of Matsumoto causing dozens of deaths and thousands of poisoning cases [15]. Two chemical attacks with sarin were carried out during the Syria conflict in 2013 and 2017 counting more than 3,000 victims and 400 deaths [16,17]. In 2017, the half-brother of North Korea's leader, Kim Jong-Nam, was assassinated inside the Kuala Lumpur airport with the nerve agent VX [17]. A year later, the ex-spy Sergei Skripal and his daughter were poisoned with Novichok in the United Kingdom. As consequence of this, 46 members of the public were

attended with poisoning symptoms and two of them died [18]. More recently, in August 2020, a nerve agent of the Novichok group was used in the poisoning of Alexei Navalny in Tomsk [19].

1.1.4. Physicochemical properties of organophosphates

In a pure state, most organophosphates are lipophilic liquids, mainly colourless, odourless or with faint odour, characterized by different physicochemical properties (Table 1.1.2). Depending on these properties, each organophosphate is absorbed, transported, accumulated or biotransformed throughout different routes (see section 1.1.5). In general, nerve agents are more volatile than pesticides (Table 1.1.2), being more susceptible to absorption by the respiratory tract [20].

Table 1.1.2. Physicochemical properties of organophosphates pesticides and nerve agents.

Chemical	Molecular weight (g/mol)	Boiling point (°C)	Vapour pressure (mmHg)	Solubility (mg/l)	Hydrolysis rate $t_{1/2}$ (days, pH 7.0)	Log K_{ow}
Chlorpyriphos	350.6	160	$2x10^{-5}$	1.4	94	4.96
Cyclosarin*	180.2	239	0.044	3700 (20°C)	n.a.	1.04
DFP*	184.2	183	0.579 (20°C)	15400	2.2	1.17
Diazinon	304.4	353.9	$9x10^{-5}$	60	23	3.3
Dichlorvos	220.9	234	0.0158	18000	61.5	1.9
Fenamiphos	303.4	375.6	$9x10^{-7}$	700	16	3.3
Malathion	330.4	156	$4x10^{-5}$	145	1	2.75
Monocrotophos	223.2	125	$2.2x10^{-6}$	Miscible	30	-0.22
Paraoxon-ethyl	275.2	170	$1.1x10^{-6}$	3640	144 (pH 7.4)	1.98
Paraoxon-methyl	247.1	100	$1.1x10^{-6}$	731	5.8 (pH 8)	1.33
Sarin*	140.1	158	2.9	Miscible	1.625	0.3
Soman*	182.2	190	0.4	21000 (20°C)	1.875 (pH 6.6)	1.82
Tabun*	162.1	248	0.037	98000	0.425	0.38
Trichlorfon	257.4	100	$1.6x10^{-6}$	120000	29	0.43
VX*	267.4	298	0.0007	30000	41.667	2.09

Note. Solubility and vapour pressure at 25°C unless otherwise specified. Log K_{ow}, octanol:water partition coefficient to estimate the capability of organophosphates for skin penetration and fatty tissue accumulation. Asterisk indicates nerve agents. Data are taken from [21].

1.1.5. Toxicokinetic of organophosphates

1.1.5.1. Exposure

Organophosphates can be absorbed throughout all exposure routes including the respiratory tract, the gastrointestinal tract, the skin and the eyes (Figure 1.2). Nerve agents with higher resistance to evaporation and more lipophilicity, such as VX, can be absorbed by skin or eye contact [20]. In contrast, more volatile compounds, such as the G-series chemicals, can be taken up by inhalation and absorbed across the respiratory tract [22]. The most common routes of exposure

to organophosphate pesticides are by accidental ingestion of contaminated food and/or water. Depending on the hydrophobicity of the chemical, organophosphates can be absorbed through the walls of the intestine, entering the blood stream [20]. Additionally, inhalation of droplets and dermal exposure during the mixing, loading and application of pesticides are two important routes of poisoning [23].

For controlled toxicological studies in model organisms, organophosphates can be administrated by subcutaneous, intravenous, intramuscular or intraperitoneal injection (see section 1.3.4.1).

1.1.5.2. Distribution and accumulation

Organophosphates distribute to other organs through blood either in solution or by covalent modification of circulation carrier proteins such as albumin, γ-globulin and butyrylcholinesterase (Figure 1.2) [24,25]. The efficiency of this process largely varies between different chemicals depending on their hydrophobicity. Highly lipophilic compounds, such as VX, have limited transfer into blood or systemic organs, accumulating in fatty tissue and creating a depot for delayed release [26]. This fact reduces the biotransformation and therefore the elimination of the organophosphate from the body [27].

1.1.5.3. Biotransformation

The transformation of organophosphates consists of the spontaneous or enzymatic hydrolysis of the leaving group, creating more soluble and less toxic compounds that can be eliminated by urinary excretion (Figure 1.2) [20]. The half-life for organophosphate hydrolysis ranges from hours to weeks (Table 1.1.2). However, the velocity of enzymatic hydrolysis is much faster, defining the rate for poison elimination. Phosphotriesterases (paraoxonases and DFPases) are the enzymes responsible for hydrolysing organophosphates. These can be found in plasma, liver or kidneys [28]. Although the physiological function of phosphotriesterases remains to be established [28,29], a correlation has been recognized between the expression or activity levels of these enzymes and the susceptibility to organophosphate toxicity. Thus, species with low levels of phosphotriesterase activity, such as birds or insects, are more sensitive to the toxic effects of organophosphates [30,31]. This fact has led to the development of modified phosphotriesterases as bioscavengers as a promising route to treat organophosphate poisoning (see section 1.3.3.2) [32].

Although the majority of organophosphate metabolic processes are detoxification reactions, some can substantially increase the toxicity of certain organophosphates such as parathion, chlorpyrifos, diazinon and diethoate (Table 1.1). These chemicals possess a P=S group which is not very reactive with serine hydrolases. However, the cytochrome P450-dependent conversion of the P=S moiety to a P=O group forms the oxon derivatives, increasing their toxicity [33]. This can

help to target their toxicity towards insects, rather than humans, who are much less efficient at the conversion to the oxon form [34].

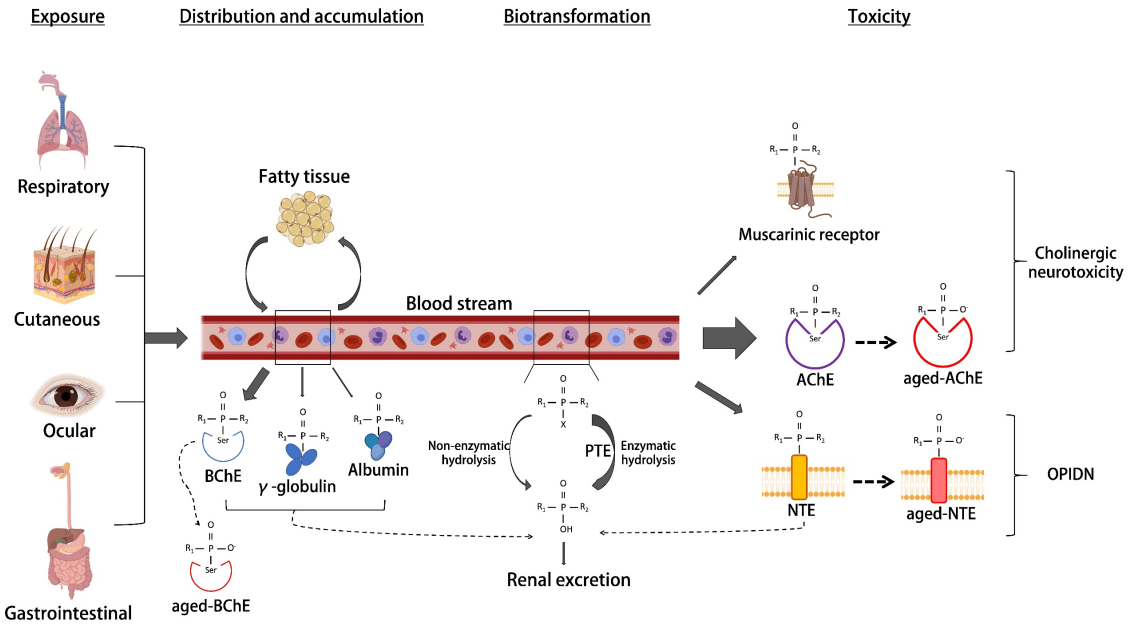

Figure 1.2. Toxicokinetic steps of organophosphates in mammals. Organophosphates exposure routes depend on their solubility, vapour pressure and octanol-water partition coefficient (Table 1.1.2). Chemicals with higher vapour pressure and lower octanol-water partition coefficient predominantly access by inhalation. Chemicals with lower vapour pressure and higher octanol-water partition coefficient access by per cutaneous absorption. After this, organophosphates reach the blood where they can be systematically distributed in solution or by blood carrier proteins transport (albumin, γ-globulin and butyrylcholinesterase) (Table 1.1.2). Highly lipophilic compounds can accumulate in the fatty tissue reducing their biotransformation and creating a deposit for delay release. Biotransformation and elimination of organophosphates by non-enzymatic or enzymatic hydrolysis throughout phosphotriesterases (PTE) reduce the amount of circulating poison reducing the toxicity. This process takes place in the blood, kidneys and liver. The binding of organophosphates to alternative targets contributes to the reduction of poison available. When organophosphates reach the central and peripheral nervous system, they bind and inhibit the function of muscarinic receptors, acetylcholinesterases (AChE) and neuropathy target esterases (NTE) and with different affinities (see section 1.1.5.4). The inhibition of acetylcholinesterases is the main cause of cholinergic neurotoxicity that could be aggravated by the inhibition of muscarinic receptors. The organophosphate bound to acetylcholinesterase, butyrylcholinesterase and neuropathy target esterase can be either hydrolysed, releasing the enzyme to be functional, or aged, creating an irreversible bound between the poison and the enzyme. The irreversible inhibition of a large proportion of neuropathy target esterase triggers the development of organophosphate-induced delayed polyneuropathy (OPIDP). Figure adapted from [20] and created with BioRender.

1.1.5.4. Toxicity

The toxicity of organophosphates is mediated by the attack of the phosphorous atom on polarized hydroxyl groups in amino acid side chains of proteins. This reaction triggers the phosphorylation of the amino acid by the release of the leaving group. The phosphorylation of the catalytic serine in the active site of acetylcholinesterases represents the most important reaction in terms of toxicity. The pathophysiological implications of acetylcholinesterase inhibition by

organophosphates are known as cholinergic syndrome or cholinergic crisis and will be detailed in section 1.2.

Despite their high affinity for acetylcholinesterases, organophosphates chemically modify other targets such as albumin [24,35,36], receptor/channel complexes [37], muscarinic and nicotinic acetylcholine receptors [38,39] and other secondary serine hydrolases (Figure 1.2). This might contribute to the toxicity of organophosphates pesticides by inducing pathophysiological situations through non-cholinergic mechanisms [37]. However, since the chemical modification of these alternative targets requires a concentration of organophosphate beyond the lethal dose for nerve agents, the binding of organophosphates to these targets would reduce the concentration of neurotoxin available to bind acetylcholinesterase and therefore the toxicity (Table 1.3) [40].

Some of the additional targets with clinical consequences following intoxication are described in this section while the mechanism and consequence of acetylcholinesterase inhibition as major determinant will be described in section 1.2 of this thesis.

- Organophosphate-induced delayed polyneuropathy

The organophosphate-induced delayed polyneuropathy (OPIDP) is a neurodegenerative disorder caused by a single exposure with certain organophosphates. Effects usually appear 10 – 20 days after the cholinergic crisis has been medically solved with standard therapy and include loss of function and ataxia of distal parts of sensory and motor axons in peripheral nerves and spinal cord [41-43].

The OPIDP syndrome is triggered by the reduction of more than 70% of the functional neuropathy target esterase (NTE) in peripheral nerves due to the phosphorylation of its catalytic serine and the subsequent aging reaction between the enzyme and the organophosphate (see section 1.2.2 for details of aging reaction) [44]. Human NTE is a patatin-like phospholipase domain-containing protein 6 that catalyses hydrolysis of membrane-associated lipids and might play a role in intracellular membrane trafficking as well as membrane homeostasis [45,46].

- Chronic organophosphate-induced neuropsychiatric disorder

The chronic organophosphate-induced neuropsychiatric disorder (COPIND) might result due to the chronic exposure to low levels of organophosphates. The syndrome is not dependent on acetylcholinesterase inhibition and patients can develop symptoms without exhibiting previous signs of cholinergic crisis [42,47,48].

The most common symptoms of the COPIND include cognitive deficit (impairment in memory, concentration, learning, attention, coordination and reaction time), mood change (anxiety, depression, psychosis, emotional lability, suicidality), chronic fatigue, autonomic dysfunction and

peripheral neuropathy (dystonia, resting tremor, postural instability and rigidity of face muscles) [47-49].

Table 1.3. Acute lethality of organophosphates. Median lethal doses (LD_{50}) from organophosphate exposure by different routes in human and model organisms. Data are given in mg/kg for oral and percutaneous exposure and in mg/m^3 for inhalation 24 hours postexposure unless otherwise is specified. Data taken from [20,21,50]. a – Given as lowest published toxic dose; b – 10 minutes postexposure; c – 4 hours postexposure; d – Given as lowest published lethal dose; e – 60 minutes postexposure; f – 2 minutes postexposure; g – 30 minutes postexposure; h – 4 minutes postexposure.

OP	Exposure route	Specie			
		Rat	Mouse	Guinea pig	Human
Chlorpyriphos	Oral	82	60	504	300[a]
	Percutaneous	202	120		
	Inhalation				
DFP	Oral	5	2		
	Percutaneous	300	72		
	Inhalation	360	440		8.1[a b]
Diazinon	Oral	66	17	250	214
	Percutaneous	180	2750		
	Inhalation	3.5[c]	1600[c]	5500[c]	
Dichlorvos	Oral	17	61		1000[d]
	Percutaneous	0.75	206		
	Inhalation	15[c]	13[a c]		
Fenamiphos	Oral	8	22.7		
	Percutaneous	80			
	Inhalation	91[c]			
Malathion	Oral	290	190	570	47[a]
	Percutaneous	4444	2330	6700	
	Inhalation		43.8[c]		
Monocrotophos	Oral	8	15		
	Percutaneous	112			
	Inhalation	63[c]			
Paraoxon-ethyl	Oral	1.8	0.76		14
	Percutaneous	4.4			
	Inhalation				
Paraoxon-methyl	Oral	32.7	21		
	Percutaneous				
	Inhalation				
Sarin	Oral	0.55			0.002[a]
	Percutaneous	2.5	1.08	8.75	0.024
	Inhalation	5.9[e]	9[e]	14.3[e]	36[f]
Soman	Oral	0.4			
	Percutaneous	7.8	7.8	9.9 - 11.1	5
	Inhalation		1[g]	827.7[h]	70[a]
Tabun	Oral	3.7			
	Percutaneous	18	0.1	35	14 – 21
	Inhalation				
Trichlorfon	Oral	450	300	420	240[a]
	Percutaneous	2	1710		
	Inhalation	1300			
VX	Oral	0.12			
	Percutaneous	0.08		34	0.086[a]
	Inhalation				

The mechanism by which organophosphates induce COPIND is still unclear. Some hypotheses are that symptoms derive from withdrawal of the chronic organophosphate exposure [51], alteration of neuropeptide metabolism [52,53], serotonin disturbances in the central nervous system [54] or neuronal damage due to the induction of oxidative stress. Reactive oxygen species induced by organophosphate exposure might trigger cell death due to the reaction with lipids, proteins and DNA, causing membrane damage, enzyme inactivation and DNA alterations, respectively [55].

1.2. Organophosphate poisoning

The reaction between organophosphates and acetylcholinesterases results in the inhibition of the enzyme function. Since acetylcholinesterase plays a crucial role terminating the cholinergic signalling, its inhibition triggers a broad range of neurotoxicological effects and eventually death. These effects are known as cholinergic syndrome or cholinergic crisis [56].

1.2.1. Acetylcholinesterase

Acetylcholinesterase is a serine hydrolase highly conserved from invertebrates to mammals [57] . Its principal biological role is the hydrolysis of the neurotransmitter acetylcholine into acetate and choline. This facilitates the termination of the impulse transmission to prevent the overstimulation of acetylcholine receptors at cholinergic synapses including neuromuscular junctions.

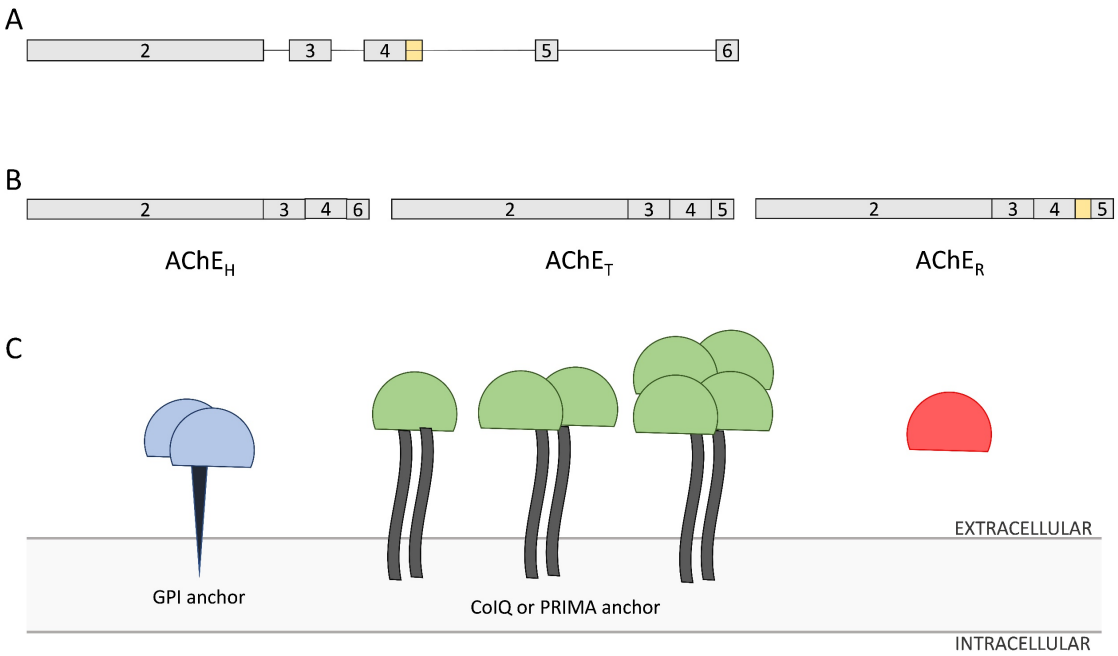

Figure 1.3. Acetylcholinesterase gene organization, RNA transcripts and protein products. A) Structure of human acetylcholinesterase gene. Exons are represented by grey rectangles and introns by single horizontal lines. Yellow square after exon 4 represents an intronic sequence alternatively spliced in the AChE$_R$ isoform. B) mRNA composition of the three AChE isoforms expressed in mammals (see text for full detail). C) Acetylcholinesterase alternative protein

products. $AChE_H$ forms dimeric structures anchored to the membrane by GPI protein. $AChE_T$ can be found as mono, di or tetrameric forms anchored to the membrane by either CoIQ or PRIMA proteins. $AChE_R$ consists of a soluble monomer. Adapted from [58,59].

1.2.1.1. Isoforms

One single gene encodes acetylcholinesterase in vertebrates that is composed by the N-terminal region containing the signal peptide, removed in the mature protein, the catalytic domain and the C-terminal region which confers specificity to the different isoforms of the enzyme (Figure 1.3) [60,61].

In mammals, exons 2 to 4 constitute the catalytic core of the enzyme and are constitutively expressed (Figure 1.3). Transcripts containing exon 6 generate the hydrophobic form of acetylcholinesterase ($AChE_H$) while transcripts harbouring exon 5 create the tailed form ($AChE_T$). The readthrough ($AChE_R$) form of the enzyme is generated by the retention of the 3' end of exon 4 as well as exon 5 in the mature transcript (Figure 1.3).

The $AChE_H$ form, also known as $AChE_E$, is a dimeric isoform expressed in haematopoietic cells that is bound to the membrane throughout a glycosylphosphatidylinositol (GPI) anchor (Figure 1.3). This membrane-anchoring structure is added by a post-translational modification due to the signal encoded by exon 6 [62-66].

The $AChE_T$ isoform is present as monomeric, dimeric and tetrameric form. The C-terminal encoded by exon 5 allows the interaction of the protein with proline-rich attachment domains of either cholinesterase-associated collagen Q (CoIQ) or proline-rich membrane anchor (PRiMA) (Figure 1.3) [59,67]. Oligomers anchored to the extracellular matrix by CoIQ are mainly expressed in the basal laminal of neuromuscular junctions while tetramers associated with PRiMA to the membrane surface are predominantly localized in the brain [68]. This isoform is also known as $AChE_S$.

The $AChE_R$ isoform creates monomers preferentially expressed in embryonic tissues and neurons. This form of the enzyme would remain soluble within the synaptic cleft [58] (Figure 1.3).

Interestingly, the balance between the different isoforms of acetylcholinesterase is altered in stress conditions as well as some neurological disorders such as Alzheimer's disease, Parkinson disease and myasthenia gravis [58]. The increase of the R isoform of acetylcholinesterase in stress conditions or after exposure to anti-cholinesterases might present a protective effect in short-term by increasing the synaptic concentration of acetylcholine and therefore the basal electrophysiological activity in the brain. However, the prologue elevation of neurotransmitter levels might trigger an acetylcholine-induced signalling cascade that might be the consequence of the long-term damage occurred in stress-related neurological disorders. This reduces the

concentration and/or capacity of muscarinic receptors at the synapse and promotes the interaction of acetylcholinesterase R isoform with other synaptic proteins causing the intensification of long-term potentiation currents in the brain [69-71].

1.2.1.2. Synthesis, transport, localization, and degradation of acetylcholinesterase

Biosynthesis, processing, and transport of acetylcholinesterases are similar across cell types requiring about 3 hours from transcription till expression at the plasma membrane. This time comprises translation, folding, post-translational modifications, assembling, and trafficking to the final destination [72].

After transcription, acetylcholinesterase mRNA is highly associated with the rough endoplasmic reticulum via Pumilio-2, an RNA-binding protein. This protein might also serve as a mechanism for transporting acetylcholinesterase mRNA to specifically the region of interest in neurons and muscles [73]. Acetylcholinesterase peptides are translated, fold, and glycosylated in the rough endoplasmic reticulum. However, depending on the cell type, about 20% of the molecules are correctly fold and maintain catalytic activity to be transported to the Golgi. Post-translational modifications at the Golgi include the addition of asparagine-linked oligosaccharides and the assembling into dimers or tetramers depending on the cell type [74]. Properly assembled acetylcholinesterase molecules are packed into transport vesicles, through a clathrin-mediated mechanism, that translocate along microtubules until they fuse with the plasma membrane [75].

Different research studies agree that acetylcholinesterase is a stable protein at the neuromuscular junction compared with other extracellular proteins [76-79]. However, the half-life calculated using H3-DFP varies between 50 hours in cell cultures till 20 days at the neuromuscular junction of live mice [76,80]. More recent estimations using fluorescent fasciculin-2 indicate that the turnover ration depends on the exposure conditions. After one single exposure to the toxin, the half-life of acetylcholinesterase is about 3 days initially and 12 days later. However, the continuous exposure to fasciculin-2 increases the removal rate up to 12 hours [77].

Removed acetylcholinesterases from synapses are mainly co-localized with acetylcholine receptors in the same intercellular compartments that transport the proteins into lysosomes for degradation [77].

1.2.1.3. The catalytic domain

The structure of the catalytic domain has a conserved hydrolases fold. This consists of a central strand of beta sheets surrounded by alpha helices. The active site is organized around 4 key determinants: the gorge, the oxyanion hole, the acyl pocket and the catalytic triad [81] (Figure 1.4). The gorge is a deep and narrow hole surrounded by 14 highly conserved aromatic residues that

penetrates more than halfway into the enzyme (Figure 1.4). The acyl pocket and the oxyanion hole, composed by aromatic (tryptophan) and non-polar (alanine/glycine) residues respectively, are located at the end of the gorge flanking the catalytic triad [81]. The catalytic triad is formed by three highly conserved interspaced amino acids that are serine, glutamate and histidine: Ser238, Glu367 and His440 in *Drosophila melanogaster*; Ser216, Glu346 and His468 in *Caenorhabditis elegans*; Ser200, Glu327 and His440 in *Torpedo californica*; Ser203, Glu334 and His447 in *Mus musculus* and *Homo sapiens* [81-85]. The gorge, acyl pocket and oxyanion hole play a key role creating the perfect environment to attract, guide and orientate the molecule to the active site in front of the catalytic triad. Once precisely positioned, the catalytic triad hydrolyses the acetylcholine molecule into choline and acetic acid (Figure 1.5A) [81,83].

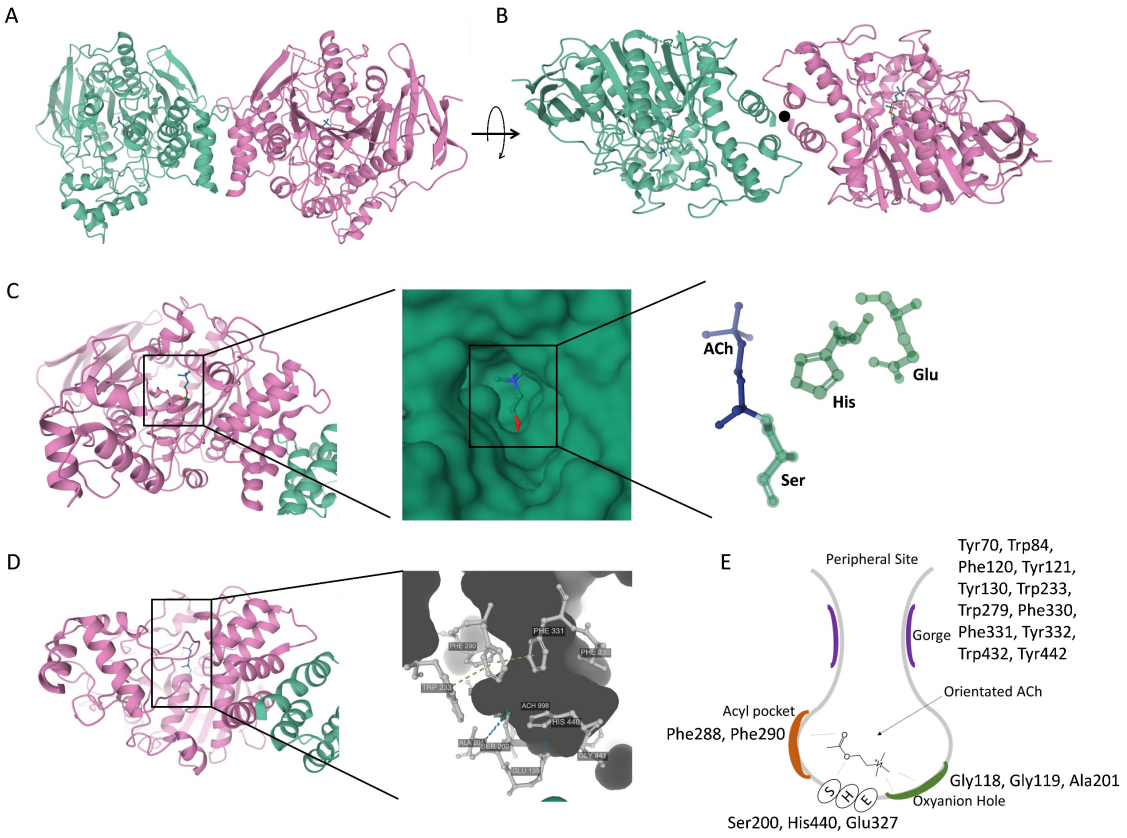

Figure 1.4. Acetylcholinesterase structure. Conformational structure of *Torpedo californica* acetylcholinesterase dimer held by a 4-helix bundle. The two monomers are represented by green and pink colours, respectively. Accession number 2ACE in PDB database [81]. A) View along the 2-fold axis. B) View down the 2-fold axis. C) Zenithal view of acetylcholinesterase binding pocket in a ribbon representation with detail of acetylcholine fitted in a molecular surface representation. The distribution of acetylcholine and the three amino acids of the catalytic triad are highlighted. D) Front view of acetylcholinesterase catalytic domain in a ribbon representation with detail of its structure and conserved amino acids responsible for the breaking down of acetylcholine. E) Schematic representation of acetylcholinesterase catalytic domain. Conserved amino acids at the gorge (purple), acyl pocket (orange), oxyanion hole (green) and catalytic triad are represented. Dotted lines represent the interaction between the acetylcholine molecule and the different structures of the acetylcholinesterase active site. Adapted from [86].

1.2.1.4. Hydrolysis of acetylcholine by acetylcholinesterase

The hydrolysis of the neurotransmitter acetylcholine by acetylcholinesterase is possible due to the proton transference carried out between the three amino acids of the catalytic triad (Figure 1.5). The side chain of serine transfers a proton to a nitrogen in the imidazole ring of the histidine side chain, which transfer a proton from the second nitrogen of the imidazole ring to the carboxyl group of glutamate. This reaction allows the nucleophilic attack of acetylcholine by the active site serine oxygen which leads the formation of acyl-serine and releases choline. Finally, the acyl-enzyme undergoes nucleophilic attack by a water molecule, assisted by the histidine 440 group, liberating acetic acid and regenerating the free enzyme (Figure 1.5) [87].

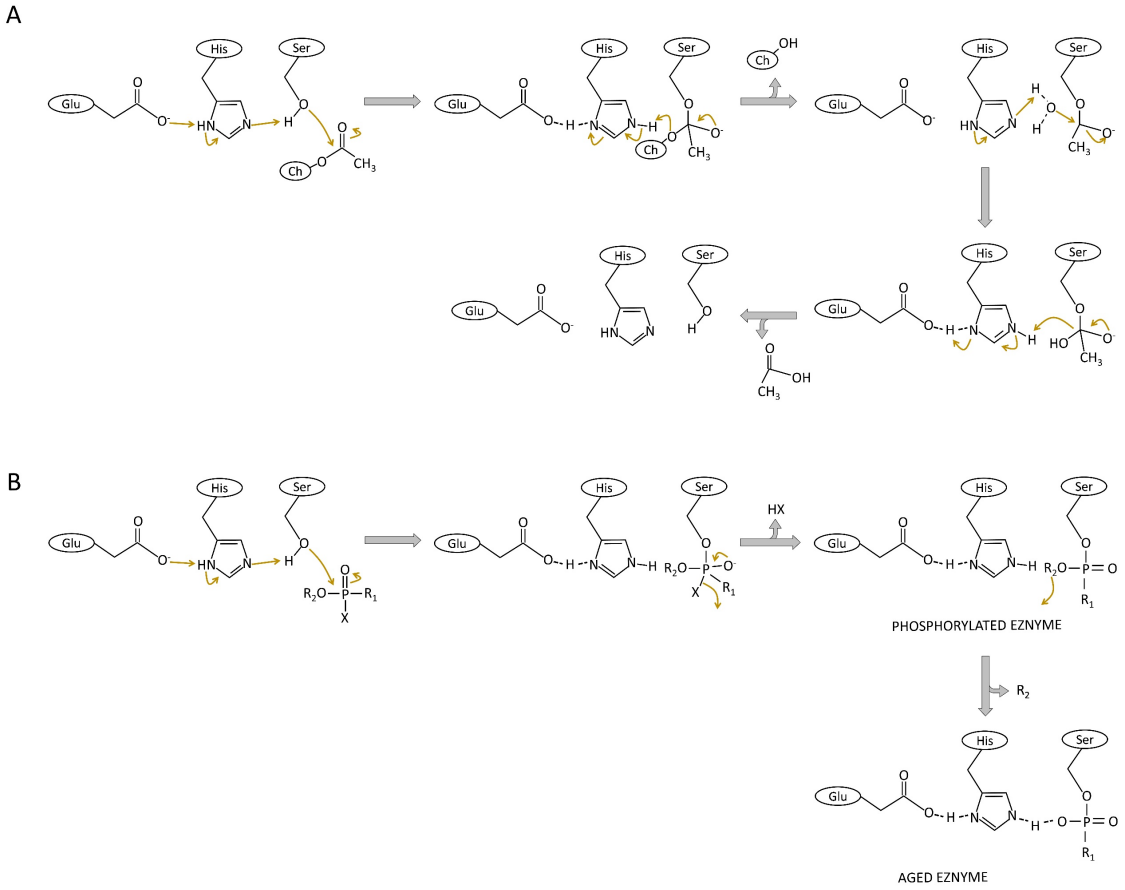

Figure 1.5. Mechanism of acetylcholine hydrolysis catalysed by acetylcholinesterase (A) and acetylcholinesterase inhibition by organophosphates and aging (B). Glu, His and Ser represent the catalytic triad glutamate, histidine and serine. Ch: choline; X: leaving group. Adapted from [88].

1.2.2. Mechanism of acetylcholinesterase inhibition by organophosphates

The mechanism of acetylcholinesterase inhibition by organophosphates is defined by a Uni-Bi Michaelis-Menten equation in which the organophosphate binds the enzyme creating an intermediate complex that can be susceptible to spontaneous hydrolysis, oxime-mediated hydrolysis or aging (Figure 1.6).

The organophosphate molecule is attracted, guided and orientated by the gorge, acyl pocket and oxyanion hole of the acetylcholinesterase in a similar manner to the original substrate, acetylcholine [81]. When the molecule is positioned in front of the catalytic triad, the nucleophilic attack of the serine oxygen to the phosphorous atom leads to the phosphorylation of the catalytic serine and the dissociation of the leaving group from the organophosphate (Figure 1.5). The kinetic of the reaction is defined by the biomolecular inhibition rate constant K_i which indicates the moles of organophosphate that bind acetylcholinesterase over time (Table 1.4).

The phosphorylated enzyme can undergo spontaneous reactivation, oxime-dependent reactivation or aging reaction, depending on the type of organophosphate reacting. The aging reaction is more likely to occur when inhibiting acetylcholinesterase with nerve agents rather than pesticides [89].

The spontaneous reactivation consists of a hydrolysis reaction of the alkyl-ester bond created by the enzyme and the organophosphate molecule and enables the re-use of the acetylcholinesterase [90]. The oxime-mediated reactivation will be described in section 1.3.2.2 of this thesis. Finally, the aging reaction is a time-dependent process consisting of the dealkylation of any side chain of the conjugated organophosphate by the addition of a water molecule. It creates a stronger O-C bond between the organophosphate and the catalytic serine leading to the irreversible inhibition of the enzyme (Figure 1.5) [91].

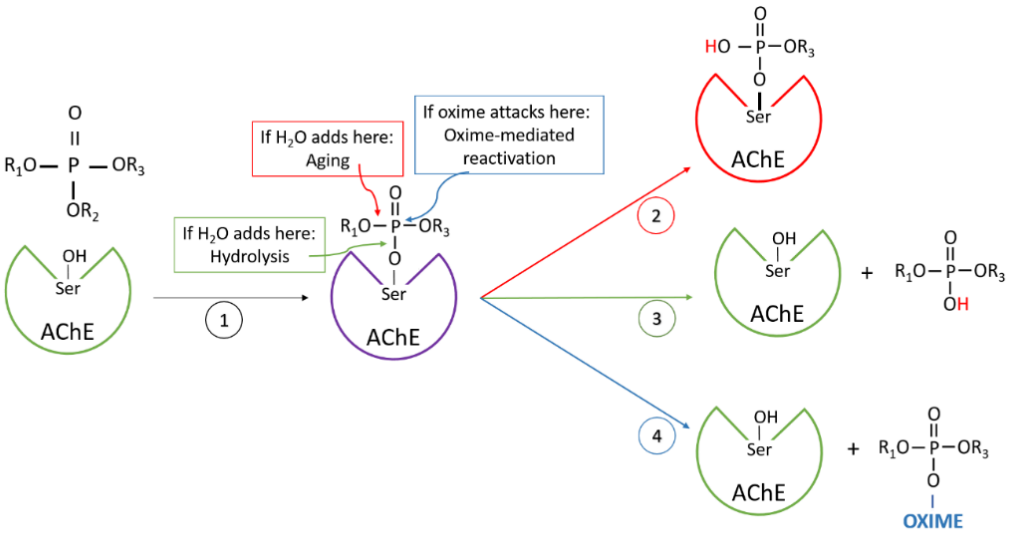

Figure 1.6. Mechanism of inhibition, aging, spontaneous reactivation and oxime-mediated reactivation between acetylcholinesterase and organophosphates. After being phosphorylated by the organophosphate (OP) molecule (1), the inhibited acetylcholinesterase can undergo either the irreversible inhibition of the enzyme by aging reaction (2) or the reactivation of the enzyme by spontaneous hydrolysis [92] or by oxime-mediated reactivation (4) (see section 1.3.2.2). For constant of inhibition (1), aging (2), spontaneous hydrolysis (3) [92] and oxime-mediated reactivation (4) values see Table 1.1. Green AChE represents active acetylcholinesterase, purple AChE corresponds to inhibited acetylcholinesterase and red AChE represents aged acetylcholinesterase. Adapted from [88].

Both the phosphorylated and the aged acetylcholinesterase are deficient in the hydrolysis of acetylcholine, triggering the progressive accumulation of the neurotransmitter in synaptic clefts and neuromuscular junctions. This causes the overstimulation of acetylcholine receptors [88]. The symptoms associated with acetylcholinesterase inhibition by organophosphates are directly related to the physiological function of acetylcholine as neurotransmitter (section 1.2.3) and the differential expression of the cholinergic receptors (section 1.2.5).

Table 1.4 Constants of inhibition, aging, spontaneous hydrolysis and oxime-mediated reactivation of some organophosphates to human acetylcholinesterase. K_i represents the inhibition constant of human acetylcholinesterase by the organophosphate molecule (step 1 in Figure 1.6). K_a represents the aging reaction constant between human acetylcholinesterase and the organophosphate molecule (step 2 in Figure 1.6). K_s corresponds to the spontaneous hydrolysis constant of the organophosphate-inhibited acetylcholinesterase (step 3 in Figure 1.6). K_r corresponds to the oxime-mediated reactivation of the organophosphate-inhibited acetylcholinesterase (step 4 in Figure 1.6) by three different oximes, obidoxime, pralidoxime and HI-6 (see section 1.3.2.2). n.d. – not determined. Table adapted from [89].

OP	K_i ($M^{-1}min^{-1}$)	K_a (min^{-1})	K_s (min^{-1})	Obidoxime K_r ($M^{-1}min^{-1}$)	Pralidoxime K_r ($M^{-1}min^{-1}$)	HI-6 K_r ($M^{-1}min^{-1}$)
Cyclosarin	$4.9x10^8$	$1.7x10^{-3}$	n.d.	418	57.6	$2.8x10^4$
DFP	$1.3x10^5$	$3.7x10^{-3}$	n.d.	940	59	10.3
Fenamiphos	$0.2x10^2$	$8.3x10^{-5}$	n.d.	150	28.8	22.5
Paraoxon-ethyl	$2.2x10^6$	$3.7x10^{-4}$	$3.7x10^{-4}$	$2.5x10^4$	910	365
Paraoxon-methyl	$1.2x10^6$	$3.1x10^{-3}$	0.017	$2.6x10^4$	$2.9x10^3$	581
Sarin	$2.7x10^7$	$3.8x10^{-3}$	n.d.	$2.9x10^4$	$9.1x10^3$	$1.4x10^4$
Tabun	$7.4x10^6$	$6x10^{-4}$	n.d.	411	14.2	n.d.
Soman	$9.2x10^7$	0.11	n.d.	n.d.	n.d.	n.d.
VX	$1.2x10^8$	$3.2x10^{-4}$	$3.5x10^{-4}$	$3.2x10^4$	$7.7x10^3$	$2.1x10^4$

1.2.3. Acetylcholine as neurotransmitter

Acetylcholine mediates synaptic transmission between neurons in the peripheral and central nervous system of mammals.

In the peripheral nervous system, acetylcholine is the main neurotransmitter released by pre and postganglionic neurons in the parasympathetic division, by preganglionic neurons in the sympathetic division and by all the motor neurons in the somatic nervous system (Figure 1.7). In this sense, the cholinergic signal intervenes in different physiological functions such as the regulation of cardiac contractions, blood pressure, breathing, intestinal peristalsis, glandular secretion as well as the skeletal muscle contraction [93].

In the central nervous system, the majority of cholinergic neurons are located in four regions: 1) the brainstem pedunculo-pontine and lateral dorsal tegmental nuclei; 2) a subset of thalamic nuclei; 3) the striatum, where cholinergic neurons serve as local interneurons; and 4) the basal

forebrain nuclei, which serve as major source of cholinergic projections to other parts of the brain such as neocortex, hippocampus and amygdala [94,95]. The cholinergic neurotransmission in the brain has a neuromodulatory role. This is achieved by the ability of cholinergic transmission of changing neuronal firing rates, altering presynaptic release of other neurotransmitters and coordinating the firing of other group of neurons [96-100].

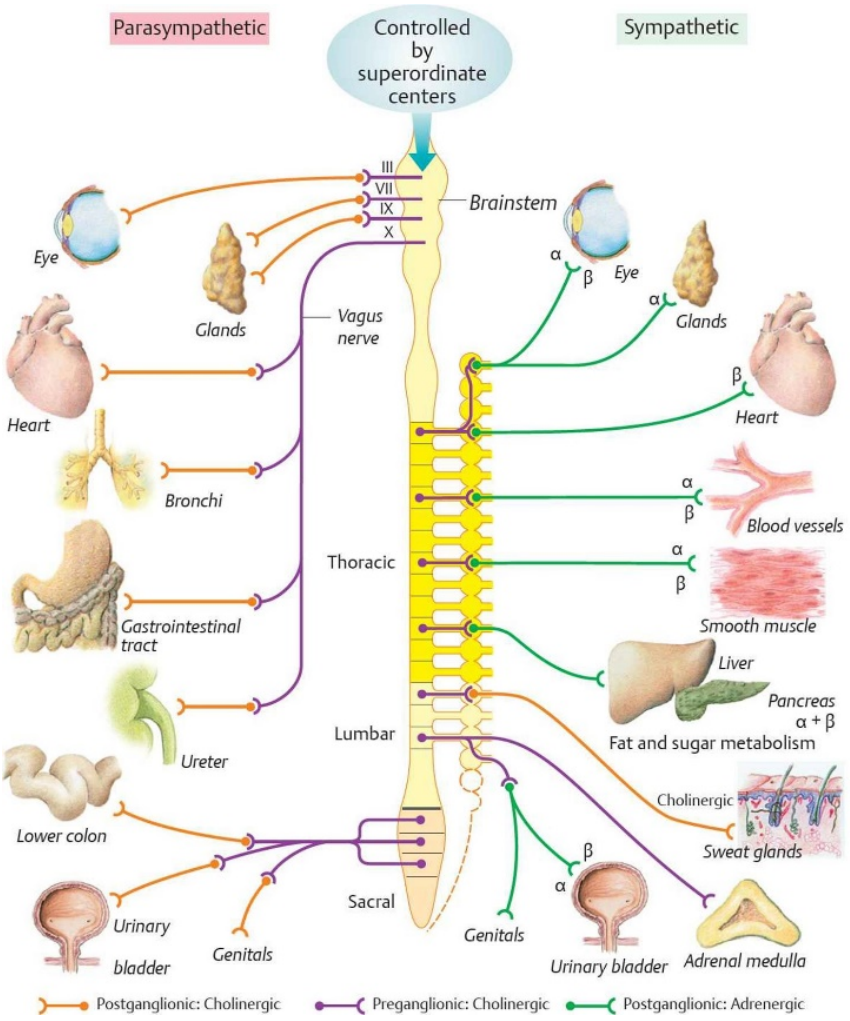

Figure 1.7. Cholinergic innervation in the autonomic nervous system. The function of visceral organs, smooth muscle and gland secretion is controlled by preganglionic cholinergic neurons in both the sympathetic and the parasympathetic division of the autonomic nervous system. Postganglionic innervation in the parasympathetic branch is governed by cholinergic signalling while postganglionic innervation in the sympathetic branch is mediated by adrenergic signalling. Adapted from [101].

1.2.4. Acetylcholine biosynthesis and synaptic release

Acetylcholine is synthesized in the cytoplasm of neurons by the enzyme choline acetyltransferase from precursors acetyl-CoA and choline (Figure 1.8). Choline for acetylcholine synthesis in mammals is primary supplied by dietary intake, phospholipases-mediated catabolism of phosphatidylcholine lipids or the recycling the choline that is generated during the catabolism of acetylcholine by acetylcholinesterases [102]. Sodium-dependent choline transporter takes up choline into the cytoplasm of cholinergic neurons. Cytoplasmic synthesized acetylcholine is uploaded to

vesicles by the ATP-dependent vesicular acetylcholine transporter [103]. Vesicles discharge acetylcholine in the synaptic cleft or neuromuscular junction by exocytosis in a calcium-dependent process [104] leading to an initial concentration of neurotransmitter of about 40,000 molecules at the release site [105]. Acetylcholine is removed from the cleft by either diffusion or hydrolysis. The rate of diffusion out of the synaptic cleft is a function of concentration as well as the properties and geometry of the cleft region [106]. Acetylcholinesterase hydrolyses acetylcholine in an estimated rate of about 2,000 molecules per second and per active site [107]. Finally, about a fifth of the neurotransmitter molecules released to the synaptic cleft bind to acetylcholine receptors for signalling transduction [105].

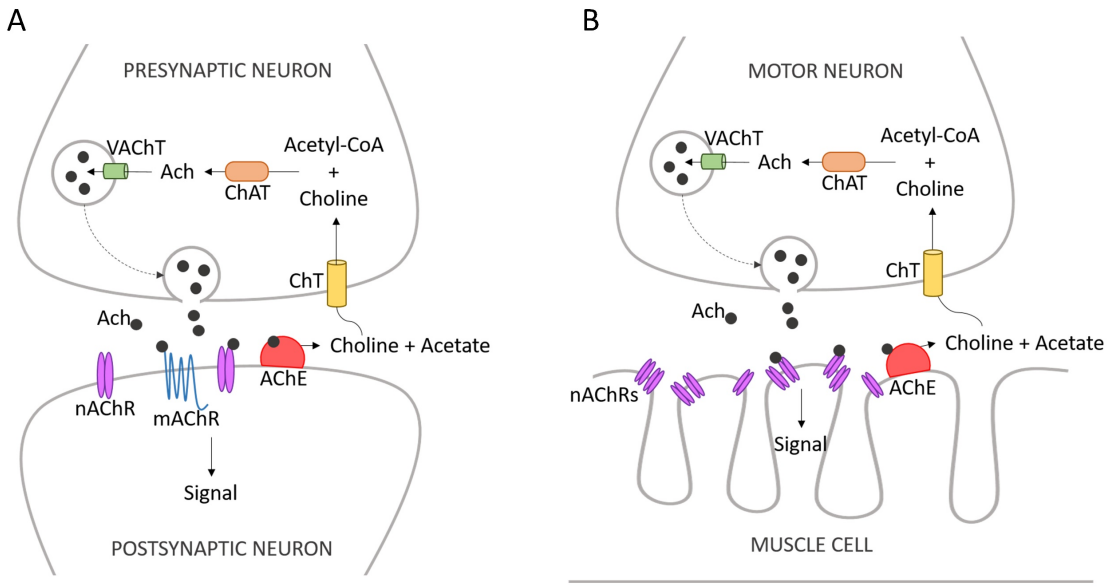

Figure 1.8. Schematic representation of synapse (A) and NMJ (B) cholinergic pathway. ACh: acetylcholine; ChAT: choline acetyltransferase; VAChT: vesicular acetylcholine transporter; nAChR: nicotinic acetylcholine receptor; mAChR: muscarinic acetylcholine receptor; AChE: acetylcholinesterase; ChT: choline transporter. See section 1.2.4 and 1.2.5 for full description.

1.2.5. Acetylcholine receptors

The acetylcholine receptors are divided into two major types: the ionotropic acetylcholine receptor and the metabotropic acetylcholine receptor. Ionotropic and metabotropic receptors are structurally, functionally and pharmacologically different.

Ionotropic receptors are members of the Cys-loop superfamily of pentameric ligand-gated channels. Nicotine has been classically defined as agonist, giving the terminology of nicotinic receptors.

Metabotropic receptors are G-coupled seven transmembrane proteins that are structurally and pharmacologically distinguished from the ionotropic acetylcholine receptors. These are sensitive

to activation by *Amanita muscaria* toxin muscarine, giving the terminology of muscarinic receptors [108].

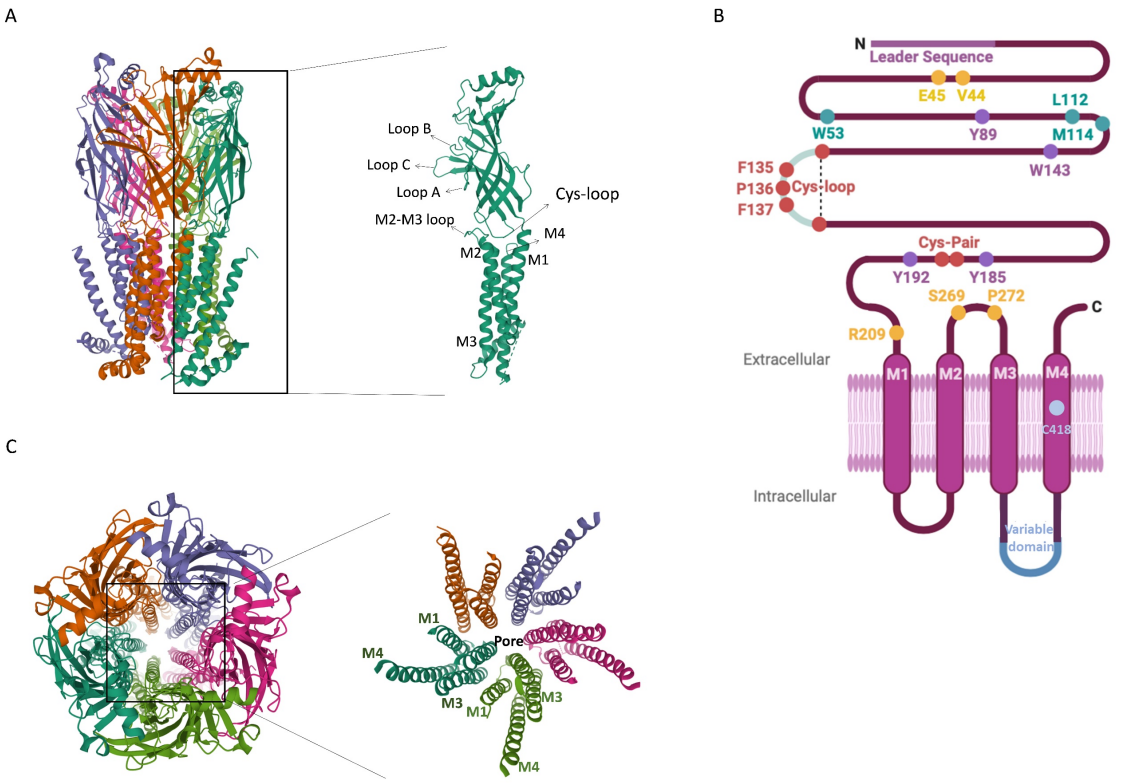

Figure 1.9. Generic structure of ionotropic acetylcholine receptors. A) Side view of the structure of nicotinic receptors in a ribbon representation with detailed view of the conformation of a single subunit. Loops A, B and C from α subunit and loops E, D and F in the adjacent subunit create the agonist binding pocket. The five subunits composing the channel are represented in different colours. Accession number 5KXI in PDB database [109]. B) Schematic linear sequence of nicotinic receptor subunits representing key structural elements: the large extracellular domain, the four transmembrane domains and the variable loop between the third and fourth transmembrane domain. Key amino acids involved in the function of nicotinic receptors are conserved in most of the subunits using Torpedo α subunit numbering system [110]. Amino acids involved in the Cys-loop and vicinal cysteines characteristics of α subunits are represented in red colour. Purple and green residues are important to the α and β contribution of the agonist-binding pocket, respectively. Amino acids involved in the gating of the receptor are represented in yellow colour. Cysteine 418 in the fourth transmembrane domain contributes to the response of nicotinic receptors by its interaction with the lipid environment. Adapted from [111]. C) Zenithal view of nicotinic receptors ion pore with detailed view of the transmembrane domains distribution of different subunits to create the channel. Accession numbers 5KXI and 1OED in PDB database [109,112].

1.2.5.1. Ionotropic acetylcholine receptor

The ionotropic nicotinic acetylcholine receptor is a Cys-loop acetylcholine-gated cation channel that mediates the fast-cholinergic signalling, opening the channel in microseconds. It consists of a cation-permeable channel formed by five homomeric or heteromeric subunits of transmembrane proteins (Figure 1.9). This core principle is conserved across phyla from invertebrates to mammals (section 1.4.6.1) [113-116]. Each subunit consists of a large and conserved extracellular N-terminal domain, three highly conserved transmembrane domains, a cytoplasmic loop between the third

and the fourth transmembrane domain variable in size and a fourth less conserved transmembrane domain with a short extracellular C-terminal domain (Figure 1.9). Subunits can be classified into α and non-α (β, δ, ϒ and ε) depending on the presence or absence of a cysteine-cysteine motif in loop C [117].

Acetylcholine binding pocket is created by the interface of loops A-C of an α subunit with loops E-F at the complementary face of the adjacent subunit (Figure 1.9). The cysteine-cysteine motif of the α subunit in loop C is essential at this step. When the agonist is bound, the Cys-loop moves creating a conformational change in the ion channel that results in the rotation of the second transmembrane domain. This is supported by the cis-trans isomerization of a highly conserved proline at the loop between the second and third transmembrane domain. The consequence is the movement of hydrophobic gating residue away from the pore and serine residues toward the pore, allowing the ion permeability [111,118].

There are 17 subunits of nicotinic receptors in vertebrates differentially expressed in muscles (α1, β1, δ, γ and ε) and neurons (α2-10 and β2-4). The combination of these subunits creates different nicotinic receptor subtypes that differ in their pharmacological and biophysical properties (Table 1.5). It implies they can be involved in the diverse functions of the cholinergic pathways in the mammalian nervous system (Figure 1.10) [119,120].

Table 1.5. Pharmacological properties to acetylcholine and physiological function of different subtypes of nicotinic receptors. Acetylcholine agonist potency is represented by the median effective concentration (EC_{50}) in μM of the subtype receptor response by two-electrode voltage-clamp when they are heterologous expressed in *Xenopus* oocytes. Agonist dose-response curve parameters determined by non-linear fitting of the Hill equation. Values are represented as mean ± standard deviation of human receptor subtypes unless otherwise is specified (references indicated on the table). Physiological function and pathology associated information was summarized from [111]. a – Data given from rat subtypes.

Subtype	EC_{50} ACh (μM)	Physiological function and pathology associated	Ref
α3α5β2	0.5 ± 0.6		[121]
α3α5β4	122 ± 20	Expression is linked with increased vulnerability to tobacco addiction	[121]
α3β2	26 ± 0.3	Dopamine release and Parkinson's disease	[121]
α3β2β3	87 ± 22 [a]		[122]
α3β4	163 ± 6	Cardiovascular and gastrointestinal actions	[121]
α4β2	3.4 ± 2.7	Cognition, neurodegeneration, pain, anxiety and depression	[123]
α4β4	22.2 ± 0.8	Cognition, neurodegeneration, pain, anxiety and depression	[124]
α6β2β3	16 ± 2.4 [a]		[122]
α7	177 ± 32	Synaptic plasticity and memory. Implicated in schizophrenia	[125]
α9	30 ± 6		[126]
α9α10	27 ± 6	Auditory function and development	[126]
α1β1δε	8.5	Muscle contraction in adults	[119]

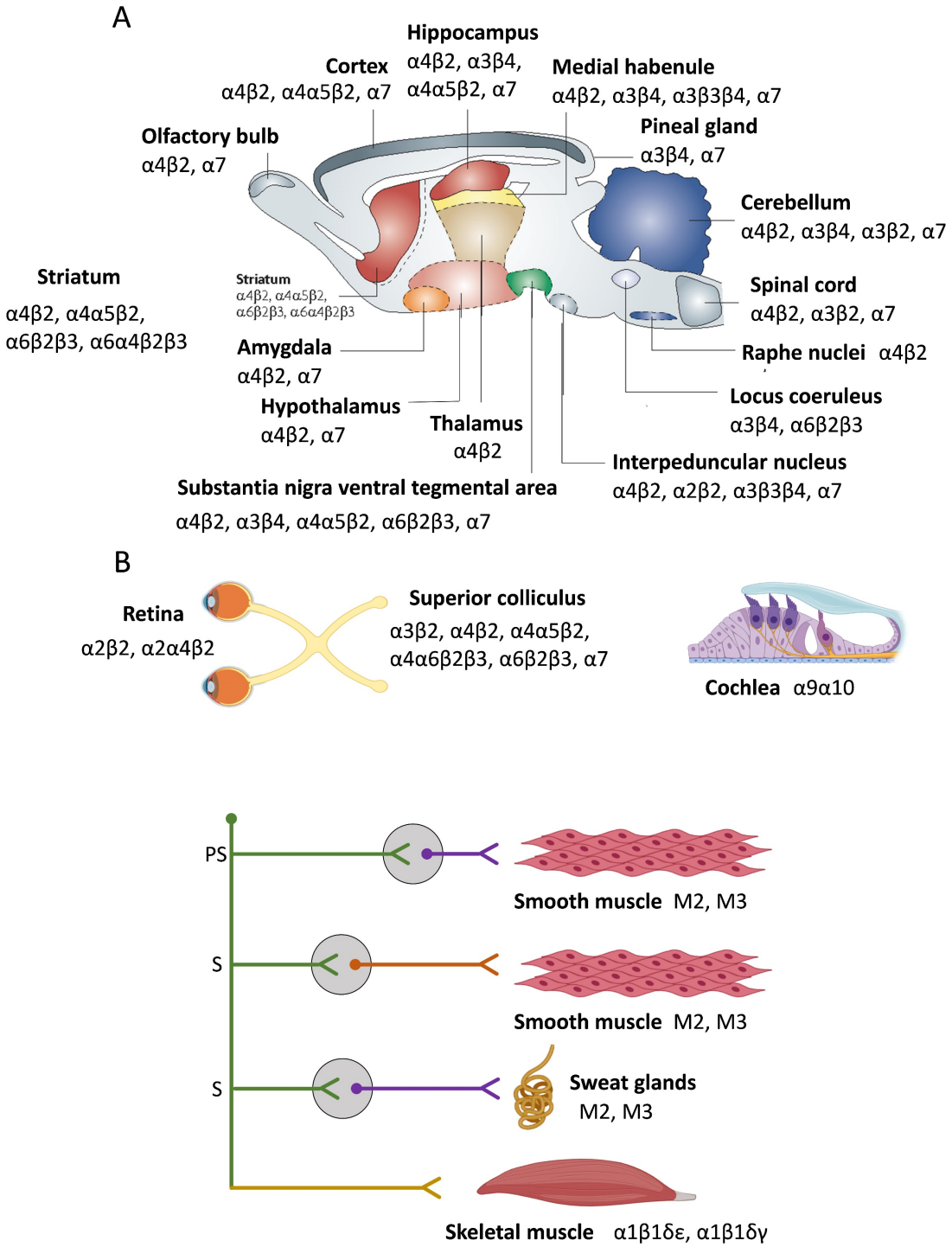

Figure 1.10 Distribution of ionotropic and metabotropic acetylcholine receptor subtypes in the central nervous system (A), visual and auditory systems (B) and peripheral nervous system (C). PS: parasympathetic branch. S: sympathetic branch. ACh: acetylcholine. NE: norepinephrine. Preganglionic neurons are represented on the left and postganglionic neurons are represented on the right of the gray circle that depicts the ganglia**.** Adapted from [127,128].

- Muscle-type nicotinic receptor

The muscle-type nicotinic receptor is exclusively expressed in skeletal muscle and triggers the contraction of the fibres upon acetylcholine binding. It consists of two subunits of α1 and the non-α subunits β1, δ and either ϒ or ε. Muscle-type nicotinic receptors containing the ϒ form are found at the foetal neuromuscular junctions and at the adult extrajunctional regions while muscle-type receptors containing the ε subunit are exclusively found at the adult neuromuscular junction [129,130]. The adult form of the nicotinic receptor is more stable to degradation, aggregates at the crest of the neuromuscular junctions and presents a faster response to agonists and a higher conductance compared with the foetal form [131]. The foetal subunit ϒ might replace the ε subunit at the adult neuromuscular junction during stress conditions suggesting it might be involved in stabilisation and/or synaptogenesis [132-134].

- Neuronal-type nicotinic receptor

The neuronal-type nicotinic receptor includes both homomeric and heteromeric receptors, with α7, α8 and α9 creating the homomeric forms of the channels. The most common heteromeric receptor is formed by 2α subunits and 3β in a pair-wise combination, however other stoichiometries have also been established [120,128].

The most abundant homomeric nicotinic receptor subtype in the nervous system of mammals is the α7 channel which is can be found in both the peripheral and the central nervous system (Figure 1.10). Among the heteromeric receptors, α4β2 is the most abundant in the mammalian brain while the combination α3β4 is the predominant subtype in the autonomic ganglia, adrenal medulla and in subsets of nerve cells in the medial habenula, nucleus interpeduncularis, dorsal medulla, pineal gland and retina (Figure 1.10) [127].

Additionally, many neuronal nicotinic receptor subunits are also expressed in non-neuronal tissues such as epithelial, endothelial, immune, mesenchymal and mesothelial cells [135].

1.2.5.2. Metabotropic acetylcholine receptor

The muscarinic acetylcholine receptor consists of a monomeric seven-pass transmembrane protein that triggers a signal throughout a G-protein (Figure 1.11) [136]. The activation of the muscarinic receptors is slower than nicotinic receptors ranging between milliseconds to seconds [108].

In mammals, five genes encode the different subtypes of muscarinic receptors, differentiated by the sequence of the third intracellular loop (i3) [137,138]. M1, M3 and M5 subtypes transduce the signal through the activation of a phospholipase C that mobilises intracellular calcium while M2

and M4 subtypes act by the inhibition of an adenylate cyclase that reduces the intracellular concentration of cAMP (Figure 1.11) [139,140].

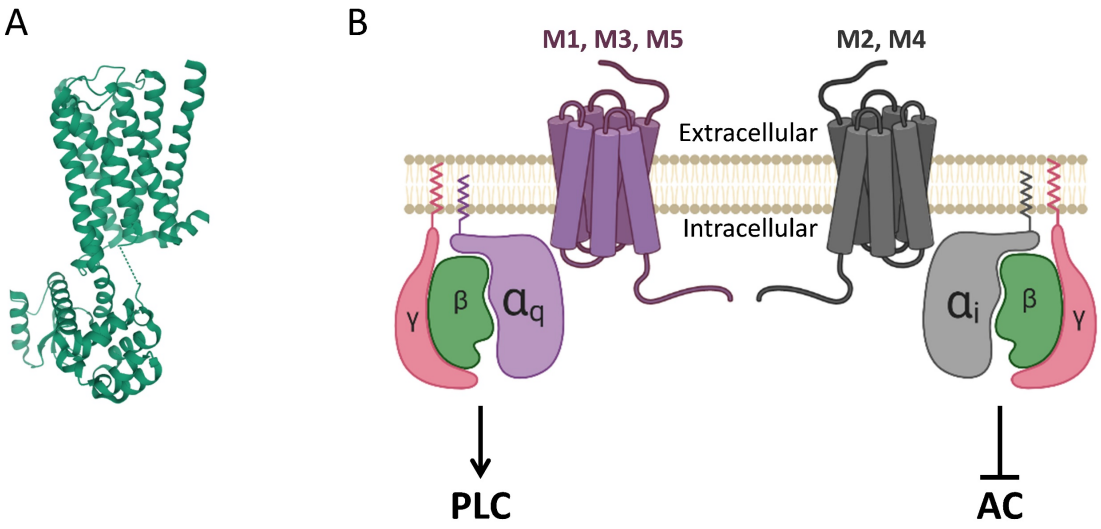

Figure 1.11. Generic structure and function of metabotropic acetylcholine receptors. A) Ribbon representation of muscarinic receptor conformation. Accession number PDB database 4DAJ [141]. B) Schematic representation of muscarinic receptors and G-proteins interaction. M1, M3 and M5 subtypes exert their function by activation of protein lipase C (PLC) through a G-protein α_q signal while M2 and M4 by inhibition of adenylate cyclase (AC) through a G-protein α_i signal.

Similar to nicotinic receptor subtypes, the different muscarinic receptor subtypes mediate a wide range of physiological functions in the central and peripheral nervous system (Figure 1.10). M1 and M4 subtypes are the most likely muscarinic receptors mediating effects on cognition, attention and sensory processing [142,143].

The M2 and M3 subtypes have been more studied for their function in the smooth muscle and glandular tissues (Figure 1.10) [144]. In fact, bradycardia, gastrointestinal distress and excessive glandular secretion are some of the symptoms developed after organophosphate intoxication mediated by the activation of these two muscarinic receptor subtypes (see section 1.3).

1.2.5.3. Pharmacology and modulation of acetylcholine receptors

As mentioned above, the different subtypes of nicotinic and muscarinic receptors exhibit differential expression and functional profile as well as distinct pharmacological and biophysical properties. In this sense, the selective modulation of certain subtypes respect to others might have a potential benefit in the control of cholinergic activity in specific conditions where the fine tune of acetylcholine signalling is impaired. These conditions include a range of neurological diseases (Alzheimer's, Parkinson's, Huntington's, chronic pain, depression and schizophrenia) [142,143,145], internal diseases (asthma, chronic pulmonary obstruction and incontinence) [146,147],

addictions (nicotine and alcohol) [148] and poisonings (carbamates and organophosphates) (see sections 1.3.1 and 1.3.2) [149].

In the past years, efforts have been made in the discovery of agonist and antagonist drugs with varying nicotinic and muscarinic subtype selectivity and target profile (Table 1.6). However, a different manner to modulate the signalling of acetylcholine receptors could be achieved by controlling their interaction with auxiliary and ancillary proteins responsible of the assembling, trafficking, maturation, location and distribution of these receptors at the synaptic cleft (Table 1.7). The fine tune of modulation is exemplified by chaperones in the maturation of nicotinic receptors. These proteins can regulate levels of nicotinic receptors at the membrane by stabilizing and sequestering subunits during the process of assembly in the endoplasmic reticulum [150]. The expression level and splicing regulation of the chaperone RIC-3 enable the functional modulation of nicotinic receptors expression and therefore the regulation of cholinergic signalling at the postsynaptic terminal (Table 1.7) [151].

Table 1.6. Drugs interacting with different nicotinic and muscarinic receptor subtypes [145,152].

Drug	Effect
ABT-089	Agonist of α4β2 and α6β2 subtypes
ABT-107	Agonist of α7 subtype
ABT-418	Agonist of α4β2 subtype
ABT-594	Agonist of α4β2 subtype
ABT-894	Agonist of α4β2 subtype
α-neurotoxins	Antagonist of α7 and muscle subtype
Arecoline	Agonist of M1, M2 and M3 subtypes. Partial agonist of M4 subtype
AR-R1779	Agonist of α7 subtype
Atropine	Antagonist of primarily M1 and M2 subtypes
AVL-3288	Positive allosteric modulator of α7 subtype
AZD 1446	Agonist of α4β2 subtype
BQCA	Positive allosteric modulator of M1 subtype
BQZ12	Positive allosteric modulator of M1 subtype
Carbachol	Agonist of all muscarinic receptor subtypes
Cotinine	Sensitizer of α7 subtype. Increase the trafficking of α4β2 receptors to the PM. Increase the expression of $(\alpha4)_2(\beta2)_3$
Epibatidine	Agonists at α4β2, α3β2, α3β4, α7, α8, muscle subtypes
Galantamine	Positive allosteric modulator of α7 subtype and AChE inhibitor
Gallamine	Antagonist of muscle subtype. Partial antagonist of α3β2 subtype
Genistein	Positive allosteric modulator of α7 subtype
GTS-21	Agonist of α7 subtype. Weak antagonist of α4β2 subtype
JNJ-39393406	Positive allosteric modulator of α7 subtype
Levamisole	Positive allosteric modulator of α3β2 and α3β4 subtypes
LY2033298	Positive allosteric modulator of M4 subtype
LY2119620	Positive allosteric modulator of M2 subtype
Mecamylamine	Antagonist of α3β4, α3β2, α4β4, and α2β4 subtypes. Partial antagonist of α2β2, α4β2, and α7 subtypes

Menthol	Increase the expression of α4β2 and α6β2β3 subtypes
ML375	Negative allosteric modulator of M5 subtype
Morantel	Positive allosteric modulator of α3β2 and α3β4. Agonist of α7 subtypes
Nicotine	Agonist of α4β2 and α7 subtypes. Increase the expression of $(\alpha4)_2(\beta2)_3$ in the cortex but not in the thalamus. Increase the expression of α3β4 subtype in heterologous system
NS1738	Positive allosteric modulator of α7 subtype
NS9283	Positive allosteric modulator of α4β2 subtype
Pilocarpine	Agonist of primarily M3 subtype
PNU 120596	Positive allosteric modulator of α7 subtype
RG 3487	Partial agonist of α7 subtype
Sazetidine-A	Agonist of α4β2 subtype
Scopolamine	Antagonist of primarily M1 and M2 subtypes
SEN-12333	Agonist of α7 subtype
SIB-1508Y	Agonist of α4β2 subtype
TC-5619	Agonist of α7 subtype
Tubocurarine	Antagonist of muscle subtype. Partial antagonist of α4β2 and α7 subtypes
Varenicline	Partial agonist of α4β2 and α7 subtype
VU0119498	Positive allosteric modulator of M3 subtype

Table 1.7. Effect of auxiliary proteins on different nicotinic and muscarinic acetylcholine receptor subtypes. PM: plasma membrane. NMJ: neuromuscular junction. Adapted from [153].

Protein	Acetylcholine receptor subtype and effect
RIC-3	At low levels, increase arrival and functional expression at the PM of α7 receptor
	Increase intracellular retention of α7 receptor when present in excess
	Reduce the acute nicotine-induced up-regulation of α4β2
UNCL	At low levels, enhance the rate of assembly and/or insertion of α3β4 subtype into the PM
	At high levels, inhibit α3β4 subtype expression
Lynx1	Non-competitive antagonist of α4β2 and α7 subtypes in heterologous systems
	Reduce the function of α3β4 in *Xenopus* oocytes
	Increase the rate and extend desensitization of α4β2 subtype
	Stabilize the assembly of α4 dimers, increasing the formation of $(\alpha4)_3(\beta2)_2$ subtype
	Stabilize muscle subtype at NMJs and modulate its sensitivity to acetylcholine
Lynx2	Forms a complex with α4β2 subtype, reducing the amount of receptor at the PM by 80%
	When co-expressed with α7 subtype, reduce acetylcholine-induced calcium influx
	Allosteric modulation of α7 and α4β2 subtypes
	Increase desensitization rate in response to acetylcholine of α4β2 subtype
Ly6h	Reduce the trafficking to the PM and the agonist-induced currents of α7 subtype
	Increase epibatidine sensitivity of the α4β2 subtype
Ly6g6e	Slow α4β2 desensitization upon acetylcholine stimulation
Lypd6	Reduce downstream signalling of α3β4 subtype stimulation
	Reduce α7-induced currents in hippocampal neurons
Lypd6b	Increase sensitivity to nicotine and reduce acetylcholine-induced whole-cell currents of $(\alpha3)_3(\beta4)_2$ subtype
PSCA	Reduce activation of α7 subtype by interfering with the α7-mediated increase in intracellular calcium concentration
SLURP-1	Allosteric antagonist of α7 subtype
	Mediate inhibition of human α3β4, α4β4, α3β2 and α9α10 subtypes
SLURP-2	Reduce acetylcholine-evoked currents of oocytes expressing α4β2 and α3β2 subtypes
	Depending on its concentration, reduce or increase acetylcholine-evoked currents of α7 subtype

NACHO	When co-transfected with α7, increase acetylcholine-evoked currents and the amount of the subtype at the PM
	Increase α4β2 currents in heterologous system
	Its knockdown exhibits a reduction of α4β2-mediated currents in hippocampal neurons
UBXN2A	Interacts with α3 and α4 nAChR subunits
	Interferes with the ubiquitination of α3 subunits, thus protecting them from proteasomal degradation
Calnexin	Associates with unassembled subunits in the ER to prevent misfolding and increase lifetime
ERp57	Associate with unassembled δ subunit in the ER to prevent misfolding and increase lifetime
BiP	Associate with α subunit in the ER to prevent misfolding and increase lifetime
ARF6	Regulate internalization and biosynthesis of the M2 subtype
DRiP78	Regulate expression levels of M2 subtype at the PM

1.3. The cholinergic syndrome

1.3.1. Symptoms of the cholinergic syndrome

The cholinergic syndrome symptoms and severity are directly related to the route of exposure, the amount of organophosphate absorbed (section 1.1.5) and the function and expression of acetylcholine receptors in the nervous system (Figure 1.10) [42,154,155]. The peripheral symptoms include miosis, nausea, vomiting, diarrhoea, salivation, lacrimation, bradycardia, arrhythmias, bronchoconstriction, bronchosecretion, involuntary defaecation and urination relate to hyperactivation of the muscarinic receptors underpinning parasympathetic function (Figure 1.10) [42]. Nicotinic receptor overstimulation in the peripheral nervous system is responsible for twitching of facial muscles and tongue, tremors, fasciculations, weakness and paralysis of diaphragm and respiratory muscles (Figure 1.10) [42]. These signs are accompanied by effects in the central nervous system such as dizziness, tremor, confusion, ataxia, headache, fatigability, seizures, convulsions, twitching and coma (Figure 1.10) [156].

Death usually occurs due to respiratory failure resulting from a combination of central and peripheral effects, viz, paralysis of muscles essential for breathing, increase bronchial secretion and/or depression of respiratory centre in the brain [42,154,155].

Patients with severe acetylcholinesterase inhibition that survive the first days after poisoning might develop a disorder of the neuromuscular junctions termed the intermediate syndrome [157,158]. Symptoms of the intermediate syndrome include muscle weakness, decreased reflexes or respiratory insufficiency due to flaccid paralysis of the muscles essential for breathing [42].

1.3.2. Current treatment of the cholinergic syndrome

The management of acute organophosphate poisoning includes a combined pharmacological and non-pharmacological countermeasures [159-161]. The initial protocol consists of reanimation of the patient (in case of unconsciousness), artificial ventilation, administration of a first dose of atropine (Figure 1.12), decontamination, supply of fluids, monitoring and administration of a first

dose of oxime (Figure 1.12) [159]. Repeated doses of atropine every 5 minutes and pralidoxime/obidoxime every 30 minutes are administrated until the patient is stabilized (heart rate higher than 80 beats per minute and blood pressure higher than 80 mmHg) [162]. Haemodialysis can be performed to remove circulating organophosphates from the blood stream [163,164].

Once the patient is stable, a number of different strategies for atropinisation and oxime administration have been proposed. Typically, a reduced dose of atropine is dispensed every certain time until artificial ventilation is not required. During this time, oxime can be infused at different intervals [159,162]. The administration of benzodiazepines is recommended as first-line therapy in patients developing seizures [165].

Monitoring and clinical judgment is needed to prevent the recurrence of cholinergic crisis due to the release of organophosphates from fatty tissue stores (see section 1.1.5.3). In this case, the protocol might need to be repeated [159].

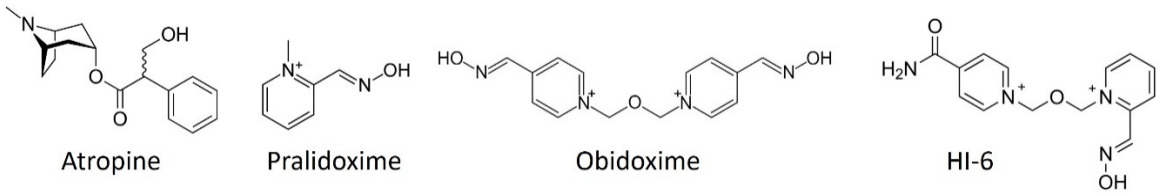

Figure 1.12. Chemical formula of antidotes used for human organophosphate poisoning. Atropine is an antagonist of muscarinic receptors. Pralidoxime, obidoxime and HI-6 are oxime drugs able to reactivate the organophosphate-inhibited acetylcholinesterase (Table 1.4).

1.3.2.1. Atropine

Atropine has been the core for the treatment of human organophosphate poisoning since the 1950s [166]. This is a competitive antagonist of muscarinic receptors able to cross the blood-brain-barrier and penetrate into the central nervous system [167]. The aim of this antidote is to reverse the cholinergic features due to the overstimulation of muscarinic receptors, in particular improving the cardiovascular function [161].

1.3.2.2. Oximes

Oximes are the second most important antidote in the treatment of organophosphate poisoning. These are highly nucleophilic chemicals able to attack the phosphorylated serine residue, breaking the bound between the neurotoxin and the catalytic amino acid and restoring the physiological function of the enzyme (Figure 1.6) [89].

Since their discovery, a large spectrum of oximes has been synthesised but only three of these have currently clinical use: pralidoxime, obidoxime and HI-6. Pralidoxime was the first oxime used as antidote for organophosphate intoxication in 1955 [168]. It is effective for the reactivation of

inhibited acetylcholinesterase by sarin or VX but not by soman or tabun. Obidoxime is the best acetylcholinesterase reactivator against intoxication with organophosphates used as pesticides but is not as effective against some nerve agents. In contrast, HI-6 is more efficient reactivating acetylcholinesterase from inhibition with certain nerve agents than from inhibitions with pesticides (Table 1.4) [162].

The reactivation process of the organophosphate-inhibited acetylcholinesterase by the oximes occurs in two steps; firstly the oxime is added to the conjugate, creating a transition state oxime-organophosphate-acetylcholinesterase, and secondly the release of the enzyme happens when the stabilization of the conjugate oxime-organophosphate occurs [169-172]. Apart from the rescue of acetylcholinesterase function, some oximes might have an important non-reactivating but direct effect in the recovery from organophosphate intoxication by their interaction with cholinergic receptors (see section 1.3.3.3) [173-178]. Although there is no evidence of this pharmacological function proved in humans, *in vitro* studies highlight the block of the cholinergic receptors by the presence of oximes in poisoned rodents, in guinea-pig diaphragm preparations as well as in human intercostal muscle preparations [172,179-183].

1.3.2.3. Benzodiazepines

The benzodiazepines, diazepam and midazolam, are anticonvulsant drugs used during the organophosphate poisoning treatment to reduce seizures [161,184]. The mode of action of benzodiazepines is by the allosteric modulation of the $GABA_A$ receptor to increase the inhibitory action of the GABAergic system in the central nervous system. Research studies in animals suggest that benzodiazepines reduce organophosphate-induced brain injury and help in preventing respiratory failures [185].

1.3.3. Limitations of the current treatment and alternatives

Although the atropine and oxime treatment has been used for the last 6 decades, its efficiency is controversial in many aspects [186]. Firstly, atropine is an antagonist of muscarinic receptors, meaning that overstimulation of the postsynaptic specialization can still occur throughout the nicotinic receptors. Furthermore, the optimal dose and protocol of atropinization has not been identified in humans and different recommendations are found in the literature varying in the dose and time of administration [187]. In this sense, a careful monitoring of cholinergic and anticholinergic toxicity symptoms is required in order to avoid excessive atropine dosing. The confounding anti-muscarinic side effects might result in tachycardia, hyperthermia, delirium, cardiovascular collapse and death [159,162]. Secondly, the acetylcholinesterase reactivation by oximes depends on several factors such as the type of organophosphate, the susceptibility of phosphorylated acetylcholinesterase to the nucleophilic attack, the velocity of aging reaction

between organophosphate and acetylcholinesterase [188,189]. In addition, oximes have poor blood-brain-barrier penetration and are inefficient at reactivating aged enzymes [189,190] .

In the last years, new therapies have been focused on the discovery of novel acetylcholinesterase reactivators, catalytic and non-catalytic bioscavengers, nicotinic receptor antagonists and false transmitters (Table 1.8).

1.3.3.1. Novel acetylcholinesterase reactivators

In the past 60 years, several thousand acetylcholinesterase reactivators have been synthesized including charged and non-charged compounds, mono- and bispyridinium oximes, oximes with different substitutes and more recently non-oxime reactivators [189,190]. Apart from being safe for human use, these compounds need to cover three main requisites to serve as antidote for human organophosphate poisoning. These include increased reactivation efficacy, broader spectrum of organophosphate mitigation and improved blood-brain-barrier penetration [190].

Among these compounds, the oxime K203 was initially considered as a universal reactivator for nerve agent inhibition in *in vitro* assays [191]. However, *in vivo* experiments demonstrated a moderate reactivation of tabun-, sarin-, and VX- inhibited acetylcholinesterase (Table 1.8) [191,192]. The oxime RS194B was also considered a promising antidote due the beneficial effect of post-exposure therapy of organophosphate poisoned mice with paraoxon, sarin and VX [193]. Nevertheless, it had no effect in soman or tabun exposed animals (Table 1.8) [194]. Finally, the non-oxime, antimalarial drug amodiaquine and its analogue ADOC demonstrated a superior reactivation compared to pralidoxime for paraoxon-, sarin- and DFP- inhibited human acetylcholinesterase but limited reactivation after VX inhibition (Table 1.8) [195,196].

1.3.3.2. Bioscavengers

Bioscavengers are enzymes, antibodies or reactive proteins that bind to the organophosphates in the blood stream to prevent them inhibiting acetylcholinesterase in the peripheral and central nervous system (section 1.1.5.3) [32,197]. These proteins can be divided into two groups: stoichiometric bioscavengers, that bind organophosphates in a 1:1 ratio; and catalytic bioscavengers, that degrade organophosphates into non-toxic compounds via a turnover process [198].

Stoichiometric bioscavengers, such as human acetylcholinesterase and butyrylcholinesterases, provided significant protection against organophosphate poisoning when they are administrated as a pre-treatment or post-treatment in different animal models [197,199]. However, the stoichiometric neutralization of organophosphates requires the administration of large doses of scavenger that is not cost-efficient and might be associated with other complications such as immunogenicity [32]. In contrast, catalytic bioscavengers with high specificity and turnover ratio

could degrade large amounts of organophosphate with a low dose of antidote. Among them, the most promising are derivatives of phosphotriesterases and paraoxonase-1 [200]. These enzymes hydrolyse V and G series of compounds and have protective effects against VX poisoning in guinea pigs [201]. Furthermore, the administration of paraoxonase-1 by gene therapy in mice offers a prophylactic protection against tabun, sarin, cyclosarin or soman intoxication (Table 1.8) [202].

Table 1.8. Summary of putative therapies for the treatment of organophosphate poisoning. The *in vitro* effect of acetylcholinesterase reactivators is compared with the reactivation potency of either obidoxime or pralidoxime (Table 1.4). The *in vitro* effect of false transmitters is referred to the corresponding acetylated compound. *In vivo* effects refer to a significant improvement of the symptomatology and/or survival rate when combined with atropine (acetylcholinesterase reactivators) or the classical therapy (bioscavengers, nicotinic antagonists and false transmitters). AChE: acetylcholinesterase. ADQ: amodiaquine. BuChE: Butyrylcholinesterase. PON-1: paraoxonase-1. MECh: monoethylcholine. DECh: diethylcholine.

Category	Antidote	*In vitro* effect	*In vivo* effect	Ref
AChE reactivator	K203	Universal reactivator after nerve agent AChE inhibition	Moderate effect against tabun, sarin, and VX poisoning in rats	191,203
	RS194B	Weak reactivator of paraoxon-, sarin-, cyclosarin-, VX- and tabun-inhibited AChE	Beneficial effect after paraoxon, sarin and VX poisoning in mice No effect after soman or tabun intoxication in mice	193,194
	ADQ ADOC	Increased reactivation of paraoxon-, sarin- and DFP- inhibited AChE Limited reactivation after VX inhibition	n.a.	195,196
Bioscavenger	BuChE		Beneficial effects against sarin, soman and VX in rats, mice, guinea pigs, pigs and monkeys. Prophylactic effect against VX and soman in guinea pigs and monkeys	204-206
	PON-1	Hydrolyse sarin, cyclosarin, tabun and soman	Beneficial effects against VX poisoning in guinea pigs Prophylactic effect against tabun, sarin, cyclosarin and soman in mice	200-202
Nicotinic antagonist	MB327	Non-competitive open channel blocker	Beneficial effect against sarin, soman and tabun intoxication in guinea pigs	183,207-210
	MB399	Non-competitive open channel blocker	Beneficial effect against sarin, soman and tabun intoxication in guinea pigs	
False transmitter	MECh	Partial agonist of M1 and M3 Partial agonist of muscle-type	Improves the survival rate of mice intoxicated with DFP and diazinon	211,212
	DECh	Partial agonist of M1 and M3 No effect on nicotinic receptors	n.a.	

1.3.3.3. Nicotinic receptor antagonists

Nicotinic receptor antagonists seem a logic antidote to manage the cholinergic toxicity of organophosphates, alike the use of the muscarinic antagonist atropine [149,213,214]. However, the

current therapy does not cover an approach for the overstimulation caused by nicotinic receptors. This is mainly due to the high toxicity caused by the complete inhibition of the nicotinic signalling (see section 1.2.5.1) [149,213]. In this sense, antagonists of nicotinic receptors need to cover two main requisites to be considered as organophosphate antidote: have tolerable physiological effects on cholinergic synapses at therapeutically relevant concentration and display partial inhibition of the receptor function when the concentration of acetylcholine is built up at the synapse to allow the maintenance of a minimum post-synaptic function [149,213]. According to these criteria, non-competitive antagonists could be the most suitable option. Among them, the bispyridinium compound MB327 and its dimethanesulfonate salt MB399 (commonly named as MB327 both) have been highlighted as the most promising non-competitive antagonist of nicotinic receptors in the treatment of organophosphate poisoning. Despite their high toxicity, the treatment with either MB327 or MB399 combined with the classical therapy improves the neuromuscular transmission and survival rate of guinea pigs after poisoning with sarin, soman or tabun (Table 1.8) [183,207-210].

1.3.3.4. False transmitters

False transmitters are analogues of acetylcholine that mimic its synthesis and function in the synapse but with reduced agonist effect on acetylcholine receptors. In this sense, false transmitters are able to decrease cholinergic transmission in physiological conditions [215], therefore they might have beneficial effects in the treatment of organophosphate poisoning by reducing the overstimulation caused by nicotinic receptors.

Monoethylcholine and diethylcholine are choline analogues that can be transported into the presynaptic terminal, acetylated, loaded into vesicles and released to the synaptic cleft or neuromuscular junction to activate receptors [216]. Acetylmonoethylcholine is a partial agonist of the muscle-type nicotinic receptor and the M1 and M3 subtypes of muscarinic receptors [211]. In contrast, acetyldiethylcholine partially activates the M1 and M3 muscarinic receptors but has no effect on nicotinic receptors (Table 1.8) [211]. Administration of either monoethylcholine or diethylcholine improves the neuromuscular junction function of soman poisoned hemi-diaphragm preparation [211]. Furthermore, the treatment with monoethylcholine improves the survival rate of mice intoxicated with DFP and diazinon (Table 1.8) [212]. This postulates these drugs as potential alternatives to treat organophosphate poisoning.

1.4. Experimental models for organophosphate poisoning investigation

The discovery of alternative therapies for organophosphate poisoning relies on the use of experimental models. These models include kinetic analysis of acetylcholinesterase activity,

electrophysiological recordings of cell cultures and/or organ preparations and toxicological assays in different vertebrate and/or invertebrate model organisms.

1.4.1. Kinetic analysis of acetylcholinesterase activity

The reactivating potency of novel oximes as well as the inhibitory potency of organophosphates are researched by the determination of acetylcholinesterase activity under specific conditions [217]. According to the 3Rs principles for the protection of animals used for scientific purposes, this should be the first step in the evaluation of new reactivators as antidotes against poisoning [218].

Human acetylcholinesterase from erythrocyte membranes is frequently used as source of enzyme. However, other blood and brain samples can be used from other species such as *Torpedo californica*, mice, rat or guinea pig [217]. The quantification of acetylcholinesterase activity is determined by the spectrophotometric Ellman's assay in which the enzyme is mixed with acetylthiocholine and DNTB [219]. Acetylcholinesterase hydrolyses acetylthiocholine into thiocholine and acetic acid. The increase in absorbance over time at 412 nm, due to the reaction between thiocholine and DNTB which produces the yellow compound 5-thio-2-nitrobenzoic acid, allows the determination of acetylcholinesterase activity using the equation in Figure 1.13 [219]. This assay is additionally used for diagnosis and therapeutic monitoring of patients poisoned with organophosphates [220,221].

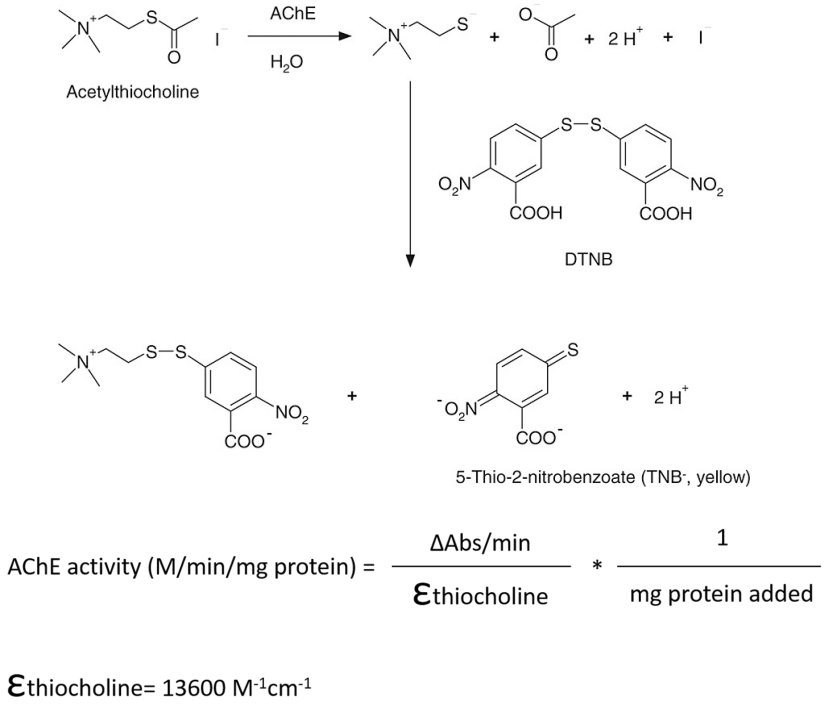

Figure 1.13. Reactions of Ellman assay for the determination of acetylcholinesterase activity [217].

Organophosphates compete with acetylthiocholine for the catalytic site of the enzyme, reducing its capacity of hydrolyse acetylthiocholine and therefore the absorbance over time. The reduction

is more pronounced in increasing concentrations of organophosphates. Therefore, the determination of absorbance over time at different concentrations of these neurotoxins allows the calculation of the biomolecular inhibition rate constant K_i (Table 1.4) [217,222]. After the complete inhibition of the enzyme activity, oxime-mediated (K_r) and spontaneous (K_s) reactivation can be determined by the increase in absorbance over time with or without a previous incubation step with the reactivator, respectively (Table 1.4). This step consists of the addition of a fixed oxime concentration during a specific time. Removing the excess of organophosphate before performing the Ellman's assay is critical in order to avoid the re-inhibition of the reactivated acetylcholinesterase [217]. The percentage of acetylcholinesterase reactivation is calculated according to the formula in Equation 1.1.

$$\%R = (1 - [(a_o - a_r)/(a_o - a_i)])*100$$

Equation 1.1. Percentage of acetylcholinesterase reactivation. a_o is activity of intact enzyme, a_i is activity of inhibited enzyme and a_r is activity of reactivated enzyme [223].

1.4.2. Cell cultures

The effect of novel antidotes on acetylcholine receptors can be quantified by either electrophysiological patch clamp recordings [224,225] or fluorescence-based methods for detecting intracellular calcium changes [211,226,227] in cell culture lines expressing different subtypes of nicotinic and/or muscarinic receptors. This is frequently the first step in the evaluation of antidotes targeting acetylcholine receptors such as nicotinic receptor antagonists or false transmitters. The most common cell lines are summarized in Table 1.9.

Table 1.9. Cell cultures used as experimental tool for investigation of alternative antidotes for organophosphate poisoning. In order to ensure single stimulation of either nicotinic or muscarinic receptors in cell lines expressing both, pre-treatment with atropine (to block muscarinic receptors) or tubocurarine (to block nicotinic receptors) is frequently used before physiological determination of the antidote function.

Cell culture	nAChR subunits	mAChR subtype	Parental cell line	Ref
CN21	α1, γ, α1, β1, δ, ε	M3	TE671 human rhabdomyosarcoma	228,229
SHSY5Y	α3, α5, α7, β2, β4	M1, M2	Human neuroblastoma	230-232
CHO-CHRM1	-	M1	Chinese hamster ovary	233
CHO-M3 (CHRM3)	-	M3	Chinese hamster ovary	233
CHO/RIC-3/hα7-nAChR cell line	α7	-	Chinese hamster ovary transfected with human cDNA for α7 and *ric-3*	224,225

For investigating false transmitters and acetylcholinesterase reactivators on acetylcholine receptors, different concentrations are applied to the cell culture line and the physiological response is quantified by any of the methods mentioned above. This allows the determination of

EC_{50} values from dose-response curves that are compared with the EC_{50} value of acetylcholine as control [211,234]. In contrast, for investigation of receptor antagonists, the response to different concentrations of the test compound is additionally measured in the presence of acetylcholine in order to determine the inhibitory response [226,227].

1.4.3. Isolated tissue preparations

The *ex vivo* phrenic nerve hemidiaphragm tissue isolated from rats, mice or guinea pigs is the most frequent preparation utilized to evaluate the recovery potency of novel antidotes on the skeletal muscle function. This additionally allows the determination of acetylcholinesterase activity in the homogenized tissue at the conclusion of the assay [178,183,211,227,235]. This experiment serves as an intermediate step between the *in vitro* and *in vivo* evaluation of antidotes.

The diaphragm contraction is measured after being stimulated by controlled tetanic pulses delivered via the phrenic nerve at fixed times. Muscle contractions are recorded before adding the organophosphate, during the organophosphate exposure, during the test antidote incubation and during a recovery period following a washout step (Figure 1.14). The concentration and/or incubation time with the organophosphate can be varied to consider the inhibition and aging kinetics of the neurotoxin's effect (Table 1.4). An additional washout step can be performed after the organophosphate exposure to remove the excess of chemical prior to measuring the recovery of the muscle function [178,183,211,227,235].

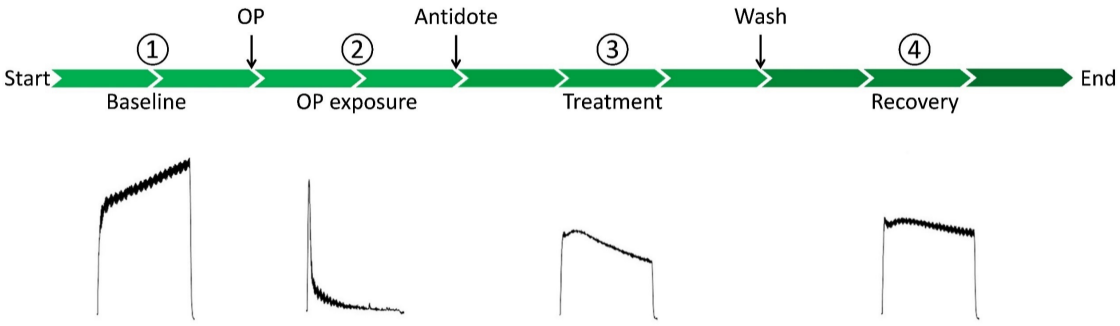

Figure 1.14. Experimental protocol and representative tetanic contractions for phrenic nerve hemidiaphragm preparations. 1. The baseline of diaphragm contraction is recorded. This defines the control tetanic contraction under the testing conditions. The tetanic stimulation of the phrenic nerve provokes the release of acetylcholine to the neuromuscular junction and the contraction of muscle fibres due to its action on muscle type nicotinic receptors. 2. Tetanic contraction is investigated after the organophosphate perfusion. Diaphragm muscles are not able to sustain tetanic contraction due to the overstimulation of the fibres and desensitisation of voltage-gated sodium channels. 3. Tetanic contraction is recorded during the treatment step after perfusion of the antidote. If successful for organophosphate treatment, the antidote exposure provokes the recovery of tetanic contraction in the diaphragm muscle. This is achieved by the decrease of cholinergic stimulation at the muscle fibres that can be accomplished by different mechanisms (sections 1.3.1 and 1.3.2). 4. Tetanic contraction during recovery after washing out excess of organophosphate and antidote. The recovery of diaphragm muscle contraction is observed by the progressive clearance of acetylcholine and the recovery from inactivation of sodium channels at the fibres in case of acetylcholinesterase is not aged by the organophosphate. If this occurs, the recording of tetanic contraction would be alike tetanus of step 2. Adapted from [211].

During organophosphate exposure, the muscle fibres are not able to sustain a tetanic contraction due to the depolarisation block and the desensitisation of voltage-gated sodium channels caused by the increased accumulation of acetylcholine. The efficacy of antidotes is then assessed by the ability to recover the tetanic contraction of muscle fibres during the treatment step (Figure 1.14).

1.4.4. *In vivo* models

The testing of new therapies in *in vivo* animal models is required in order to assess the efficiency of antidotes against organophosphate poisoning in a whole organism where additional toxicokinetic aspects that may confound efficacy of toxin and/or antidote can be considered. For this, mammalian and non-mammalian model organisms are utilized. The acute organophosphate toxicity that mammalian models exhibit closely resembles signs and symptoms exhibited by humans. These *in vivo* assays are also required in order to demonstrate functional recovery of peripheral and central cholinergic transmission in the presence of the test antidote. However, due to the severity of the experimental protocol for the mammalian model and therefore the associated ethical considerations, this step is a bottleneck in the discovery of more efficient therapies [218]. In addition, these methods do not allow a high-throughput drug discovery platform in a whole organism scenario. For these reasons, non-mammalian model organisms are being increasingly recognized as alternative tools to research organophosphate poisoning and antidotes (Figure 1.15).

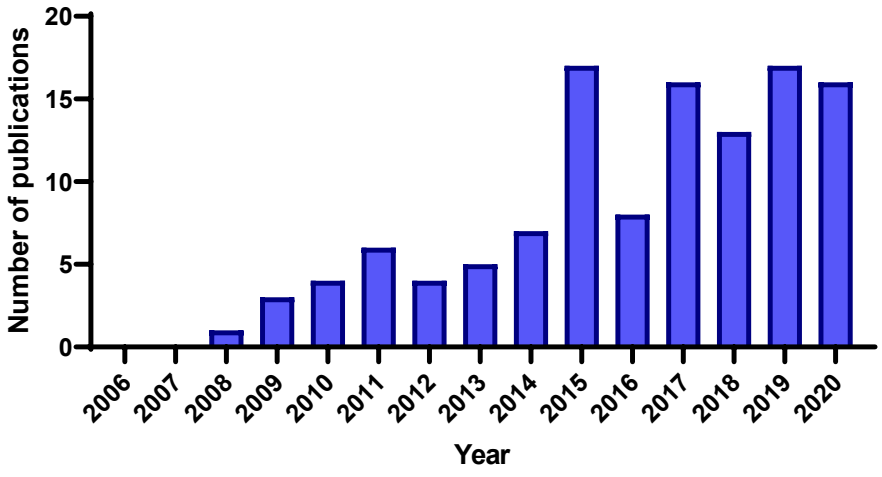

Figure 1.15. Number of publications where non-mammalian organisms have been used to model organophosphate toxicity in the past 15 years. Non-mammalian models include the zebrafish *Danio rerio*, the freshwater planarians *Schmidtea mediterranea* and *Dugesia japonica* and the non-parasitic nematode *Caenorhabditis elegans*. Data obtained from PubMed.

1.4.4.1. Mammalian model organisms

Different mammalian species have been used as model organisms for organophosphate investigation ranging from small rodents such as rats, mice and guinea pigs to large animals such as pigs and non-human primates [236]. In these models, the LD_{50} value for different

organophosphates correlates with the IC_{50} value for acetylcholinesterase inhibition from brain and blood samples from the same species [237,238]. This is consistent with the organophosphate toxicity in those models being triggered by the inhibition of the enzyme function [236].

The classical experiment for assessing the efficiency of novel therapies in mammalian models is the investigation of LD_{50} values after organophosphate intoxication in the presence of the new antidote and, usually, in combination with the standard therapy. Four or five different organophosphate doses are administrated by subcutaneous, intravenous, intramuscular or intraperitoneal injection (section 1.1.5.1). Standard antidotes with and without the test compound are administrated at a dose corresponding to their 10 – 20% LD_{50} value a few minutes before or after organophosphate exposure. Poisoning symptoms are monitored for a defined time-period and LD_{50} calculated using probit analysis of death occurring usually 3, 6 or 24 hours after organophosphate administration. This protocol additionally allows the evaluation of the new therapy against specific symptoms such as seizures or respiratory frequency [179,239-241]. LD_{50} value for the new antidote needs to be previously quantified by exposing animals to different concentrations of the test compound and analysis mortality after a certain time-period [242].

Another standard method is the comparison of Kaplan-Meier survival curves after a fixed dose challenge of organophosphate in the presence or absence of the new antidote, frequently combined with the standard therapy [243]. A fixed dose of organophosphate between LD_{50} and LD_{75} is administrated by any of the routes mentioned above, followed by the administration of the test compound at different doses or saline solution for control group. Poisoning symptoms are monitored, and Kaplan-Meier curves are fitted by scoring the mortality rate at different end-point times in each treatment condition [244]

1.4.4.2. Non-mammalian model organisms

Non-mammalian models have emerged as alternative platforms to research organophosphate toxicity and antidotes. The four main animals included in this group are the zebrafish *Danio rerio* [245,246], the freshwater planarians *Schmidtea mediterranea* and *Dugesia japonica* [247,248] and the non-parasitic nematode *Caenorhabditis elegans* [249,250]. These species are genetically tractable models, easy to maintain and reproduce, with short life cycles and large number of offspring. The molecular and cellular basis of the cholinergic pathway in these three model organisms is highly conserved to each other and to the mammalian pathway. In particular, and in contrast to insect models, this includes the control and organization of the neuromuscular junction by acetylcholine signalling [246,247,251]. Usefully, these models exhibit well-characterized cholinergic-dependent behaviours that can be readily scored in high-throughput screening protocols. The quantification of these behaviours can be automated for improving the turnover of the screening [252-254].

In addition, experimentation with the freshwater planarian, the non-parasitic nematode, or the zebrafish larvae during the first 120 hours post-fertilization faithfully complies with the 3Rs principles of animal experimental techniques (replacement, reduction and refinement) [255]. These are not defined as protected animals for scientific purpose according to the EU Directive 2010/63/EU, hence, they do not fall into the regulatory frameworks dealing with experimentation on animals [218]

The most common experimental protocol to assess organophosphate toxicity in these models is the quantification of different cholinergic-dependent behaviours for a defined time-period. This allows the calculation of EC_{50} values using logarithmical analysis. LD_{50} values or Kaplan-Meier curves can also be calculated in survival assays.

Some of the behaviours analysed in zebrafish are locomotory responses and the contraction of axial muscle fibres (length of the trunk). The inhibition of these behaviours by organophosphates are dose-depend and well correlated to organophosphate intoxication and *in vitro* acetylcholinesterase inhibition in the fish [246,256]. In addition, animals co-exposed to the organophosphate chlorpyrifos-oxon and pralidoxime exhibit a partial improvement of the locomotory behaviours compared to non-oxime exposed animals [246].

Mobility and regeneration assays are the most frequently used to investigate organophosphate toxicity in planaria. Impairments in these phenotypes have been correlated with acetylcholinesterase function by *in vitro* assays [247,248,257]. Although oximes have not been tested in planarian models, the exposure to certain phosphotriesterases as bioscavengers decreases toxicity in animals exposed to organophosphates [248,257].

Finally, the suitability of the nematode *C. elegans* as model organism for organophosphate toxicity and antidotes will be reviewed in the next sections and is assessed in this thesis. The transparency, small size, ease of cultivation, large brood size, genetically identical offspring and quick life cycle are some of the features that make this organism model a perfect candidate for a wide range of eukaryotic biological and pharmacological research. Furthermore, *C. elegans* has easily quantifiable behaviours that can be linked with specific molecular pathways. It makes the nematodes a suitable organism model for drug testing.

1.5. *Caenorhabditis elegans* as model organism for organophosphate toxicity

C. elegans is a round, transparent, free-living nematode introduced to the scientific community in 1963 by Sydney Brenner [258]. The strain isolated was called Bristol N2 and is considered the wild type strain usually maintained on agar medium plates containing a patch of *Escherichia coli* OP50 strain as source of food.

1.5.1. Anatomy

Adult nematodes are composed of a cuticle that protects them from the external environment, an epidermis that secretes the cuticle, a musculature that controls different movements and digestive, nervous and reproductive systems. The internal organs of the worm are submerged into the interstitial fluid contained by the body cavity or pseudocoelom.

Nematodes are hermaphrodites (XX) but males (X0) can be generated by a spontaneous process of non-disjunction of the X chromosome with a low frequency (~0.1%). However, the rate of male production can be increased in the lab by controlling the embryogenesis conditions to induce either temperature or population stress.

1.5.2. Life cycle

The life cycle depends on the temperature and lasts from 3 days incubated at 25°C until 4 days at 15°C (Figure 1.16). Briefly, adults lay about 250 genetically identical eggs that hatch into incompletely developed L1 larval stages. The larva feeds on environmental bacteria and develops into three more stages (L1-L4) before reaching the adult stage. A moult marks the end of each larval stage when the old cuticle is shed and a new one is synthetized. During this period, nematodes enter a brief lethargy, which is marked by decreased locomotory and feeding activity.

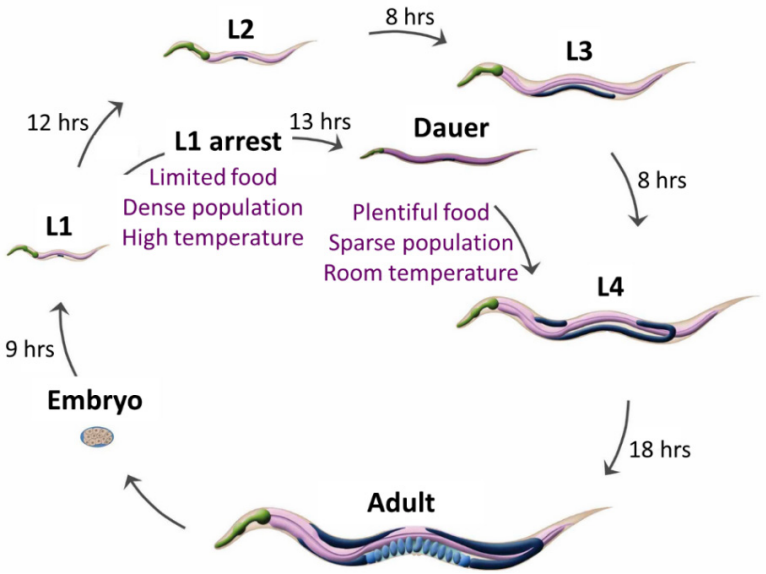

Figure 1.16. *C. elegans* cycle of life. Adult-laid embryos hatch and develop into four larval stages (L1-L4) before being reproductive. The larval stages are separated by the moults where the old cuticle is removed and a new one in synthetized. L1 arrest and dauer are highly resistant stages that develop from L1 in stress environmental conditions. The time indicated between stages corresponds to nematodes growing at 20ºC. Figure taken from www.wormatlas.org.

In harsh environmental conditions, larvae of *C. elegans* are able to arrest development for a longer survival either in L1 stage, known as "L1 arrest" or "L1 diapause", or after the second moult leading to a new larval stage known as dauer. The L1 arrested nematodes are morphologically

identical to L1 but with increased resistance to stress conditions. Dauer nematodes are a different larval stage showing a stronger cuticle that surrounds the whole animal. At these developmental stages, nematodes are able to survive for several months. When the environmental conditions are favourable, dauer larval stage moults and continues development into L4 stage.

1.5.3. Nervous system

The nervous system in hermaphrodite nematodes consists of 302 neurons and 56 glial cells, which together form about 6,300 chemical synapses and 1,400 neuromuscular junctions. This neuronal wiring diagram has been determined by mapping the neurons and characterizing the major chemical interactions between them [259-261].

Although *C. elegans* nervous system lacks the anatomical complexity of higher organisms, the physiological and genetic organization shows a high degree of similarity with the mammalian nervous system. In fact, *C. elegans* exhibits neuronal targets for several drugs and neurotoxins affecting the human neurophysiology, such as fluoxetine, reserpine, nicotine and organophosphates [262-265].

Chemical, thermal, mechanical and proprioceptive cues are detected by sensory neurons which send the information to motor neurons that execute the behavioural outcomes. Frequently, interneurons relay the information between sensory and motor neurons [259,260]. Acetylcholine, GABA, glutamate, serotonin, dopamine, tyramine, octopamine and several neurogenic peptides have been identified in *C. elegans* [266]. The formation, trafficking and release of synaptic vesicles are carried out by analogous processes to those observed in mammals [267].

Specifically, acetylcholine biosynthesis, release, signalling and degradation is carried out by equivalent molecular pathways, controlled by *C. elegans* genes orthologues of mammalian genes (section 1.2.4 and 1.2.5) (Table 1.10 and Figure 1.8).

Table 1.10. *H. sapiens* and *C. elegans* genes encoding key proteins in the cholinergic pathway. *C. elegans* genes are orthologues to the respective human gene (Figure 1.8). *C. elegans* genes encoding nicotinic and muscarinic receptors are displayed in Table 1.12 and Table 1.13, respectively. ChAT: choline acetyltransferase; VAChT: vesicular acetylcholine transporter; mAChR: muscarinic acetylcholine receptor; AChE: acetylcholinesterase; ChT: choline transporter. Data were taken from [268,269].

Protein	*H. sapiens* gene	*C. elegans* gene
ChAT	*CHAT*	*cha-1*
VAChT	*SLC18A3*	*unc-17*
mAChR	*CHRM1, CHRM2, CHRM3, CHRM4, CHRM5*	*gar-1, gar-2, gar-3*
AChE	*ACHE*	*ace-1, ace-2, ace-3, ace-4*
ChT	*SLC5A7*	*cho-1*

1.5.4. Acetylcholine biosynthesis and synaptic release

Acetylcholine is synthetized in the cytoplasm of the presynaptic terminal by the choline acetyl transferase which is encoded by *cha-1* gene (Table 1.10). This enzyme transfers an acetyl group from acetyl-CoA to choline [251]. Choline for acetylcholine synthesis is supplied by catabolism of phosphatidylcholine and recycling of choline transported from the synaptic cleft by a choline transporter (CHO-1) after acetylcholinesterase-dependent degradation of acetylcholine [270]. The vesicular acetylcholine transporter, encoded by the gene *unc-17*, loads acetylcholine into vesicles that are released from the presynaptic terminal by a conserved machinery of proteins [251,267].

The acetylcholine released at the synaptic cleft or neuromuscular junction is removed by either diffusion or hydrolysis. Acetylcholinesterase, encoded by four genes (*ace-1*; *ace-2*; *ace-3* and *ace-4*), catalyses the hydrolysis of acetylcholine into choline and acetate (section 1.4.5). Finally, a proportion of the acetylcholine at the synaptic cleft or neuromuscular junction binds to the receptors at the postsynaptic specialization for signal transduction (section 1.4.6).

1.5.5. Acetylcholinesterase

Four genes encode acetylcholinesterases in the nematode *C. elegans*: *ace-1*, *ace-2*, *ace-3* and *ace-4*, however, no activity has been detected for ACE-4 protein. The three acetylcholinesterase genes encoding functional enzymes co-expressed in the pharyngeal muscle pm5. However, they exhibit no overlapping expression in the rest of the animal (Table 1.11) [271]. Single mutant nematodes lacking ACE-1 or ACE-2 proteins have a modest alteration in locomotion while double mutants show a severely uncoordinated locomotion (section 1.4.7.1) [272,273]. Mutants deficient in the acetylcholinesterase ACE-3 do not exhibit any phenotypic feature and the triple mutant *ace-1;ace-2;ace-3* is lethal. This indicates that ACE-1 and ACE-2 represent the major core of acetylcholinesterase activity in the worm. Nevertheless, ACE-3 supports acetylcholinesterase activity to allow the survival of the double mutant *ace-1;ace-2* [274].

ACE-1 is encoded by the *ace-1* gene, composed by ten exons and expressed mainly in muscles: body wall, pm5 pharyngeal and anal muscle cells as well as head mesoderm cells (Table 1.11) [275]. Interestingly, the C-terminal encoded by exons 9 and 10 presents a high similarity to the T-type C-terminal of the vertebrate acetylcholinesterases [276,277]. Both, *C. elegans* ACE-1 and vertebrate $AChE_T$, present a strong conserved tryptophan amphiphilic tetramerization (WAT) domain consisting of seven aromatic residues that facilitates the formation of tetramers and the association with the Proline Rich Attachment Domain of the membrane proteins as shown in vertebrates (Figure 1.3 and Table 1.11) [264].

ACE-2 consists of nine exons mainly expressed in neurons, specifically in sensory endings, cephalic neurons around the pharyngeal bulb, neurons in anal ganglia, hypodermal cells and pharyngeal muscle cells (Table 1.11) [271,275]. In contrast, ACE-3 consists of eight exons expressed exclusively in pharyngeal muscle cells as well as in two medial canal-associated neurons (Table 1.11) [271,275]. The final exons of both, *ace-2* and *ace-3* genes, encode a hydrophobic C-terminal, eventually associated into dimers linked to the membrane surface throughout a GPI anchor, homologous to the vertebrates $AChE_H$ type (Figure 1.3 and Table 1.11) [264].

ACE-3 accounts for only 5% of the total acetylcholinesterase activity in the nematode, exhibiting a higher affinity for butyrylcholine than for acetylcholine [264]. Furthermore, this enzyme is resistant to some inhibitors such as the carbamates eserine or aldicarb as well as the inhibitory ligands gallamine and propidium [278]. Interestingly, the expression level of *ace-3* gene is up-regulated in the presence of the organophosphate phoxim. As ACE-3 is not resistant to phoxim inhibition, it might indicate a possible function of this acetylcholinesterase in the detoxification process of the phoxim organophosphate poisoning [279].

Table 1.11. Summary of *C. elegans* acetylcholinesterase. Genomic and protein structures, isoforms, mode of anchoring to the membrane and expression of the four genes encoding acetylcholinesterase in the nematode. n.d. – not determined. For C. elegans anatomy and description refer to [280]. Data taken from [264,271].

Gene	Exons	Isoform	Quaternary structure	Membrane anchoring	Expression
ace-1	1-10	T	Tetramers	n.d.	Body wall muscle Pharyngeal muscle (pm5) Anal muscle
ace-2	1-9	H	Dimers	GPI	Sensorial projections Head neurons Anal ganglion neurons Hypodermal cells Pharyngeal muscle (pm5)
ace-3	1-8	H	Dimers	GPI	Pharyngeal muscle (pm3, pm4, pm5, pm7) Two medial canal-associated neurons
ace-4	1-11	n.d.	n.d.	n.d.	*ace-3* co-expression

Finally, *ace-4* gene is the first gene of the tandem formed by *ace-4* and *ace-3* genes, with 356 nucleotides between the stop codon of *ace-4* and the putative start codon of *ace-3*. ACE-4 corresponds to a non-catalytic form of acetylcholinesterase due to a replacement of E200Q next to the catalytic serine at the active site. Interestingly, vertebrate acetylcholinesterases expressing a similar missense mutation (E199Q) introduced by directed mutagenesis present only 2% of the initial catalytic activity [281]. The high identity of these two enzymes and the lack of acetylcholinesterase activity of ACE-4 might indicate a duplication event of the gene *ace-3* to

generate *ace-4* [264]. Surprisingly, *ace-4* mRNA is undetectable suggesting the cleavage of the polycistronic operon occurs early after transcription [282].

Although the quaternary structure of *C. elegans* acetylcholinesterases is not available, the similarity between *C. elegans* and the vertebrate enzyme predicts an equivalent mechanism for acetylcholine hydrolysis and organophosphate inhibition (Figure 1.17) (sections 1.2.1 and 1.2.2). Indeed, inhibition of acetylcholinesterase by organophosphates triggers impairments in the phenotype of *C. elegans* that are directly related with the physiological function of acetylcholine as neurotransmitter and the differential expression of cholinergic receptors.

A

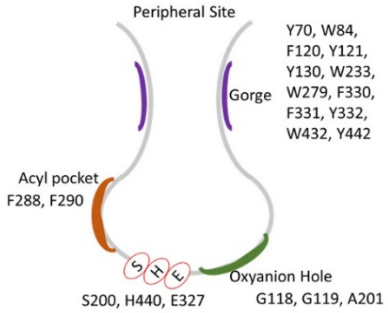

B

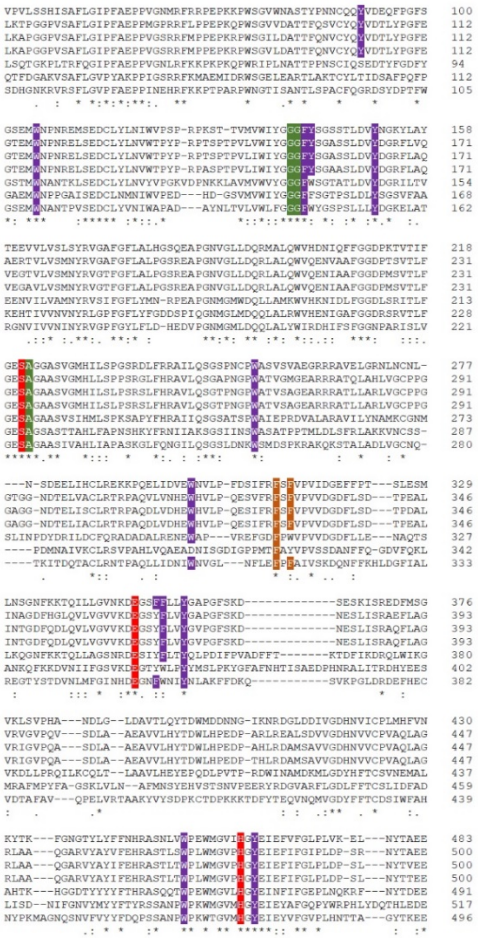

C

	Torpedo californica	*Homo sapiens*	*Rattus norvegicus*	*Mus musculus*
ACE-1	41.18	40.75	42.01	42.01
ACE-2	34.22	32.94	33.8	33.45
ACE-3	34.36	33.22	33.69	34.04

Figure 1.17. *C. elegans* acetylcholinesterase protein compared to acetylcholinesterase sequences of human and other model organisms. A) Schematic representation of acetylcholinesterase active site (Figure 1.4). Amino acids in the gorge guide the acetylcholine molecule into the active site and amino acids in both, the oxyanion hole and acyl pocket, orientate the molecule in front of the catalytic triad (serine, histidine and glutamic acid). The conserved amino acids in the different parts of the active site are represented next to them and correspond to *Torpedo californica* acetylcholinesterase sequence (Figure 1.4) [81]. B) Protein alignment of *Torpedo californica* (P04058), *Homo sapiens* (NP_001289550.1), *Rattus norvegicus* (NP_742006.1), *Mus musculus* (NP_001276939.1) and *C. elegans* ACE-1 (NP_510660.1), ACE-2 (NP_491141.1) and ACE-3 (NP_496963.1). Accession numbers correspond to ncbi database. Conserved amino acids from the gorge, acyl pocket, oxyanion hole and catalytic triad are highlighted in purple, orange, green and red, respectively. The majority of them are conserved between *C. elegans* and other organism models acetylcholinesterases. C) Percentage of identity between *C. elegans* and vertebrates acetylcholinesterase proteins.

1.5.6. Acetylcholine receptors

Ionotropic and metabotropic receptors are involved in the acetylcholine signalling in *C. elegans* [283-288]. Ionotropic receptors are members of the Cys-loop superfamily of ligand-gated ion channels responsible for the fast-cholinergic transmission in the postsynaptic neurons and muscles [287-289].

Metabotropic receptors are G-protein coupled receptors that are able to extend neurotransmission into multiple intracellular signalling pathways [290-292].

1.5.6.1. Ionotropic acetylcholine receptor

There are 34 subunits of ionotropic receptors in *C. elegans* differentially expressed in muscles and neurons. Among these, 30 genes encode for subunits that create acetylcholine-gated cation channels homologues to mammalian acetylcholine receptors while 4 genes encode for subunits that form acetylcholine-gated chloride channels allowing a cholinergic inhibitory transmission. These receptors exhibit more homology to serotonin-gated chloride channels than to acetylcholine-gated cation channels and are exclusively expressed in nematodes [293,294].

Similar to mammalian receptors (section 1.2.5), the combination of these subunits creates different subtypes that differ in their pharmacological and biophysical properties (Table 1.12).

- Acetylcholine-gated anion channels

The amino acid sequence of acetylcholine-gated chloride channel subunits (ACC-1, ACC-2, ACC-3 and ACC-4) exhibit conserved features of Cys-loop receptor subunits: large extracellular N-terminal that binds acetylcholine and four transmembrane domains that create the pore. However, neither the loops forming the ligand-binding pocket nor the adjacent cysteines in loop C of acetylcholine-gated cation channel subunits are conserved in anion channel subunits [294]. This suggests a different acetylcholine-binding site and might explain the unusual pharmacology (Table 1.12).

The subunits ACC-1 and ACC-2 can create the homomeric receptors ACC-1R and ACC-2R, respectively (Table 1.12). In addition, ACC-1 can create heteromeric receptors with ACC-3 and ACC-2 can create heteromeric receptors with ACC-4 when the subunits are heterologous expressed in *Xenopus* oocytes [294]. Expression of *acc-3* has not been observed in the nematode, therefore ACC-3-containing subtype is not considered to support any physiological function [261]. However, expression of *acc-4* gene is reported in all cholinergic neurons [261]. Since *Xenopus* oocytes co-expressing ACC-2 and ACC-4 are insensitive to acetylcholine, the insertion of ACC-4 into the ACC-2R receptor might create a mechanism to control the excitability of cholinergic neurons in the worm by presynaptic modulation of neurotransmitter release [261,294].

Table 1.12. Subunit composition, pharmacology and expression pattern of ionotropic acetylcholine receptor subtypes in *C. elegans*. ACC-1R and ACC-2R corresponds to acetylcholine-gated chloride channels. L-type, N-type, ACR-2R, EAT-2R and DEG-3R corresponds to acetylcholine-gated cation channels. Acetylcholine agonist potency is represented by the median effective concentration (EC_{50}) of the subtype receptor response measured by two-electrode voltage-clamp when the indicated subunits are expressed in *Xenopus* oocytes. The indicated auxiliary proteins were co-injected along with the corresponding subunits to assess pharmacology of the receptor subtype. Agonist dose-response curve parameters were determined by non-linear fitting of the Hill equation. Values are represented as mean ± standard deviation. A – agonist, AN – antagonist, NAM – negative allosteric modulator, OCB – open channel blocker, ACh – acetylcholine, Glu – glutamate, DA - dopamine, SN – sensory neuron, IN – interneuron, MN – motor neuron. For neurons terminology and description refer to [280]. Asterisk indicates partial action of the drug on the receptor.

Subtype	Subunit	Auxiliary	EC_{50} ACh (μM)	Pharmacology	Expression	Ref
ACC-1R	ACC-1	-	0.3 ± 0.0	Arecoline (A) D-tubocurarine (AN) Strychnine (AN)	VA, VB, VC (ACh MN) M1, M3 (Glu MN)	[294]
ACC-2R	ACC-2	-	9.5 ± 0.1	Arecoline (A) D-tubocurarine (AN) Strychnine (AN)	RIA, RIG, AIZ (Glu IN) URX, RIH (ACh IN)	[294]
L-type	UNC-36 UNC-38 UNC-29 LEV-1 LEV-8	RIC-3 UNC-50 UNC-74	26 ± 3.2	Levamisole (A) Nicotine (NAM)	Body wall muscle	[265]
N-type	ACR-16	RIC-3	31 ± 0.5	Nicotine (A)	ADE, CEP (DA SN) AVA, RIB, SIB (ACh IN) DB, SMD (ACh MN) Anal, body wall muscles	[265]
ACR-2R	UNC-63 UNC-38 ACR-12 ACR-2 ACR-3	RIC-3 UNC-50 UNC-74	14.1 ± 1.2	Mecamylamine (OCB) Nicotine (A)*	DA, DB, VA, VB (ACh MN)	[295]
EAT-2R	EAT-2	EAT-18	5.0 ± 0.0	Nicotine (A) D-tubocurarine (AN)	Pharyngeal muscle (pm4)	[296]
DEG-3R	DEG-3 DES-2	-	2900 ± 0.5	D-tubocurarine (AN) Strychnine (AN)	PVD (Glu IN) IL2 (ACh SN)	[297]

- Acetylcholine-gated cation channels

Acetylcholine-gated cation channel subunits exhibit conserved amino acid sequences and predicted transmembrane topology compared to vertebrate subunits. Furthermore, the key amino acids responsible for acetylcholine binding and receptor gating in higher organisms are also present in *C. elegans*. This implies structural and functional similarities between the nematode and the mammalian receptor (Figure 1.18).

30 genes of *C. elegans* have been identified to encode functional receptor subunits when expressed in oocytes; however, most of them have an unknown role in nervous system function and/or behaviour [283,298]. The subunits present in *C. elegans* (22 of which are α) can combine in a

homomeric or heteromeric manner defining the receptor function and pharmacology (Table 1.12) [121,299].

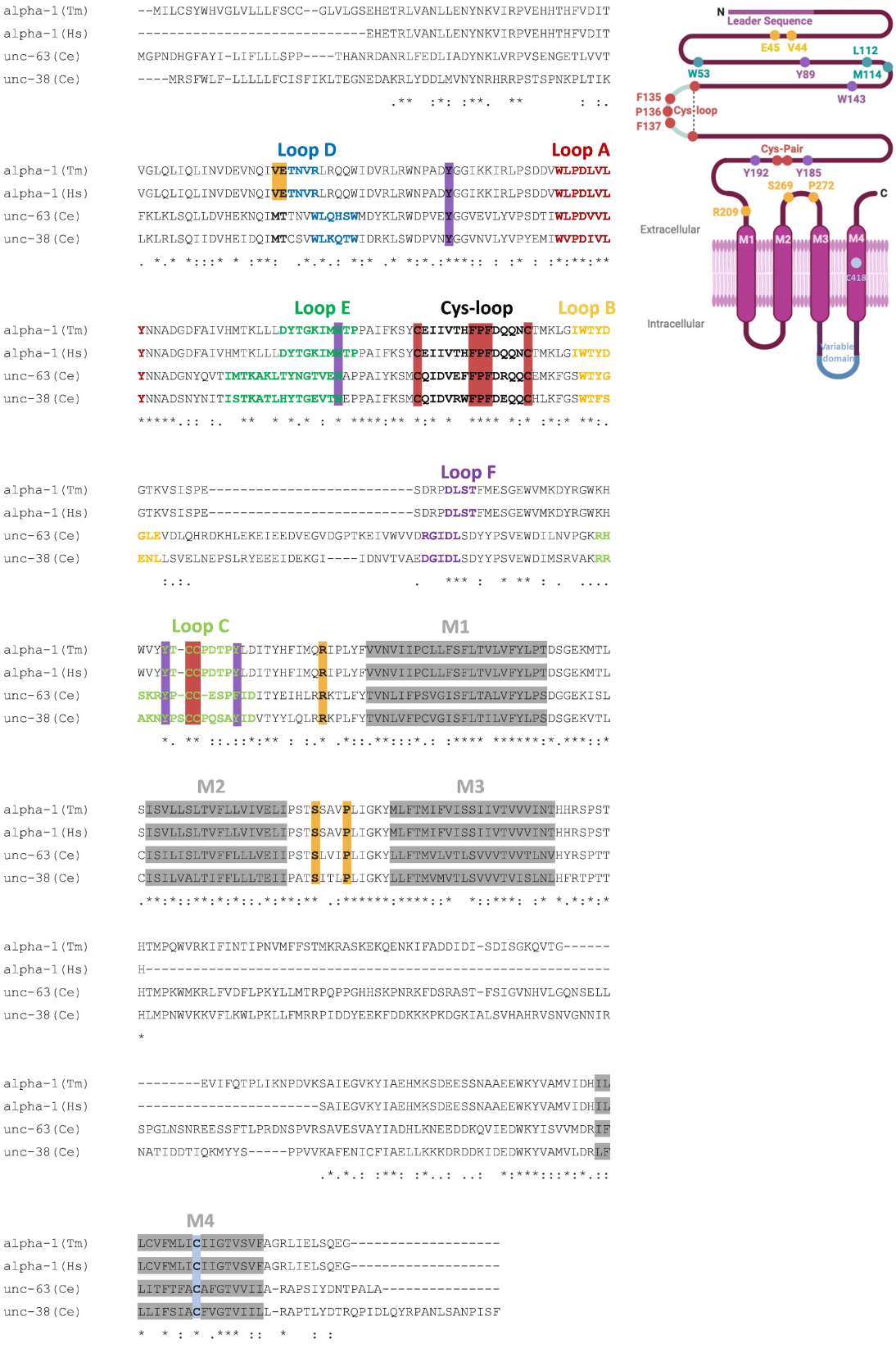

Figure 1.18. Protein alignment of vertebrate and *C. elegans* α subunit. Protein sequence of α1 subunit from *Torpedo marmorata* (Tm) and *Homo sapiens* (Hs) were used as representative for

vertebrate α subunits. Protein sequence of UNC-63 and UNC-38 were used as representative of α subunits in the nematode. Loop D, A, E, B, F and C involved in the agonist binding are represented by blue, red, green, yellow, violet and light green lettering, respectively. Black and bold letters indicate the Cys-loop. The four transmembrane domains are highlighted in grey. Red, purple, yellow and blue highlighted amino acids correspond to highly conserved residues at the vertebrate receptor involved in the nicotinic receptor function (Figure 1.9). These are conserved in the nematode subunits. Accession numbers are P02711.1 for *Torpedo marmorata* α1; NP_000070 for *Homo sapiens* α1; NP_491533.2 for *C. elegans* UNC-36; NP_491472.1 for *C. elegans* UNC-38 in ncbi database.

1.5.6.2. Metabotropic acetylcholine receptor

There are three genes encoding G protein-linked acetylcholine receptors in *C. elegans* (*gar-1*, *gar-2* and *gar-3*) (Table 1.13). These are alternatively spliced to generate eight distinct isoforms differentiated by the sequence of the third intracellular loop (i3) (section 1.2.5.2) [286,300-302]. Three isoforms are generated by alternative splicing of the *gar-1* and *gar-2* genes, respectively. Although GAR-1 and GAR-2 are rather similar, they present differences in the expression pattern and the pharmacological characteristics to each other (Table 1.13) [301,302]. However, the two isoforms (GAR-3a and GAR-3b) generated by alternative splicing of *gar-3* gene differ in the third intracellular loop (i3) being structurally and pharmacologically comparable to mammalian muscarinic receptors (section 1.2.5.2) [303]. Furthermore, expression of GAR-3 receptor in Chinese hamster ovary (CHO) demonstrated the activation of phospholipase C (similar to mammalian M1, M3 and M5 subtypes (Figure 1.11)) but the specific expression of the isoform GAR-3b couples both stimulation and inhibition of pathways modulating the intracellular cAMP level (similar to mammalian M2 and M4 subtypes(Figure 1.11)) [303,304].

Table 1.13. Pharmacology and expression pattern of metabotropic acetylcholine receptors in *C. elegans*. The gene and expression are indicated for the three genes encoding muscarinic receptors in *C. elegans*. Acetylcholine agonist potency is represented by the median effective concentration of the subtype receptor response measured by two-electrode voltage-clamp when the indicated isoform is expressed in Chinese hamster ovary cells. Agonist dose-response curve parameters were determined by non-linear fitting of the Hill equation. Values are represented as mean ± standard deviation. A – agonist, AN – antagonist, ACh – acetylcholine, Glu – glutamate, SN – sensory neuron, IN – interneuron, MN – motor neuron. Asterisk indicates male specific neuron. For neurons and muscles terminology and description refer to [280].

Subtype	Effector	EC50 ACh (μM)	Pharmacology	Expression	Ref
GAR-1	-	-	Atropine (AN)	PVM (ACh SN)	300
GAR-2	G_i	~ 0.035	-	AIY (ACh IN) HSN (ACh & 5-HT MN) VA, VB, VC, DA, DB, DC (ACh MN) DD, VD (GABA MN)	305
GAR-3a	G_q	17.9 ± 3.7	Carbachol (A) Scopolamine (AN) Atropine (AN)	DD, VD (GABA MN) I3 (ACh IN) PCA (Glu SN)* PCB, SPC (ACh SN)* Anal depressor, body wall, spicule protractor and pharyngeal muscles	286,304
GAR-3b	G_i	32.8 ± 4.3	Carbachol (A) Scopolamine (AN) Atropine (AN)		

1.5.6.3. Pharmacology and modulation of *C. elegans* acetylcholine receptors

As summarized in Table 1.12 and Table 1.13, the different subtypes of acetylcholine receptors in *C. elegans* exhibit distinct pharmacological properties and expression pattern. Among them, the L-type, N-type, ACR-2R, EAT-2R and GAR-3 receptor subtypes are expressed in distinct neuromuscular junctions, being involved in the different phenotypes controlled by these structures in the nematodes [306,307].

Neuromuscular-dependent behaviours are altered by the exposure to drugs that modify the acetylcholine receptor signal in the corresponding muscle. These phenotypes can be additionally exhibited by mutant worms deficient in either any of the subunits composing the receptor subtype or auxiliary proteins responsible for assembling, trafficking, maturation, location and distribution of these receptors at the synaptic specialization (Figure 1.19 and Table 1.14). In addition, these mutants are resistant to the drug action. This paradigm allows the efficient screening of molecular components involved in the proper function of the acetylcholine receptor. In fact, some of these were discovered in the nematode before the bona fide identification of orthologues in vertebrates [151,308,309]. More importantly, this paradigm could allow the identification of alternative potential targets of organophosphate toxicity as well as antidotes against organophosphate poisoning.

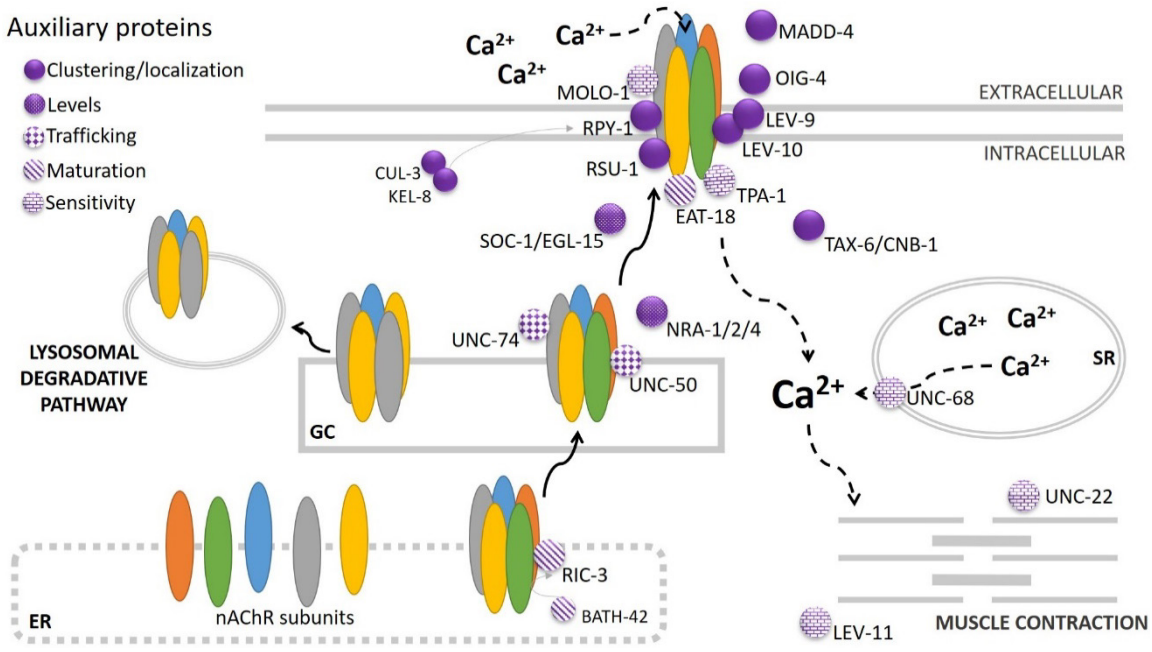

Figure 1.19. Schematic representation of auxiliary proteins involved in clustering/localization, levels, trafficking, maturation and/or sensitivity of *C. elegans* nicotinic receptors. ER – endoplasmic reticulum. GC – Golgi complex. SR – sarcoplasmic reticulum. See Table 1.14 for full detail.

Table 1.14. Effect of auxiliary proteins on nicotinic receptor subtypes in *C. elegans*. Refer to Table 1.12 for receptor subtypes. BWM – body wall muscle, ER – endoplasmic reticulum, NMJ – neuromuscular junction.

Protein	Function
CBN-1 **TAX-6**	Redistribution of N-type receptor at BWM
CRLD-1	Interact with L-type receptor at the ER and promote the assembly of subunits [310]
EAT-18	Functional expression of the EAT-2R subtype [296]
EGL-15 **SOC-1**	Required for maintenance of the normal level of L-type and GABA receptor at BWM [311]
EMC-6	Required for protein folding of the L-type, N-type and GABA receptor at BWM [312]
LEV-9 **LEV-10** **OIG-4**	Involved in L-type receptor clustering at BWM [313-315]
MADD-4	Leads the localization of the L-type cholinergic receptor clusters at NMJ [316]
MOLO-1	Positive allosteric modulator of L-type receptor at BWM [317].
NRA-1	Control the expression level, targeting or stabilizing the L-type receptor at BWM [311]
NRA-2 **NRA-4**	Control the composition of the receptor or the trafficking of certain receptor assemblies from the ER to the cellular surface [318]
RIC-3	Chaperone of L-type, N-type and ACR-2R subtypes [265]
BATH-42	Maintain the proper level of the chaperone RIC-3 [319]
RPY-1	Clustering and location of UNC-29-containing subtype [320,321]
CUL-3 **KEL-8**	Responsible RPY-1 degradation [320]
RSU-1	Prevent the formation of extra synaptic L-type clusters at BWM [322]
TPA-1	Necessary for nicotine-induced expression and/or biological activity of UNC-29-containing receptor subtype [323]
UNC-50	ER associated protein responsible for the trafficking of L-type and ACR-2R [324]
UNC-74	Functional expression of L-type and ACR-2R [265]

1.5.7. Neuromuscular junction and associated phenotypes

There are four distinct neuromuscular junctions that are responsible for the locomotion, feeding, reproduction and defaecation of nematodes. These connections are located at the body wall, pharynx, vulva and enteric muscles, respectively. In males, an additional neuromuscular junction organization, placed at the spicule protractor muscles, supports the mating behaviour.

Acetylcholine released by motor neurons controls muscle contraction and this signalling supports the different behaviours of the worm upon sensory input [251]. However, the role of this neurotransmitter is not clear for the function of the vulva and enteric neuromuscular organs (sections 1.4.7.3 and 1.4.7.4).

Although the different neuromuscular junctions of *C. elegans* are governed by apparently unrelated motor neurons and exhibit distinct organization and molecular composition, there is a certain degree of coupling between locomotion and the other behaviours. For example, the speed and pattern of locomotion is modulated in coordination with reproduction and defaecation, respectively [325,326]. Furthermore, the optical silencing of body wall muscles induces the cessation of feeding [327].

1.5.7.1. Body wall neuromuscular junction

The body wall neuromuscular junctions of *C. elegans* are formed by 75 motor neurons that signal onto 79 body wall muscles running along the length of the nematode. The motor neurons belong to eight different classes innervating either the dorsal part of the animal (AS, DA, DB and DD) or the ventral (VA, VB, VC and VD) (Figure 1.20). This circuit is contained in the pseudocoelom, the fluid-filled body cavity of nematodes.

The acetylcholine released by the dorsal motor neurons AS, DA and DB activates cholinergic receptors expressed at the dorsal body wall muscles, causing their contraction, and also receptors expressed on the VD motor neuron, triggering the relaxation of the ventral body wall muscles by the release of GABA (Figure 1.20). Similarly, acetylcholine released by the ventral motor neurons VA and VB generates the contraction of the ventral body wall muscle but also the relaxation of the dorsal by the activation of DD motor neuron that release GABA as consequence (Figure 1.20) [328]. In this way, a smooth body bend is produced when the worm is crawling. This circuit is governed by a subset of sensory and inter neurons that interrupt the forward locomotion promoting changes in the sense and direction of the movement in response of sensory and proprioceptive cues.

This relatively simple mechanism offers different phenotypical options associated with the body wall acetylcholine signalling.

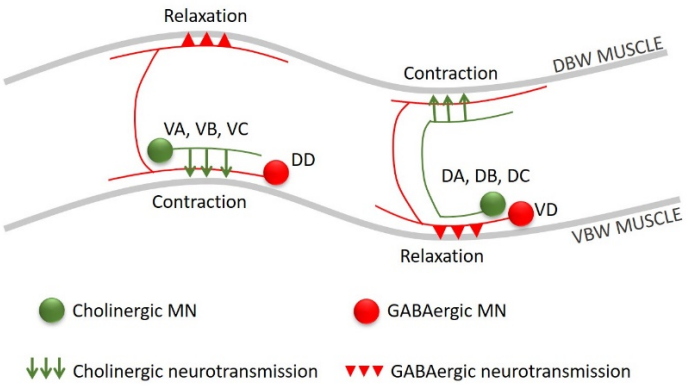

Figure 1.20. Locomotory circuit of *C. elegans*. The acetylcholine released by the cholinergic motor neurons evoke the contraction of the body wall muscle where they synapse as well as the relaxation of the opposite body wall muscle by the activation of the GABAergic neurons. VBW – ventral body wall. DBW – dorsal body wall. Adapted from [280].

- Body bend, speed, body length and paralysis

Four different phenotypes are directly related with the body wall neuromuscular function. These are the quantification of body bends, speed, body length and paralysis. A body bend is considered when the part of the worm behind the pharynx reaches a maximum bend in the opposite direction to the previous one [329]. The speed refers to the average distance moved by a single worm per unit time. The body length quantification consists of recording of the size of the worms from the lips till the tail [330]. Paralysis is determined by the quantification of immobilized worms out the total number of worms on the same experimental plate. In this case, to distinguish paralysis phenotype from physiological locomotion disruption, any movement should be detecting after mechanical stimulation of the nematodes [331,332].

Impairments in the body wall excitability by alteration of L-type, N-type and/or ACR-2R signalling (Table 1.12) results in reduction of the body bends, decreased speed, variation of the body size and paralysis [330,331]. In fact, the characterization of these phenotypes in mutant strains exposed to either levamisole or aldicarb has been classically used as screening platform to identify molecular components for the correct L-type and N-type function [315,331-333].

Speed has been the most used phenotype to assess toxicity of organophosphate pesticides in *C. elegans*. Overall, this phenotype exhibits good correlation with acetylcholinesterase activity in exposed worms (section 1.4.8) [249,334,335].

1.5.7.2. Pharyngeal neuromuscular junction

The pharyngeal circuit is formed by 20 neurons that signal on 8 types of muscles. These muscles are radially disposed around a lumen that opens upon contraction and sucks liquid from the surrounding environment along with suspended bacteria. The pharyngeal muscles are organized in three different functional parts. The anterior, middle and posterior part of the pharynx, named as corpus, isthmus and terminal bulb, respectively [336].

The pharyngeal circuit responsible of food intake is isolated from the pseudocoelom by a basal lamina. A single synapse exists between pharyngeal (I1) and extrapharyngeal (RIP) neurons. However, the absence of RIP neuron results in an essentially normal pharyngeal and electrophysiological behaviour, indicating the importance of a neurohumoral signalling from the extrapharyngeal nervous system in the control of feeding (Figure 1.21) [336].

Laser ablation and optogenetic activation/inhibition of individual and/or groups of pharyngeal neurons highlighted the role of the internal nervous system in controlling the muscle contraction. Among the 20 neurons composing the pharyngeal circuit, only the M4 motor neuron is essential for feeding and hence for life [337]. Animals lacking the other 19 pharyngeal neurons exhibit a slow

and uncoordinated pharyngeal movement that allows feeding and therefore development [338]. Nevertheless, some neurons such as MC, M3, and NSM are required for an efficient feeding behaviour [338-341] (Figure 1.21).

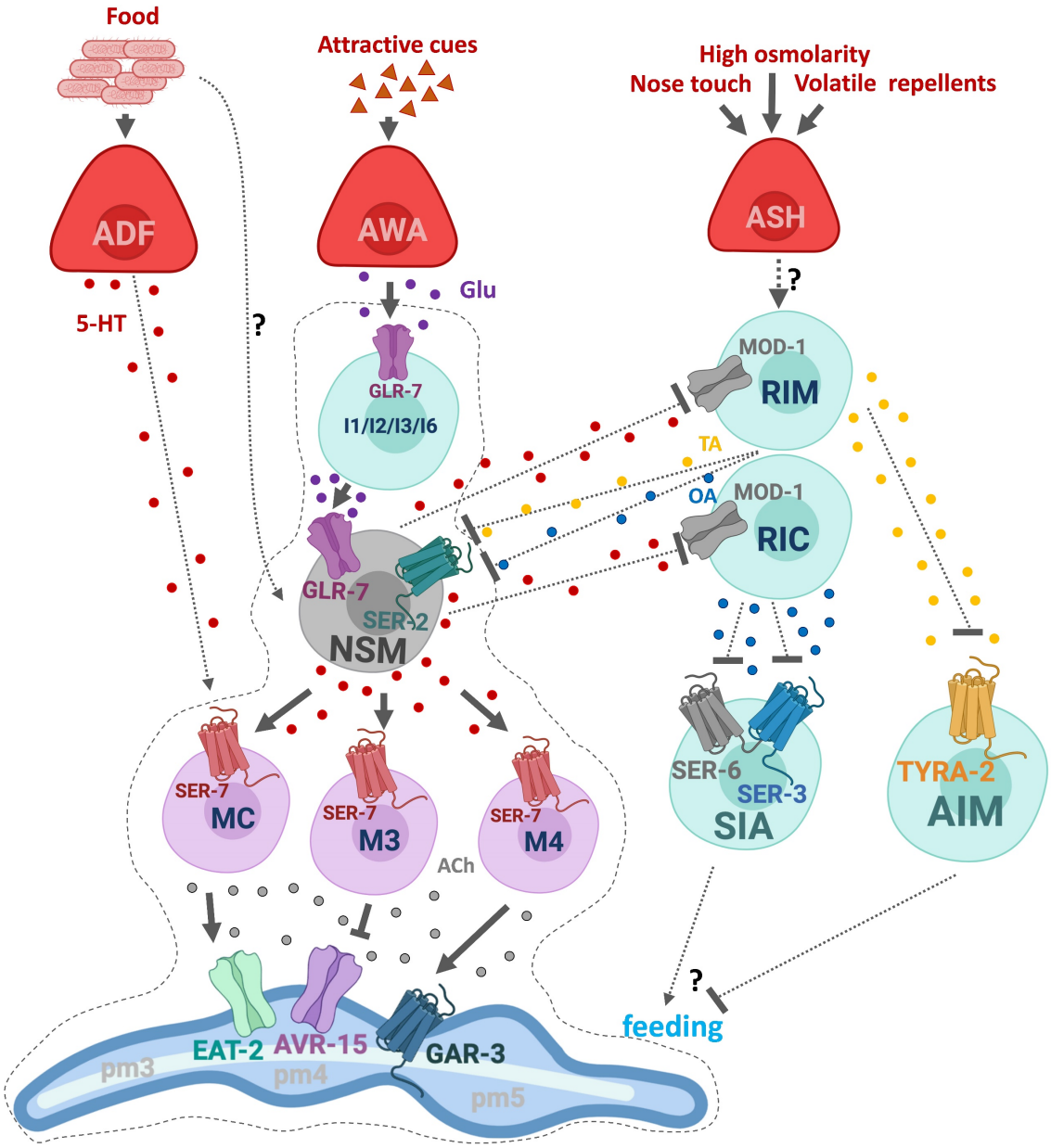

Figure 1.21. Molecular circuit controlling pharyngeal neuromuscular junction function on food. The presence of food in the close proximity of the nematode triggers the increase of the pharyngeal movement by different routes. Gustatory cues are detected by dendrite projections of the ADF and other amphid neurons that release serotonin in consequence [342]. This binds to the serotonin metabotropic receptor SER-7 located at MC motor neuron via an endocrine signal [342]. Activation of MC motor neuron provokes the release of acetylcholine that binds to EAT-2R at the corpus to induce pharyngeal muscle contraction [307]. Olfactory cues are detected by AWA and other chemosensory neurons that release glutamate in consequence. The neurotransmitter binds to GLR-7 (glutamate-gated ion channel) expressed at different pharyngeal interneurons that respond releasing glutamate to activate NSM neuron. This provokes the release of serotonin by the NSM neuron [343]. Activation of NSM in response to food might additionally happen by other mechanisms. For example, by serotonin humoral signal from the vulva motor neuron HSN [343]. The serotonin released NSM signals the motor neurons MC, M3 and M4 throughout a SER-7 dependent pathway [344]. MC and M4 release acetylcholine that control muscle contraction at the corpus and isthmus,

respectively [307,337]. EAT-2R is located at the synapse with MC and its activation elicits the contraction of the muscle at the corpus [296,307]. The contraction of muscles at the isthmus is the consequence of M4 acetylcholine release signalling the muscarinic receptor GAR-3 and the calcium wave travelling from the corpus to the terminal bulb [342,345]. M3 releases glutamate in response to serotonin and pharyngeal muscle contraction. This leads the relaxation of the pharyngeal muscle mediated by AVR-15, a glutamate-gated chloride channel [346]. The fast relaxation of pharyngeal muscles by M3 shorten the pump duration, increasing the pumping frequency [340,346]. NSM integrates other chemical and mechanical cues from the animal surroundings to modulate the feeding behaviour in consequence [347]. These environmental conditions are detected by ASH and other amphid neurons that cause the activation of RIC/RIM interneurons by a mechanism still unravelled. RIM/RIC and NSM are negatively regulated by a serotonin signal. Likewise, the serotonin released by NSM silences RIM/RIC by signalling throughout MOD-1 (serotonin-gated chloride channel) while tyramine/octopamine released by RIM/RIC, respectively, silence NSM by signalling throughout SER-2. This mechanism allows the fine regulation of feeding under contradictory environmental conditions. In addition, RIM/RIC released neurotransmitters induce the suppression of feeding by an NSM unrelated mechanism. This is achieved by an undescribed pathway that implies the signalling of SIA and AIM interneurons. Dotted arrows indicate humoral signal. Neurotransmitter signalling is colour coded as indicated: serotonin (5-HT) in red; glutamate (Glu) in purple; tyramine (TA) in yellow; octopamine (OA) in blue and acetylcholine (ACh) in grey. The basal lamina that separates pharyngeal and extra pharyngeal circuit is represented by a dotted line [343,347]. For neurons terminology and description refer to [280]. Created with BioRender.

- Pharyngeal pumping and isthmus peristalsis

The feeding behaviour in *C. elegans* is defined by two pharyngeal movements, pharyngeal pumping and isthmus peristalsis (Figure 1.22). The simultaneous contraction of the corpus and the terminal bulb, known as pharyngeal pumping, filters and transports bacteria from the surroundings of the animal to the isthmus [348]. The peristalsis movement of the isthmus drives the bacteria throughout this part to the terminal bulb where the grinder mashes them before directing to the intestine [337]. Pharyngeal pumping and isthmus peristalsis are not coupled, that is, an isthmus peristalsis happens each 3 or 4 pharyngeal pumping movements. These two feeding phenotypes are regulated by different environmental cues (Figure 1.21). Among them, food is the most potent factor that defines pumping. For example, wild type nematodes change the pharyngeal pumping rate per minute from 20 to 250 in response to the presence of food [349].

The quantification of pumping rate per unit time has been classically used to determine pharyngeal function. A pump is defined by a cycle of backward and forward movement of the grinder at the terminal bulb (Figure 1.22) [350]. This protocol can be performed by either visual observation or automated platforms for higher-throughput screenings [351,352]. Indirect measurement can also be performed by quantifying the depletion of food in suspension when nematodes are incubated in liquid media [353]. This methodology has been used to determine a dose-dependent response of feeding to sublethal doses of dichlorvos that correlates with the acetylcholinesterase activity in the exposed worms (section 1.4.8) [353].

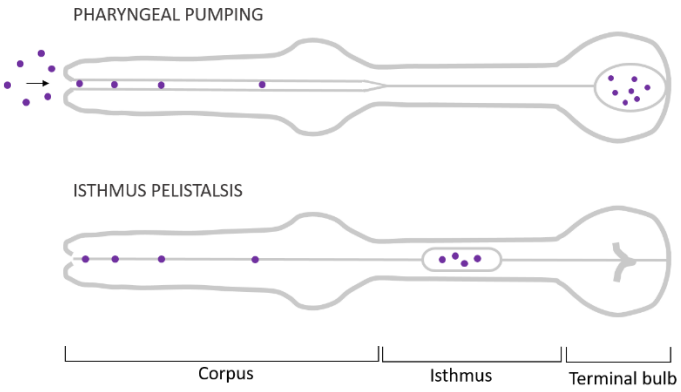

Figure 1.22. *C. elegans* pharynx and pharyngeal movements for feeding. During pharyngeal pumping the muscles of the corpus and terminal bulb contract allowing the access of food into the pharyngeal lumen. Bacteria pass from the corpus to the terminal bulb by the isthmus peristalsis. At the terminal bulb, bacteria are mashed at the grinder before passing to the intestine. Purple circles represent bacteria. Figure adapted from [280].

1.5.7.3. Vulva neuromuscular junction

The vulva neuromuscular junctions are formed by 2 serotonergic neurons (HSNs) and 6 cholinergic ventral neurons (VCs) that synapse onto 16 uterine and vulva muscles whose contraction expels eggs for the reproduction of nematodes (Figure 1.23) [354]. Despite the simplicity of the system, the full mechanism by which nematodes lay eggs is still unclear. The specific contraction of the vulva muscles vm2 is critical for the expulsion of the egg. Vm2 muscle expresses nicotinic receptor subunits such as UNC-29 and UNC-38 [323,355]. However, the contraction of vulva muscles is triggered by the serotonin released from HSN motor neuron that signals throughout a SER-7 receptor [344]. Furthermore, the role of acetylcholine in egg-laying is controversial. While levamisole and nicotine stimulate vulva muscle contraction [356,357], mutants deficient in acetylcholine such as *unc-17* or *cha-1* are egg-laying hyperactive. However, the excess of acetylcholine produced by aldicarb causes the opposite effect, decreasing the number of eggs laid [357]. This indicates that acetylcholine can activate the receptors directly expressed on the muscles but may drive release of additional signals that inhibit the egg laying circuit [357,358].

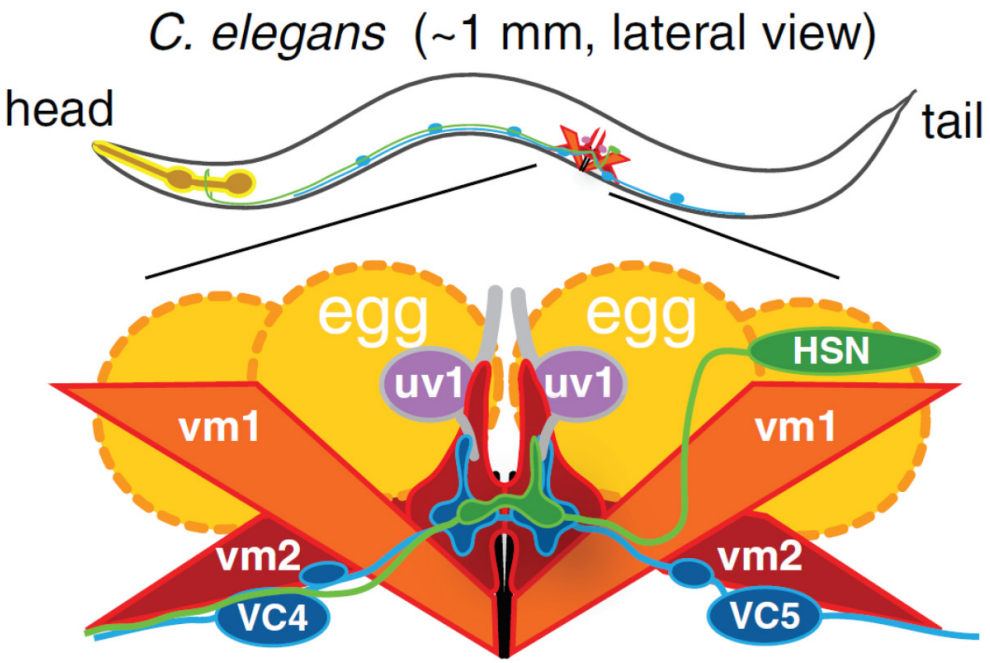

Figure 1.23. Schematic representation of vulva circuit in *C. elegans*. The vulva muscles vm1 and vm2 are cross-disposed muscles around the vulva. Serotonin released by HSN neuron elicits the contraction of vm2 which in turn stimulate the uterine muscles. This signalling is critical for the expulsion of the egg from the uterus to the environment [354,358]. Ventral VC motor neurons release acetylcholine to vm1. However, this process seems to be less important for laying eggs. For neurons and muscles terminology and description refer to [280]. Figure taken from [358].

- Egg-laying

Egg-laying is the effect of depositing eggs into the environment by the adult hermaphrodites caused by a rhythmic behaviour that alternates an active state that lasts a few minutes and a quiescent period of about 20 minutes. During the active state, each worm can deposit about 5 eggs [358,359]. The scoring of number of eggs deposited per worm and per unit time is indicative of the vulva muscle function.

Despite the disputed role of acetylcholine during egg-laying, a dose-dependent decrease in fertility has been observed in nematodes exposed to monocrotophos. This phenotype correlates with acetylcholinesterase activity in those worms (section 1.4.8) [360].

1.5.7.4. Enteric neuromuscular junction

The enteric neuromuscular junctions are formed by two polymodal motor and interneurons (DVB and AVL) that signal to three types of enteric muscles (anal, sphincter and stomato-intestinal) (Figure 1.24). DVB and AVL neurons release GABA to the muscles that provokes the contraction of anal and stomato-intestinal muscles via EXP-1 input (GABA-gated cation channel) and the relaxation of the sphincter muscle via UNC-49 signalling (GABA-gated chloride channel) [361]. Stomato-intestinal muscles are disposed wrapping around the posterior region of the intestine and their contraction pressurizes the gut content near the posterior end of the intestine. The sphincter muscle circles the intestine at its junction with the rectum, allowing the passage of the

intestine content to the rectum. Finally, the contraction of anal muscles facilitates the expulsion of the rectum content [361].

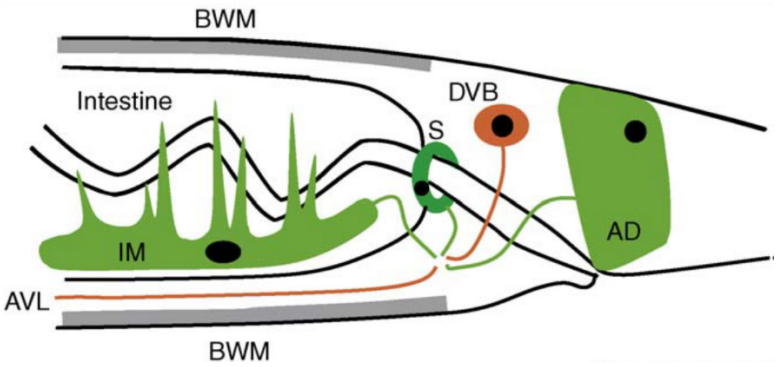

Figure 1.24. Schematic representation of neurons and muscles responsible for defaecation. Refer to text for full description. IM – stomato-intestinal muscle. BWM – body wall muscle. S – sphincter. AD – anal depressor muscle. AVL and DVB correspond to neurons. For neurons and muscles terminology and description refer to [280]. Figure taken from [361].

- Defaecation motor program

The defaecation motor program has clocklike properties being activated once every 55 seconds in wild type strain at 20°C. However, it can be modulated by environmental factors such as temperature or food availability. During each defaecation, nematodes contract the four quadrants of the posterior body wall muscles, increasing the pressure in the intestine and pushing the fluid inside to the anterior part of the body. About 1 second after, the four quadrants of the anterior body wall muscles contract, causing the fluid to flow posteriorly where is collected in the anal region. Finally, the contraction of the enteric muscles triggers the expulsion of the gut content [361,362].

Although the control of enteric muscles is governed by GABA, mutant nematodes lacking *cha-1* gene exhibit a dramatically increased defaecation cycle length, being each 30 minutes in some mutant nematodes. It might indicate an active function of the acetylcholine pathway controlling the timing of the defaecation cycle [362]. Furthermore, ACR-8 and ACR-16 are expressed in anal muscles although their function is not known.

1.5.8. Insights into *C. elegans* as model of organophosphate toxicity

Previous research studies have used the nematode *C. elegans* as model organism for modelling organophosphate acute and chronic toxicity as well as identifying alternative molecular pathways that contribute to this toxicity. Surprisingly, there is not any research study focused on the identification of alternative targets to treat organophosphate poisoning.

1.5.8.1. Modelling organophosphate toxicity

As mentioned above, the most used phenotype to quantify acute toxicity in *C. elegans* has been speed of locomotion. At least 19 organophosphate pesticides have been demonstrated to reduce

the velocity of worms with different efficacies. Among them, dichlorvos, paraoxon-ethyl, parathion and fenamiphos have been the most potent inhibitors of the nematode locomotion [249,334]. Furthermore, pharyngeal pumping and egg-laying are inhibited in nematodes exposed to dichlorvos and monocrotophos, respectively [353,360]. All of these organophosphate compounds are able to inhibit acetylcholinesterase activity of exposed nematodes, indicating a correlation between the phenotype and the classical mode of action for organophosphates [249,334,353,360].

Despite the effort made describing the biochemical and phenotypical effect during intoxication, there is not any research study that includes the quantification of behavioural and acetylcholinesterase activity recovery after poisoning.

1.5.8.2. Finding alternative modes of actions

Due to the genetic tractability of *C. elegans*, the research of alternative targets that might affect organophosphate toxicity has been addressed by determination of the gene expression profile during intoxication and recovery (Table 1.15) [363-365].

The upregulation of genes involved in stress response and myogenesis observed in distinct research studies after the exposure of different organophosphates suggests changes in metabolic processes. This highlights mitochondria dysfunction as a potential non-target organophosphate toxicity effect that might augment organophosphate-mediated disruption of acetylcholine signalling [363-365]. In fact, this mechanism has been additionally involved in cell death of cultures treated with organophosphates [366].

Table 1.15. Summary of the main *C. elegans* molecular pathways affected by the exposure to organophosphates. Genes involved in the molecular pathways indicated are differentially up-regulated during the early response (2 – 8 h exposure time), medium response (14 – 26 h exposure time), late response (72 h postexposure time) and recovery (14 – 20 h after the organophosphate is washed out) from the specified compound. Incubations were performed from adult worms in all conditions. Data taken from [363-365].

Poisoning time-course	Organophosphate tested	Molecular pathways affected
Early	Dichlorvos	Immune and stress response Development β-oxidation
Medium	Dichlorvos, fenamiphos, mefloquine	Immune and stress response Myogenesis Axon regeneration and guidance Apoptosis
Late	Chlorpyrifos and diazinon	Immune and stress response Detoxification Lipid transport and metabolism
Recovery	Dichlorvos	Myogenesis Axon regeneration and guidance Apoptosis

1.6. Aims and objectives

The objective of this thesis has been the investigation of organophosphate intoxication in the model organism *C. elegans* to establish a new platform for the discovery of alternative pathways to address the cholinergic toxicity.

In the first chapter of this thesis, behavioural and biochemical approaches were used to identify pharyngeal pumping as the most suitable phenotype to research organophosphate intoxication and recovery. However, the second chapter describes how the pharyngeal function is controlled by the pharyngeal neuromuscular junction but modulated by body wall neuromuscular junction input. Finally, an organophosphate-induced plasticity in the pharyngeal phenotype is described in the last chapter. Modulation of the L-type receptor signal is proposed as mechanism triggering this plasticity effect. This aligns with the idea of using nicotinic receptors as drug targets to develop new antidotes for organophosphate poisoning (section 1.3.3.3). The modulation of the receptor was additionally achieved by manipulation of auxiliary proteins involved in its synaptic location and sensitivity. This opens new insights into other pathways for identifying alternative targets to treat organophosphate poisoning.

Chapter 2

C. elegans pharyngeal pumping provides a whole organism bio-assay to investigate anti-cholinesterase intoxication and antidotes

Patricia G. Izquierdo [a], Vincent O'Connor [a], A. Christopher Green [b], Lindy Holden-Dye [a], John E.H. Tattersall [b]

[a] Biological Sciences, Institute for Life Sciences, University of Southampton, Southampton, United Kingdom.

[b] Dstl, Defence Science and Technology Laboratory, Porton Down, Salisbury, Wiltshire, SP4 0JQ, United Kingdom.

Key words. Organophosphate, aldicarb, DFP, paraoxon, oxime, neuromuscular junction.

Author for correspondence:

Patricia G. Izquierdo: P.Gonzalez@soton.ac.uk

Published as: Izquierdo, P. G., O'Connor, V., Green, A. C., Holden-Dye, L., and Tattersall, J. E. H. (2020) *C. elegans* pharyngeal pumping provides a whole organism bio-assay to investigate anti-cholinesterase intoxication and antidotes. *Neurotoxicology* **82**, 50-62. https://doi.org/10.1016/j.neuro.2020.11.001

Research Highlights

- *C. elegans* pharyngeal pumping inhibition by organophosphates correlates with worm acetylcholinesterase inhibition by the anti-cholinesterases.
- The recovery of the pharyngeal function in *C. elegans* in the presence of obidoxime is due to the recovery of the acetylcholinesterase function after anti-cholinesterase intoxication.
- The pharyngeal neuromuscular function represents a quantitative bio-assay for investigation of anti-cholinesterase toxicity and recovery with excellent 3Rs potential.

2.1. Abstract

Inhibition of acetylcholinesterase by either organophosphates or carbamates causes anti-cholinesterase poisoning. This arises through a wide range of neurotoxic effects triggered by the overstimulation of the cholinergic receptors at synapses and neuromuscular junctions. Without intervention, this poisoning can lead to profound toxic effects, including death, and the incomplete efficacy of the current treatments, particularly for oxime-insensitive agents, provokes the need to find better antidotes. Here we show how the non-parasitic nematode *Caenorhabditis elegans* offers an excellent tool for investigating the acetylcholinesterase intoxication. The *C. elegans* neuromuscular junctions show a high degree of molecular and functional conservation with the cholinergic transmission that operates in the autonomic, central and neuromuscular synapses in mammals. In fact, the anti-cholinesterase intoxication of the worm's body wall neuromuscular junction has been unprecedented in understanding molecular determinants of cholinergic function in nematodes and other organisms. We extend the use of the model organism's feeding behaviour as a tool to investigate carbamate and organophosphate mode of action. We show that inhibition of the cholinergic-dependent rhythmic pumping of the pharyngeal muscle correlates with the inhibition of the acetylcholinesterase activity caused by aldicarb, paraoxons and DFP exposure. Further, this bio-assay allows one to address oxime dependent reversal of cholinesterase inhibition in the context of whole organism recovery. Interestingly, the recovery of the pharyngeal function after such anti-cholinesterase poisoning represents a sensitive and easily quantifiable phenotype that is indicative of the spontaneous recovery or irreversible modification of the worm acetylcholinesterase after inhibition. These observations highlight the pharynx of *C. elegans* as a new tractable approach to explore anti-cholinesterase intoxication and recovery with the potential to resolve critical genetic determinants of these neurotoxins' mode of action.

2.2. Introduction

Organophosphates and carbamates are potent acetylcholinesterase inhibitors [88,367]. This enzyme is key in terminating the cholinergic transmission that controls neuromuscular junction and important central synapse function [368,369]. This mode of action has led to the development of these compounds for widespread use as pesticides based on the central role of cholinergic transmission in the animal and plant parasitic life cycle [370]. This widespread use of anti-cholinesterases as pesticides has an associated human intoxication issue. At least two million cases of poisoning per year result in an estimated 200,000 deaths [11-13,162]. Additionally, acetylcholinesterase inhibitors with high human toxicity were developed as nerve agents for chemical warfare and terrorism [88,371].

The toxicological effect of organophosphates and carbamates is exerted through the covalent modification of acetylcholinesterase [88,367]. The anti-cholinesterase drugs are orientated in the catalytic centre of the enzyme in a similar manner to acetylcholine [81]. When the molecule is positioned at the catalytic triad (Ser-Glu-His), the phosphorylation (OP) or carbamylation (carbamate) of the serine leads to inactivation of the acetylcholinesterase [81]. This inhibition results in the accumulation of the acetylcholine in the synaptic cleft causing the potential continued agonist activation of the two distinct classes of cholinergic receptors, muscarinic and nicotinic [372]. This overstimulation of the cholinergic target cells causes a wide range of neurotoxic effects. The first manifestations of the associated cholinergic syndrome cause autonomic disturbances including excessive sweating, lacrimation, salivation as well as cramps, bradycardia and miosis [42,367]. Fatality occurs primarily due to disruption of the respiratory centres in the brain and/or transmission failure at the respiratory muscles [42].

After enzyme inactivation, spontaneous reactivation occurs via hydrolysis of the bond created between the enzyme and the inhibitor molecule and enables the re-use of the acetylcholinesterase [88]. This reversibility is important in managing recovery from intoxication. The rate at which it happens depends on the organophosphate or carbamate molecule and shows strong variation between distinct classes of anti-cholinesterase [89]. However, the chemistry of the organophosphate attack is complicated by an ancillary reaction termed aging that leads to an irreversible inhibition in the OP-inhibited acetylcholinesterase [88,90]. The dealkylation of any side chain of the conjugated OP creates a bond resistant to hydrolysis between the inhibitor and the catalytic serine [91]. It is a time-dependent reaction whose rate is extremely variable depending on the chemical structure of the intoxicating OP molecule [89].

Artificial ventilation is used to preserve breathing. This mitigation is supported by a pharmacological treatment that consists of atropine, benzodiazepine and oximes. Oximes are

potent nucleophile molecules able to hydrolyse and reverse the acetylcholinesterase inhibition [162]. However, the success of reactivating acetylcholinesterase by oximes depends on which of the various OP molecules has produced the inhibition. For example, obidoxime seems to be more efficient for reactivating acetylcholinesterase after the inhibition of OP pesticides but not nerve agents. The efficiency of 2-pralidoxime is demonstrated after the inhibition of acetylcholinesterase with sarin or VX but not by soman or tabun. Lastly, there is not any reactivator able to recover the acetylcholinesterase activity after the aging reaction [89].

The limitations of the current treatment, poor health condition of the surviving victims and the fatalities reported have become a major public health concern [11,373]. Mammal animal models have been used to address this situation, with species ranging from small rodents to large mammals, including non-human primates [236]. The signs and LD_{50} values of anti-cholinesterase poisoning in these models are well correlated to the IC_{50} of acetylcholinesterase inhibition in both brain and blood samples [237,238]. However, since the development of the current treatment, between 1950s and 1960s, it has not been significantly improved. Taking into consideration this fact as well as the 3Rs principles for animal research [374,375], the genetically tractable model organism *C. elegans* is proposed in this study. It has been widely used in neurotoxicological studies including organophosphates [249,250,334,335,353,360,363-365]. This is advantaged by highly conserved molecular pathways between the nematode and humans. There is a rich cholinergic signalling network in which acetylcholine controls the worm's nervous system and is essential for neuromuscular transmission [251,261]. The cholinergic neuromuscular transmission, which excites distinct muscles, underpins biologically critical functions such as locomotion, egg-laying and the feeding behaviour [250,251]. As in mammals, acetylcholinesterase is key in terminating the cholinergic signal to prevent hyperstimulation. The three *C. elegans* acetylcholinesterases are orthologues to the three human acetylcholinesterase isoforms [59,264,376]. In particular, the catalytic centre of the nematode enzyme is highly conserved to mammals and harbours the key amino acids involved in the inhibition and aging reactions [264]. Finally, nematodes are protected from external conditions by a cuticle that controls the drug access to the nervous system and internal organs [377,378]. However, this barrier is very different from other mammalian barriers that protects the central nervous system. This can facilitate the initial screening of antidotes against organophosphate poisoning by not limiting the drug accessibility.

We have investigated how anti-cholinesterases act on the high rate of pharyngeal pumping. This is essential to the feeding of worms when they are in the presence of bacteria [339,379,380]. We show that whole organism measurement of pharyngeal movements represents a sensitive phenotype that allows us to evaluate effects of OP intoxication. Furthermore, the inhibition of nematode acetylcholinesterases was better correlated to the inhibition of the pharyngeal pumping than to

the paralysis of the body wall muscles. We validated the pharyngeal pumping as a tool to probe spontaneous recovery as well as the reversible and irreversible inhibition associated with aging. This was confirmed by biochemical analysis of the nematode acetylcholinesterase activity. Thus, the pharynx offers a powerful bio-assay to investigate organophosphate intoxication and approaches by which chemical mitigation can be used to treat poisoning.

2.3. Materials and methods

2.3.1. *C. elegans* maintenance

All the experiments were performed using N2 Wild-type *C. elegans* strain obtained from Caenorhabditis Genetics Center (https://cgc.umn.edu/) and maintained under standard conditions [258]. Briefly, nematodes were grown at 20°C on Nematode Growth Medium (NGM) agar plates seeded with *E. coli* OP50 as source of food.

2.3.2. Drug stocks

Carbamate (aldicarb) and organophosphates (paraoxon-ethyl, paraoxon-methyl and DFP) were acquired from Merck and dissolved in 70% ethanol and 100% DMSO, respectively. The oximes, obidoxime and 2-pralidoxime, were provided by DSTL Porton Down (UK) and dissolved in distilled autoclaved water. The drug stocks were kept at 4°C, as manufacturer recommended temperature, in a locked cabinet according with standard security protocols. Dissolved compounds were used within one month or discarded.

Acetylthiocholine iodide (ATCh) and 5,5'-dithio-bis-2-nitrobenzoic acid (DTNB) were obtained from Merck (https://www.sigmaaldrich.com/united-kingdom.html) and dissolved in phosphate buffer 0.1 M pH7.4 directly before use.

2.3.3. Behavioural assays

All behavioural experiments were performed on a standard developmental stage: young hermaphrodite adults (L4 + 1 day) at room temperature (20°C). Worms were allowed to develop from eggs at 20°C through the larval stages L1, L2, L3. Worms were viewed under a Nikon SMZ800 binocular zoom microscope and were recognized as L4 by the temporary appearance (8 hours window) of the vulva saddle. These worms were selected the day before the experiment and placed on fresh OP50 seeded plates. They were used 16-24 hours after as L4 +1. Nematodes were picked onto the bacterial lawn 10 min before starting observations.

Paralysis and body length were scored as previously described [330,331]. Briefly, nematodes were picked onto the bacterial lawn containing either aldicarb or vehicle control. Paralysis was scored by quantifying the number of animals not moving out the total of worms on the plate at indicated times. These snapshots involved scoring for 30 secs. Nematodes were considered paralysed when

no movement was detected after prodding three times with a platinum wire [331]. To measure body length, images of the worms were taken at the specified times. These images of the nematodes were binarized and skeletonized using ImageJ software. The length of the skeleton was used to determine the body length of the nematodes [330].

Pharyngeal pumping on food in the presence of aldicarb or organophosphates was scored at indicated times after transferring worms to either anti-cholinesterase containing plates or vehicle control plates (10 min, 1 h, 2 h, 6 h, and 24 h after picking onto assay plates). Pumping was quantified visually by counting the number of grinder movements observed under binocular microscope using a timer and a counter. The pump rate was quantified for a minimum of 3 min per worm at each time point and the mean was used as pumps per minute.

Nematodes exhibited a strong aversive behaviour to anti-cholinesterases that difficulted the behavioural analysis (Figure 2.1. Aversive behaviour response of *C. elegans* to anti-cholinesterase drugs. Nematodes onto anti-cholinesterases plates tend to leave both the patch of food and the NGM agar plate in a dose-time dependent response. This aversive behaviour is stronger for organophosphates than for aldicarb. Data are shown as mean ± SEM. ap<0.001 for both worms on food and total number of worms on plate; bp<0.001 for worms on food but not for total number of worms on plate.. During the experiment with low concentrations of aldicarb or organophosphates, worms left the patch of food and the plate before being paralysed for the action of the drug. Animals that left the patch of food during the experiment with aldicarb, paraoxon-ethyl and paraoxon-methyl were picked back to the bacterial lawn. They had to be on the lawn for at least 10 min before the start of observations to be counted [381]. Nematodes that left the plate during the experiment were not considered for the experiment.

The estimates of IC_{50} were made by measuring the body wall and pharyngeal function at varying drug concentrations after 24 hours incubation relative to worms placed on drug free vehicle control plates. The percentages of inhibition relative to these controls were used to estimate IC_{50}.

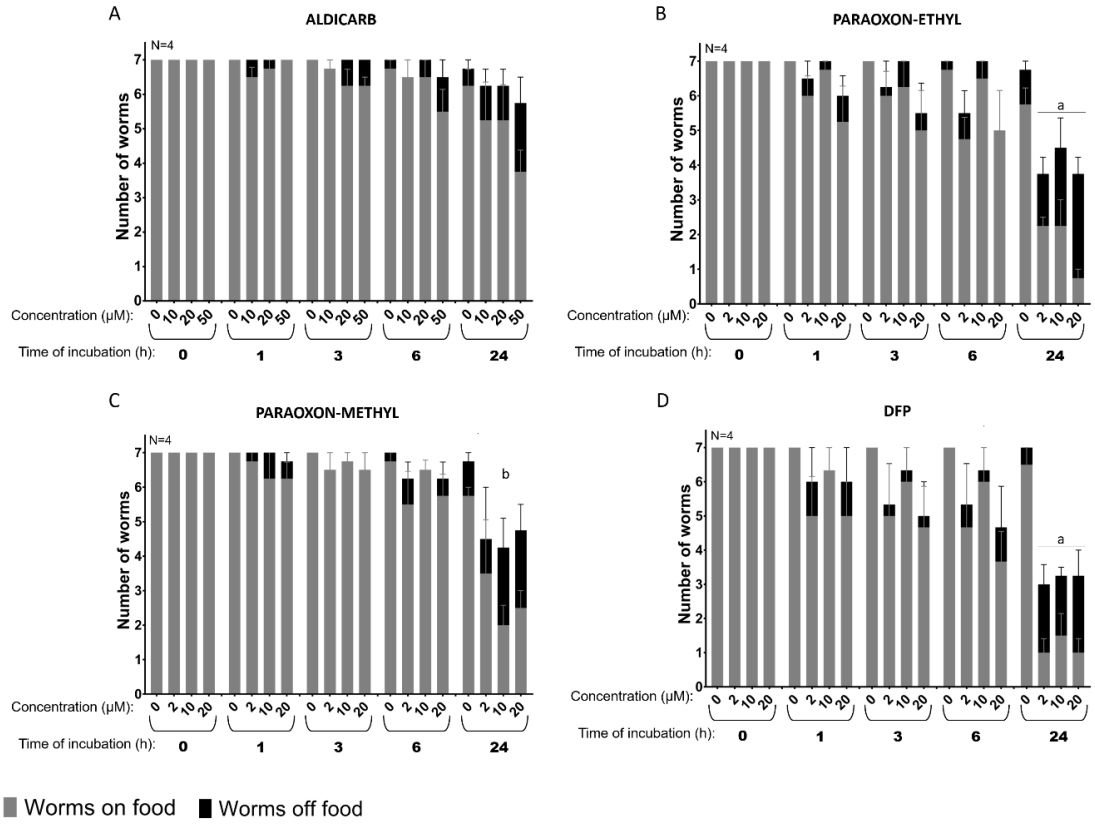

Figure 2.1. Aversive behaviour response of *C. elegans* to anti-cholinesterase drugs. Nematodes onto anti-cholinesterases plates tend to leave both the patch of food and the NGM agar plate in a dose-time dependent response. This aversive behaviour is stronger for organophosphates than for aldicarb. Data are shown as mean ± SEM. ap<0.001 for both worms on food and total number of worms on plate; bp<0.001 for worms on food but not for total number of worms on plate.

2.3.4. Plate husbandry

Experiments were performed in 6-well plates containing a final NGM volume of 3 ml with exception of DFP intoxication assays (section 2.5). Anti-cholinesterase and oximes containing plates were prepared the day before of each experiment by adding an aliquot of a concentrated stock in the melted NGM, tempered after heating to approximately 60ºC. 50 µl of OP50 *E. coli* bacteria one $OD_{600\,nm}$ was dropped on the plate when the media was solidified. After 1 hour in the fume hood, the dried bacterial plates were sealed and kept in dark at 4ºC until next day. Plates were left at room temperature for at least 30 min before starting the experiment. There was no observable change in the bacterial lawn of anti-cholinesterase/oxime-containing and control plates, therefore no effect of the anti-cholinesterase or oxime on the *E. coli* growth was discernible [382]. The final concentration of vehicle in the behavioural assay was 0.07% ethanol for aldicarb-containing plates and 0.1% of DMSO for organophosphate-containing plates. Control plates contained the same concentration of vehicle than assay plates. Neither vehicle concentrations alone had any effect in the phenotypes tested.

2.3.5. Intoxication with the organophosphate DFP

The organophosphate DFP equilibrates across the individual wells of the 6-well culture plates. This was evidenced by the inhibition of pumping and paralysis of worms placed on non-DFP wells adjacent to DFP laced agar (data not shown). This potent cross-contamination by DFP concentrations precluded the use of 6-well plates. Therefore, 9 cm Petri dishes were used containing a final volume of 20 ml NGM. DFP was added to the melted NGM as mentioned above to obtain the indicated final concentrations between 2 µM and 500 µM. Non-DFP containing plates were used as control. After solidification, 200 µl of *E. coli* OP50 $OD_{600\,nm}$ = 1 was spread evenly over the complete surface of the NGM. This full food coverage was needed to mitigate the potent drive for worms to leave food that was particularly strong in the case of the DFP treatments (Figure 2.1). Seeded plates were incubated for 1 hour and then they were kept until the next day as mentioned in section 2.3.

2.3.6. Recovery from organophosphate intoxication

To study the recovery of pharyngeal pumping after organophosphate intoxication, L4 + 1 worms were intoxicated on organophosphate-containing plates for 24 hours. The intoxicating concentration was calculated based on estimating the lowest concentration that gave the maximal inhibition of pumping after 24 hours of exposure. After incubation on organophosphate laced plates for 24 h, the nematodes were transferred onto either non-drug containing plates or oxime-containing plates. From here, the recovery from full inhibition was measured by recording the pump rate at indicated times after being placed on no-drug or oxime plates. Neither obidoxime nor pralidoxime alone had an effect on the pharyngeal pumping rate at concentrations between 0.5 mM and 2 mM (Figure 2.2).

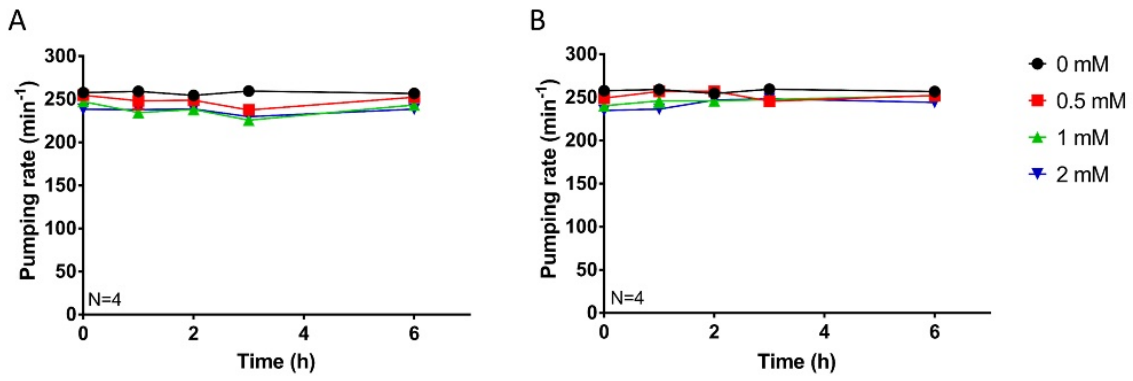

Figure 2.2. Pharyngeal pumping rate phenotype of *C. elegans* wild type adults exposed to oximes plates. Pharyngeal pumping rate per minute was quantified at different end-point times for synchronized L4 + 1 nematodes exposed to increasing concentration of plates containing obidoxime (A) or pralidoxime (B). Neither obidoxime nor pralidoxime had any effect in the pharyngeal function of *C. elegans*. Data are shown as mean ± SEM of four worms in four independent experiments.

2.3.7. Pharynx dissection procedure

Pharynxes of young hermaphrodite wild type adults were dissected according to previously published methods [383]. Briefly, nematodes were placed into dissection plates containing 3 ml of cold Dent's solution supplemented with 0.2% bovine serum albumin (Merck). Dishes with nematodes were incubated at 4°C for 5 min to reduce the thrashing activity. In order to dissect the lips from the rest of the body, an incision at the mouth of the worms was made with a surgical scalpel blade while viewing under a binocular microscope Nikon SMZ800. Due to the internal pressure of the worm, the incision provokes the ejection of internal structures exposing the pharynx. When the pharynx's terminal bulb was clearly observed outside the cuticle, a second incision was made at the pharyngeal-intestinal valve to isolate the intact pharynx from the rest of the intestines.

2.3.8. Aldicarb intoxication assays with isolated pharynxes

Isolated pharynxes were removed from dissection dishes using non-sticky tips and transferred in 10 µl to a 3 ml Dent's media (containing 0.2% BSA). After washing, isolated pharynxes were transferred into dissection dishes with 3 ml Dent's containing either 5 µM of aldicarb or vehicle control. Pharynxes were incubated 5 min before imaging.

Isolated pharynxes were imaged using a Nikon Eclipse X microscope with a DIC optics with 40x Plan Fluor air objective. Images were acquired through a Hamamatsu Photonics camera and visualized for recording with IC capture software (The Imaging Source©).

2.3.9. Acetylcholinesterase activity determination

Total worm homogenates were generated from synchronized L4/adult worms. For this, 12 gravid worms were maintained for 4 hours on OP50 seeded 5.5 cm plates, in which time they accumulated freshly laid eggs. The adult worms were removed, and plates were incubated 3 days at room temperature. This generated approximately 250 age-synchronized L4/adults on bacteria depleted plates. Worms from a minimum of 40 plates (approx. 10,000 worms) were harvested and washed three times with 0.1 M phosphate buffer pH7.4 in order to remove all the remaining bacteria. Nematodes were transferred to a glass homogenizer and incubated for 30 min on ice with a final concentration of 0.15% of n-octyl-glucoside as detergent to permeabilize the cuticle and release cellular content [384]. The n-octyl-glucoside did not alter the acetylcholinesterase activity (data not shown). Mouse brain homogenate was used in parallel to validate the acetylcholinesterase activity quantification protocols in *C. elegans* and compare with previously published data. To generate mouse forebrain homogenate, freshly dissected tissue was homogenized in 10 volumes of phosphate buffer (w/v). This was kindly provided by Aleksandra

Pitera (Southampton University, UK). Worm/mouse protein homogenate was stored at -80°C until use when they were defrosted on ice.

Acetylcholinesterase activity was measured using a modified colorimetric Ellman's assay [219]. The assay mixture contained 0.2 mg/ml of worm/mouse homogenate comprising the acetylcholinesterase enzyme, 0.48 mM acetylthiocholine (ATCh) as substrate and 0.32 mM 5,5-dithio-bis-(2-nitrobenzoic acid) (DTNB) as chromophore in a final volume of 200 µl of 0.1 M phosphate buffer pH7.4. The increase in absorbance at 410 nm was measured at 1 min intervals for 15 min at room temperature using a FLUOstar Optima microplate reader (BMG Labtech). The change in absorbance against time due to the production of 5-thio-2-nitro-benzoic acid and its extinction coefficient was utilized to calculate the acetylcholinesterase activity (µmoles/min). This was normalized to the protein content of worm/mouse homogenate determined by standard Bradford protocol [385]. The enzyme activity in the homogenate was expressed as µmoles/min/mg protein.

2.3.10. Acetylcholinesterase activity after whole worm aldicarb/paraoxon-ethyl intoxication

To estimate the acetylcholinesterase activity after aldicarb and paraoxon-ethyl intoxication, nematodes were synchronized as in section 2.7. When worms reached the L4/adult stage, an aliquot of 12 µl aldicarb or paraoxon-ethyl stock was added to the worm-containing plates (12 ml) to generate the indicated final concentration of 50 µM or 500 µM, for aldicarb, and 100 µM for paraoxon-ethyl. Control plates were made by adding 12 µl of 70% ethanol or 100% DMSO for aldicarb and paraoxon-ethyl respectively. A minimum of 40 plates were used per condition. After 24 hours of incubation at room temperature the control and aldicarb/paraoxon-ethyl intoxicated worms were harvested, washed and treated to generate the worm homogenate. Nematodes were kept on ice during the whole process to prevent recovery of the acetylcholinesterase activity through reversibility of the reaction. Acetylcholinesterase activity assays were carried out directly after the worm protein extraction.

2.3.11. Acetylcholinesterase activity of worm/mouse brain homogenate after inhibition by organophosphates

A stock solution of organophosphate was appropriately diluted in 0.1 M phosphate buffer pH7.4 just before the experiment to ensure a low concentration of DMSO in the final dilution for acetylcholinesterase activity quantification. The final concentration of vehicle in the biochemical assay was 0.000025%.

Worm/mouse brain homogenate in phosphate buffer (0.1 M pH7.4) as described above was placed in a 96-well plate. At 0 min, 15 min, 30 min, 35 min, 40 min, 43 min, 44 min, 44.3 min, 44.6 min and 45 min, these volumes were supplemented with organophosphate to the indicated final concentration in 50 µl final volume. This incubation contained 120 µg of worm/mouse protein and 1 µM organophosphate. After 45 min, acetylcholinesterase activity assay was scored for all the samples as described above (section 2.7) by addition of DNTB and acetylthiocholine in a final volume of 200 µl with 0.1 M phosphate buffer pH7.4. This gave a time series in which the time of incubation with the organophosphate was 20 s, 40 s, 1 min, 2 min, 5 min, 10 min, 15 min, 30 min and 45 min. An acetylcholinesterase assay without the presence of the OP was used as control.

Either single or double decay exponential curve was fitted to these time courses to determine the best-fit mode of inhibition of acetylcholinesterase by each organophosphate.

2.3.12. Acetylcholinesterase reactivation after inhibition with organophosphate drugs

Organophosphate-inhibited acetylcholinesterase was prepared by incubating 2.4 mg/ml of worm/mouse homogenate with 2 µM of any organophosphate in a final volume of 320 µl for 1 hour at room temperature. The mixture was centrifuged at 14000 rpm for 30 min and the supernatant was discarded to remove the excess of organophosphate. The pellet containing the inhibited acetylcholinesterase was resuspended with 320 µl of phosphate buffer (0.1 M pH7.4) and maintained at room temperature. For control, non-exposed 2.4 mg/ml worm/mouse protein was used in parallel. Following organophosphate removal, aliquots were taken at subsequent time intervals to determine acetylcholinesterase activity after incubating the mixture 1 min in the presence or absence of 100 µM obidoxime [89]. The concentration of obidoxime used was previously described to research spontaneous recovery and aging reaction in human acetylcholinesterase inhibited by paraoxon-ethyl, paraoxon-methyl or DFP [89].

The percentage of reactivation (%R) was calculated using the following formula [223]:

$$\%R = (1 - [(a_o - a_r) / (a_o - a_i)]) * 100$$

where a_o is activity of intact enzyme, a_i is activity of inhibited enzyme and a_r is activity of reactivated enzyme. Acetylcholinesterase activity that does not recover upon incubation with obidoxime is considered to have arisen from a dealkylation reaction that ages the modified enzyme [89]. Mouse brain acetylcholinesterase was used in order to validate the protocol and compare the nature of organophosphate mode of action in the two organisms [386].

2.3.13. Statistical analysis

Data were analysed using GraphPad Prism 7 and are given as mean ± SEM. Statistical significance was assessed using either one-way or two-way ANOVA test followed by post hoc analysis with Bonferroni corrections when applicable. Bonferroni corrections were selected to avoid false positives. The sample size N of each experiment is specified in the figure.

2.4. Results

2.4.1. Quantifying anti-cholinesterase induced changes in cholinergic neuromuscular function with whole organism behaviour

We first investigated distinct behaviours that are underpinned by cholinergic neuromuscular junction function in *C. elegans*. This identified that locomotion/paralysis, contraction mediated shrinkage of body length and the rate of pharyngeal pumping showed a clear concentration-time dependent inhibition with respect to this class of anti-cholinesterase. The carbamate aldicarb was used as representative of the acetylcholinesterase inhibitors. The aldicarb-induced hypercontraction of the body wall muscles elicited both paralysis and decrease of the body length of the nematodes (Figure 2.3). However, the lowest concentrations of aldicarb tested (2 µM, 10 µM and 50 µM) failed to paralyse the worms, even though the nematodes incubated on 50 µM aldicarb plates for 24 hours looked uncoordinated and were significantly shorter than control nematodes (Figure 2.3).

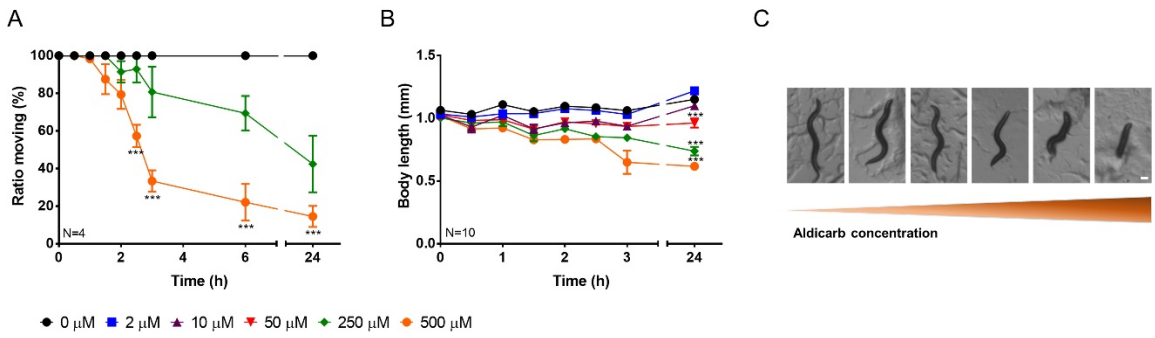

Figure 2.3. Nematodes exposed to aldicarb exhibited paralysis and hypercontraction of body wall muscles. A) The number of synchronized L4 + 1 nematodes moving as percentage the total worms on the plate was scored at different times in the face of a range of concentrations of aldicarb. The ratio moving of nematodes exposed to 2 µM, 10 µM and 50 µM was identical to the control. Data are shown as mean ± SEM of four different experiments. B) The body length of synchronized L4 + 1 nematodes exposed to different concentrations of aldicarb plates was scored by taking micrographs at different times of incubation and the length quantified. Data are shown as mean ± SEM of the length of ten worms in five different experiments. C) Body length of nematodes incubated on different concentrations of aldicarb plates for 24 hours. From the left to the right the concentration of aldicarb was: 0 µM (control), 2 µM, 10 µM, 50 µM, 250 µM and 500 µM. Scale bar represents 100 µm. *p<0.05; **p<0.01; ***p<0.001 by two-way ANOVA test.

In a similar way, the aldicarb treatment caused a dose-dependent inhibition of pharyngeal pumping. (Figure 2.4). This paralysis is likely mediated by the elevated acetylcholine associated

with cholinesterase inhibition. The consequence is the hyperstimulation of the radial muscle contractions that underpin rhythmic pumping mediated by a pacemaker cholinergic transmission [339,379,380]. This notion is supported by experiments in which the isolated pharynx is exposed to physiological Dent's solution with or without 5 µM aldicarb for 5 min (Figure 2.4B). In the carbamate-treated isolated pharynx, we observed the predicted hypercontraction of the pharyngeal radial muscle evidence by the sustained opening of the pharyngeal lumen (Figure 2.4B). In contrast to body wall muscles, the whole organism paralysis of the pharyngeal muscle was observed with the lowest concentrations tested within 6 hours of incubation on the aldicarb-containing plate and from the first hour of intoxication onto 50 µM plates.

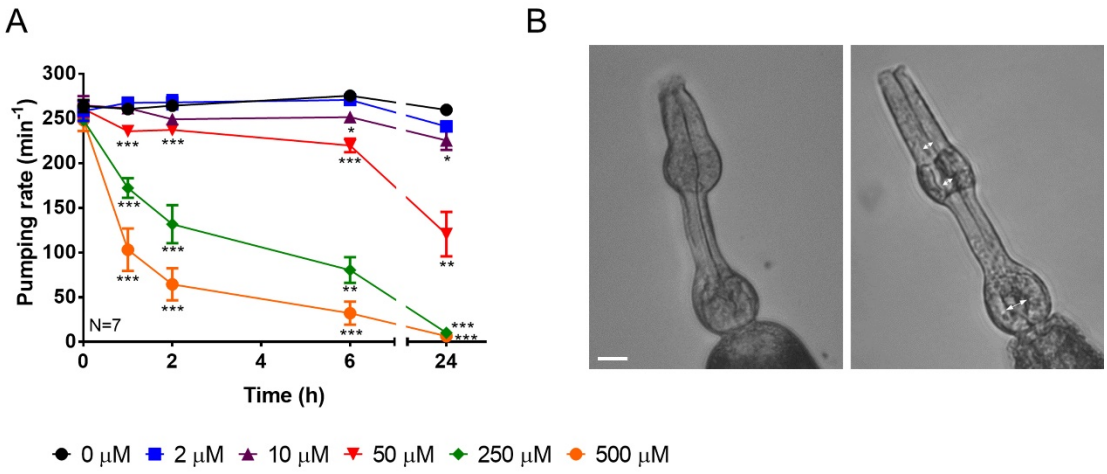

Figure 2.4. Pharyngeal pumping of *C. elegans* exposed to aldicarb exhibited a gradual concentration-time dependent paralysis due to the hypercontraction of the radial muscles in the pharynx. A) Pharyngeal pumping rate per minute was quantified at different end-point times for synchronized L4 + 1 nematodes exposed to a range of concentration of aldicarb plates. An increased concentration-dependent response over the time is observed. Data are shown as mean ± SEM of the pumping rate of 7 worms in four independent experiments. B) Isolated pharynxes of *C. elegans* were exposed to Dent's solution as control (left panel) or 5 µM of aldicarb (right panel). The hypercontraction of the radial muscles caused the opening of the pharyngeal lumen (indicated by the white arrows). Scale bar represents 1 µm. *p<0.05; **p<0.01; ***p<0.001 by two-way ANOVA test.

The IC_{50} values calculated after 24 hours of intoxication indicated that pharyngeal pumping rate and body length were the most sensitive behaviours to anti-cholinesterase intoxication, being 5-fold lower than paralysis IC_{50} value (Figure 2.5). Moreover, the pharyngeal pumping rate discriminated the incremental effect of increasing concentrations of cholinesterase inhibition. Furthermore, this whole organism bio-assay of cholinergic neuromuscular junction was more sensitive than body length in resolving the low concentration as well as discerning anti-cholinergic effects at shorter incubation times.

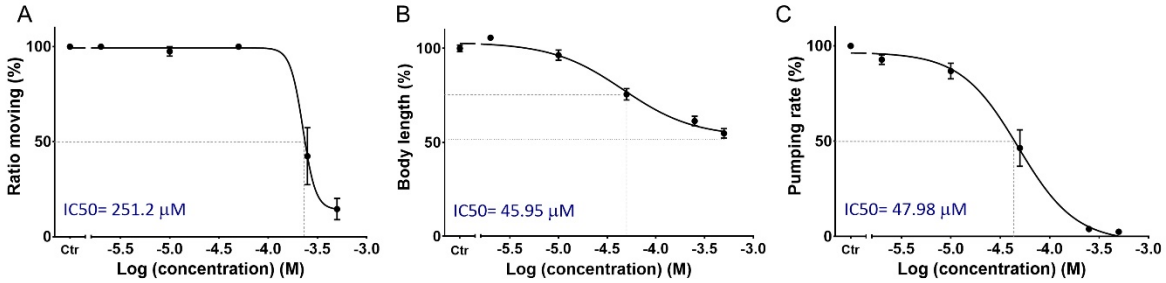

Figure 2.5. Aldicarb concentration-dependent sensitivity in cholinergic neuromuscular junction dependent behaviours. A) The percentage of ratio moving corresponds to the number of worms moving out of the total number of worms on plates after 24 hours of intoxication. B) Body length was expressed as percentage of the unexposed body length after 24 hours of incubation. C) Pharyngeal pump rate was expressed as percentage of the pharyngeal pumping of unexposed nematodes after 24 hours of incubation. Data are shown as mean ± SEM.

2.4.2. *C. elegans* acetylcholinesterase activity is reduced by the presence of aldicarb.

In order to demonstrate that aldicarb inhibits acetylcholinesterase activity in the treated *C. elegans*, intoxicated worms on 50 µM and 500 µM aldicarb plates were harvested and homogenized. The acetylcholinesterase activity in the homogenates was measured and compared with non-treated animals (Figure 2.6A). Nematodes intoxicated onto aldicarb plates for 24 hours exhibited a reduction in the acetylcholinesterase activity that was dependent on the inhibitor concentration (Figure 2.6A). Interestingly, the inhibition of enzyme activity was greater than the reduction in any of the neuromuscular junction dependent phenotypes investigated. Nematodes incubated on 50 µM aldicarb displayed 15% of the acetylcholinesterase activity found in control homogenates (Figure 2.6A). In contrast, locomotion, body length and pharyngeal pumping were 100%, 83% and 53%, respectively, compared to the corresponding control (Figure 2.6B, 2.6C, 2.6D). Similarly, the acetylcholinesterase activity of nematodes after 24 hours of incubation on 500 µM aldicarb plates was 3.4% while the ratio of worms moving, body length and pumping rate was 14.6%, 53.9% and 2.5%, respectively, compared to the corresponding control of non-treated worms (Figure 2.6). It is noteworthy that the *in vitro* assay consists on an evaluation of the three acetylcholinesterases' activities expressed in the whole worm while the phenotypical analysis quantifies a site-specific inhibition that depends on the neuromuscular junction properties such as the neuronal input or the muscle excitability.

These data indicate the high safety factor associated with cholinesterase function in which low levels of acetylcholinesterase activity can maintain the behavioural function. This is consistent with previous data from mammal models in which the function was preserved despite profound enzyme inhibition [387].

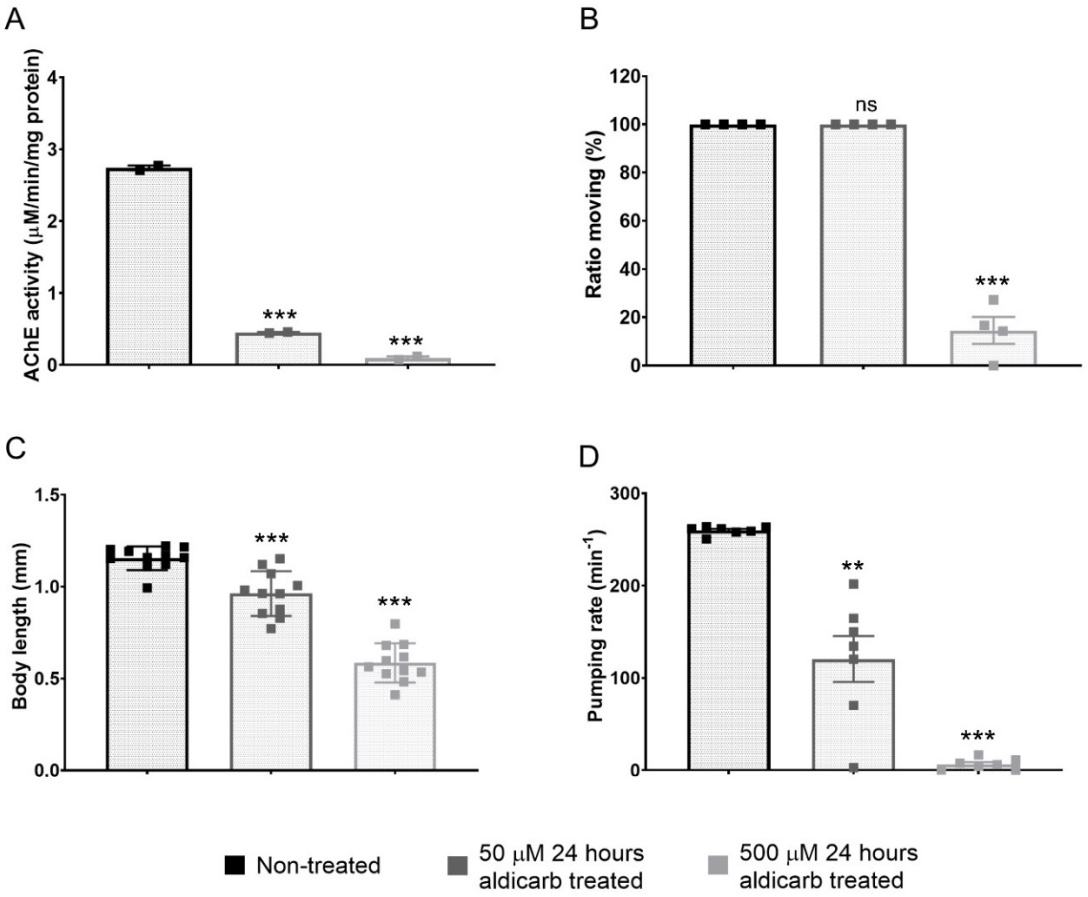

Figure 2.6. *C. elegans* acetylcholinesterase activity associated with reduced pharyngeal pumping rate and motility behaviours after 24 hours of intoxication. A) *C. elegans* acetylcholinesterase activity associated with homogenates from synchronized L4/adult worms isolated after 24 hours of incubation onto empty, 50 μM and 500 μM aldicarb plates. Treated worms were homogenized and enzyme activity measured using a modified Ellman's assay. Data are shown as mean ± SEM of two independent experiments. B) The ratio moving was scored as the animals moving after 24 hours of exposure onto empty, 50 μM and 500 μM aldicarb plates as percentage of the total worms on the corresponding plate. Data are shown as mean ± SEM of four independent experiments. C) Body length of L4 + 1 nematodes was scored after 24 hours exposed to 50 μM, 500 μM aldicarb or unexposed. Data are shown as mean ± SEM of the length of 10 worms in five independent experiments. D) Pharyngeal pumping rate of unexposed, 50 μM and 500 μM aldicarb exposed L4+1 synchronized nematodes after 24 hours of intoxication. Data are shown as mean ± SEM of seven worms in four independent experiments. $^{ns}p>0.05$; $^{**}p<0.01$; $^{***}p<0.001$ by one-way ANOVA test.

2.4.3. Pharyngeal microcircuits are more sensitive to irreversible acetylcholinesterase inhibitors than to the carbamate aldicarb

In order to test the effect of irreversible organophosphate anti-cholinesterase inhibitors in the pharynx of *C. elegans*, concentration-time dependent curves were generated for pumping rate in the presence of paraoxon-ethyl, paraoxon-methyl and diisopropylfluorophosphate (DFP) (Figure 2.7). Paraoxon-ethyl and –methyl were used as representative of organophosphate pesticides. In mammals, both compounds exhibit similar acetylcholinesterase inhibition rate constants [89]. In contrast, the spontaneous hydrolysis and aging constants for them are distinct, indicating paraoxon-methyl is more likely to age the enzyme after inducing inhibition [89]. DFP was used as

representative of organophosphate nerve agents. DFP exhibits a higher inhibition and lower aging constant of mammal acetylcholinesterase compared to the paraoxon derivatives. Unlike these compounds, DFP does not show spontaneous hydrolysis, facilitating its use as a nerve agent [89].

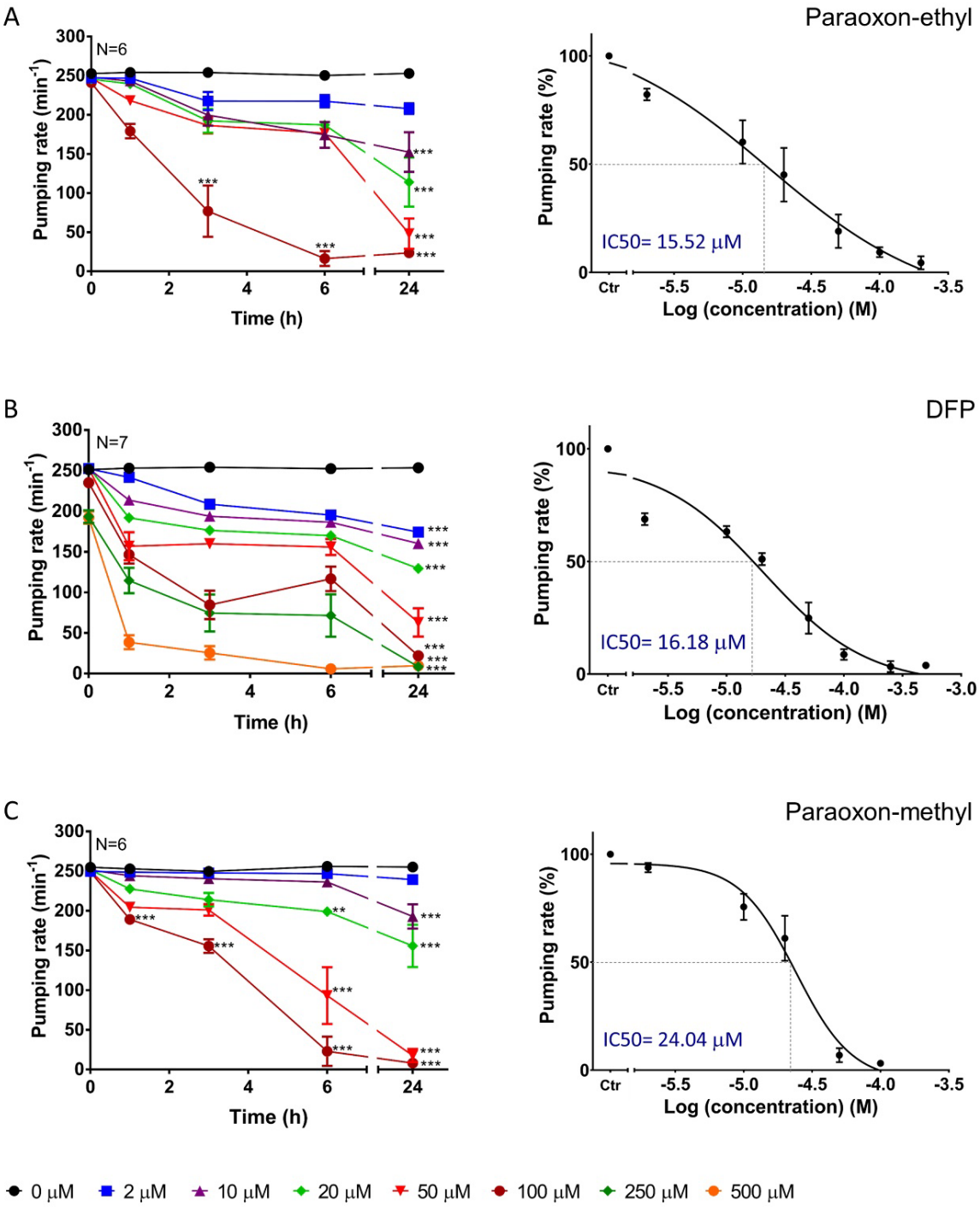

Figure 2.7. Pharyngeal pumping of *C. elegans* exposed to organophosphates. Pharyngeal pumping rate was quantified at indicated times with a range of concentrations of paraoxon-ethyl (A), DFP (B) and paraoxon-methyl (C). The IC_{50} values were calculated from the pump rate recorded at 24 hours of exposure to drug relative to untreated vehicle control. Data are shown as mean ± SEM of 6/7 worms in four independent experiments. *p<0.05; **p<0.01; ***p<0.001 by two-way ANOVA test.

The potency of all the organophosphates to inhibit pharyngeal pumping (Figure 2.7) was much greater than observed with the carbamate (Figure 2.4 and Figure 2.5). The potency of inhibition of pharyngeal pumping was similar for each organophosphate. The estimated IC_{50} values for paraoxon-ethyl, DFP and paraoxon-methyl were 15.52 µM, 16.18 µM and 24.04 µM, respectively (Figure 2.7A, 2.7B and 2.7C).

To demonstrate that the pharyngeal inhibition in the presence of organophosphates scales to acetylcholinesterase function, protein homogenate was extracted from exposed and non-exposed nematodes. Paraoxon-ethyl was used as representative example of the enzyme inhibitor treatment. The acetylcholinesterase activity of nematodes exposed to 100 µM paraoxon-ethyl for 24 hours corresponded to 4.6% of the activity found in control homogenates. Similarly, the pharyngeal function of nematodes exposed to this treatment was 9.3% compared to the corresponding non-treated control worms (Figure 2.8). This side by side comparison between pharyngeal pumping and acetylcholinesterase activity showed that the full inhibition of pharyngeal pumping is matched by a similar large inhibition of the acetylcholinesterase function.

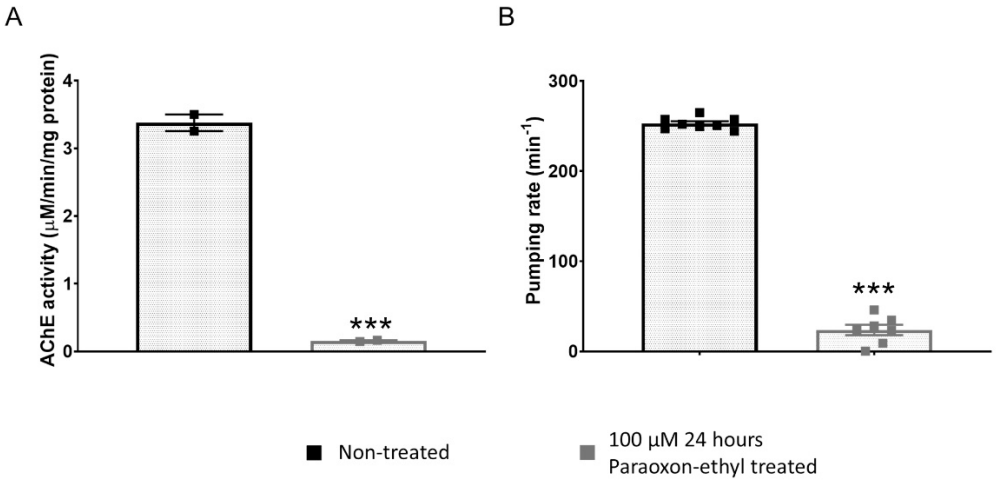

Figure 2.8. Comparison of *C. elegans* acetylcholinesterase activity and pharyngeal pumping following treatment with the organophosphate paraoxon-ethyl. A) *C. elegans* acetylcholinesterase activity in homogenates from adult worms isolated after 24 hours of incubation on empty or 100 µM paraoxon-ethyl plates. Data are shown as mean ± SEM of two independent experiments. B) Pharyngeal pumping rate of unexposed and 100 µM paraoxon-ethyl exposed adult nematodes after 24 hours of intoxication. Data are shown as mean ± SEM of seven worms in four independent experiments. $^{ns}p>0.05$; $^{**}p<0.01$; $^{***}p<0.001$ by one-way ANOVA test.

2.4.4. *C. elegans* acetylcholinesterase activity is reduced by the presence of organophosphate compounds.

To characterise the inhibition of *C. elegans* acetylcholinesterase by the paraoxon derivatives and DFP, organophosphates were added to untreated worm protein. To benchmark this approach, parallel experiments using mouse brain homogenates were run. Acetylcholinesterase activity

from the protein homogenates was quantified after the exposure of a single concentration of the organophosphate at increasing times of incubation (Figure 2.9).

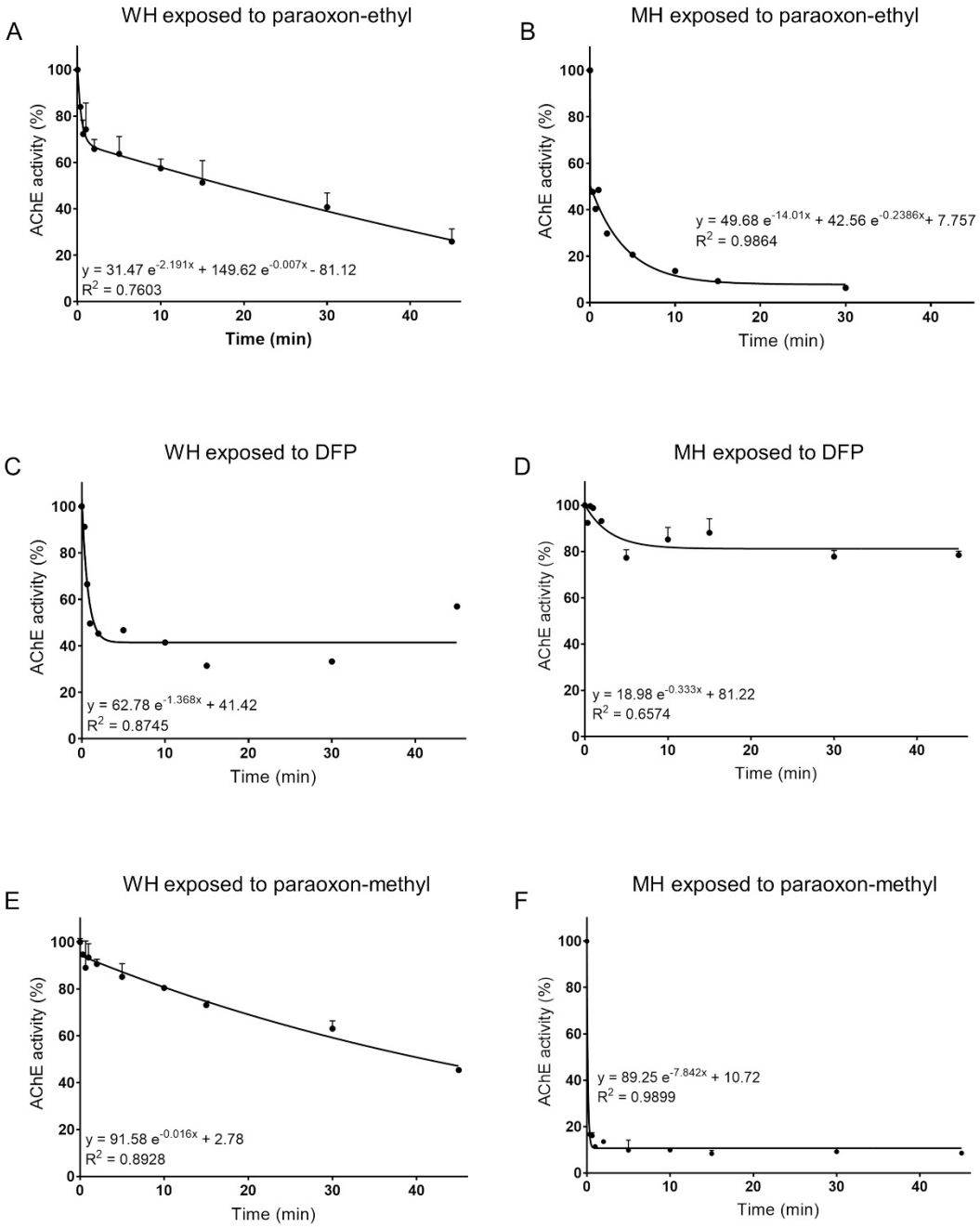

Figure 2.9. Paraoxon-ethyl, DFP or paraoxon-methyl show a time dependent inhibition of the acetylcholinesterase activity associated with *C. elegans* and mouse brain homogenates. Worm (WH) and mouse brain (MH) homogenates were incubated in addition of 1 µM of paraoxon-ethyl, DFP or paraoxon-methyl to allow timed incubation of the enzyme inactivation before synchronized measurement of homogenate associated acetylcholinesterase activity. Acetylcholinesterase activity was expressed as percentage of the unexposed homogenate activity. Two-phase exponential decay curve was ascribed as the best fit for the inhibition of nematode (A) and mouse (B) acetylcholinesterase activity at different end-point times of incubation with paraoxon-ethyl. Single exponential decay curve was fitted to the inhibition of worm (C) and mouse (D) acetylcholinesterase with DFP. One-phase inhibition of worm (E) and mouse (F) acetylcholinesterase inhibition with paraoxon-methyl at different end-point times of incubation with the organophosphate.

Paraoxon-ethyl inhibition over time showed two different phases in both the *C. elegans* and mouse homogenate (Figure 2.9A and 2.9B). The inhibition rate was greater early during intoxication relative to later exposure times.

Upon incubation with DFP, both the nematode and mouse acetylcholinesterase activity were diminished within the first 2 min of exposure, after which it levelled off to a steady state inhibition (Figure 2.9C and 2.9D). However, the steady state inhibition of worm acetylcholinesterase occurred about 60% of the total activity while the inhibition of mouse acetylcholinesterase was only 20%. This might indicate that *C. elegans* acetylcholinesterase is more susceptible for DFP inhibition than the mouse enzyme in the conditions assayed.

Paraoxon-methyl inhibition over the time in *C. elegans* and mouse homogenate fitted a single decay curve. Nevertheless, the inhibition of worm acetylcholinesterase is progressive over the time while the reduction of the mouse acetylcholinesterase activity is more rapid, reaching steady state within 1 min of incubation (Figure 2.9E and 2.9F).

Overall, the reduction of the pharyngeal pumping rate in the presence of the anti-cholinesterases was associated with a time and concentration dependent inhibition of the nematode acetylcholinesterase. Based on the degree of organophosphate-induced inhibition of behaviour and homogenate associated acetylcholinesterase activity, the results suggest that DFP is more efficient than paraoxon-ethyl, which is more efficient than paraoxon-methyl, even if the IC_{50} values and homogenate inhibition reached similar values at the longest incubation time (Figure 2.7 and Figure 2.9).

2.4.5. Recovery of pharyngeal function from organophosphates intoxication

To investigate if pharyngeal pumping recovered from anti-cholinesterase intoxication, nematodes were incubated with inhibitors for 24 hours. The intoxicated nematodes were then transferred onto control plates, or ones treated with either obidoxime or pralidoxime. These oximes, which did not affect pumping themselves, were investigated to see if their known ability to facilitate recovery is manifest in *C. elegans* (Figure 2.10).

Nematodes intoxicated with 100 µM paraoxon-ethyl exhibited a fast recovery of the pharyngeal function, which was complete at 4 hours after being transferred onto empty plates (Figure 2.10B). Recovery was accelerated when nematodes were removed from organophosphate and placed onto either the obidoxime or the pralidoxime plates. Obidoxime was the most effective of the two compounds tested in rescuing the pharyngeal activity, with a half-time of recovery of 1 hour compared to 1.33 hours on pralidoxime or 2 hours on control plates (Figure 2.10B). In contrast, nematodes incubated on either 100 µM paraoxon-methyl or 250 µM DFP plates for 24 hours did not show complete recovery when transferred to drug free plates (Figure 2.10C and 2.10D).

Moreover, the exposure of intoxicated worms to either of the oximes tested did not improve the rescue of the pharyngeal function.

Overall, the complete, fast and oxime-sensitive recovery of the pharyngeal function after paraoxon-ethyl exposure indicates that paraoxon-ethyl is not able to age the worm acetylcholinesterase and the presence of oximes facilitates the reactivation of the inhibited enzyme. In contrast, the slow, incomplete and oxime-insensitive recovery of the pumping rate after either paraoxon-methyl or DFP intoxication suggests these compounds irreversibly inhibit *C. elegans* acetylcholinesterase.

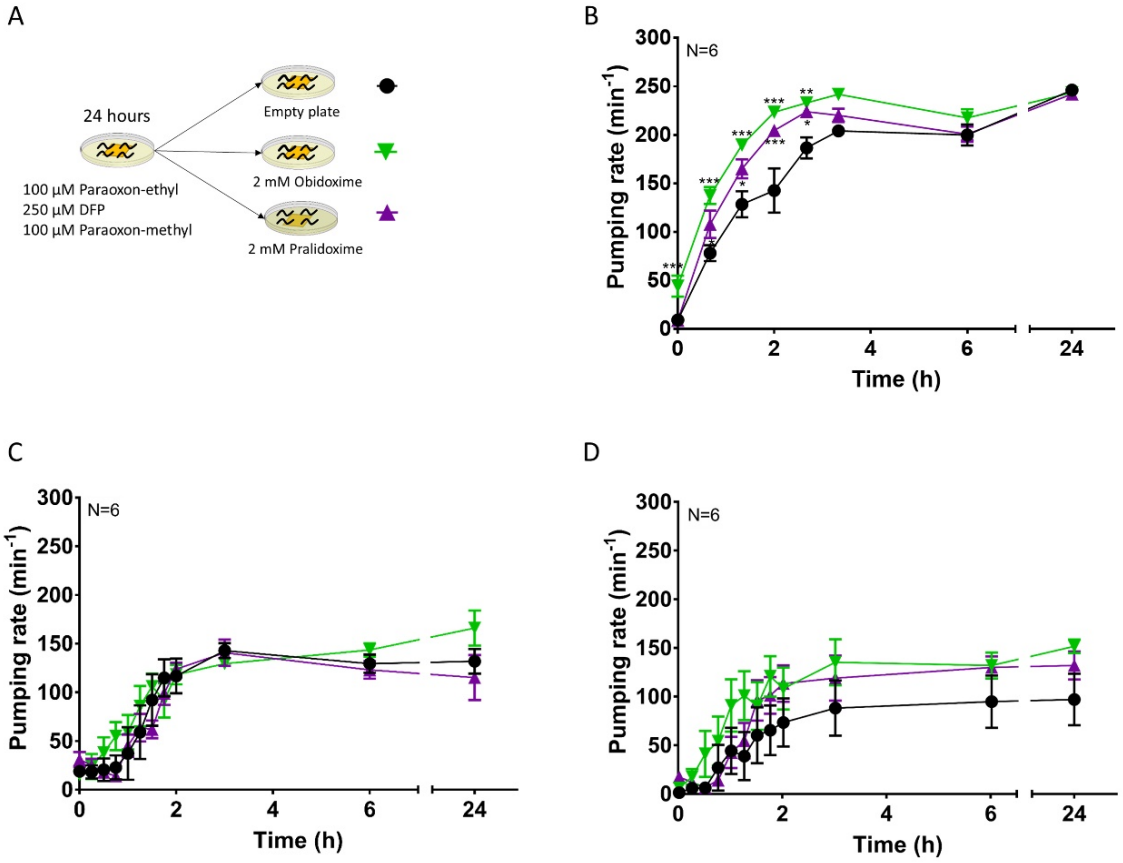

Figure 2.10. Spontaneous and oxime induced recovery of pharyngeal pumping inhibition from organophosphates intoxication. A) Experimental design of pharyngeal function recovery after 100 µM paraoxon-ethyl, 250 µM DFP or 100 µM paraoxon-methyl intoxication. Synchronized L4 + 1 nematodes were incubated on drug-containing plates for 24 hours. After transfer to control, obidoxime or pralidoxime containing plates pumping was scored at indicated times. B) Nematodes intoxicated on paraoxon-ethyl plates exhibited a fast and complete recovery of pumping enhanced by oxime treatment. C) Nematodes intoxicated on DFP plates for 24 hours displayed slow, incomplete and oxime-insensitive recovery. D) Recovery from paraoxon-methyl was incomplete and oxime-independent. Data are shown as mean ± SEM of six worms in six independent experiments. *p<0.05; **p<0.01; ***p<0.001 by two-way ANOVA test.

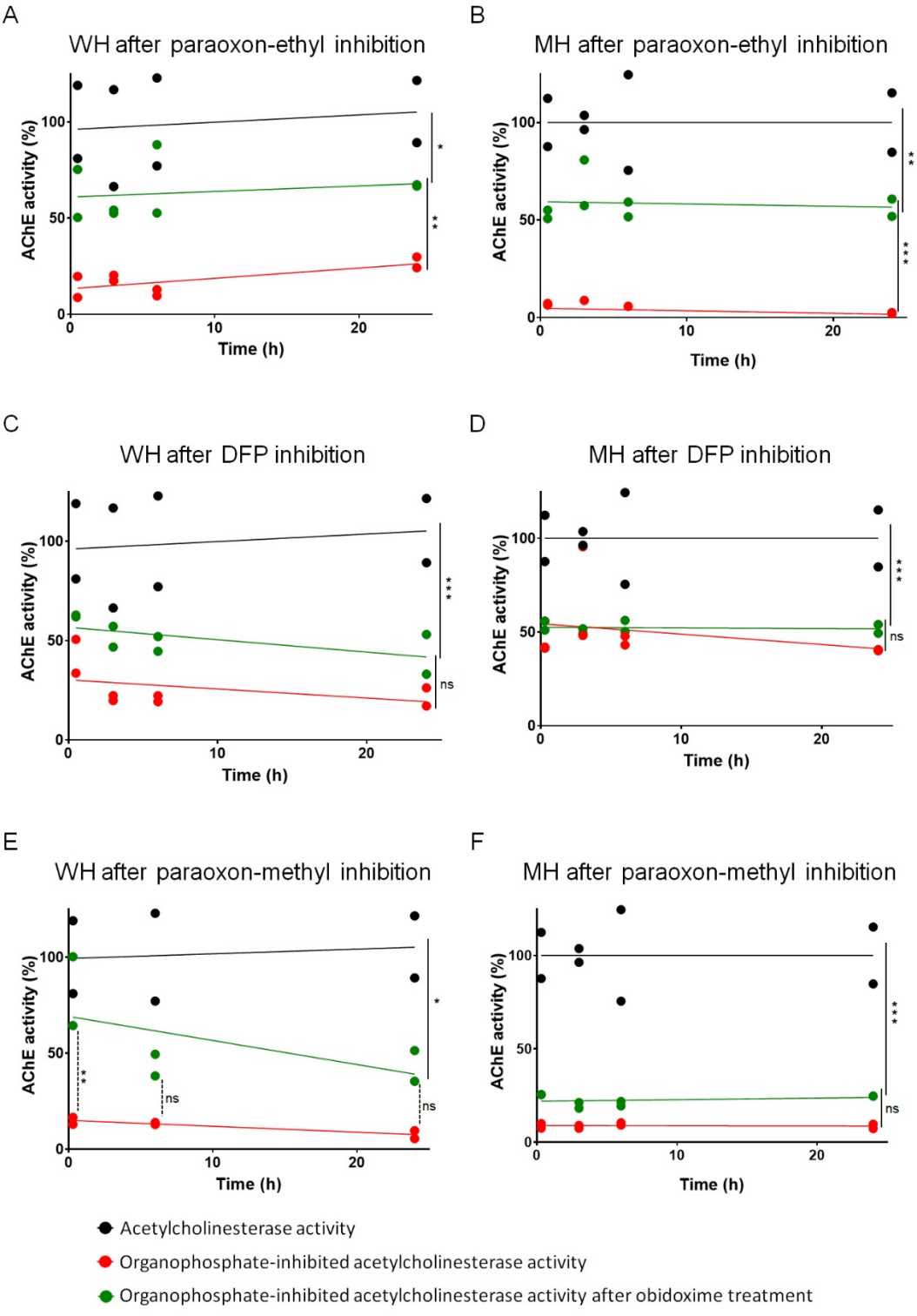

G

Time (h)	P-ethyl	DFP	P-methyl
0.5	46.4 ± 12.1	35.1 ± 7.6	102 ± 11.3
6	53 ± 22.7	34.8 ± 9	47.7 ± 20.4
24	42.3 ± 2.1	27.4 ± 8.6	43.8 ± 16.4

H

Time (h)	P-ethyl	DFP	P-methyl
0.5	43.7 ± 2.3	25.7 ± 0.4	21.2 ± 1
6	43.8 ± 10.2	26.1 ± 23.8	16.5 ± 1
24	47.8 ± 3.4	25.7 ± 0.4	21.2 ± 1

Figure 2.11. *C. elegans* and mouse acetylcholinesterase is aged after the inhibition with either DFP or paraoxon-methyl. OP-inhibited worm (WH) or mouse (MH) acetylcholinesterase activity was quantified in the presence or absence of a single concentration of obidoxime. Untreated homogenates were used as controls. Acetylcholinesterase activities were represented as the percentage of activity referred to the untreated control. A) Worm homogenate inhibited by paraoxon-ethyl exhibited an 80% reduction of the acetylcholinesterase activity that was partially recovered by the obidoxime treatment. B) Mouse homogenate acetylcholinesterase inhibited by paraoxon-ethyl displayed a partial recovery of its activity after obidoxime treatment. C) The obidoxime treatment did not significantly improved the acetylcholinesterase activity of the worm acetylcholinesterase inhibited by DFP. D) Mouse acetylcholinesterase activity was reduced after DFP treatment in 50%. Nevertheless, there is not recovery of the enzyme activity after the obidoxime treatment. E) Worm homogenate exposed to paraoxon-methyl displayed a reduction of the acetylcholinesterase activity that can be recovered by the obidoxime treatment after 30 min of incubation. However, there is not recovery in the consequent end-point times tested. F) The inhibition of mouse acetylcholinesterase activity by paraoxon-methyl was not recovered by the obidoxime treatment. G) Percentage of reactivation for *C. elegans* inhibited acetylcholinesterase after obidoxime treatment. H) Percentage of reactivation for mouse homogenate inhibited acetylcholinesterase after obidoxime treatment. *p<0.05; **p<0.01; ***p<0.001 by two-way ANOVA test.

2.4.6. Nematode acetylcholinesterase recovery after organophosphate inhibition

To test if the organophosphates that inhibit pharyngeal pumping irreversibly modify the worm acetylcholinesterase, we investigated the recovery of the organophosphate-inhibited homogenates with and without the post-intoxication addition of obidoxime.

Both worm and mouse acetylcholinesterase inhibited by paraoxon-ethyl had a significant but incomplete recovery by obidoxime (Figure 2.11A and 2.11B).

As already observed (Figure 2.9C and 2.9D), the inhibition of worm acetylcholinesterase by DFP was greater than the inhibition of mouse acetylcholinesterase (Figure 2.11C and 2.11D). After the incubation step with obidoxime, there was no significant recovery of the acetylcholinesterase activity supporting enzyme inhibition by this organophosphate had progressed through an irreversible reaction.

Finally, worm/mouse acetylcholinesterase exposed to paraoxon-methyl exhibited a nearly complete reduction of the activity (Figure 2.11E and 2.11F). The presence of obidoxime did not improve the acetylcholinesterase activity of the mouse paraoxon-methyl enzyme indicating a rapid irreversible inhibition (Figure 2.11F). Nonetheless, the effect of obidoxime in the worm paraoxon-methyl inhibited acetylcholinesterase indicated a time-dependent process. At 30 min after removing the excess of organophosphate, the presence of obidoxime recovered the total acetylcholinesterase activity, indicating a reversible reaction of inhibition at this time point. At subsequent times beyond 30 min, there was no improvement in the acetylcholinesterase activity of paraoxon-methyl inhibited enzyme by the incubation with obidoxime (Figure 2.11E).

2.5. Discussion

2.5.1. Pharyngeal pumping rate as mechanism for evaluating the effect of anti-cholinesterase intoxication

In the present study, we have used whole organism intoxication of *C. elegans* to investigate carbamate and organophosphate poisoning of cholinesterase. We have demonstrated that pharyngeal pumping is the most sensitive bio-assay to investigate organophosphate intoxication and recovery that shows a better association to *in vitro* acetylcholinesterase activity.

The study verifies previous results that worm behaviours are dependent on cholinergic transmission and therefore suitable to investigate anti-cholinesterase intoxication [249,250,334,360,388]. Most of the previous studies were focused on the direct effect of anti-cholinesterases on *C. elegans* movement, either in liquid or solid culture. In the case of an effect on pharyngeal function, this has been indirectly assumed by scoring residual food levels in liquid culture in the absence and presence of drug [334,388,389]. However, the recovery of these behaviours after acetylcholinesterase inhibition has never been probed. This is an important area for investigating mitigation approaches and cross-referencing to the similarity of core mode of action in the model organisms and humans.

The pharyngeal pump depends on acetylcholine excitation of the pharyngeal muscles to drive the contraction and relaxation cycle that allows the food intake [307,339,388]. This readily scored behaviour on food offers a distinct route to test acetylcholinesterase intoxication and recovery. Comparing the sensitivity of the pump rate to intoxication relative to the shrinkage of the worm or the binary scoring of paralysis suggests this assay may be more sensitive and better suited to discern the incremental concentration-dependent and recovery effects. The assay, which is conducted on the worms on food, has a good dynamic range. Pumping is elevated from about 40 to 250 pumps per minute when worms enter the food and the concentration-dependent inhibition of this activity by the anti-cholinesterase appears to operate across this dynamic range. Indeed, when judged as an observer based bio-assay, it is more sensitive than locomotion, previously described as a phenotype for assessing organophosphate intoxication [249,335,360]. The pharyngeal neuromuscular innervation of *C. elegans* consists of a subset of cholinergic and glutamatergic neurons that synapse onto the radial muscles of the pharynx [336,390]. The release of acetylcholine mainly by the MC and M4 motor neurons results in the contraction of the muscles causing the opening of the lumen and therefore the entering of bacteria [336,390]. In the presence of anti-cholinergic compounds, the pharyngeal muscles remain hypercontracted and the lumen continuously open (Figure 2.4B) causing the paralysis of the pharyngeal movement (Figure 2.4A). We demonstrated that the reduction of the pumping rate was better correlated with the

inhibition of the acetylcholinesterase activity by aldicarb compared to body wall neuromuscular junction phenotypes (Figure 2.6). This fact might be due to a differential sensitivity of the pharyngeal circuits to intoxication with acetylcholinesterase inhibitors compared to body wall circuits. The ingestion of the anti-cholinesterase compounds with the bacteria while feeding might be a faster access pathway for the inhibitors than throughout the cuticle. However, the pharyngeal movement quantification is also a better discriminatory assay, ranging the impact of intoxication from 0 to 250 pumps/min while there is not such an incremental effect in the paralysis of the locomotion.

The intoxication of the pharyngeal muscles by organophosphates caused a reduction of the pumping rate, which gave the rank order of potency of toxicity: paraoxon-ethyl > DFP > paraoxon-methyl with slight differences of the IC_{50} values between them (Figure 2.7). Similar to mammalian investigations, the acute toxicity of organophosphates was associated with the block of the acetylcholinesterase activity by the inhibitors (Figure 2.9). In fact, the biochemical reduction of acetylcholinesterase activity during exposure indicates a similar ranking of toxicity as the one measured with pharyngeal pumping (Figure 2.7 and Figure 2.9A, 2.9C, 2.9E). It might indicate that organophosphates can easily access the worm acetylcholinesterases when the nematodes are on inhibitor-containing plates. They block enzyme activity, causing the hypercontraction of the pharyngeal muscles and therefore the paralysis of the feeding.

The action of organophosphates in the mouse homogenate indicates that acetylcholinesterase is more susceptible to the inhibition by either paraoxon-ethyl or -methyl than by DFP (Figure 2.9B, 2.9D, 2.9F). This is consistent with acute toxicity and kinetic data previously published for murine models poisoned with organophosphates where LD_{50} values and inhibition constants for DFP are slightly higher than for paraoxon-ethyl or –methyl, independently of the mode of administration [50,391,392].

The different rank of toxicity for OP intoxication between *C. elegans* and mouse acetylcholinesterase might indicate a difference in the kinetics of inhibition by the OP between the two organisms. Key amino acids in the gorge, oxyanion hole, acyl pocket and catalytic triad are conserved in *C. elegans* compared to other model organisms (Figure 1.17). However, structural changes in the protein outside the core region might explain the variation in the toxicity to different OPs. This variance has been previously described among the diverse organism models probed for their reactivity acetylcholinesterase inhibition and recovery [89,391-394]. Despite the different rank of toxicity, both *C. elegans* and mouse DFP-inhibited acetylcholinesterase exhibited no recovery after obidoxime treatment (Figure 2.11C and 2.11D), which is consistent with the absence of recovery observed in the pharyngeal pumping after DFP intoxication (Figure 2.10C).

2.5.2. Pharyngeal pumping rate as a metric for evaluating spontaneous recovery and reactivation after organophosphate intoxication

The recovery of the acetylcholinesterase activity is key to treat the cholinergic syndrome. Oxime treatment in humans after OP poisoning offers an established supporting therapy [162]. However, the recovery and the oxime efficiency is an OP-dependent process [89]. In mammalian models, the rate of the reaction and the efficiency of possible therapies can be analysed biochemically by quantifying the acetylcholinesterase activity either in blood or brain samples of intoxicated animals [50,395,396]. We describe here a simple *in vivo* experiment in a model organism that is potentially indicative of the chemical state of the acetylcholinesterase active site after the organophosphate intoxication. The recovery of the pharyngeal function after paraoxon-ethyl exposure and the improvement by the oximes (Figure 2.10B) supports an oxime-sensitive reaction between the OP and the worm acetylcholinesterase (Figure 2.11A). In biochemical experiments using worm protein, we observed a reduction of acetylcholinesterase activity that can be rescued by the incubation with obidoxime (Figure 2.11A). In contrast, the inefficiency of the oxime treatment after paraoxon-methyl or DFP inhibition indicates an irreversible modification of the nematode enzyme by these organophosphates (Figure 2.11C and 2.11E). This was manifest by the failure to recover pharyngeal function when intoxicated worms are transferred onto either empty or oxime-containing plates (Figure 2.10C and 2.10D).

The biochemical study of spontaneous recovery and oxime-sensitive reaction in mouse acetylcholinesterase is consistent with previously published data [386,397]. Non-aged acetylcholinesterase after the exposure of paraoxon-ethyl was able to recover partially the activity in the presence of obidoxime (Figure 2.11B) while the aged acetylcholinesterase that predominates after either paraoxon-methyl or DFP inhibition could not be rescued by the oxime treatment (Figure 2.11D and 2.11F) [386,397].

To conclude, the analysis of the nematode pharyngeal function after OP intoxication might be indicative of the acetylcholinesterase state after the enzyme inhibition, spontaneous and obidoxime-induced reactivation. The simplicity of this methodology makes *C. elegans* pharynx an attractive bio-assay for high-throughput drug-screening of new reactivators, aligning with 3Rs principles. This can be combined with automated methods to quantify pharyngeal pumping to facilitate the process [351,352].

2.6. Conclusion

In previous studies, *C. elegans* body wall phenotypes have been used to understand acetylcholinesterase inhibition by organophosphate exposure and, in some of them; it was correlated with the quantification of acetylcholinesterase activity in the worm [334,335,360]. Here, we

demonstrated that the pharyngeal function represents a more precise phenotype to understand acetylcholinesterase inhibition by OP drugs. Interestingly, the rescue of the phenotype was also correlated with the rate of the acetylcholinesterase reaction upon OP inhibition as well as the efficiency of the reactivators. It makes the pharynx of *C. elegans* an attractive tool for discovering new drugs able to reactivate the inhibited acetylcholinesterase. Furthermore, clear benchmarking of this class of neurotoxicological agents in a tractable bio-assay in *C. elegans* means that genetic manipulation of these effects can be probed. This provides a new approach to investigate mitigation of such neurotoxicity that may translate to human poisoning.

2.7. Acknowledgements

We thank Dr Aleksandra Pitera and Dr Katrin Deinhardt for providing mouse brain homogenate. Additionally, *C. elegans* strains were provided by the CGC, which is funded by NIH Office of Research Infrastructure Programs (P40 OD010440).

2.8. Author contributions

Patricia G. Izquierdo: Conceptualization, Data curation, Formal analysis, Investigation, Methodology, Validation, Visualization, Roles/Writing - original draft. **Vincent O'Connor**: Conceptualization, Funding acquisition, Methodology, Supervision, Writing - review & editing. **Christopher Green**: Conceptualization, Funding acquisition, Methodology, Supervision, Writing - review & editing. **Lindy Holden-Dye**: Conceptualization, Funding acquisition, Methodology, Supervision, Writing - review & editing. **John Tattersall**: Conceptualization, Funding acquisition, Methodology, Supervision, Writing - review & editing.

2.9. Funding

This work was equally funded by the University of Southampton (United Kingdom) and the Defence Science and Technology Laboratory, Porton Down, Wiltshire (United Kingdom).

2.10. Conflict of interest

The authors declare that they have no conflicts of interest with the contents of this article.

Chapter 3

Cholinergic signalling at the body wall neuromuscular junction couples to distal inhibition of feeding in *C. elegans*

Patricia G. Izquierdo [1], Thibana Thisainathan [1], James H. Atkins [1], Christian J. Lewis [1], John E.H. Tattersall [2], A. Christopher Green [2], Lindy Holden-Dye [1], Vincent O'Connor [1].

[1] Biological Sciences, Institute for Life Sciences, University of Southampton, Southampton, United Kingdom.

[2] Dstl, Defence Science and Technology Laboratory, Porton Down, Salisbury, Wiltshire, SP4 0JQ, United Kingdom.

Key words. Acetylcholinesterase inhibitor, levamisole, pharyngeal pumping, inter-tissue communication, neuromuscular junction, tissue specific rescue.

Author for correspondence:

Patricia G. Izquierdo: P.Gonzalez@soton.ac.uk

Running title: Distal inhibition of feeding by body wall cholinergic signalling

Deposited as: Izquierdo, P.G., Thisainathan, T., Atkins, J.H., Lewis, C.J., Tattersall, J. E. H., Green, A. C., Holden-Dye, L. and O'Connor, V. (2021) Cholinergic signalling at the body wall neuromuscular junction couples to distal inhibition of feeding in *C. elegans*. *BioRxiv*. https://doi.org/10.1101/2021.02.12.430967.

Accepted to Journal of Biological Chemistry (JBC) with revision as: Izquierdo, P. G., T. Thisainathan, J. H. Atkins, C. J. Lewis, J. E. H. Tattersall, A. C. Green, L. Holden-Dye and V. O'Connor (2021) Cholinergic signalling at the body wall neuromuscular junction couples to distal inhibition of feeding in *C. elegans*.

3.1. Abstract

Complex biological functions within organisms are frequently orchestrated by systemic communication between tissues. In the model organism *C. elegans*, the pharyngeal and body wall neuromuscular junctions are two discrete structures that control feeding and locomotion, respectively. These distinct tissues are controlled by separate, well-defined neural circuits. Nonetheless, the emergent behaviours, feeding and locomotion, are coordinated to guarantee the efficiency of food intake. We show that pharmacological hyperactivation of cholinergic transmission at the body wall muscle reduces the rate of pumping behaviour. This was evidenced by a systematic screening of the cholinesterase inhibitor aldicarb's effect on the rate of pharyngeal pumping on food in mutant worms. The screening revealed that the key determinant of the inhibitory effect of aldicarb on pharyngeal pumping is the L-type nicotinic acetylcholine receptor expressed in body wall muscle. This idea was reinforced by the observation that selective hyperstimulation of the body wall muscle L-type receptor by the agonist levamisole inhibited pumping. Overall, our results reveal that body wall cholinergic transmission controls locomotion and simultaneously couples a distal inhibition of feeding.

3.2. Introduction

The communication between tissues has an important role in physiological processes in health, disease and stress conditions [398,399]. The communication between the skeletal muscle, liver and adipose tissue during exercise is a clear example of tissue communication to control energy metabolism and insulin sensitivity in that particular stress condition [400]. The imbalance of that communication causes an increase of energy expenditure associated with chronic disease or cachexia [401]. This complex process is conserved from invertebrates to mammals and can be modelled in simpler organisms such as the fruit fly *Drosophila melanogaster* [402-404].

The survival of the model organism *Caenorhabditis elegans* depends on two essential behaviours, feeding and locomotion, as well as the ability to modify them according to the environmental cues. The external presence of food is a potent stimulus that modulates the rate of feeding by increasing pharyngeal movements and the intake of the external bacterial food source [338,381,405]. Interestingly, nematodes can modify their locomotory patterns according to food availability, changing between dwelling and roaming [406,407]. In this sense, the quality and quantity of food ingested emerges as an important environmental factor to modulate the worm's motility that is directly controlled by the neuromuscular body wall [407,408]. Similarly, mechanical stimulation or the optogenetic silencing of the body wall musculature reduces the feeding rate of *C. elegans* that is otherwise directly governed by the neuromuscular cholinergic transmission at the pharynx [327,409,410]. This supports the notion that locomotory function might provide additional pathways that contribute to regulation of the pharyngeal circuits that control feeding.

Morphologically, the pharynx is divided into three different parts: the corpus, the isthmus and the terminal bulb. Two pharyngeal movements are responsible for the transport of bacteria by ingestion via the buccal cavity to the intestines [336,339,411]. The coordinated contraction-relaxation cycle of the corpus and the terminal bulb causes the opening of the lumen in these parts of the pharynx that results in the aspiration of bacteria into the cavity. This rhythmic movement is named pharyngeal pumping and is caused by the release of acetylcholine and glutamate from the MC and M3 pharyngeal neurons that contract and relax the pharyngeal muscle, respectively [307,340]. The bacteria accumulated in the corpus during the pumping are directed to the terminal bulb by the progressive wavelike contractions of the muscles in the isthmus. This peristalsis movement depends on acetylcholine released from the pharyngeal motor neuron M4 [337,379]. One of the 20 pharyngeal neurons that more widely supports regulation of feeding. This circuit is isolated from the rest of the animal by a basal lamina [336]. A single synaptic connection is described between the pharynx and the rest of the animal (I2-RIP). However, disruption of this connection does not cause any defect in the feeding phenotype, indicating that this anatomical route does not mediate a strong determinant of the pharyngeal modulation of feeding [411]. This points to a more important

role of neuromodulatory signalling via biogenic amines and peptides, involving volume transmission [381].

The molecular composition of the transmitter functions that control the pharyngeal neuromuscular junction and the feeding phenotype is poorly described. The glutamate-gated chloride channel AVR-15 acts postsynaptically in the pharyngeal muscle to sense glutamate released from the motor neuron M3 that cause muscle relaxation [340,346]. EAT-2 is a Cys-loop acetylcholine receptor subunit localized at the synapse between the pharyngeal MC motor neuron and the muscle at the corpus. It requires the auxiliary protein EAT-18 to allow EAT-2 essential function in initiating contraction [296,307]. Mutations in *avr-15* and *eat-2* phenocopy the feeding behaviour of nematodes with M3 and MC ablated neurons, respectively, highlighting the critical role these receptor components play [307,340,346]. The feeding phenotype additionally requires the release of acetylcholine by the motor neuron M4, triggering isthmus peristalsis [337]. However, there is not any mutation in an acetylcholine receptor that phenocopies the M4 ablation and the molecular determinants of this feeding critical function are unknown.

In order to better understand the pharyngeal neuromuscular junction of *C. elegans*, we performed a targeted screen of the pumping behaviour on food with defined molecular determinants of cholinergic transmission in the presence or absence of aldicarb. This acetylcholinesterase inhibitor has been previously used to induce paralysis of movement and this led to the discovery of molecular components at the body wall neuromuscular junctions in *C. elegans* [331,332]. We found that the genes conferring significant drug sensitivity of the pharyngeal paralysis are surprisingly located in the body wall neuromuscular junction. Additionally, we describe how the stimulation of the L-type receptor at the body wall muscle by the specific agonist levamisole reduced the pharyngeal pumping rate. This indicates an unexpected communication between the body wall neuromuscular junction that controls locomotion and the distinct and physically separated pharyngeal circuit that controls feeding.

3.3. Materials and methods

3.3.1. *C. elegans* maintenance and strains

Nematodes were maintained at 20°C on NGM plates supplemented with *E. coli* OP50 strain as a source of food [258]. *C. elegans* mutant strains are listed in Table 1 and were provided by Caenorhabditis Genetics Center (CGC) unless otherwise specified. Mutant strains EN39 *oig-4 (kr39)* II, EN300 *rsu-1 (kr300)* III and EN100 *molo-1 (kr100)* III were kindly provided by Jean-Louis Bessereau Lab (Institut NeuroMyoGène, France). ZZ427 *lev-1 (x427)* and transgenic lines AQ585 corresponding to N2; *Ex[Plev-1::gfp; rol-6]* genotype and AQ749 corresponding to ZZ427 *lev-1 (x427)* IV*; Is[Plev-1::lev-1::HA::gfp; rol-6]* genotype were kindly provided by William Schafer Lab

(MRC Laboratory of Molecular Biology, UK). The transgenic lines GE24 *pha-1 (e2123)* III; *Ex[Punc-17::gfp; pha-1 (+)]* and N2; *Is[Peat-4::ChR2::mrfp]* were previously available in the laboratory stock.

The following transgenic lines were generated in this work: VLP1: CB211 *lev-1 (e211)* IV; *Ex[Punc-122::gfp]*; VLP2: CB211 *lev-1 (e211)* IV; *Ex[Punc-122::gfp; Pmyo-3::lev-1]*; VLP3: ZZ427 *lev-1 (x427)* IV; *Ex[Punc-122::gfp]*; VLP4: ZZ427 *lev-1 (x427)* IV; *Ex[Punc-122::gfp; Pmyo-3::lev-1]*; VLP5: CB211 *lev-1 (e211)* IV; *Ex[Punc-122::gfp; Plev-1::lev-1]*; VLP6: ZZ427 *lev-1 (x427)* IV; *Ex[Punc-122::gfp; Plev-1:lev-1]*.

3.3.2. Generation of lev-1 rescue constructs.

PCR amplifications were performed using Phusion High-Fidelity PCR Master Mix with HF Buffer (Thermo Fisher Scientific) following manufacturer instructions unless otherwise is specified.

PCR was used to amplify sequence for the *myo-3* promoter. 2.3 kb upstream of *myo-3* was amplified using the primers 5' TCCTCTAGATGGATCTAGTGGTCGTGG 3' and 5' ACCAAGCTTGGGCTGCAGGTCGGCT 3' (58°C annealing temperature). This was subsequently cloned into pWormgate expression vector using the indicated restriction sites incorporated into the 5' end of the oligonucleotides indicated above (HindIII/XbaI).

The primers 5' ATGCTAGCTCTCATAACACTCAAGAAAACCCA 3' and 5' CCTCTATCCTCCACCACCTCCTAAC 3' were used to amplify 3.536 kb of *lev-1 locus* corresponding to 3.5 kb upstream of the starting codon and 36 pb of exon one. PCR conditions for amplification were: initial 3 min at 98ºC following of 34 cycles consisting of 1 min at 98ºC, annealing 1 min at 57ºC, extension 3:30 min at 72ºC and a final extension 10 min at 72ºC. Amplification product was cloned into pWormgate expression vector using the restriction site NheI underlined in forward primer and the naturally occurred XbaI restriction site 4 pb upstream of the *lev-1* starting codon.

cDNA of *lev-1* was amplified from a *C. elegans* cDNA library (OriGene) using 5' AGAGAGAATGATGTTAGGAGG 3' and 5' AGTTGAAAATGAAAGAATAATGG 3' (55°C annealing temperature) forward and reverse primers, respectively. The PCR product was subcloned into pCR8/GW/TOPO following manufacturer protocol and subsequently cloned into pWormgate plasmid containing either *Pmyo-3* or *Plev-1* in order to generate *Pmyo-3::lev-1* and *Plev-1::lev-1* plasmids, respectively. The sequence of the plasmids was validated by Sanger sequencing before microinjection.

3.3.3. Generation of transgenic lines.

The marker plasmid *Punc-122::gfp* was kindly provided by Antonio Miranda Lab (Instituto de Biomedicina de Sevilla, Spain). It drives the expression of GFP specifically in coelomocytes of *C. elegans* [412].

The microinjection procedure was performed as previously described [413]. A concentration of 50 ng/µl of the marker plasmid *Punc-122::gfp* was injected into one day old adults of the CB211 *lev-1 (e211)* IV and ZZ427 *lev-1 (x427)* IV mutant background to generate the transgenic strains VLP1 and VLP3, respectively. A mixture of 50 ng/µl of *Punc-122::gfp* plasmid and 50 ng/µl of *Pmyo-3::lev-1* plasmid was microinjected into adults of CB211 and ZZ427 strains to produce the transgenic lines VLP2 and VLP4, respectively. Finally, transgenic strains VLP5 and VLP6 were generated by microinjecting adults of the *lev-1 (e211)* and *lev-1 (x427)* mutant backgrounds with a mixture of 50 ng/µl of *Punc-122::gfp* plasmid and 50 ng/µl of *Plev-1::lev-1* plasmid, respectively.

The genotype of CB211 and ZZ427 strains was authenticated by PCR amplification of the *lev-1* gene and subsequent sequencing of the PCR product before microinjection was carried out.

3.3.4. Plate husbandry

Aldicarb and levamisole hydrochloride (Merck) were dissolved in 70% ethanol and water, respectively. The stock drugs were kept at 4°C and used within a month or discarded.

Behavioural experiments were performed at room temperature (20°C) in 6-well plates that were prepared the day before of each experiment. Drug-containing plates were made by adding a 1:1000 aliquot of the concentrated stock to molten tempered NGM agar to give the indicated concentration of aldicarb (500 µM) and levamisole (10 µM to 500 µM). For aldicarb control plates, a similar aliquot of 70% ethanol was added to the molten agar. The final concentration of ethanol for control and aldicarb-containing plates was 0.07%. This concentration of ethanol did not affect any of the behavioural tests performed in this work (data not shown).

For protracted intoxication experiments, 50 µl of OP50 bacteria culture OD_{600} 1 was pipetted onto the solidified NGM assay plates containing either drug or vehicle. For the first 10 min of exposure to levamisole (early intoxication experiment), assay plates were seeded with 100 µl of OP50 bacteria culture of one OD_{600} that was spread evenly over the complete surface of the NGM agar. After seeding, plates were left in the laminar flow hood for one hour to facilitate drying of the bacterial lawn. 6-well plates containing either levamisole or aldicarb with bacterial lawn were then stored in dark at 4°C until next day. Assay plates were incubated at room temperature for at least 30 min before starting the experiment. Contrary to assay plates with other cholinergic drugs

[382], we did not observe any difference in the density or integrity of the bacterial lawn between control and drugged plates.

3.3.5. Behavioural observations

A pharyngeal pump as a cycle consists of contraction-relaxation of the terminal bulb in the pharyngeal muscle. Each pump was discerned by the backward-forward movement of the grinder structure in the terminal bulb. The quantification was made visually under a binocular dissecting microscope Nikon SMZ800 (x60 magnification) using a clicker counter.

For protracted intoxication experiments, synchronized nematodes one day older than L4 stage (L4 + 1) were transferred onto the assay plates and the pumping measured after 24 hours for aldicarb intoxication assays and after 10 min, 1, 3, 6 and 24 hours for levamisole intoxication experiments. Nematodes that left the patch of food during the experiment were picked back to the bacterial lawn and the pumping rate was scored after waiting for between 10-15 min.

For the first 10 min of exposure to levamisole, synchronized (L4 + 1) adults were picked onto either control or levamisole-containing plates. The delay between each pump was scored for the consecutive 10 min straight after transferring each worm using Countdown Timer tool from www.WormWeb.org website. It was then translated into pumping rate per second.

3.3.6. Pharynx dissection procedure

Dissection of the pharynxes was performed according to previously published methods [383]. Young adult (L4 + 1) worms were placed into dissection plates containing 3 ml of Dent's solution (glucose 10 mM, HEPES 10 mM, NaCl 140 mM, KCl 6 mM, $CaCl_2$ 3 mM, $MgCl_2$ 1 mM) supplemented with 0.2% bovine serum albumin (Merck). Dishes were incubated at 4°C for 5 min to reduce the thrashing activity of the nematodes and then placed under a binocular microscope Nikon SMZ800. The lips of the worms were dissected from the rest of the body by making an incision with a surgical scalpel blade. Due to the internal pressure of the inside organs of the worm, the content is ejected outside the cuticle of the nematode leaving the pharynx and its embedded circuit exposed. When the terminal bulb was clearly observed outside the cuticle, a second incision was made at the pharyngeal-intestinal valve to isolate the pharynx from the rest of the intestines (Figure 3.4). Pharynxes lacking more than half of the procorpus after dissecting were not considered for either imaging or for RT-PCR.

3.3.7. Differential interference contrast (DIC) and fluorescence imaging of pharyngeal structure and transgene expression.

Isolated pharynxes were removed from dissection dishes using non-sticky tips within 10 µl of solution. Fat and debris were carefully removed from the pharynxes by two sequential transfers,

in a volume of 10 µl, through two changes of 3 ml Dent's 0.2% BSA media. After washing, the pharynxes were placed on a thin pad of 2% agarose previously deposited and solidified on a microscope slide. A 24x24 mm coverslip was gently located on top before observations were made. Objectives of 10x/0.30, 60x A/1.40 (oil) and 100x A/1.40 (oil) fitted in a Nikon Eclipse (E800) microscope were used to collect images through both DIC and epifluorescence filters. A Nikon C-SHG1 high pressure mercury lamp was used for illumination in fluorescence micrographs.

Images were acquired through a Hamamatsu Photonics camera software, and were cropped to size, assembled, and processed using Abode PhotoShop® (Adobe Systems) and ImageJ (NIH) software.

Two transgenic strains harbouring *Punc-17::gfp* and *Peat-4::rfp* were used as control of the dissection procedure. They are both transcriptional reporters of cholinergic and glutamatergic neurons, respectively. Isolated pharynxes from the two transgenic strains were isolated and imaged following the previously explained protocol. Fluorescent from distinct neurons was observed upon the dissection procedure (data not shown) indicating the pharyngeal neurons were preserved in the isolated pharynx preparations.

3.3.8. RT-PCR from whole worms and isolated pharynxes

RT-PCR for single worm and isolated pharynxes was performed following previously published method with modifications [414]. A single worm or isolated pharynxes were placed into 1 µl of worm lysis buffer containing a final concentration of 5 mM Tris pH8, 0.25 mM EDTA, 0.5% Triton X100, 0.5% Tween 20 and 1 mg/ml proteinase K. After a brief centrifugation, the mixture containing either the single worm or the isolated pharynxes, was incubated at 65°C for 10 min and at 85°C for 1 min into a T100™ thermocycler (Bio-Rad). The heated lysate was subsequently used in cDNA synthesis with SuperScript™ III Reverse Transcriptase kit in a total volume of 20 µl following manufacturer protocol (Invitrogen™). 5 µl of the resulting cDNA was used for a final volume of 20 µl PCR with indicated oligo primers. PCR amplifications were performed employing Phusion High-Fidelity PCR Master Mix with HF Buffer (Thermo Scientific™) following manufacturer's recommendations.

The primers used for the PCR extensions were 5' GGACAGGGAGCCGAGAAGAC 3' and 5' GAAGCATCGTTAAGGAAAGTCAGG 3' (64°C annealing temperature) for *myo-2*; 5' GTGAATAGTCAGTTGGTGATGG 3' and 5' TGCGAAAATAAGTGCTGTGGTG 3' (66°C annealing temperature) for *eat-2*; 5' CTGCTCGTCCTTTTGATTCC 3' and 5'- GTTTCCCTTCACAGTTACCAC -3' (58°C annealing temperature) for *myo-3*; 5' ATGTTAGGAGGTGGTGGAGG 3' and 5' GTTGAACGAGAGAGTTGTATCC 3' (66°C annealing temperature) for *lev-1*.

3.3.9. Statistical analysis

The collection of the data was performed blind, so the experimenter was unaware of the genotype and the drug present, absent or concentration tested in each trial.

Data were analysed using GraphPad Prism 8 and are displayed as mean ± SEM. Statistical significance was assessed using two-way ANOVA followed by post hoc analysis with Bonferroni corrections where applicable. This post hoc test was selected among others to avoid false positives. The sample size N of each experiment is specified in the corresponding figure.

3.4. Results

3.4.1. The determinants that control pharyngeal function are distinct from the determinants that control pharyngeal sensitivity to aldicarb.

In order to investigate the cholinergic regulation of the feeding behaviour, the well-characterized protocol of aldicarb-induced paralysis was performed [331,332]. This assay has been extensively used to find molecular determinants at the neuromuscular junction of the body wall muscle on the basis of resistance or hypersensitivity to paralysis of locomotion when nematodes are incubated on aldicarb-containing agar plates [331]. We previously demonstrated that aldicarb and other cholinesterase inhibitors also cause a dose-dependent inhibition of the pharyngeal function (Figure 2.4 and Figure 2.7) [415]. This inhibition was associated with the pharynx exhibiting hypercontraction observed by the opening of the lumen (Figure 2.4) [415]. This implied that aldicarb intoxication in the context of the whole organism would result from drug-induced hyperactivation of the cholinergic transmission. In this sense, we hypothesized that molecular determinants in the pharynx would confer resistance or hypersensitivity to aldicarb-induced paralysis of feeding behaviour.

We screened the pharyngeal function of different mutant worms in the presence or absence of the cholinesterase inhibitor aldicarb under the conditions we previously optimized [415]. The results of this screening are listed in Table 1. It consisted of 53 mutant strains deficient in cholinergic and other neurotransmitters signalling. The components of the cholinergic pathway tested included alpha and non-alpha subunits of the acetylcholine-gated cation channel [299], subunits of the nematode selective acetylcholine-gated chloride channel [294], muscarinic acetylcholine receptors [300,303,305,416], acetylcholinesterases [59,67,264] and auxiliary proteins involved in the proper function of the cholinergic receptors [265,296,307,311,313-315,317,322,333,417,418] (Table 3.1). This analysis can be conveniently summarized by ascribing responses into three different groups of mutants regarding their pharyngeal pumping on food in the absence and presence of aldicarb (Figure 3.1).

Table 3.1. Pharyngeal pumping rate on food in the absence or presence of aldicarb. Synchronized L4 + 1 nematodes were incubated for 24 hours onto seeded plates containing aldicarb or vehicle control before pumping rate per minute was quantified. Wild type strain is highlighted in green. Refer to figure 3.1 for colour code. nAChR: acetylcholine-gated cation channel; mAChRs: muscarinic acetylcholine receptors; AChEs: acetylcholinesterases; APs: auxiliary proteins; NTs: neurotransmitters. Statistical analysis corresponds to the comparison between each strain and the N2 wild type control in each condition (off and on aldicarb). The quantification of pumping rate on and off aldicarb of mutant deficient in acetylcholine-gated chloride channel subunits, muscarinic acetylcholine receptors, acetylcholinesterases, auxiliary proteins involved in the location of nicotinic receptors and neurotransmitter signalling were performed by James H. Atkins. Statistical analysis was not considered due to non-normal distribution of the sample in some of the observations.

Classification	**Strain**	**Gene**	**Allele**	**Pumps/min ± SEM**	**N**	**Pumps/min ± SEM**	**N**
	N2			249.4 ± 1.7	52	9.5 ± 1.9	48
alpha-nAChR subunits	DH404	*unc-63*	*b404*	178.4 ± 5.9	12	47.1 ± 14.9	12
	VC1041	*lev-8*	*ok1519*	251 ± 4	6	23.2 ± 12	5
	ZZ20	*unc-38*	*x20*	230.8 ± 4.3	9	22.8 ± 4.5	9
	CB904	*unc-38*	*e264*	221 ± 4.6	12	8 ± 2.3	12
	TU1747	*deg-3*	*u662*	143.9 ± 23.3	8	7.1 ± 4.2	8
	NC293	*acr-5*	*ok180*	253.8 ± 1.5	9	4.3 ± 1.5	9
	RB2294	*acr-6*	*ok3117*	185.1 ± 6	9	14.3 ± 9	9
	FX863	*acr-7*	*tm863*	256.4 ± 1.9	9	3.3 ± 1.7	9
	RB1195	*acr-8*	*ok1240*	244.1 ± 2.4	9	13.5 ± 3.9	9
	RB2262	*acr-10*	*ok3064*	196.3 ±20.4	6	2 ± 1	6
	RB1263	*acr-11*	*ok1345*	252.6 ± 1.6	9	3.1 ± 2	8
	VC188	*acr-12*	*ok367*	252.6 ± 2.1	9	76.8 ± 15.7	9
	RB1172	*acr-15*	*ok1214*	251.8 ± 0.8	7	31.9 ± 9.1	7
	RB918	*acr-16*	*ok789*	242.9 ± 1.1	9	0.9 ± 0.5	9
	RB1226	*acr-18*	*ok1285*	236.8 ± 3.5	9	1.6 ± 0.5	9
	DA1674	*acr-19*	*ad1674*	246.3 ± 3	8	3.3 ± 0.9	8
	RB1250	*acr-21*	*ok1314*	240 ± 3.2	8	1.9 ± 0.8	8
	RB2119	*acr-23*	*ok2804*	230.2 ± 2	9	2.3 ± 0.7	9
non-alpha nAChR subunits	CB193	*unc-29*	*e193*	227.3 ± 3.3	8	52.3 ± 10.2	7
	CB211	*lev-1*	*e211*	244.8 ± 2.7	15	131.7 ± 15.8	15
	ZZ427	*lev-1*	*x427*	253.7 ± 8.9	4	113.2 ± 36.2	4
	DA465	*eat-2*	*ad465*	50.3 ± 2.7	14	0.5 ± 0.2	11
	RB1559	*acr-2*	*ok1887*	254.4 ± 2	8	62.5 ± 20.8	8
	RB1659	*acr-3*	*ok2049*	235.8 ± 6.8	9	21.8 ± 6.8	9
	VC649	*acr-9*	*ok933*	217.3 ± 5.6	9	11.3 ± 3.7	9
	RB1132	*acr-14*	*ok1155*	250.8 ± 1.5	9	0.8 ± 0.4	9
	FX627	*acr-22*	*tm627*	227.1 ± 7.1	7	5.9 ± 2.2	7
ACh-gated Cl channel subunits	VC1757	*acc-2*	*ok2216*	210.4 ± 20	9	20.5 ± 8.7	5
	RB2490	*acc-3*	*ok3450*	153.7 ± 13.6	8	39.2 ± 14.3	7
	RB1832	*acc-4*	*ok2371*	225.3 ± 15.7	4	5.5 ± 4.1	4

mAChRs	RB896	*gar-1*	*ok755*	222.3 ± 3.8	4	24.8 ± 23.8	4
	RB756	*gar-2*	*ok520*	224.6 ± 4.6	6	12.5 ± 4.4	4
	VC670	*gar-3*	*gk337*	252.8 ± 3.4	6	7 ± 6.3	4
AChEs	VC505	*ace-1*	*ok663*	226.3 ± 12	5	2.8 ± 2.4	4
	GG202	*ace-2*	*g72*	235.5 ± 2.8	3	6.8 ± 3.7	3
	PR1300	*ace-3*	*dc2*	235.6 ± 6.9	4	3.6 ± 3.1	4
Ancillary proteins	MF200	*ric-3*	*hm9*	201 ± 11.3	6	74.1 ± 17.1	6
	CB306	*unc-50*	*e306*	223 ± 7.5	4	8.7 ± 4.3	3
	CB883	*unc-74*	*e883*	232.1 ± 2.1	4	5.9 ± 3.7	4
APs involved in location of nAChRs	RB1717	*lev-9*	*ok2166*	236.5 ± 6	6	94.9 ± 33.2	4
	ZZ17	*lev-10*	*x17*	239.7 ± 3.5	6	83.6 ± 25	4
	EN39	*oig-4*	*kr39*	227.4 ± 10.7	4	7 ± 5.3	3
	EN300	*rsu-1*	*kr300*	243.9 ± 4.9	4	20.4 ± 18.4	4
Other APs	DA1110	*eat-18*	*ad1110*	65.9 ± 3.3	6	1.6 ± 0.7	4
	PR675	*tax-6*	*p675*	222.1 ± 7.8	4	17.1 ± 7.5	4
	KJ300	*cnb-1*	*jh103*	193.6 ± 6.3	6	1.8 ± 0.8	6
	HK30	*unc-68*	*kh30*	231.2 ± 9	4	21.3 ± 11.6	4
	EN100	*molo-1*	*kr100*	249.4 ± 2.7	6	19.4 ± 3.7	4
NTs signalling	MT6308	*eat-4*	*ky5*	211.6 ± 7	4	9.6 ± 8.9	5
	VC862	*cho-1*	*ok1069*	206 ± 19.4	4	29 ± 12.7	4
	GR1321	*tph-1*	*mg280*	217.1 ± 6	4	13.3 ± 8.3	3
	RB681	*cat-1*	*ok411*	241.5 ± 7.4	4	30.5 ± 5.5	3
	CB156	*unc-25*	*e156*	225 ± 2.6	4	3.8 ± 2	4

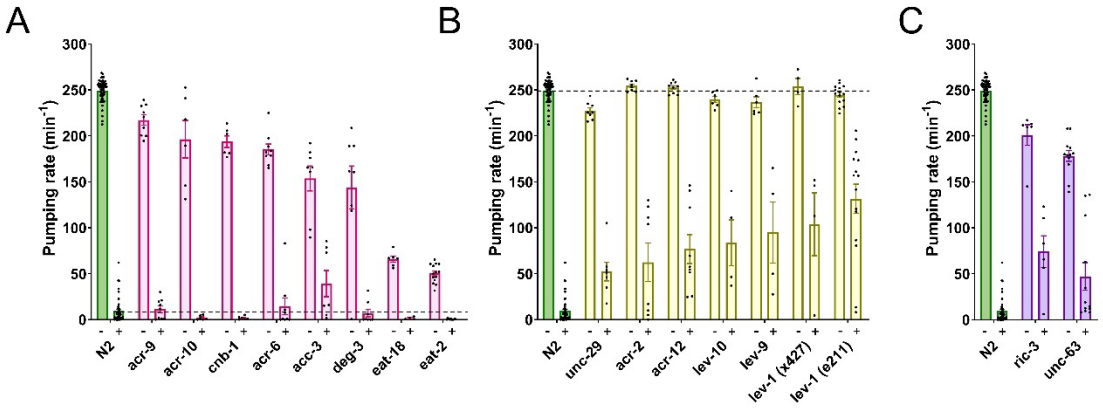

Figure 3.1. Molecular determinants that control pharyngeal function might be distinct from the determinants that confer pharyngeal resistance to aldicarb. Pharyngeal pumping on food in the absence (-) or presence (+) of 500 µM aldicarb. A) Mutant nematodes deficient in the non-alpha acetylcholine-gated cation channel subunits ACR-9 and EAT-2; the alpha acetylcholine-gated cation channel subunits ACR-10, ACR-6 and DEG-3; the acetylcholine-gated chloride channel subunit ACC-3 and the acetylcholine receptor auxiliary proteins EAT-18 and CNB-1 exhibited a reduction of the pumping rate on food but a normal sensitivity to aldicarb compared to the wild type control. These mutants are represented in pink in this figure and in Table 3.1. B) Mutant nematodes deficient in the non-alpha acetylcholine-gated cation channel subunits UNC-29, LEV-1 and ACR-2; the alpha acetylcholine-gated cation channel subunit ACR-12 and the

acetylcholine receptor auxiliary proteins LEV-9 and LEV-10 exhibited normal pumping rate on food but increased resistant to aldicarb compared to the wild type worms. These mutants are highlighted in yellow in this figure and in Table 3.1. C) Nematodes deficient in the ancillary protein RIC-3 and the alpha acetylcholine-gated cation channel subunit UNC-63 presented both phenotypes, reduced pumping rate on food and resistance to aldicarb compared to the wild type control. These group of mutants is represented in purple in both this figure and in Table 3.1. Data are shown as mean ± SEM of the pumping per minute. Statistical analysis was not performed due to non-normal distribution of the sample in some of the observations. Refer to Table 3.1 for N numbers.

One class of mutants showed reduced pumping rate in the absence of aldicarb but wild type inhibition of pharyngeal pumping in the presence of the drug (Figure 3.1A). This class of mutants clearly harbours an important contribution to feeding at physiological levels of cholinergic stimulation when nematodes are on food. However, despite this essential contribution, no resistance to the inhibition was observed when the cholinergic stimulation increased as a consequence of aldicarb exposure. According to this, we identified this class of mutants as "physiological determinants" of the feeding phenotype. This is exemplified by the *eat-2* and *eat-18* mutants. In addition, mutant nematodes deficient in the subunits of the acetylcholine-gated cation channel DEG-3, ACR-6, ACR-9 and ACR-10, the subunit of the acetylcholine-gated chloride channel ACC-3 and the calcineurin CNB-1 exhibited a similar pattern of reduced pumping when they are off drug and similar pharyngeal inhibition on aldicarb compared to the response shown by the N2 wild type (Figure 3.1A).

The second class of mutants essentially described the opposite of the above. These mutants showed normal pumping rate on food relative to N2 but clear resistance to the aldicarb-induced inhibition of the pharyngeal function observed in the wild type treated worms (Figure 3.1B). The effect of this second class of determinants in the pharyngeal function was only apparent when the cholinergic transmission was overstimulated beyond the physiological levels by preventing acetylcholine degradation due to acetylcholinesterase inhibition by aldicarb. Therefore, we named this group "pharmacological determinants" of feeding. These mutants included the well characterized subunits of the acetylcholine-gated cation channel UNC-29, ACR-2, ACR-12 and LEV-1, along with the auxiliary proteins LEV-9 and LEV-10 (Figure 3.1B). Interestingly, all the pharmacological determinants of the pharyngeal function are essential determinants of the body wall neuromuscular junction that controls locomotion [283,295,315,333].

Finally, the third class of mutants showed clear deficiency in the two distinct contexts, namely pumping on food in the absence of drug, and resistance to aldicarb-induced inhibition of the pharyngeal function (Figure 3.1C). Only two genes of those tested were encompassed in this group (Figure 3.1C), the alpha subunit of the L-type receptor UNC-63 and the chaperone of the nicotinic receptors RIC-3 [289,309].

Overall, the results suggest an unexpected divergence in cholinergic determinants of the pharyngeal function. Some of these control the physiological transmission that underpins fast pumping rate on food and others the hypothesized aldicarb-dependent process that executes an inhibition of feeding in the presence of the drug.

3.4.2. The pharyngeal function of *C. elegans* exposed to levamisole exhibits a complex dose- and time- dependent inhibition.

The pharmacological determinants of the pharyngeal function highlighted in the previous screening with aldicarb (Figure 3.1B) are known to underpin the mode of action of the nematode selective pharmacological agent levamisole. This drug acts as an agonist of the body wall muscle nicotinic L-type receptor causing a spastic paralysis, essential for its use as a nematicide [419-421]. Although distinct in its mode of action, levamisole, like aldicarb intoxication, leads to a hyperstimulation of the cholinergic synapses in the nematodes [421].

Accordingly, we investigated the levamisole response in the pharyngeal circuit by quantifying the pharyngeal pumping of wild type worms to increasing concentrations of drug over time (Figure 3.2). Interestingly, nematodes displayed a profound initial inhibition of pharyngeal pumping rate when they were placed on levamisole-containing plates (Figure 3.2A). This reduction of the pharyngeal pumping was observed after control worms recovered from the mechanical stimulation caused by the picking process, which inhibits the feeding temporally (Figure 3.2A) [409]. The IC_{50} value calculated after 10 minutes of incubation onto levamisole plates was 140.3 µM (Figure 3.2B).

After this initial inhibition of the pharyngeal function by levamisole, wild type nematodes exhibited a partial recovery of the pumping rate over time at the lowest concentrations tested (10 µM and 50 µM) but the pumping was profoundly inhibited at the highest doses (250 µM and 500 µM) (Figure 3.2C). This recovery of the pharyngeal function impacted on the IC_{50} value calculated, being 199.5 µM after 24 hours of incubation on levamisole-containing plates (Figure 3.2D).

The fact that both levamisole and aldicarb inhibit pumping rate on wild type worms, and that inhibition is additionally reduced in *lev-1* deficient mutants for both drugs support the hypothesis that the pharmacological hyperstimulation of the cholinergic system by either aldicarb or levamisole inhibits pharyngeal pumping by a common mechanism.

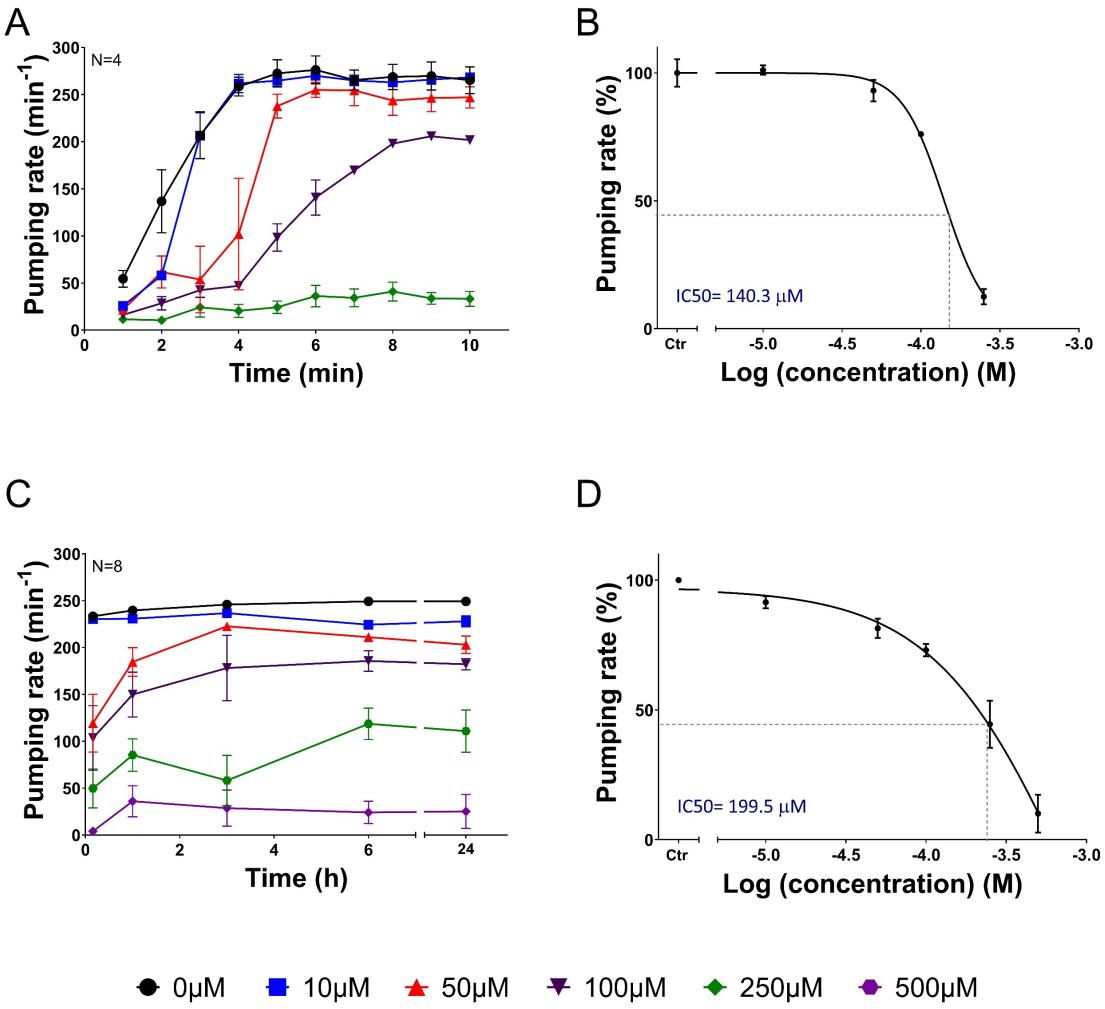

Figure 3.2. Pharyngeal function of *C. elegans* exposed to levamisole exhibited a complex concentration and time-dependent inhibition. A) Pharyngeal pumping was quantified for synchronized L4 + 1 nematodes immediately after transferring to either naïve or levamisole-containing plates. The initial picking-mediated inhibition of pumping [409] was recovered within 4 min. Nematodes picked onto levamisole-containing plates displayed a delayed dose-dependent recovery of the pharyngeal function after picking. Data are shown as mean + SEM of the pumping rate of 4 worms in 4 different experiments. The experiment was performed by Christian J. Lewis. B) IC_{50} value for pharyngeal inhibition by levamisole after 10 min of incubation. C) Pharyngeal pumping rate was quantified for synchronized L4 + 1 nematodes at different range of concentrations of levamisole over the time. An increased dose-dependent response was observed. Data are shown as mean + SEM of the pumping rate of 8 worms in 4 different experiments per dose. The experiment was performed by James H. Atkins. D) IC_{50} value for pharyngeal inhibition by levamisole after 24 hours of exposure. Data are shown as mean + SEM of the pumping per minute of 8 nematodes in 4 independent experiments. Statistical analysis was not considered due to low N number presented in graph 3.2A.

3.4.3. The extra-pharyngeal nicotinic receptor subunit LEV-1 is a key determinant of levamisole inhibition of pharyngeal pumping.

To more clearly resolve the molecular pathway through which the pharyngeal inhibition is mediated, we focused on the quantification of the pharyngeal function of *lev-1* deficient strains in the presence of levamisole (Figure 3.3). The LEV-1 subunit was highlighted in our screen due to the selective contribution to aldicarb-induced modulation of the feeding (Figure 3.1B). In addition,

the LEV-1 subunit was originally identified as a determinant of body wall muscle sensitivity to levamisole [283].

Strains deficient in *lev-1* displayed a similar inhibition of the pharyngeal function as wild type worms after 10 minutes of incubation on 250 µM levamisole plates (Figure 3.3). However, the pumping rate completely recovered over the time, being similar to the non-drug exposed nematodes after 3 hours of incubation (Figure 3.3B and 3.3C). This phenotype was consistent in the two *lev-1* deficient strains tested, indicating the LEV-1 subunit of the nicotinic receptor is not responsible for the pharyngeal inhibition by levamisole at early exposure times, but its function is indeed required at the later exposure times.

These results highlight two distinct components of a complex response to worm intoxication by levamisole. While the rapid effect is independent of *lev-1*, the late sustained inhibition is clearly *lev-1* dependent. This points to an overlapping mechanism for the aldicarb and levamisole-induced inhibition of the pharynx at protracted intoxication conditions. This mechanism is mediated by a LEV-1 containing receptor.

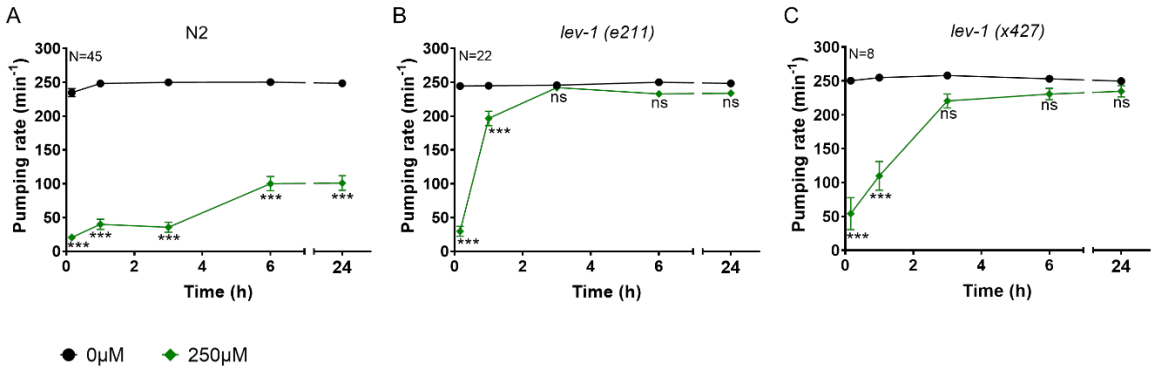

Figure 3.3. The non-alpha subunit LEV-1 of the heteromeric cholinergic receptor is responsible of the pharyngeal inhibition in the presence of levamisole at later end-point times. A) Pharyngeal pumping was measured in the presence or absence of 250 µM of levamisole. Data are shown as mean ± SEM of the pumping rate of 45 worms in at least 25 independent experiments. B) Pumping rate of CB211 *lev-1* strain in the presence or absence of 250 µM levamisole. Data are shown as mean ± SEM of 22 worms in at least 10 independent experiments. C) Pharyngeal pumping rate of ZZ427 *lev-1* mutant strain nematodes onto naïve or levamisole-containing plates. Data are shown as mean ± SEM of the pumping per minute of 8 nematodes in 4 independent experiments. Statistical analysis corresponds to the comparison between pumping rate on and off levamisole plates in each end-point time of incubation $^{ns}p>0.05$; ***$p<0.001$ by two-way ANOVA test. The experiment was performed by James H. Atkins and Thibana Thisainathan.

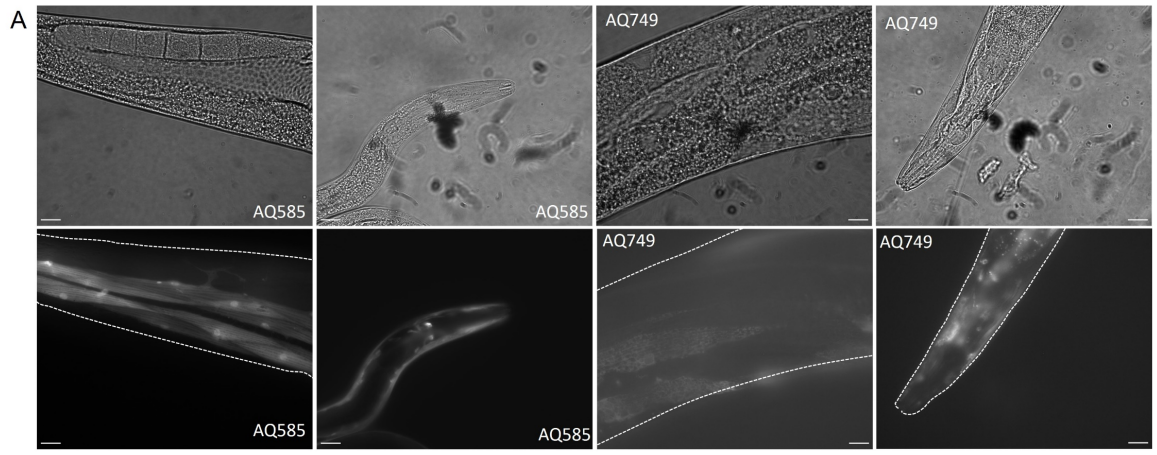
A
AQ585
AQ585
AQ749
AQ749
AQ585
AQ585
AQ749
AQ749

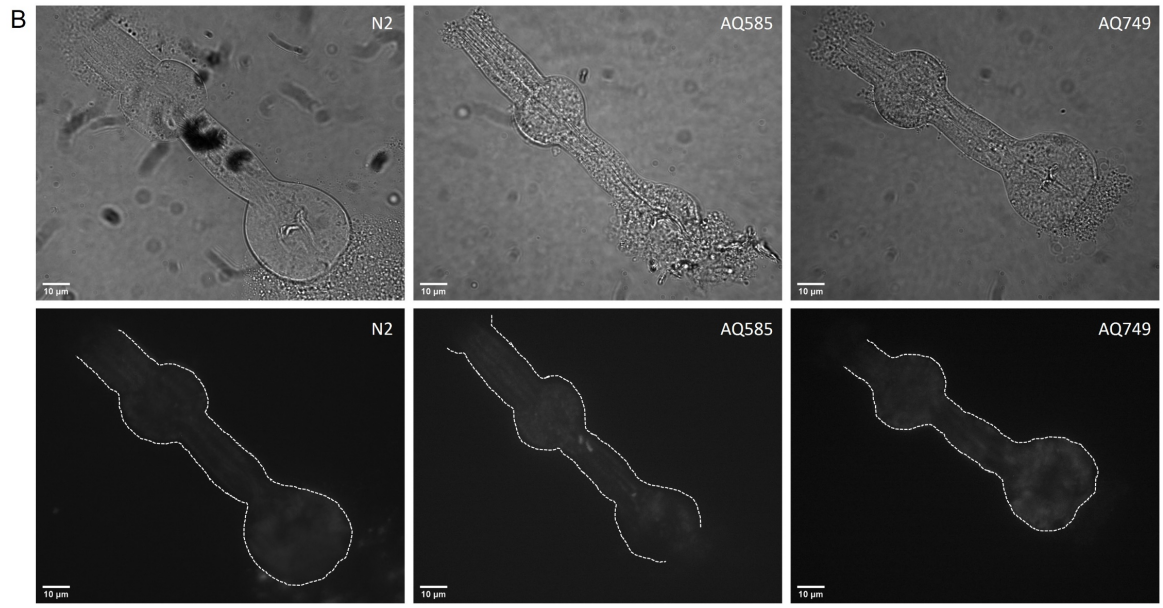
B
N2
AQ585
AQ749
N2
AQ585
AQ749
10 µm

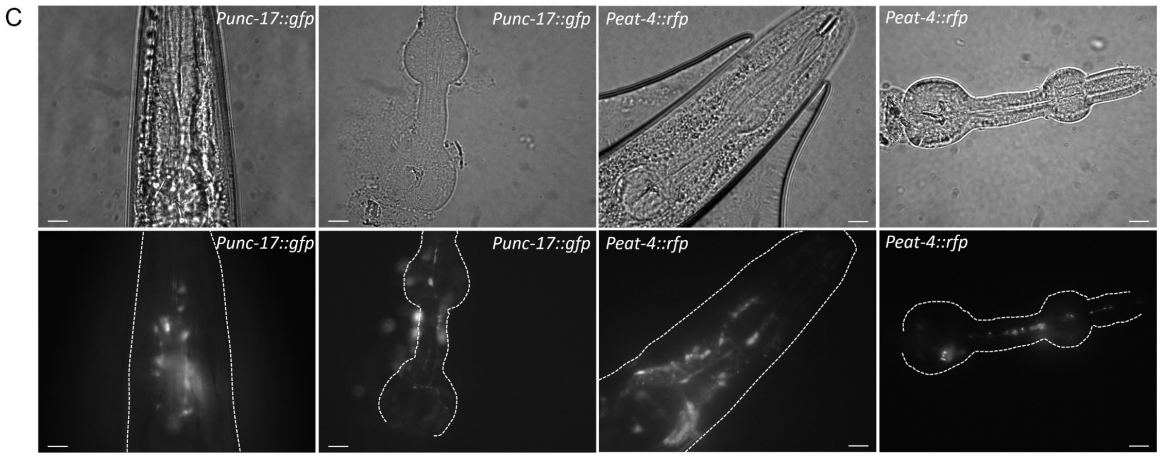
C
Punc-17::gfp
Punc-17::gfp
Peat-4::rfp
Peat-4::rfp
Punc-17::gfp
Punc-17::gfp
Peat-4::rfp
Peat-4::rfp

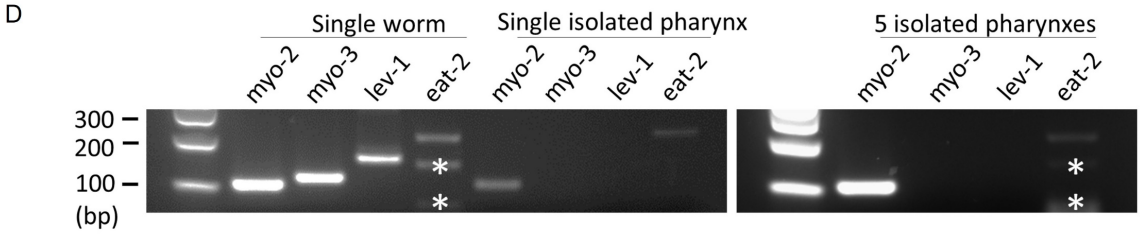
D
Single worm
Single isolated pharynx
5 isolated pharynxes
myo-2
myo-3
lev-1
eat-2
300
200
100
(bp)

Figure 3.4. The determinants that control aldicarb and levamisole sensitivity in the pharynx are not expressed in the pharyngeal muscle of embedded circuits. A) Representative images of *lev-1* expression in two transgenic lines. The strain AQ585 corresponds to a transcriptional reporter that expressed GFP under *lev-1* promoter in a wild type background. The strain AQ749 corresponds to a translational reporter expressing the coding sequence of *lev-1* tagged with GFP under the control of *lev-1* naïve promoter in a *lev-1* (x427) deficient background. As previously described, the expression of *lev-1* is observed in body wall muscle and other head and body neurons. B) Isolated pharynxes of transgenic lines AQ585 and AQ749 indicate there is not expression of LEV-1 in the pharyngeal circuit. Dissected pharynxes of N2 wild type worms were used as negative control. C) Representative images of cholinergic and glutamatergic neurons in the head region and in the pharyngeal circuit of isolated pharynxes used as positive control of pharynx dissection procedure. Expression of GFP in cholinergic neurons is driven by *Punc-17* and RFP is expressed in glutamatergic neurons under the control of *Peat-4*. Photos from A, B and C were taken by James H. Atkins. Scale bar represents 10 µm. D) RT-PCR of N2 wild type isolated pharynxes demonstrates there is not expression of *lev-1* in the pharyngeal circuits. cDNA was reverse transcribed from a single worm, a single isolated pharynx or five isolated pharynxes RNA of wild type nematodes. PCR was performed using specific primers for *myo-2* and *eat-2* as positive control and *myo-3* as negative control of the expression in the pharynx. White asterisks correspond to unspecific amplification.

Due to the pivotal role played by LEV-1, we sought to detail its expression beyond the well characterized body wall muscle expression [283]. We first investigated the expression of *lev-1* in the pharyngeal circuit of *C. elegans* using existing GFP translational reporters previously used to address functional expression of *lev-1* [422]. Our analysis of these strains supported previous descriptions about the location in the body wall muscle cells as well as nerve ring, dorsal and ventral nerve cord [289,422]. However, previous investigations highlighted that some pharyngeal gene expression can be masked by overlying nerve ring expression [423]. In order to address this, pharynxes from transgenic worms carrying transcriptional (AQ585) and translational (AQ749) GFP reporters [422] were isolated and imaged to test for fluorescent signal (Figure 3.4A). We did not observe GFP fluorescence in any of the preparations, indicating LEV-1 does not occur in the isolated muscle or in its associated basal lamina embedded pharyngeal circuit (Figure 3.4A). This was reinforced utilizing RT-PCR with primers designed to specifically amplify *lev-1* from mRNA extracted from the isolated pharynxes of wild type worms (Figure 3.4B). The amplification of *myo-2* and *eat-2* were used as positive controls to demonstrate that the quality of mRNA was sufficient to amplify high and low copy number of transcripts. Selective amplification of *myo-3* was used as a negative control to show loss of body wall muscle transcripts as a consequence of anatomically isolating the pharynx. The mRNA of *lev-1* was not detected in the pharyngeal circuit of *C. elegans* worms (Figure 3.4B).

Taken together, these results indicate that the major pharmacological determinant of the drug-induced pharyngeal inhibition phenotype exerts its function outside the pharyngeal circuit.

3.4.4. LEV-1 is required in the body wall muscle to mediate levamisole inhibition of pharyngeal pumping.

In view of the significance of LEV-1 in the body wall neuromuscular junction, we investigated tissue specific rescue of LEV-1 at the musculature controlling the locomotion. For this, we generated transgenic lines of *lev-1* deficient nematodes expressing the wild type cDNA version of the gene under the control of either *lev-1* or *myo-3* promoter. This experiment was replicated with two distinct *lev-1* deficient mutant strains (Figure 3.5).

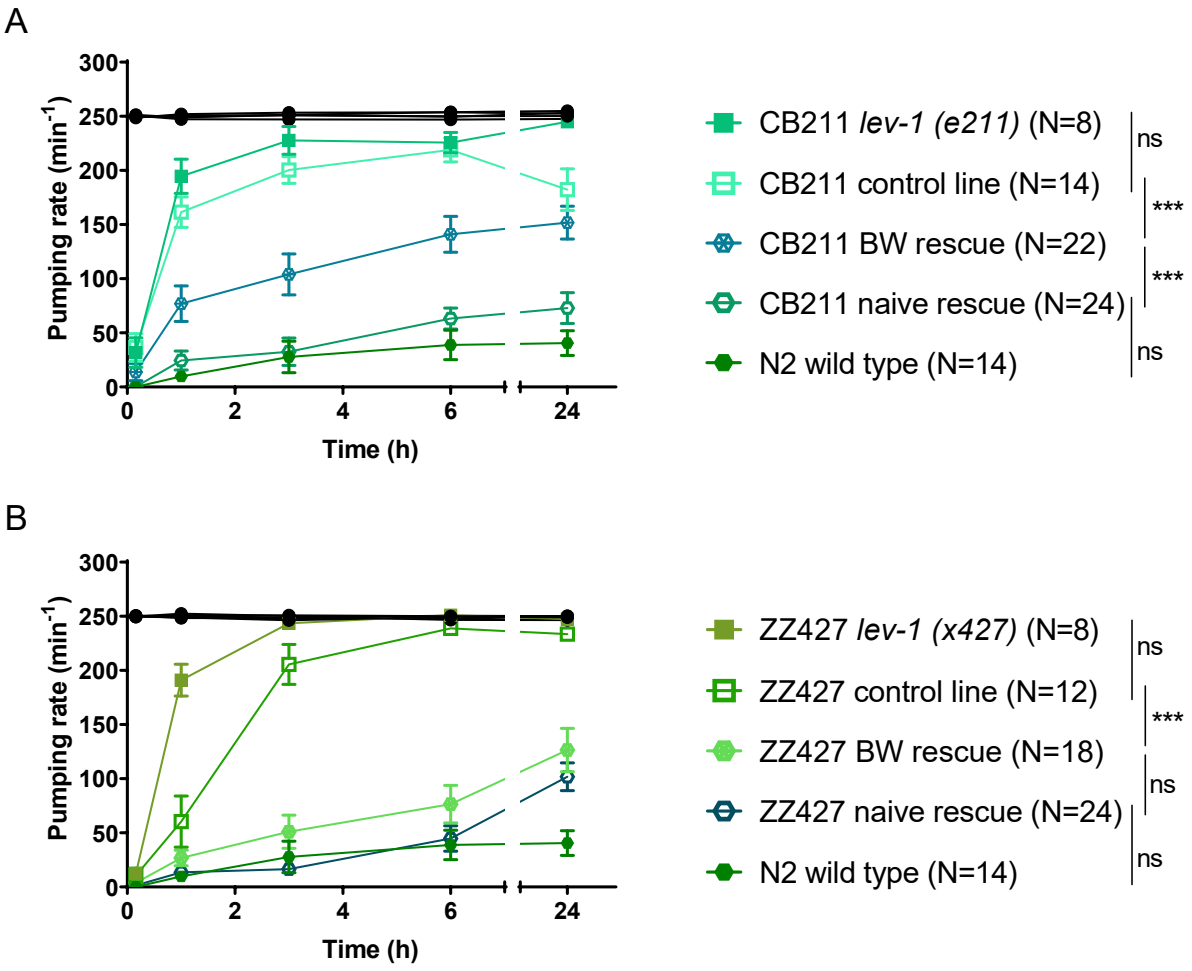

Figure 3.5. LEV-1 wild type expression in body wall muscles of *lev-1* mutant nematodes restores the levamisole induced inhibition of the pharyngeal function. A) Pharyngeal pumping in the absence (black) or presence (green) of 250 µM levamisole at different end-point times for N2, CB211 *lev-1 (e211)* mutant strain and transgenic lines expressing *lev-1* under either its own promoter (naïve rescue) or body wall muscle promoter (BW) into a CB211 background. Transgenic control lines were made by expressing GFP in coelomocytes of a *lev-1 (e211)*. Data are shown as mean ± SEM of the pumping rate of 14 worms in at least 7 different experiments for N2 wild type, 8 worms in at least 5 independent experiments for CB211 *lev-1 (e211)* mutant strain, 14 worms from two different lines in at least 4 independent experiments per line for control transgenic line, 22 worms from four different lines in at least 3 different experiments per line for body wall rescue transgenic lines and 24 worms from four different lines in at least 3 different experiments per line for naïve rescue lines. B) Pharyngeal pumping in the absence (black) or presence (green) of 250 µM levamisole at different end-point times for N2, ZZ427 *lev-1 (x427)* mutant strain and transgenic lines expressing lev-1 under either its own promoter (naïve rescue) or body wall muscle promoter (BW) into a ZZ427 background. Transgenic control lines were made by expressing GFP in

coelomocytes of a *lev-1 (x427)*. Data are shown as mean ± SEM of the pumping rate of 14 worms in at least 7 different experiments for N2 wild type, 8 worms in at least 5 independent experiments for ZZ427 *lev-1 (x427)* mutant strain, 12 worms from two different lines in at least 3 independent experiments per line for control transgenic line, 18 worms from three different lines in at least 3 different experiments per line for body wall rescue transgenic lines and 24 worms from four different lines in at least 3 different experiments per line for naïve rescue lines. $^{ns}p>0.05$; ***$p<0.001$ by two-way ANOVA test.

The naïve expression of *lev-1* rescued the wild type pharyngeal sensitivity to levamisole in the two *lev-1* deficient mutants tested (Figure 3.5). Furthermore, the phenotype was partially rescued in the *lev-1 (e211)* mutant strain (Figure 3.5A) and fully rescued in the *lev-1 (x427)* mutant strain (Figure 3.5B) when the wild type version of the cDNA was selectively expressed in the body wall musculature under the control of the *myo-3* promoter.

These results indicate that the inhibition of the pharyngeal function by levamisole exposure is driven by the LEV-1 signalling at the body wall muscle.

3.4.5. The pharyngeal sensitivity to levamisole is not mediated by a neuroendocrine signal

Pharyngeal pumping rate in mutants deficient in major transmitters was investigated after 6 hours of incubation with levamisole (Figure 3.6), a time at which inhibition of pumping rate by this drug was dependent on the LEV-1 function at the body wall neuromuscular junction (Figure 3.3 and Figure 3.5). These strains included those deficient in *unc-25 (e156)*, *eat-4 (ky5)*, *cat-1 (ok411)*, *tph-1 (mg280)*, *tdc-1 (n3419)*, *tbh-1 (n3247)* and *egl-3 (n150)*.

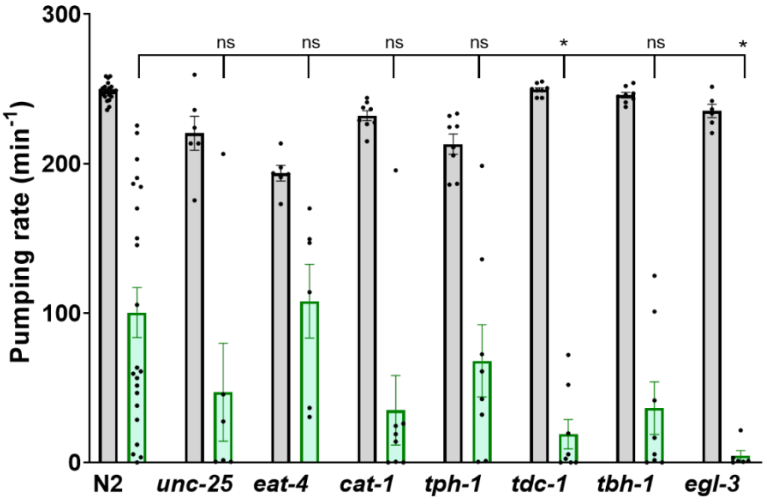

Figure 3.6. The inhibitory effect of levamisole in the pharyngeal function is independent of neurotransmitter or peptidergic signalling. Pumping rate of indicated neuromodulatory deficient mutants on food in the absence (grey column) or presence (green column) of 250 µM of levamisole after 6 hours incubation. Statistical analysis corresponds to the comparison between pumping rate on levamisole for N2 wild type and the different mutant strains. Data are shown as mean + SEM. $^{ns}p>0.05$; *$p<0.05$ by two-way ANOVA test. The experiment was performed by James H. Atkins.

Nematodes deficient in the neurotransmitters GABA (*unc-25*), glutamate (*eat-4*), the biogenic amines (*cat-1*), serotonin (*tph-1*), octopamine (*tbh-1*), or both tyramine and octopamine (*tdc-1*) as well as nematodes deficient in the majority of neuropeptides (*egl-3*) exhibited a similar response to levamisole compared with the wild type nematodes. Since none of the mutant strains tested phenocopy the response observed in *lev-1* deficient worms, it indicates limited contribution of these major transmitter pathways to the levamisole-induced inhibition of the pharyngeal circuit or the underlying pharyngeal muscle pumping (Figure 3.6).

3.5. Discussion

The screening performed in the present study was designed to identify molecular determinants that control the pharmacological inhibition of pumping during cholinergic hyperstimulation while comparing the cholinergic dependent intrinsic ability to respond to food [381]. Following this we clearly defined three groups of determinants.

3.5.1. Physiological determinants of pharyngeal function

Although the pharyngeal muscle has two important cholinergic inputs in MC and M4 controlling its core function, there are additional cholinergic neurons of unknown function [336]. Our study highlights an important class of mutants, including *eat-2* and *eat-18*, which are fundamental to sustain high pumping rate on food in physiological conditions (Figure 3.1A). Indeed, our comparative approach strongly reinforces the critical role of the EAT-2/EAT-18 dependent receptor [296,307]. The subunits of the nicotinic receptor ACR-6, ACR-10, DEG-3 and ACR-9 [299], the acetylcholine-gated chloride channel subunit ACC-3 [294] and the calcineurin CNB-1 [417] are included in this group (Figure 3.7). This may have a value in better understanding additional roles of cholinergic signalling and associated receptors in feeding behaviour. However, further investigations will be required in order to identify the molecular pathways in which the physiological determinants of the feeding phenotype exert their function.

Interestingly, none of the mutants included in this group displayed additional resistance to aldicarb-induced inhibition of the pharyngeal function (Figure 3.1A). It indicates that the physiological determinants responsible for the essential control of the pharynx are quite distinct from those that drive the inhibition in the presence of aldicarb. Indeed, the distinct nature of mutants reinforces this proposition (Figure 3.7).

3.5.2. Pharmacological determinants of pharyngeal function

In the present study, we have used the aldicarb-induced paralysis protocol [331,332] to investigate determinants that regulate the pharyngeal pumping behaviour. However, this has highlighted a distinct non-pharyngeal modulation of drug-induced feeding inhibition. These investigations have

been built on our previous observations indicating that aldicarb and other anti-cholinesterases cause a profound inhibition of the pharyngeal pumping [415]. It was underpinned by a spastic paralysis of the radial muscles in the pharynx evidenced by an overt opening of the lumen [415]. The prediction of our initial investigations was explained by assuming that aldicarb-dependent inhibition of acetylcholinesterase leads to an excess of input to the pharyngeal muscle from the two cholinergic motor neurons, MC and M4 [337,339,341,424]. In contrast to this view, we demonstrated here that LEV-1 and other molecular components of the body wall neuromuscular junction are strong determinants of the aldicarb-induced inhibition of the pharyngeal function (Figure 3.1B). This points to the pivotal role of the body wall muscle receptor in controlling locomotion and pharyngeal pumping in conditions where the pharmacological stimulation of the cholinergic signal causes an excitation of the musculature beyond the physiological levels (Figure 3.7). This is reinforced by two observations: the failure to detect the *lev-1* expression in the pharynx (Figure 3.4) and the tissue-specific rescue experiments in the *lev-1* mutant backgrounds (Figure 3.5). The introduction of the wild type version of *lev-1* in the body wall muscle had a strong rescue effect of the levamisole-induced inhibition of pumping (Figure 3.5). However, we note that *lev-1* is expressed more widely than body wall muscle. Therefore, the expression in the nerve cord and nerve ring could additionally contribute to the integrity of the response.

Overall, these results suggest that paralysis of locomotion by the signalling of the L-type receptor modulates pharyngeal function by inhibiting the pumping rate in that particular stress condition. Indeed, feeding can continue after the ablation of the pharyngeal neurons [338] but can be completely abolished by mechanical stimulation of the nematodes [409] or optical silencing of the body wall musculature [327]. In the present study, we demonstrated that the pharmacological stimulation of the cholinergic signal at the body wall neuromuscular junction causes the reduction of the pharyngeal pumping (Figure 3.7). This is a clear example of inter-tissue communication that is advantageous to the worm, allowing the coupling of two distinct functions. The mechanism underpinning the communication between the body wall and the pharyngeal neuromuscular junction is still unknown. Previously published observations highlighted the implication of dense core vesicle release as well as innexins as part of this mechanism [327]. Using our pharmacological paradigm, we did not identify clear routes of chemical transmission responsible for the coupling between feeding and locomotion. Further investigations will be needed in order to underpin the signalling between the body wall and the pharyngeal circuits.

3.5.3. Determinants playing a role in both scenarios

A final class of mutants that emerged from the screen includes *unc-63* and *ric-3* deficient strains. These two mutants are the only one tested that exhibited a deficit in the pumping rate on food in the absence of aldicarb, and a resistance to the inhibition of pumping in the presence of the drug

(Figure 3.1C). The central role of UNC-63 and RIC-3 in the composition and maturation of the body wall L-type receptor at the body wall muscle [265,289] explains why its deficiency impacts on the ability of aldicarb to induced the pharyngeal inhibition (Figure 3.7). However, the fact that these mutants also impart the loss of the physiological pump rate on food suggests an under investigated role of UNC-63 and RIC-3 function within the pharyngeal circuit. This highlights paucity of understanding of the cholinergic determinants in pharyngeal function and how our screening approach may provide information about this in the future.

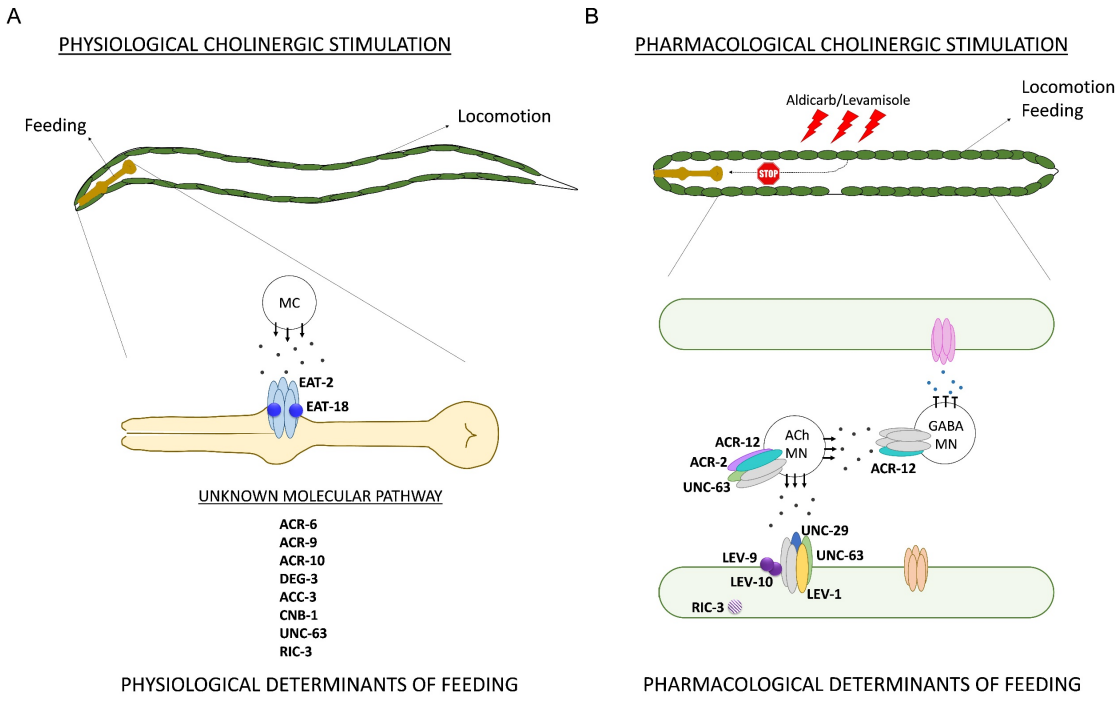

Figure 3.7. Physiological and pharmacological determinants of the feeding phenotype. The determinants of the pharyngeal function are distinct in the two contexts probed in this study. A) When nematodes are on food the cholinergic transmission stimulates pumping that underpins physiological feeding. The determinants of the pumping rate are EAT-2 and EAT-18, transducing the MC cholinergic signal in the pharyngeal muscle [296,307]. The subunits of the nicotinic receptor ACR-6, ACR-9, ACR-10, DEG-3, ACC-3, UNC-63, the calcineurin subunit CNB-1 and the ancillary protein RIC-3 were identified as additional molecular determinants of pumping rate on food. B) The pharmacological overstimulation of the cholinergic pathway by aldicarb or levamisole drives a hypercontraction of the body wall muscle that imposes inhibition of the pumping rate. In this context, the determinants of the L-type receptor at the body wall musculature that underpin locomotion impart resistance to hypercontraction mediated inhibition of the feeding phenotype. These determinants are the subunits of the nicotinic receptors UNC-63, UNC-29, LEV-1, ACR-2, ACR-12 and their auxiliary proteins LEV-9, LEV-10 and RIC-3.

3.6. Conclusion

In the *C. elegans* model organism, the ability of the pharynx to act as an interceptive cue for food to globally affect motility has been previously established [407]. In the present work, we demonstrated that the pharmacological activation of the body wall circuit allows the distal inhibition of the pharyngeal pumping rate. This highlights a reverse route in which the tone of the

musculature that controls locomotion impacts the circuit controlling the feeding behaviour. This fact provides insight into how the physiological state of one tissue can indirectly, but profoundly, impose control on distinct organs with an unrelated function. Acute regulation of pumping by the locomotory circuit has been noted [327,409], however, the advantages and mechanisms for allowing this remain to be resolved. In a wider sense, this kind of inter-tissue communication can report stress or disease in the whole organism's physiology. In *C. elegans*, the hypercontraction of body wall muscles might act as an aversive cue that impacts in the feeding rate of the worm in a similar manner to the signals that are involved in disease in higher animals that impact on the appetite and feeding during cachexia [425].

3.7. Acknowledgements

We thank Dr Jean-Louis Bessereau, Dr Denise Walker and Dr William Schafer for sharing strains; Dr Antonio Miranda-Vizuete for sharing *Punc-122::gfp* marker plasmid.

We thank Emeritus Professor Robert Walker, Dr Fernando Calahorro, Helena Rawsthorne-Manning and Johanna Haszczyn for critical reading of the manuscript and for detailed comments.

Additional *C. elegans* strains were provided by the CGC, which is funded by NIH Office of Research Infrastructure Programs (P40 OD010440).

3.8. Author contributions

Patricia G. Izquierdo: Conceptualization, Data curation, Formal analysis, Investigation, Methodology, Validation, Visualization, Roles/Writing - original draft. **Thibana Thisainathan**: Investigation. **James Atkins**: Investigation. **Christian J. Lewis**: Investigation. **John Tattersall**: Conceptualization, Funding acquisition, Methodology, Supervision, Writing - review & editing. **Christopher Green**: Conceptualization, Funding acquisition, Methodology, Supervision, Writing - review & editing. **Lindy Holden-Dye**: Conceptualization, Funding acquisition, Methodology, Supervision, Writing - review & editing. **Vincent O'Connor**: Conceptualization, Funding acquisition, Methodology, Supervision, Writing - review & editing.

3.9. Funding

This work was funded by the University of Southampton (United Kingdom) and the Defence Science and Technology Laboratory, Porton Down, Wiltshire (United Kingdom).

3.10. Conflict of interest

The authors declare that they have no conflicts of interest with the contents of this article.

Chapter 4

A new route to mitigate organophosphate intoxication through modulation of molecular determinants of nicotinic acetylcholine receptor function

Patricia G. Izquierdo [a], Claude L. Charvet [b], Cedric Neveu [b], A. Christopher Green [c], John E.H. Tattersall [c] Lindy Holden-Dye [a], Vincent O'Connor [a]

[a] Biological Sciences, Institute for Life Sciences, University of Southampton, Southampton, SO17 1BJ, United Kingdom.

[b] French National Institute for Agricultural Research (INRA), Infectiologie Animale et Santé Publique, Nouzilly, France.

[c] Dstl, Defence Science and Technology Laboratory, Porton Down, Salisbury, Wiltshire, SP4 0JQ, United Kingdom.

Key words. Carbamate, organophosphate, nicotinic receptor, aldicarb, paraoxon, oxime, neuromuscular junction, cholinergic plasticity, plasticity-promoting treatment.

Author for correspondence:

Patricia G. Izquierdo: P.Gonzalez@soton.ac.uk

Deposited as: Izquierdo, P. G., Charvet, C. L., Neveu, C., Green, A. C., Tattersall, J. E., Holden-Dye, L., & O'Connor, V. (2021). Organophosphate intoxication in C. elegans reveals a new route to mitigate poisoning through the modulation of determinants responsible for nicotinic acetylcholine receptor function. *BioRxiv*. https://doi.org/10.1101/2021.05.01.442241.

4.1. Abstract

Plasticity is a reactive mechanism that allows the adaptation of living organisms to changing environmental cues. The exploitation of this physiological process has a clear benefit to promote the recovery from a wide range of neurological disorders. Here, we investigate if plasticity-promoting treatments could provide an untapped route to alternate the classically used antidotes against organophosphate and carbamate poisoning. Both neurotoxins bind and inhibit acetylcholinesterase, a key enzyme in terminating the acetylcholine signal that controls a conserved transmission between cholinergic neurons and neuromuscular junctions from invertebrates to humans. Preventing the synaptic breakdown of the neurotransmitter causes the overstimulation of the cholinergic transmission and therefore, spastic paralysis of essential muscle contraction. Here, we report that the model organism *C. elegans* develops a differential plasticity in the face of carbamates and organophosphates intoxication. Interestingly, the mitigating plasticity observed in organophosphate-exposed worms impacts on the recovery of neuromuscular phenotypes that are initially impaired by the drug. The intoxication and plasticity phenomena are underpinned by overstimulation of acetylcholine receptors at the neuromuscular junction. We observed that intrinsic determinants of the receptor's location and sensitivity modulate the extent of the subsequent plasticity in the context of persistent cholinergic stimulation. These determinants mediate the efficacy of synaptic signalling causing a sustained mitigating plasticity during the poisoning. Our results indicate that pharmacological intervention of nicotinic receptors and/or scaffolding proteins that support receptor function might provide a novel treatment route for anti-cholinesterase poisoning.

4.2. Introduction

Molecular plasticity is a conserved mechanism from invertebrates to mammals involved in the adaptation and survival of the living organisms. This principle requires the reorganization of a signalling cascade in order to modulate the strength of the signal in response to intrinsic or extrinsic stimuli. [426-428]. The expression of such molecular mechanism is fundamental to neural plasticity and underpins the reactive changes associated with distinct forms of synaptic homeostasis [429-431]. Pharmacological modulation of the naturally occurring plasticity could be beneficial to treat a wide range of conditions that imply damage in the nervous system. This idea could be extended to conditions in which neurotoxin's poisoning impair neurotransmitter signalling. Acetylcholinesterase inhibitors, organophosphates and carbamates, are an important class of such neurotoxins. Anti-cholinesterase poisoning raises the concentration of acetylcholine at the synapses beyond the physiological levels and triggers persistent stimulation of the nicotinic type and muscarinic type receptors [88,367]. Since acetylcholine governs signalling between neurons in the central and peripheral nervous system and all the neuromuscular junctions [368,369], there is a wide spectrum of symptoms associated with anti-cholinesterase poisoning, known as cholinergic syndrome [42,367]. Asphyxia is the main cause of death and is produced by the uncontrolled stimulation of the nicotinic receptors at the neuromuscular junction of respiratory muscles [42]. The core of the treatment consists of the artificial ventilation of the victim and the injection of atropine, an antagonist of the muscarinic receptors [162]. It is usually supplemented with an oxime treatment to revert the inhibition of acetylcholinesterase and an anticonvulsant drug to minimize seizures during the initial cholinergic crisis [162,188,432,433]. However, the success of this treatment depends on factors such as the time of reaction, the dose of atropine administrated or the type of cholinesterase inhibitor intoxicating [162,187,190]. In this scenario, developing alternative strategies is of critical necessity [11,373].

The cholinergic signalling, whether organizing central or peripheral transmission, exhibits highly plastic mechanisms that modulate the strength of the acetylcholine signalling. Structural changes in the cholinergic circuit have been demonstrated after a brain injury and this has an implication in the recovery from symptoms observed after rehabilitation [434]. Cholinergic receptors are an additional checkpoint to regulate the level of acetylcholine signalling. Presynaptic expression of muscarinic receptors can modify the release of acetylcholine to the synaptic cleft [435,436]. Recent observations highlighted that some acetylcholinesterase inhibitors such as DFP can negatively regulate acetylcholine release by a presynaptic muscarinic receptor mediated mechanism [437].

Fast cholinergic synaptic transmission is mediated by nicotinic receptors, acetylcholine-gated cation channels formed by five subunits in homomeric or heteromeric combination [438]. Since multiple genes encode for nicotinic receptor subunits, the combinatorial complexity might

provide another opportunity to modulate the cholinergic signal [438]. Receptor subtypes exhibit different biophysical properties and some subtypes can be predominately expressed respect to others depending on external stimuli. For example, the ε subunit might be replaced by the foetal subunit ϒ in nicotinic receptors at the adult neuromuscular junction during stress conditions, conferring different signalling properties [131,132,134]. Nicotine exposure is another external cue that predominantly enhances the expression of some nicotinic receptor subtypes respect to others in the brain [439-442]. Finally, the interaction of nicotinic receptors with auxiliary proteins modifies their trafficking, clustering, sensitivity or motility between synaptic and extra synaptic domains [317,443-447]. Understanding the molecular mechanisms that regulate the cholinergic signal at all levels would be critical to develop plasticity-promoting treatments in the context of anti-cholinesterase intoxication.

Despite its simplicity, the free-living nematode *C. elegans* can develop behavioural plasticity by two different paradigms known as associative and non-associative [448,449]. The preconditioning of nematodes to nicotine and other environmental cues such as starvation or temperature modifies the consequent phenotype of these worms when they are post-exposed to the same signal [406,450-452]. Alternatively, the chronic exposure to certain odours or mechanical stimuli triggers the habituation of the behaviour to such conditions in nematodes continuously subdued to the overstimulation of chemosensory and mechanosensory circuits, respectively [409,453]. The genetic amenability of the nematode combined with a well-defined set of behaviours and the characterization of its nervous system make *C. elegans* an attractive model organism to research the genetics of behavioural plasticity [448].

In previous experiments, we built on the established work of others and demonstrated the potential of the organism model *C. elegans* to investigate acetylcholinesterase intoxication and recovery [415]. Specifically, we highlighted the measurement of pumping rate on food as a suitable cholinergic-dependent behaviour that is dose-time dependent inhibited by the presence of anti-cholinesterases but can be restored when nematodes are removed from the drug condition [415]. Here, we demonstrate that nematodes express a cholinergic plasticity in two different paradigms, the precondition to low doses of the drug and the chronic stimulation with high intoxicating concentrations. The preconditioning paradigm with the organophosphate paraoxon-ethyl intensified the behavioural effect of the drug when nematodes are post-exposed. However, the incubation to large concentrations of paraoxon-ethyl triggers a mitigating behavioural plasticity observed by the spontaneous recovery of the cholinergic-dependent pharyngeal pumping that underlies feeding. We identified mutants that impact the synaptic organization and/or sensitivity of the nicotinic receptors at the neuromuscular junction as important determinants controlling the scale of plasticity in a positive or negative manner. This finding provokes the notion that new

approaches can be used to modulate the tone of the nicotinic acetylcholine receptor function during organophosphate intoxication. Importantly, this modulation might mitigate the effects of the drug poisoning opening new insights to develop alternative strategies to treat anti-cholinesterase intoxication.

4.3. Materials and methods

4.3.1. *C. elegans* maintenance and strains

Nematodes were maintained according standard procedure [258]. Briefly, nematodes strains were grown on NMG plates at 20°C seeded with *E. coli* OP50 as source of food. Mutant strains EN39 *oig-4 (kr39)* II, EN300 *rsu-1 (kr300)* III and EN100 *molo-1 (kr100)* III were kindly provided by Jean-Louis Bessereau Lab (Institut NeuroMyoGène, France). ZZ427 *lev-1 (x427)* IV was kindly provided by William Schafer Lab (MRC Laboratory of Molecular Biology, UK). The transgenic lines VLP1: CB211 *lev-1 (e211)* IV; *Ex[Punc-122::gfp]*; VLP2: CB211 *lev-1 (e211)* IV; *Ex[Punc-122::gfp; Pmyo-3::lev-1]* were previously available in the laboratory stock [454]. The following strains were acquired from CGC: N2 wild type, DA465 *eat-2 (ad465)* II, VC670 *gar-3 (gk337)* V, PR1300 *ace-3 (dc2)* II, MF200 *ric-3 (hm9)* IV, CB211 *lev-1 (e211)* IV, CB193 *unc-29 (e193)* I, CB1071 *unc-29 (e1072)* I.

The following transgenic lines were generated in this work: VLP10: CB193 *unc-29 (e193)* I; Ex[*Punc-122::gfp*]; VLP11: CB193 *unc-29 (e193)* I; Ex[*Punc-122::gfp; Pmyo-3::unc-29*].

4.3.2. Generation of *unc-29* rescue constructs.

The genomic region corresponding to 3.8 kb of *unc-29 locus* was amplified using the forward and reverse primers 5'- CAGATCTCTTATGAGGACCAACCGAC -3' and 5'-CTCTCAAAGTCAAAAAAAGGCGAGGAG -3' (58°C annealing temperature), respectively. The PCR product was sub-cloned into pCR8/GW/TOPO following the manufacturer protocol and subsequently cloned into pWormgate plasmid containing 2.3 kb of *myo-3* promoter [454].

PCR amplifications were performed using Phusion High-Fidelity PCR Master Mix with HF Buffer (Thermo Fisher Scientific) following manufacturer instructions.

4.3.3. Generation of transgenic lines.

The marker plasmid was kindly gifted by Antonio Miranda Lab (Instituto de Biomedicina de Sevilla, Spain). It drives the expression of GFP specifically in coelomocytes of *C. elegans* [412].

Control and rescue transgenic lines of *unc-29* were generated by microinjection of the corresponding plasmids into one day old adults of CB193 *unc-29 (e193)* I mutant strain [413]. A concentration of 50 ng/µl of the marker plasmid *Punc-122::gfp* was injected to generate the

transgenic strain VLP10. A mixture of 50 ng/µl of *Punc-122::gfp* plasmid and 50 ng/µl of *Pmyo-3::unc-29* plasmid was microinjected to generate the transgenic strain VLP11.

The genotype of CB193 strain was authenticated by PCR amplification of the *unc-29 locus* and subsequently sequencing of the PCR product before microinjection was carried out.

4.3.4. Sequencing of mutant alleles

Mutations in *lev-1* and *unc*-29 mutant strains were analysed by PCR amplification (Table 4.1) of the corresponding genomic fragment followed by Sanger sequencing. RT-PCR was additionally performed to describe mutation in CB1072 *unc-29 (e1072)* strain following previously published protocols [454]. Briefly, a single worm from either CB1072 or N2 wild type strain was lysed and subsequently used for cDNA synthesis using SuperScript™ III Reverse Transcriptase kit in a total volume of 20 µl following manufacturer protocol (Invitrogen™). 5 µl of the resulting cDNA was added to a final volume of 20 µl PCR reaction with indicated oligo primers (Table 4.1).

PCR amplifications were performed employing Phusion High-Fidelity PCR Master Mix with HF Buffer (Thermo Scientific™) following manufacturer's recommendations.

Table 4.1. Primer sequences and PCR conditions for mutation analysis of alleles in *lev-1* and *unc-29*

Allele	Sample	Primers	Annealing temperature (°C)	Amplification product (pb)
e193	gDNA	5'- GGTATTTGGAAGTTGGACTGTG -3' 5'- GCTCAGATGCCGATTTTGGG -3'	56	752
e1072	gDNA	5'- CAGATCTCTTATGAGGACCAACCGAC -3' 5'- CTCTCAAAGTCAAAAAAAGGCGAGGAG -3'	58	3,870
e1072	cDNA	5'- ATTCTCTCATTCAGCCAGTCC -3' 5'- GCTCAGATGCCGATTTTGGG -3'	55	937
e211	gDNA	5'- TGAAATAGAAAACGTGGGGG -3' 5'- AAAAGTTGAAAATGAAAGAATAATGG -3'	58	965
x427	gDNA	5' AGAGAGAATGATGTTAGGAGG 3' 5' AGTTGAAAATGAAAGAATAATGG 3'	55	4,940

4.3.5. Generation of *lev-1* and *unc-29* mutant cRNAs

The generation of lev-1 and unc-29 mutant cRNAs was performed by Claude L. Charvet at the French National Institute for Agricultural Research.

C. elegans lev-1 and *unc*-29 cDNAs were cloned into the pTB207 expression vector. This vector has previously reported as suitable for transcription *in vitro* [265]. The *e211* (G461E) and the *e193* (S258P) mutations were respectively inserted in the LEV-1 and UNC-29 subunits by PCR using the Q5 site-directed mutagenesis kit according to the manufacturer's recommendations (New England Biolabs). The forward and reverse primers used were 5'- GTTCTTTGAGGCAACAGTTGG -3' / 5'- CCGTACAACAAAAACCGATCCA -3' for G461E substitution in *lev-1* cDNA, and 5'

ATTCTTTCACCAACATCTTCTACA -3' / 5'- CTTTGATACAAGAAGCAAGAACAC -3' for S258P substitution in *unc*-29 cDNA. Underlined sequences indicate the mutated codons. The resulting mutant clones were sequence-checked prior linearization (Eurofins Genomics). Respective wild-type and mutant subunit cRNAs were synthesized *in vitro* with the mMessage mMachine T7 transcription kit (Invitrogen), titrated and checked for integrity. Mixes of cRNAs containing 50 ng/µl of each cRNA encoding the *C. elegans* levamisole-sensitive acetylcholine receptor (UNC-63, UNC-38, UNC-29, LEV-1 and LEV-8) subunits of interest and ancillary factors (RIC-3, UNC-50 and UNC-74) were prepared in RNase-free water [265].

4.3.6. Oocyte electrophysiology

The oocyte electrophysiology was performed by Claude L. Charvet at the French National Institute for Agricultural Research.

To investigate the functional expression of the mutated LEV-1 or UNC-29 subunits, *C. elegans* L-type nicotinic receptors, either with wild type or modified subunits, were reconstituted in *Xenopus laevis* oocytes and assayed under voltage-clamp as previously described [455]. Briefly, 36 nl of cRNA mix were microinjected in defolliculated *Xenopus* oocytes (Ecocyte Bioscience) using a Nanoject II microinjector (Drummond). After 4 days incubation, BAPTA-AM-treated oocytes were voltage-clamped at a holding potential of -60 mV and electrophysiological recordings were carried out as described previously [455]. Whole cell acetylcholine current responses were collected and analysed using the pCLAMP 10.4 package (Molecular Devices).

4.3.7. Drug stocks

Aldicarb and paraoxon-ethyl were acquired from Merck. Aldicarb was dissolved in 70% ethanol and paraoxon-ethyl was dissolved in 100% DMSO. The drug stocks were kept at 4°C and used within one month or discarded. Obidoxime was provided by Dstl Porton Down (UK) and dissolved in distilled autoclaved water directly before use. Acetylcholine was purchased from Merk and dissolved in recording buffer (100 mM NaCl, 2.5 mM KCl, 1 mM $CaCl_2.2H_2O$, 5 mM HEPES, pH 7.3)

4.3.8. Assay plates preparation

Anti-cholinesterase and obidoxime plates were prepared as previously described [454 415]. Briefly, assay plates were made by adding a 1:1000 aliquot of the more concentrated drug stock to the molten but tempered NGM agar to obtain the indicated concentration of either aldicarb (50 µM and 250 µM) or paraoxon-ethyl (20 µM to 1 mM). 3 ml of the NGM containing the drug or the vehicle control was poured in each well of 6-well plates. After the agar solidified, plates were supplemented with 50 µl of *E. coli* OP50 (OD_{600} 1) to act as the food source. The bacterial lawn was dried on the assay plates by incubating for 1 hour in a laminar flow hood. Assay plates were finally maintained at 4°C in dark overnight. Plates were used within one day of being prepared

and left at room temperature for at least 30 min before starting the experiment. There was no observable change in the bacterial lawn of drugged and control plates, therefore no effect of the anti-cholinesterase on the *E. coli* growth was discernible at any of the concentrations tested [382].

The final concentration of vehicle in the drug-containing and control plates was 0.07% ethanol for aldicarb assay plates and 0.1% DMSO for paraoxon-ethyl assay plates. Neither vehicle concentrations alone affected the phenotypes tested.

4.3.9. Behavioural assays

Behavioural experiments were performed at room temperature (20°C).

Pharyngeal pump rate on food was quantified by visual observation under a Nikon SMZ800 binocular microscope, using a timer and a general counter. The pumping rate was defined by the number of grinder movements per minute per worm. The pump rate was quantified for a minimum of 3 times for 1 minute each and the mean was used as pumps per minute.

The body length was measured as previously described [330,415]. Briefly, images of the worms were acquired through a Hamamatsu Photonics camera and visualized for recording with IC capture software (The Imaging Source©). These images were binarized and skeletonized using ImageJ software. The length of the skeleton was used to determine the body length of the nematodes.

The quantification of body length or pumping rate of nematodes that died during the course of the experiment due to anti-cholinesterase exposure, were not considered for any of the end-point times scored for the preconditioning experiments with acetylcholinesterase inhibitors or for the protracted intoxication with paraoxon-ethyl. This ensured that the expression of plasticity was due to an adaptation process and not due to a mechanism in response of dead. The mortality rate is specified in Table 4.2.

4.3.10. Preconditioning experiments with acetylcholinesterase inhibitors

Synchronized L4 stage worms were incubated on the preconditioning plates containing either drug or vehicle control. The concentration of acetylcholinesterase inhibitor used for preconditioning was selected as one that decreased the pharyngeal pumping rate to half of the maximal response following 24 hours exposure. This was 50 µM for aldicarb and 20 µM for paraoxon-ethyl [415]. After the pre-conditioning, nematodes were transferred onto non-drug containing plates to allow the recovery of the pharyngeal function for 2 hours or 3 hours for aldicarb or paraoxon-ethyl preconditioned worms, respectively. Obidoxime plates were used during the recovery step from paraoxon-ethyl intoxication to facilitate the recovery of acetylcholinesterase after the drug inhibition [415]. Finally, nematodes were picked onto plates containing five times the concentration of drug used in the preceding preconditioning step (250

µM aldicarb or 100 µM paraoxon-ethyl). The pumping rate was measured at the indicated point times (10 min, 1, 3, 6 and 24 hours) after transferring the worms to the final control or drug treated observation plate.

Table 4.2. Mortality rate of each strain and condition. The mortality rate was calculated by counting the animals dead during the course of the experiment out the total number of worms used in the specified condition per strain. A corresponds to aldicarb, PE corresponds to paraoxon-ethyl; obi corresponds to obidoxime.

Strain	Condition	Mortality (%)	Figure
N2	50 µM A	0	4.1
N2	0 → 0 → 250 µM A	26.7	4.2
N2	50 µM A → 0 → 250 µM A	23.3	4.2
N2	0 → 0 → 100 µM PE	0	4.3
N2	20 µM PE → 0 → 100 µM PE	0	4.3
N2	20 µM PE → 2 mM obi → 100 µM PE	0	4.3
N2	50 µM A → 0 → 100 µM PE	0	4.4
N2	500 µM PE	9	4.5; 4.6; 4.7; 4.8; 4.9; 4.13
ace-3 (dc2)	500 µM PE	0	4.6
eat-2 (ad465)	500 µM PE	33.3	4.6
gar-3 (gk337)	500 µM PE	40	4.6
avr-15 (ad1051)	500 µM PE	14.3	4.6
N2	1 mM PE	14.3	4.7
ric-3 (hm9)	500 µM PE	0	4.7
ric-3 (hm9)	1 mM PE	0	4.7
lev-1 (e211)	500 µM PE	0	4.7; 4.8; 4.9
lev-1 (e211)	1 mM PE	11.1	4.7
unc-29 (e193)	500 µM PE	0	4.7; 4.8; 4.9
unc-29 (e193)	1 mM PE	0	4.7
lev-1 control	500 µM PE	0	4.8
lev-1 BW rescue	500 µM PE	8.3	4.8
unc-29 control	500 µM PE	0	4.8
unc-29 BW rescue	500 µM PE	0	4.8
lev-1 (x427)	500 µM PE	0	4.9
unc-29 (e1072)	500 µM PE	0	4.9
molo-1 (kr100)	500 µM PE	12.5	4.9
oig-4 (kr39)	500 µM PE	46.7	4.13
rsu-1 (kr300)	500 µM PE	22.2	4.13

4.3.11. Protracted intoxication with paraoxon-ethyl

Synchronized L4 plus 1 stage nematodes were picked to either paraoxon-ethyl or vehicle control plates. Pharyngeal pump rate and body length was quantified at specified times after transferring to the assay plates (10 min, 1, 3, 6 and 24 hours). Nematodes often leave the patch of food during the first hour after transferring onto paraoxon-containing plates. They were picked back to the bacterial lawn at least 10 minutes before pump rate was measured.

4.3.12. Statistical analysis

The collection of data was performed blind, viz, the experimenter was unaware of the genotype tested in each trial.

Data were analysed using GraphPad Prism 8 and are displayed as mean ± SEM. Statistical significance was assessed using two-way ANOVA followed by post hoc analysis with Bonferroni corrections where applicable. This post hoc test was selected among others to avoid false positives. The sample size N of each experiment is specified in the corresponding figure.

4.4. Results

4.4.1. The pharyngeal microcircuit of C. elegans exhibits mitigating aldicarb-induced plasticity after preconditioning with sub-maximal dose of the drug.

C. elegans is able to adapt to environmental conditions depending on their previous experience [449,456,457]. As a paradigm of behavioural plasticity in *C. elegans*, we investigated how the preconditioning to acetylcholinesterase inhibitors impacted on the subsequent response to drug treatment. This was done by quantifying pumping phenotype on food, a cholinergic-dependent behaviour that exhibits a dose-time dependent inhibition to the exposure of anti-cholinesterases [415]. We observed that nematodes exposed to 50 µM aldicarb for 24 hours exhibited a 50% drug-dependent inhibition of the pharyngeal function. However, recovery from inhibition was observed 2 hours after being removed from the drug (Figure 4.1). This implies a reversible pharmacological inhibition of the enzyme without affecting the underpinning functions that control the tested behaviour.

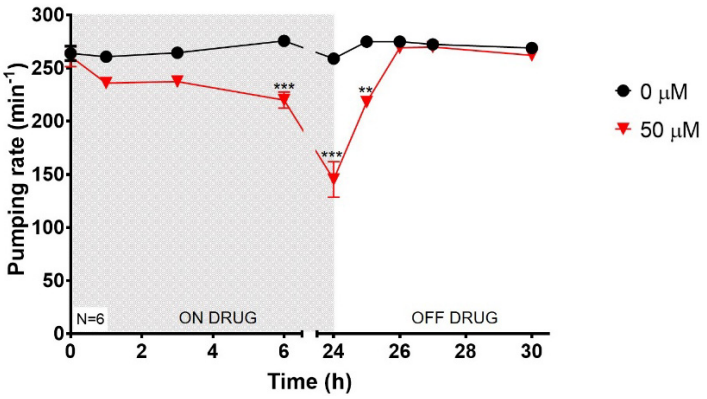

Figure 4.1. Worms intoxicated with sub-lethal dose of aldicarb exhibited recovery of the pharyngeal function after 2 hours of being removed from the drug-containing plate. Pharyngeal pumping rate per minute was quantified at different end-point times for synchronized L4 + 1 nematodes exposed to a sub-lethal dose of aldicarb. Nematodes were then transferred onto non-drug containing plates where the recovery of the pharyngeal function was observed within two hours of being removed from the drug. Shaded box indicates period of treatment. Data are shown as mean ± SEM of 6 worms in at least 3 independent experiments. Statistical significance between exposed and non-exposed nematodes was calculated by two-way ANOVA test followed by Bonferroni corrections. **p≤0.01; ***p≤0.001.

Based on the above, nematodes were incubated either in control plates or 50 µM aldicarb-containing plates for 24 hours and then transferred onto non-drugged plates for 2 hours to allow the recovery of the pharyngeal function. Finally, control and aldicarb-treated worms were intoxicated on plates containing fivefold increase of anti-cholinesterase concentration where pump rate on food was measured. (Figure 4.2A). Wild type nematodes exposed to the maximal concentration of aldicarb exhibited a time-dependent inhibition of the feeding phenotype, being completely abolished after 24 hours of incubation [415]. Interestingly, the pharyngeal pumping rate of nematodes pre-exposed to the cholinesterase inhibitor aldicarb was less susceptible to inhibition than non-preconditioned worms when they were subsequently intoxicated with the maximal dose. This was clearly evidenced at 6 and 24 hours of being transferred to the 250 µM of aldicarb-containing plates (Figure 4.2B).

The result indicates that the preconditioning step with aldicarb induces a mitigating plasticity in the pharyngeal phenotype of pre-exposed worms when they are subsequently exposed to a maximal drug concentration.

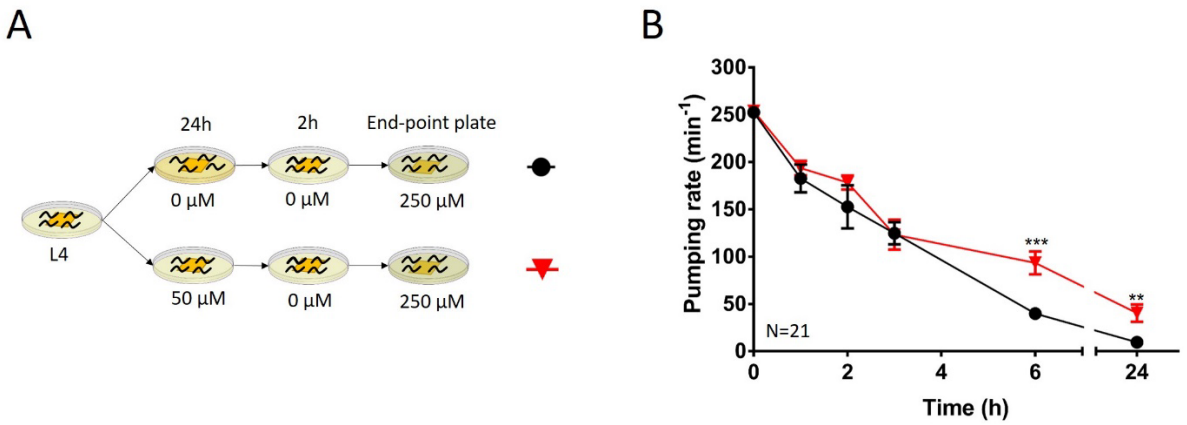

Figure 4.2. Nematodes preconditioned with aldicarb exhibit a late reduction in sensitivity of the pharyngeal circuits to the exposure of an increased dose of the drug. A) Synchronized L4 worms were intoxicated onto 50 µM aldicarb plates. Non-exposed nematodes were used as control. After 24 hours, they were transferred onto non-drug containing plates to allow the recovery of the pharyngeal function before exposing them to 250 µM aldicarb plates where the pharyngeal pumping rate was scored. B) Preconditioned worms exhibited higher pharyngeal pumping rate than non-preconditioned animals after 6 and 24 hours of being transferred onto the maximal dose plates. Data are shown as mean ± SEM of 21 worms in at least 11 independent experiments. 8 worms out 29 died during the experiment in both groups, the control and the preconditioning. Statistical significance between preconditioned and non-preconditioned nematodes was calculated by two-way ANOVA test followed by Bonferroni corrections. **p≤0.01; ***p≤0.001.

4.4.2. Preconditioning with sub-maximal dose of paraoxon-ethyl leads to an aggravating plasticity effect in the pharyngeal phenotype.

Carbamates and organophosphates are two distinct groups of cholinesterase inhibitors that cause similar cholinergic toxicity [88]. In order to investigate the behavioural plasticity of the feeding phenotype that emerges from organophosphate preconditioning, we performed an equivalent experiment to the above described with the organophosphate paraoxon-ethyl (Figure 4.3A). We previously demonstrated that paraoxon-ethyl inhibits *C. elegans* acetylcholinesterases in a reversible manner (Figure 2.10) [415]. This triggers an inhibition of the pharyngeal function that is recoverable when nematodes are removed from drugged plates [415]. In the present study, wild type nematodes were preconditioned for 24 hours on plates containing 20 µM of paraoxon-ethyl. Similar to aldicarb experiment, this concentration and time of exposure was selected to reduce the pumping phenotype by half of the maximal response after 24 hours of intoxication. The inhibition was recovered after 3 hours of being removed from the drugged plates. Finally, the preconditioned and non-preconditioned worms were transferred to 100 µM paraoxon-ethyl, a fivefold higher concentration than used in the preceding preconditioning step (Figure 4.3A).

In contrast to the results observed for aldicarb, the pre-exposure to paraoxon-ethyl caused an aggravated inhibition of pumping compared to the control non-precondition treatment. This was evidenced by the residual pumping observed after 3 hours of transferring nematodes to the maximal concentration plates (Figure 4.3B). This intensified inhibition could be explained by either an increased sensitivity to paraoxon-ethyl of preconditioned worms or an incomplete recovery of

the acetylcholinesterase inhibition imposed by the initial exposure phase of the protocol. Recovery studies from other organophosphate pesticides intoxication demonstrate that acetylcholinesterase activity was incompletely recovered even when nematodes present a normal phenotype based on visual observations [363,458]. In order to investigate this, we supplemented the recovery plate with 2 mM obidoxime (Figure 4.3C). We previously demonstrated that obidoxime improves the acetylcholinesterase activity and the pharyngeal function of *C. elegans* during the recovery from paraoxon-ethyl inhibition (Figure 2.10) [415]. Similar to previous observations, preconditioned nematodes remained more susceptible to the maximal dose of paraoxon-ethyl at 3 hours of incubation compared to those never exposed to the drug (Figure 4.3D). This indicates that the aggravated behavioural plasticity observed in the preconditioned nematodes with paraoxon-ethyl is due to an increased sensitivity to the drug rather than a residual inhibition of the worm acetylcholinesterase.

The distinct pattern of plasticity observed between aldicarb and paraoxon-ethyl preconditioned worms suggests differences in the drug-dependent mechanism of adaptation to the acetylcholinesterase inhibition by carbamates and organophosphates despite sharing a core mode of action.

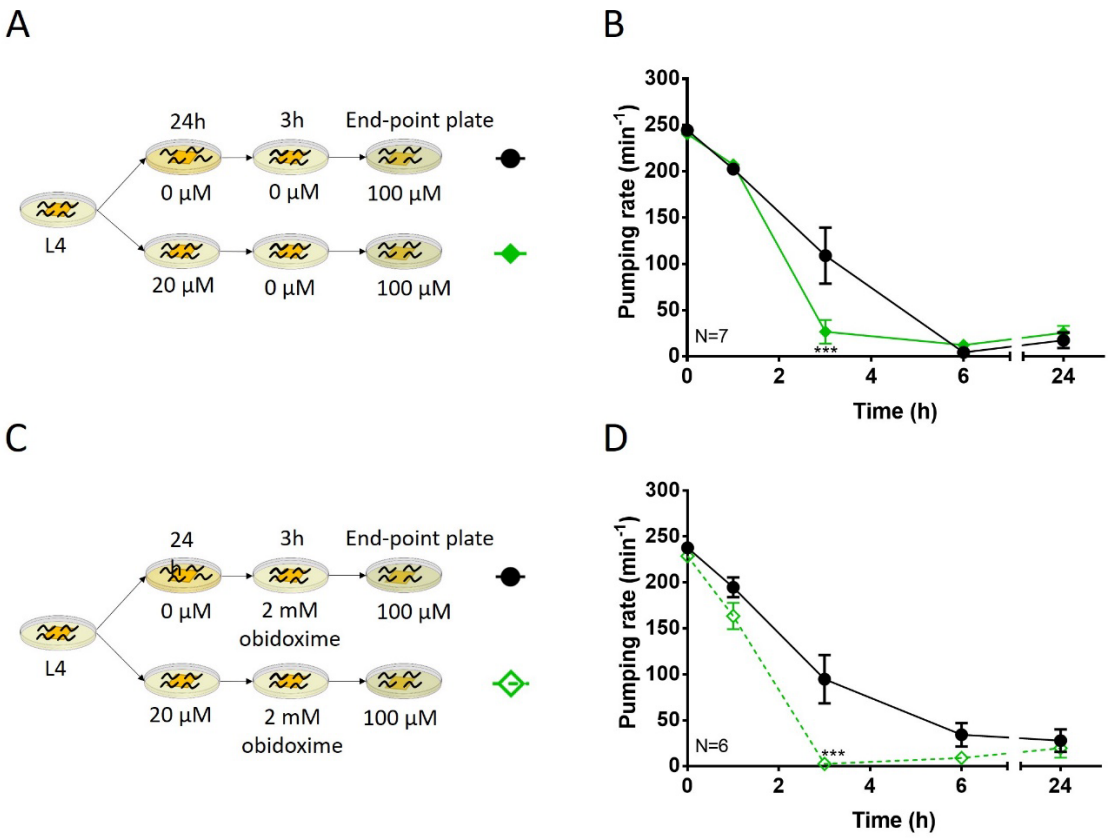

Figure 4.3. Nematodes preconditioned with paraoxon-ethyl are sensitized to subsequent OP inhibition of the pharyngeal pumping. A) Synchronized L4 worms were incubated onto either non-drug or 20 µM paraoxon-ethyl containing plates. After 24 hours, they were transferred onto non-drug containing plates to allow the recovery of the pharyngeal function. Following, they were

picked onto 100 µM paraoxon-ethyl plates where the pharyngeal pumping was scored. B) OP-preconditioned nematodes exhibited a greater reduction of the pharyngeal pumping after 3h transfer to 100 µM paraoxon-ethyl plates compared to the non-preconditioned animals. Data are shown as mean ± SEM of 7 worms in at least 4 independent experiments. A worm out of 8 died during the experiment in the preconditioning group. C) Nematodes were preconditioned as indicated in A, however, obidoxime was added to the recovery plate to promote the rescue of the acetylcholinesterase activity after paraoxon-ethyl inhibition. D) Preconditioned nematodes exhibited a similar response to maximal dose of paraoxon-ethyl when they were allowed to recover in the presence or in the absence of obidoxime. Data are shown as mean ± SEM of 6 worms in at least 3 independent experiment. Statistical significance between preconditioned and non-preconditioned nematodes was calculated by two-way ANOVA test followed by Bonferroni corrections. ***p≤0.001.

4.4.3. Aldicarb preconditioning treatment avoid the synaptic plasticity of nematodes post-exposed to paraoxon-ethyl

In order to interrogate the nature of the distinct preconditioning outcomes with carbamates and organophosphates, nematodes were pre-exposed with aldicarb and then post-exposed to paraoxon-ethyl (Figure 4.4A). Preconditioned and non-preconditioned nematodes to 50 µM aldicarb for 24 hours exhibited a similar inhibition pattern of the pumping rate when they were subsequently exposed to 100 µM paraoxon-ethyl (Figure 4.4B).

Overall, the preconditioning with aldicarb provoked the adaptation of the pharyngeal circuit to post-exposure with aldicarb but not to the post-exposure with paraoxon-ethyl. This reinforced our hypothesis that nematodes are able to adapt to anti-cholinesterase drug exposure by the previous experience. However, this is achieved by distinct mechanisms for carbamates and organophosphates. This clearly indicates that carbamates are not a well-suited model to detail investigation of the processes that underlie organophosphate intoxication, recovery and plasticity, even though they exhibit identical mode of inhibition to acetylcholinesterase [88].

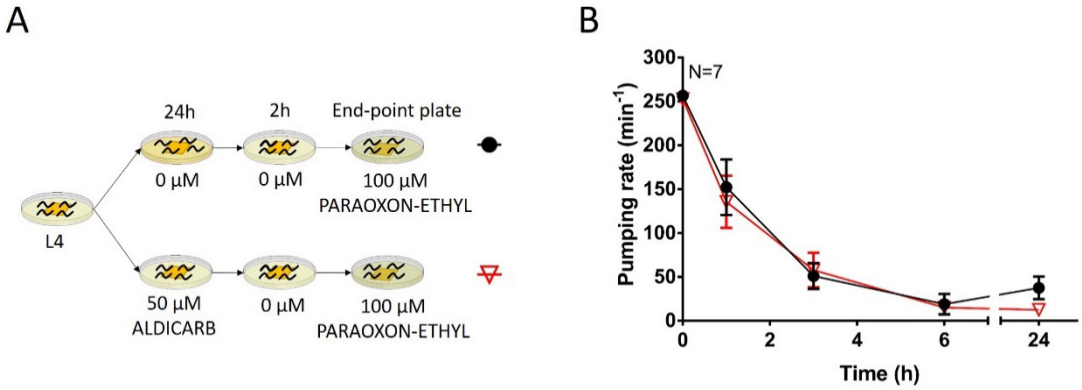

Figure 4.4. Aldicarb-preconditioned and non-preconditioned nematodes exhibit a similar pharyngeal function when exposed to maximal dose of paraoxon-ethyl. A) Synchronized L4 worms were incubated on either vehicle control or 50 µM aldicarb plates for 24 hours. After recovery on non-drug containing plates, they were exposed to a maximal dose of paraoxon-ethyl of 100 µM where pumping was measured. B) Aldicarb pre-exposed nematodes exhibit a similar sensitivity to maximal dose of paraoxon-ethyl than non-preconditioned worms. Data are shown as mean ± SEM of 7 worms in at least 4 independent experiments.

4.4.4. *C. elegans* adults exhibit spontaneous recovery of the neuromuscular junction function in the presence of higher doses of paraoxon-ethyl

A different mode of adaptation in *C. elegans* can follow upon the chronic exposure to exaggerated concentration of the stimulus [449]. In the context of organophosphate poisoning, this implies a high level of acetylcholinesterase inhibition that triggers the hyperstimulation of the cholinergic receptors in the postsynaptic terminal and therefore, a pronounced effect in the cholinergic-dependent behaviours of nematodes [415]. In order to investigate how the cholinergic system of *C. elegans* responds to inhibition with exaggerated concentrations of organophosphates, we quantified the pumping rate during the sustained exposure of wild type nematodes to 500 µM paraoxon-ethyl. The concentration was calculated as 25-fold higher than the IC_{50} value for the pharyngeal phenotype at 24 hours and would model lethal doses that represent highly toxic environmental exposure [415]. This overstimulation of the cholinergic circuit initially caused the complete inhibition of pharyngeal pumping by 3 hours of incubation in the drug (Figure 4.5A). Remarkably, after this first inhibition and despite the sustained exposure to paraoxon-ethyl, nematodes exhibited a spontaneous recovery of the pumping rate at 6 hours. This recovery of the feeding phenotype was not sustained, and the pump rate was subsequently abolished at the 24 hours of exposure to paraoxon-ethyl (Figure 4.5A).

The effect of the sustained exposure to 500 µM paraoxon-ethyl was additionally investigated in a different cholinergic-dependent phenotype at the level of the body wall neuromuscular junction by measuring body length. As expected, the intoxication with paraoxon-ethyl caused hypercontraction of the body wall muscles, being evidenced by the shrinkage of nematodes. Wild type worms poisoned with 500 µM paraoxon-ethyl exhibited a 50% reduction of the body length compared to non-exposed nematodes at 1 hour of incubation on drugged plates (Figure 4.5B). We previously demonstrated that this reduction is the maximum level of shrinkage nematodes can reach when they are incubated to anti-cholinesterases (Figure 2.5) [415]. Similar to the pharyngeal function, the body length was partially recovered at 6 hours of incubation despite the continued presence of the drug. This recovery was transitory and reversed, as the maximum shrinkage was again observed at 24 hours of exposure (Figure 4.5B).

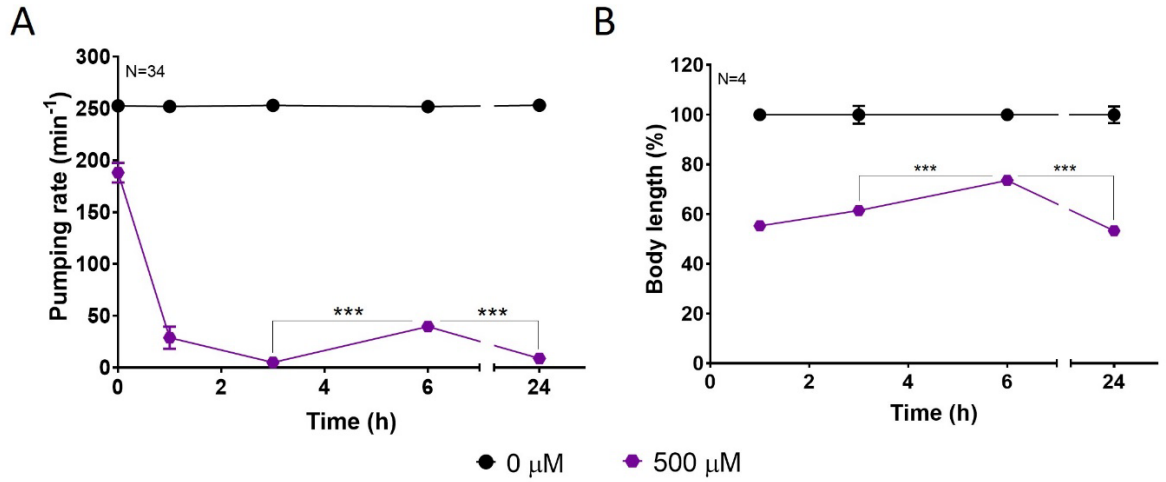

Figure 4.5. Pharyngeal and body wall neuromuscular behaviours exhibit a paraoxon-ethyl intoxication pattern characterized by three phases, an initial inhibition, a spontaneous recovery and a consequent inhibition. A) Pharyngeal pumping in nematodes exposed to 500 µM paraoxon-ethyl displays a complete inhibition of pumping at 3 hours that is spontaneously recovered at 6 hours. The complete inhibition of pumping is observed after 24 hours of exposure. Data are shown as mean ± SEM of 34 worms in at least 19 independent experiments. 4 worms out of 38 died during the experiment in the paraoxon-ethyl intoxicated group. B) Nematodes were exposed to 500 µM paraoxon-ethyl and body length recorded 1, 3, 6 and 24 hours of exposure. Percentage of body length is referenced against the corresponding age-matched untreated control. The three phases of intoxication were observed: initial shrinkage of nematodes at 3 hours, spontaneous body length recovery after 6 hours and the subsequent shrinkage of length at 24 hours of exposure. Data are shown as mean ± SEM of 4 independent worms in 4 independent experiments. Statistical significance was calculated by two-way ANOVA test followed by Bonferroni corrections. **p≤0.01; ***p≤0.001.

Overall, the results indicate that the overstimulation of the cholinergic pathways by high doses of paraoxon-ethyl triggers a pharyngeal and body wall behavioural response characterized by three phases: an initial inhibition, a partial and transitory spontaneous recovery and a subsequent inhibition. This highlights an adaptation process of the behaviours tested even in the continuous presence of paraoxon-ethyl. Furthermore, the identical expression of mitigating plasticity in these two phenotypes when nematodes are continuously exposed to the drug suggests a conserved mechanism underpinning the spontaneous recovery of the cholinergic function for the pumping rate and the body length.

4.4.5. The molecular determinants of the pharyngeal neuromuscular junction are not involved in the cholinergic plasticity observed in the pharynx

Uncovering the signalling pathways that underpin the capacity of cholinergic-dependent behaviours to exhibit mitigating plasticity might imply the expansion of treatments that palliate aspects of organophosphate intoxication. In order to identify molecular components of this cholinergic plasticity, we compared the pumping rate of different mutant worms with the wild type control in the presence or absence of 500 µM paraoxon-ethyl at 3, 6 and 24 hours of exposure. We defined these time points as key intervals in the experiment to detect initial inhibition, spontaneous recovery and subsequent inhibition. The screening utilized the pharyngeal

pumping as bio-assay since we previously demonstrated the potential of this phenotype in the research of organophosphate intoxication and recovery (Chapter 2) [415].

We first screened the pumping rate of strains containing mutations in important components of the pharyngeal neuromuscular junction (Figure 4.6). This included the acetylcholinesterase ACE-3 [264,271], the nicotinic receptor subunit EAT-2 [296,307], the muscarinic receptor GAR-3 [288] and the glutamate-gated chloride channel subunit AVR-15 [346]. All these proteins are critical to the contraction-relaxation cycle of the pharyngeal muscles responsible for the pumping rate. All mutants tested, except *eat-2 (ad465)*, exhibited the three phases pattern of initial inhibition of pumping, rebound recovery and reoccurring inhibition similar to the wild type control exposed to paraoxon-ethyl (Figure 4.6). This indicates that these proteins are not key determinants of the drug-induced plasticity in the pharyngeal pumping phenotype.

The pumping rate of *eat-2 (ad465)* deficient worms exposed to paraoxon-ethyl was continuously inhibited over the time lacking the spontaneous recovery observed in wild type nematodes at 6 hours of incubation (Figure 4.6). This might hint a role in the paraoxon-induced plasticity in the feeding phenotype, but this possibility should be tempered by the intrinsic blunting of food-induced pumping. Likewise, the profound reduction of pumping rate displayed by this strain could preclude the observation of the spontaneous recovery even present.

Overall, it indicates that the spontaneous recovery observed in the pharyngeal function of nematodes exposed to paraoxon-ethyl is not determined by molecular components of the pharyngeal neuromuscular junction.

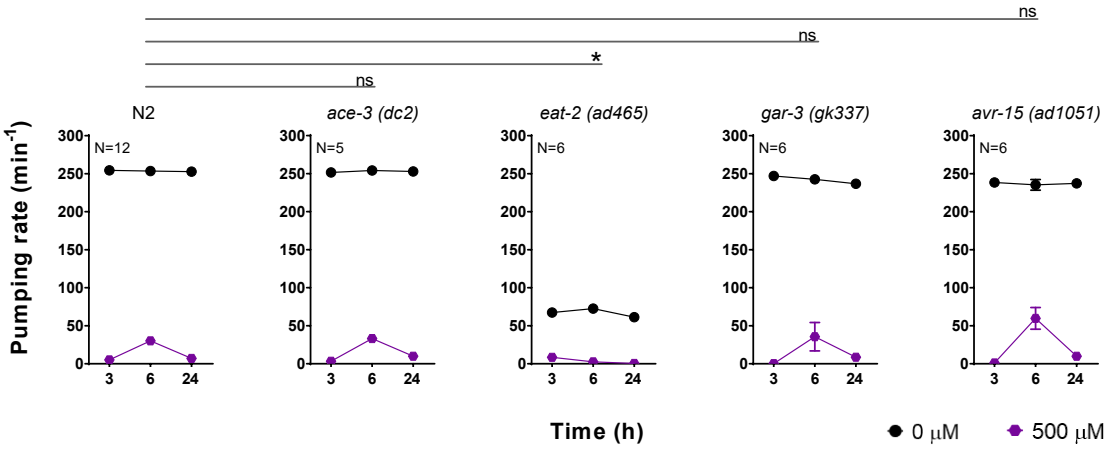

Figure 4.6. The paraoxon-ethyl induced plasticity in the pharyngeal circuit is not elicited by the neuromuscular junction components of the pharynx. N2 wild type nematodes continuously exposed to 500 µM paraoxon-ethyl exhibited spontaneous recovery of the pharyngeal function at 6 hours followed by a subsequent inhibition at 24 hours. Data are shown as mean ± SEM of 16 worms in at least 8 independent experiments. The acetylcholinesterase ACE-3 of *C. elegans* is specifically expressed in the pharyngeal muscles composing the isthmus [271]. ACE-3 deficient nematodes exposed to 500 µM paraoxon-ethyl exhibit a similar spontaneous recovery followed by inhibition of the pharyngeal pumping rate compared to wild-type worms. Data are shown as mean ± SEM of 5 worms in at least 3 independent experiments. Nematodes lacking EAT-2 did not exhibit

the spontaneous recovery observed in wild type worms. Data are shown as mean ± SEM of 6 worms in at least 3 independent experiments. The muscarinic receptor GAR-3 is expressed in the isthmus and is involved in the feeding movement [459]. Mutant nematodes lacking GAR-3 exhibited a similar paraoxon-induced plasticity of the pumping rate compared to the wild type worms. Data are shown as mean ± SEM of 6 worms in at least 3 independent experiments. E) *avr-15* encodes a glutamate-gated chloride channel subunit responsible for the relaxation of the pharyngeal muscle upon contraction [346]. *avr-15* mutant worms exhibit a similar pattern of pharyngeal pumping rate than wild type animals intoxicated onto 500 µM paraoxon-ethyl plates. Data are shown as mean ± SEM of 6 worms in at least 3 independent experiments. Statistical significance was calculated by two-way ANOVA test followed by Bonferroni corrections. $^{ns}p>0.05$; *$p\leq0.05$.

4.4.6. The molecular determinants of the cholinergic plasticity in the pharynx are located at the body wall neuromuscular junction

We previously demonstrated that pharmacological activation of the body wall neuromuscular junction by either aldicarb or levamisole exerts an indirect inhibition of the pharyngeal pumping (Chapter 3) [454]. The chaperone RIC-3 and the L-type receptor subunits UNC-29 and LEV-1 are key determinants of this response and therefore are known as pharmacological determinants of the pharyngeal function [454].

According to this, we investigated if these determinants could be involved in the paraoxon-induced plasticity observed in the feeding phenotype of wild type worms. The pumping rate of *ric-3*, *unc-29* and *lev-1* mutant nematodes was measured in the presence or absence of 500 µM paraoxon-ethyl at 3, 6 and 24 hours and the results were compared with the wild type control.

We observed that nematodes deficient in the ancillary protein RIC-3 and the non-alpha LEV-1 subunit of the L-type receptor exhibited a strong resistance to the pharyngeal inhibition by 500 µM paraoxon-ethyl (Figure 4.7). This is consistent with our previous observations using the cholinesterase inhibitor aldicarb [454]. In addition, these mutants did not show an obvious drug-induced plasticity of the pumping rate at this concentration (Figure 4.7). However, the intrinsic resistance to inhibition of the pharyngeal pumping by paraoxon-ethyl experienced by these two strains could preclude the observation or the actual expression of the drug-induced plasticity characteristic of the N2 wild type. Accordingly, we exposed nematodes deficient in *ric-3 (hm9)* or *lev-1 (e211)* to a higher dose of the cholinesterase inhibitor. The pumping rate of both strains intoxicated with 1 mM paraoxon-ethyl exhibited the initial inhibition and the spontaneous recovery phases mimicking the wild type response. However, the subsequent inhibition of the pharyngeal function observed in wild type animals is absent in *ric-3 (hm9)* and *lev-1 (e211)* strain (Figure 4.7)

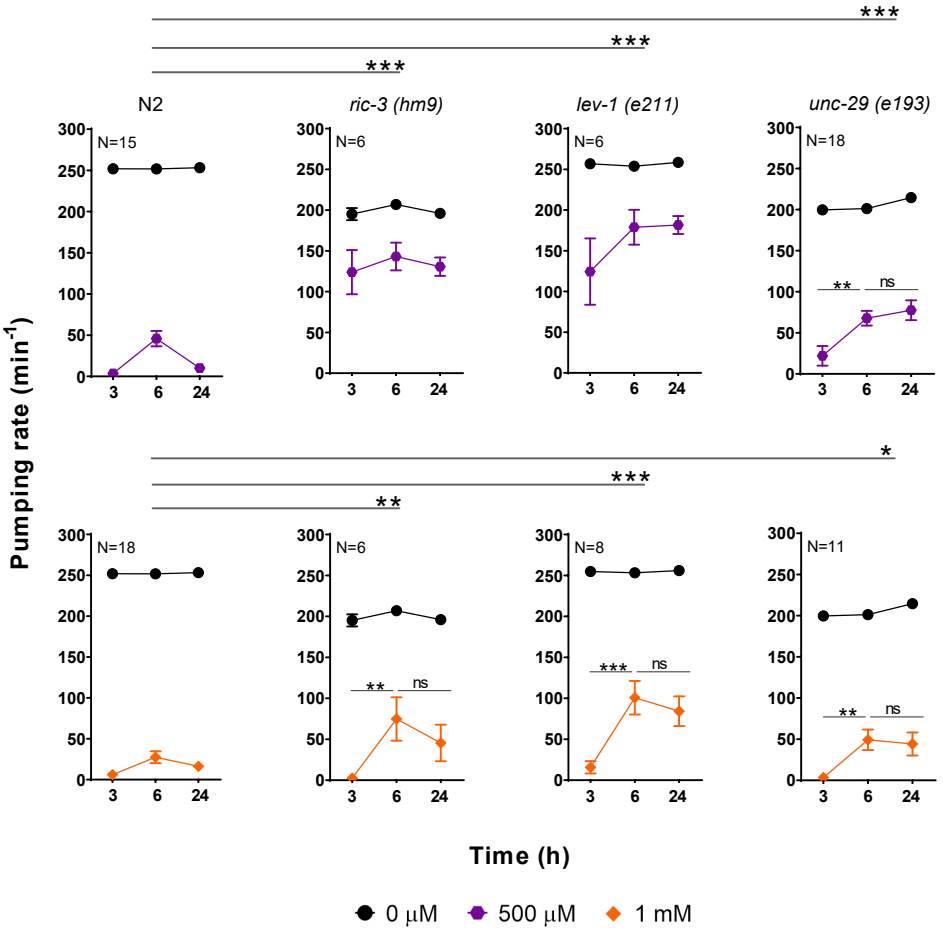

Figure 4.7. Nematodes deficient in the non-alpha subunits of the L-type body wall muscle receptor, LEV-1 and UNC-29, exhibited a sustain recovery of the pharyngeal function in paraoxon-ethyl. Paraoxon-ethyl induced plasticity of the pharyngeal function in wild type nematodes exposed to 500 µM and 1 mM. Data are shown as mean ± SEM of 15 worms in 8 independent experiments or 18 worms in 9 independent experiments, respectively. Nematodes deficient in the chaperone protein RIC-3 exhibited resistance to the inhibition of the pumping in the presence of 500 µM of paraoxon-ethyl. The exposure to 1 mM concentration inhibited the pumping rate after 3 hours and triggered a spontaneous recovery of the pharyngeal phenotype that is sustained for up to 24 hours. Data are shown as mean ± SEM of 6 worms in 3 independent experiments for each concentration. *lev-1* encodes a non-alpha subunit of the L-type receptor. LEV-1 lacking nematodes phenocopy the paraoxon-ethyl induced plasticity response of *ric-3* deficient nematodes. Data are shown as mean ± SEM of 6 worms in 3 independent experiments for 500 µM exposure or 8 worms in 4 independent experiments for 1 mM exposure. UNC-29 is the other non-alpha subunit of the L-type receptor. Nematodes deficient in UNC-29 exhibited wild type resistance to paraoxon-ethyl but sustained recovery of the pharyngeal function after 24 hours in 500 µM and 1 mM. Data are shown as mean ± SEM of 18 worms in 9 independent experiments or 11 worms in 6 independent experiments, respectively. Statistical significance was calculated by two-way ANOVA test followed by Bonferroni corrections. $^{ns}p>0.05$; *p≤0.05; **p≤0.01; ***p≤0.001.

Compared to wild type nematodes, both lev-1 and ric-3 mutants exhibited a sustained recovery of the pharyngeal function after the spontaneous recovery. Likewise, after the complete inhibition of the pharyngeal function after 3 hours of exposure, *ric-3 (hm9)* and *lev-1 (e211)* deficient worms displayed an exaggerated and prolonged spontaneous recovery of the pharyngeal function in the presence of the drug compared to the wild type worms (Figure 4.7).

Interestingly, nematodes deficient in the other non-alpha UNC-29 subunit of the L-type receptor were not resistant to the pharyngeal inhibition by paraoxon-ethyl (Figure 4.7). However, this strain presented a similar pronounced and sustained spontaneous recovery of the pharyngeal function than *lev-1 (e211)* and *ric-3 (hm9)* nematodes in the presence of 500 µM and 1 mM of paraoxon-ethyl. The three mutant strains, *ric-3 (hm9), lev-1 (e211)* and *unc-29 (e193)*, lacked the subsequent inhibition of pumping that follows the spontaneous recovery happened in the wild type worms (Figure 4.7). These data show that the sustained plasticity is not a peculiarity of mutants that are insensitive to pharyngeal inhibition by paraoxon-ethyl, indicating a dissociation between the determinants of drug sensitivity and drug-induced plasticity. While RIC-3 and LEV-1 are involved in both processes, UNC-29 is only involved in the expression of the subsequent inhibition that occurs after the spontaneous recovery observed in wild type worms exposed to 500 µM paraoxon-ethyl.

In order to address this, we performed the paraoxon-ethyl intoxication experiment with transgenic lines of *lev-1 (e211)* and *unc-29 (e193)* mutant background (Figure 4.8). The introduction of the wild type version of *lev-1* and *unc-29* in their respective mutant strain rescued the pharyngeal sensitivity to paraoxon-ethyl. This reinforces our previous data indicating that LEV-1 and UNC-29 are both pharmacological determinants of the pharyngeal function [454]. However, while the introduction of *lev-1* into CB211 strain rescued the three phases distinctive of the organophosphate-induced plasticity observed in the pharyngeal phenotype of wild type worms (Figure 4.8A), the introduction of *unc-29* into CB193 strain did not (Figure 4.8B). This highlights the importance of the LEV-1 subunit, and therefore the body wall L-type receptor, in the subsequent inhibition of the pharyngeal function that occurs after the spontaneous recovery in the presence of paraoxon-ethyl.

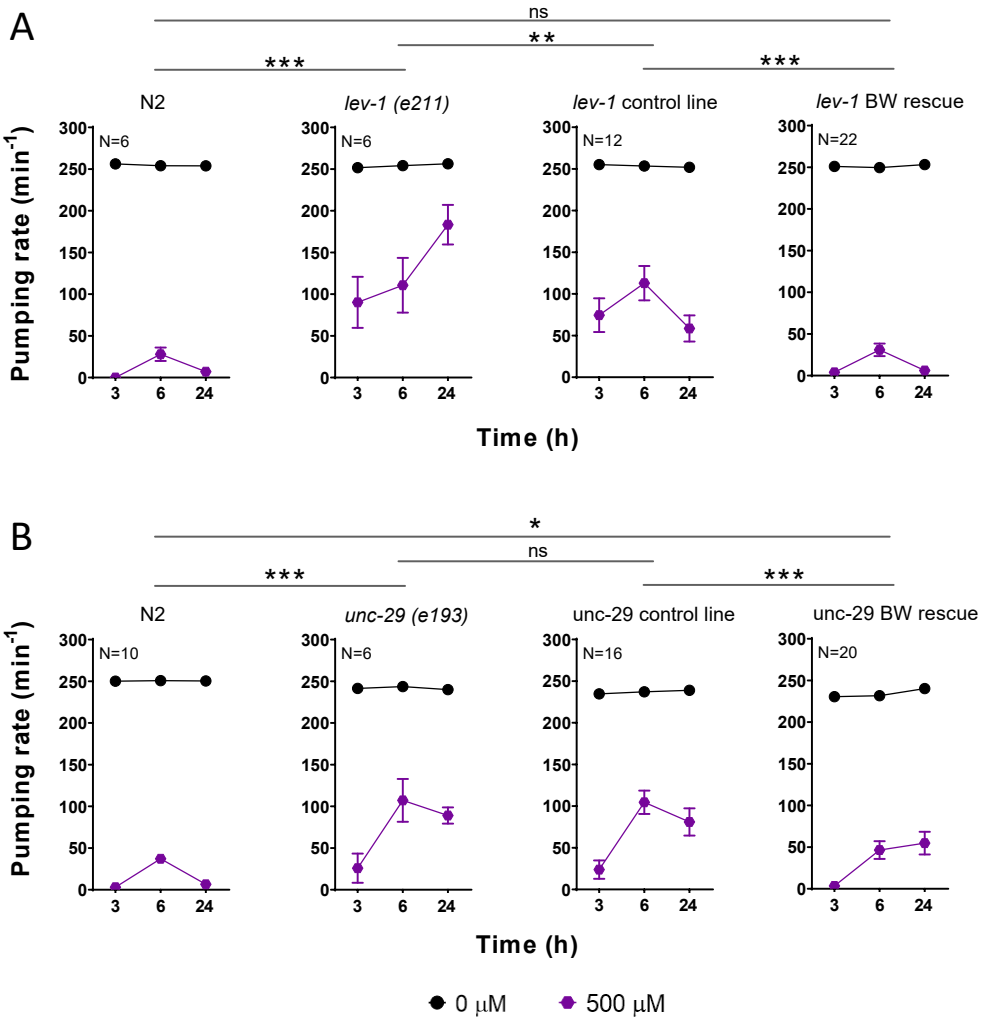

Figure 4.8. Body wall muscle rescue of the non-alpha subunits LEV-1 and UNC-29 restores wild type sensitivity to prolonged paraoxon-ethyl exposure. A) The pharyngeal sensitivity and the three phases characteristic of drug-induced plasticity to paraoxon-ethyl in the *lev-1* deficient worms were restored by introducing the wild type version of the gene selectively in the body wall muscles under control of the *myo-3* promoter. Data are shown as mean ± SEM of 6 worms in 3 independent experiments for N2 and *lev-1 (e211)* strains; 12 worms in 6 independent experiments of 2 independent lines for *lev-1* control line and 22 worms in 11 independent experiments of 4 independent lines for *lev-1* BW rescue. B) The introduction of the wild type UNC-29 in the body wall muscles of *unc-29* mutant worms rescued the consequent inhibition of the pharyngeal function that follows the spontaneous recovery in paraoxon-ethyl exposed worms. Data are shown as mean ± SEM of 10 worms in 5 independent experiments for N2; 6 worms in 3 independent experiments for *unc-29 (e193)*; 16 worms in 8 independent experiments of 3 independent lines for *unc-29* control line and 20 worms in 10 independent experiments of 3 independent lines for *unc-29* BW rescue. Statistical significance was calculated by two-way ANOVA test followed by Bonferroni corrections. $^{ns}p>0.05$; **p≤0.01; ***p≤0.001.

4.4.7. The sensitivity of the L-type receptor at the body wall muscle is responsible of the pumping inhibition that follows the spontaneous recovery in the presence of paraoxon-ethyl

LEV-1 and UNC-29 are the two non-alpha subunits that combine with the three alpha subunits UNC-63, UNC-38 and LEV-8 to compose the L-type receptor at the body wall muscles of nematodes [265]. However, the non-alpha subunits of these receptors create the binding pocket for

neurotransmitter only when they are combined with other alpha subunit [460]. To investigate the specificity of these two subunits in the paraoxon-ethyl plasticity response, we analysed the behaviour of different mutant strains in these genes in the presence of 500 µM of the cholinesterase inhibitor (Figure 4.9). The *x427* allele of *lev-1* consists of 1,267 pb deletion that contains exon 4. This results in a LEV-1 protein that lacks the first, second and third transmembrane domains (Figure 4.10). The *e211* mutation consists of a missense substitution of glycine to glutamic acid in the fourth transmembrane domain of LEV-1 (Figure 4.10). Interestingly, nematodes with the *x427* allele of *lev-1* exhibited wild type sensitivity to paraoxon-ethyl and lacked the sustained recovery of the pharyngeal pumping in the presence of the drug characteristic of the strain harbouring the *e211* mutation (Figure 4.7 and Figure 4.9).

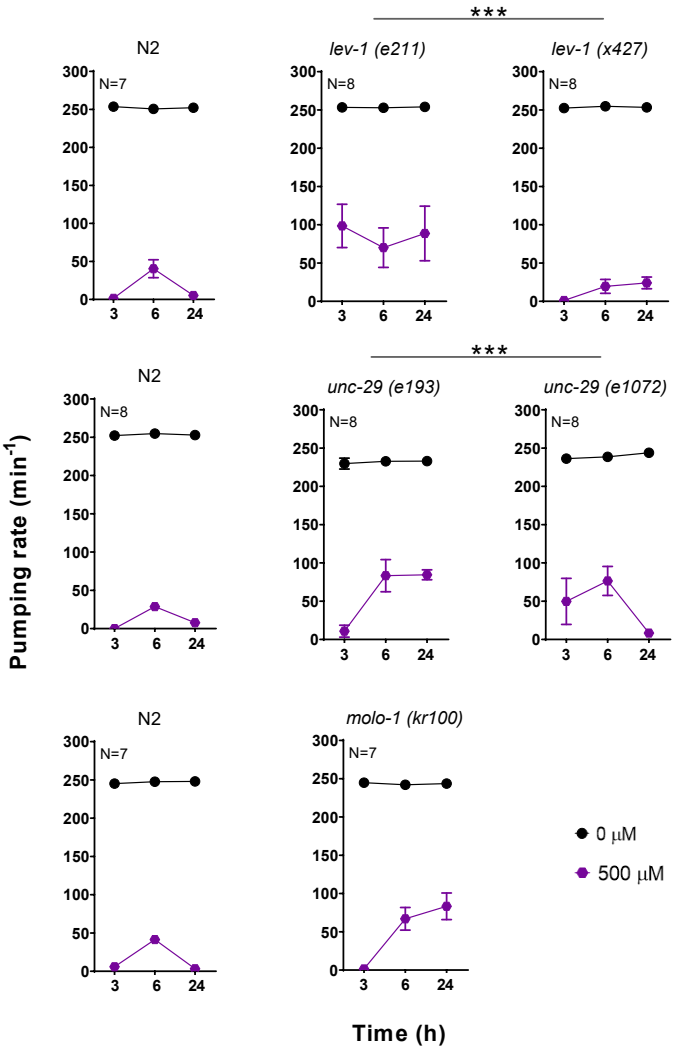

Figure 4.9. The efficacy of the L-type receptor is a significant determinant of the spontaneous recovery of pharyngeal pumping in nematodes exposed to paraoxon-ethyl. Paraoxon-induced pharyngeal plasticity in wild type nematodes incubated with 500 µM of acetylcholinesterase inhibitor. Data are shown as mean ± SEM of 7 worms in at least 4 independent experiments for *lev-1* mutants control, 8 worms in at least 4 independent experiments for *unc-29* mutants control and 7 worms in at least 4 independent experiments for *molo-1* mutant control. *lev-1 (e211)* mutant strain contains a single point mutation in the fourth transmembrane domain. This confers resistance to paraoxon-ethyl induced inhibition of the pharyngeal pumping. Data are shown as mean ± SEM of 8 worms in at least 4 independent experiments. The mutation

of *lev-1 (x427)* strain consists of a rearrangement of the genomic sequence that prevents the transcription of the gene into a protein [283]. This is the reference null-mutant of LEV-1. This mutation does not allow the expression of the mitigating plasticity in pharyngeal pumping observed in wild type worms exposed to paraoxon-ethyl. Data are mean ± SEM of 8 worms in at least 4 independent experiments. The mutation of *unc-29 (e193)* strain consists of a single point proline to serine in the loop connecting the second and third transmembrane domain of the subunit. This proline is highly conserved in the Cys-loop receptor subunits and is implicated with the gating of the receptor [111,461,462]. This mutation conferred a sustained paraoxon-ethyl induced plasticity. Data are shown as mean ± SEM of 8 worms in at least 4 independent experiments. In contrast, the null-mutant *unc-29 (e1072)* exhibited resistance to the pharyngeal inhibition by paraoxon-ethyl but did not express paraoxon-ethyl induced plasticity. Data are shown as mean ± SEM of 8 worms in at least 4 independent experiments. MOLO-1 is an auxiliary protein implicated in the positive modulation of the L-type receptor without affecting the location [317]. *molo-1* lacking worms exposed to paraoxon-ethyl exhibited spontaneous recovery of the pharyngeal function that was sustained over the time compared to wild type worms. Data are shown as mean ± SEM of 7 worms in at least 4 independent experiments. Statistical significance was calculated by two-way ANOVA test followed by Bonferroni corrections. ***p≤0.001.

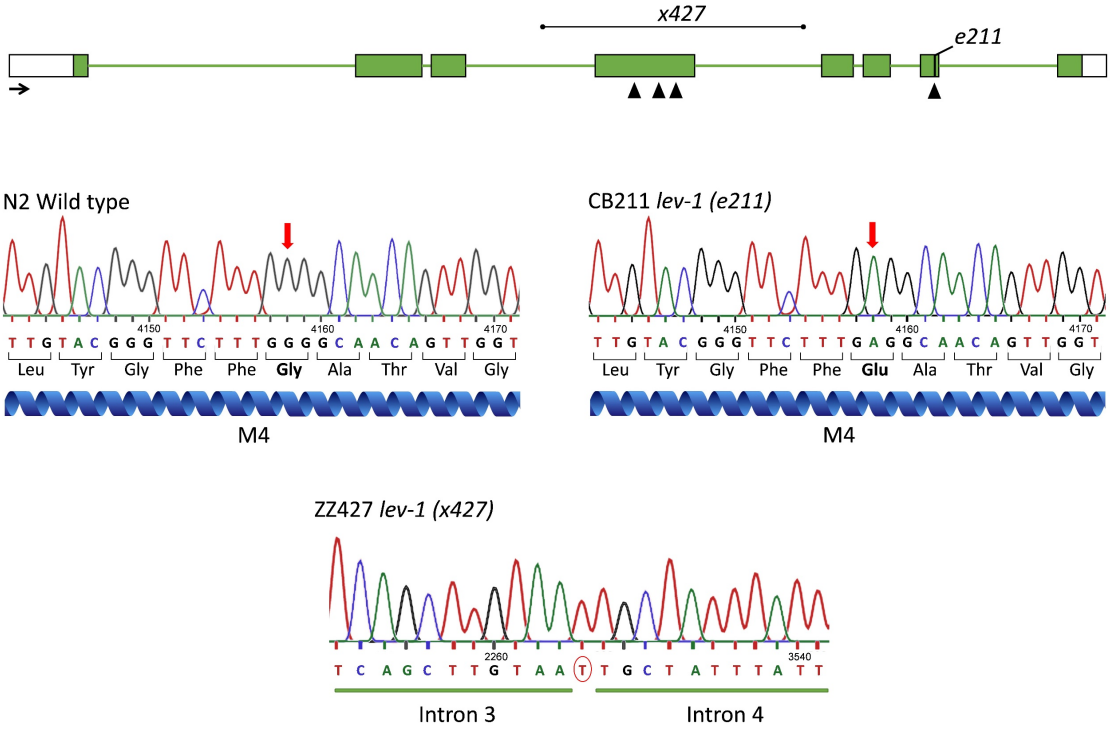

Figure 4.10. *lev-1* mutant alleles of strains CB211 and ZZ427. Genomic organization of *lev-1 locus* indicating the position of the single point mutation in *e211* and the deletion in *x427* alleles. CB211 *lev-1 (e211)* mutant strain contained a G to A missense mutation identified in exon 7 of the genomic DNA. This provokes a glycine to glutamic acid substitution at the fourth transmembrane domain (M4). The strain ZZ427 *lev-1 (x427)* contains a deletion of 1,267 pb from intron 3 to intron 4 and an T insertion. This causes a LEV-1 protein lacking the first, second and third transmembrane domain. Black arrow represents 100 pb and the sense of transcription. Black triangles in the genomic DNA represents the position of the four transmembrane domains. Chromatograms corresponds to the 5' to 3' readout of the minus strand. The position indicated in each chromatogram corresponds to the position of the respective base from the ATG starting codon in the genomic DNA of N2 wild type.

The strain CB1072 is considered a null mutant strain of *unc-29* [463]. The *e1072* allele contains a G to A base substitution in the splicing acceptor site of intron 8 (Figure 4.11). This causes a new splice acceptor that utilizes the first G in exon 9 creating a frameshift mutation and a premature stop codon between the first and the second transmembrane domain of the protein (Figure 4.11).

However, the *e193* allele contains a missense mutation that substitutes a conserved proline for a serine in the loop connecting the second and third transmembrane domain (Figure 4.11). Similar to *lev-1* deficient strains, the null mutant allele of *unc-29 (e1072)* did not exhibit the sustained recovery of the pharyngeal function in the presence of paraoxon-ethyl characteristic of the *e193* allele (Figure 4.9).

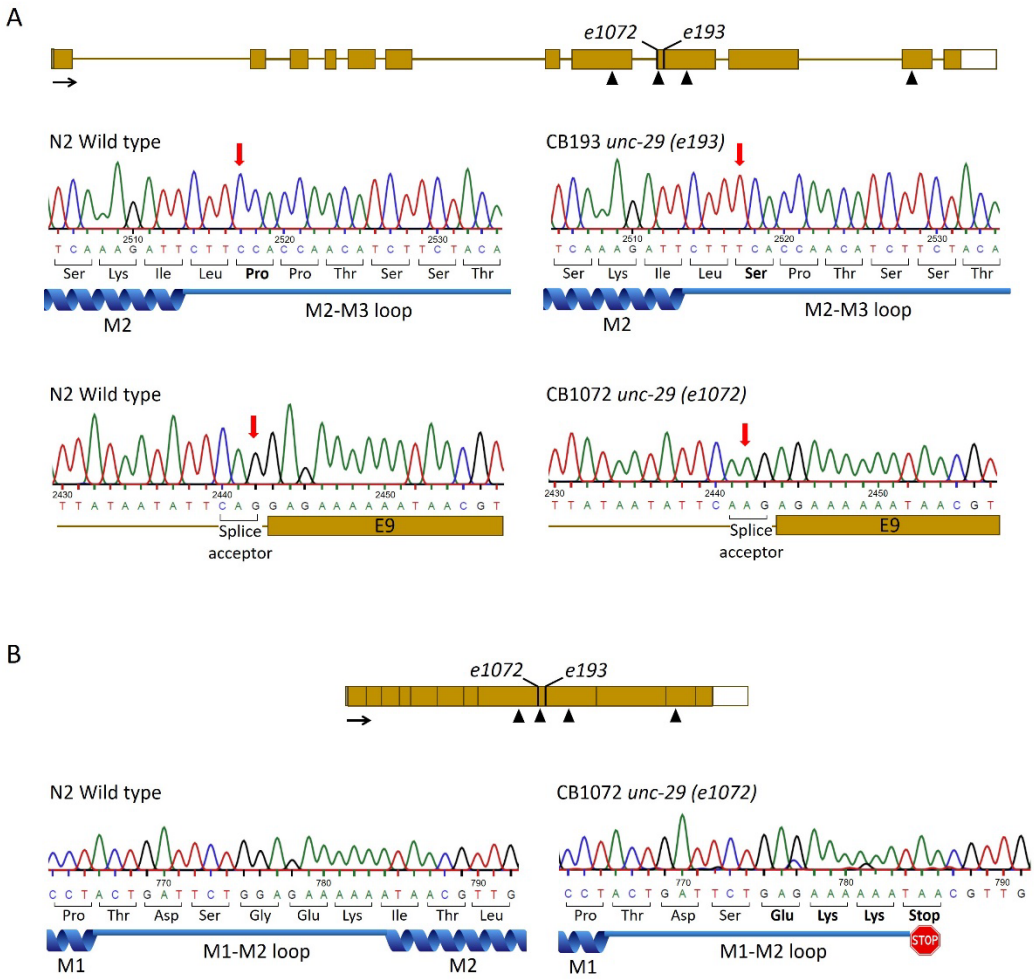

Figure 4.11. *unc-29* mutant alleles of strains CB193 and CB1072. A) Genomic organization of *unc-29 locus* indicating the position of the single point mutation in *e193* and *e1072* alleles. CB193 *unc-29 (e193)* mutant strain contained a C to T missense mutation identified in exon 9 of the genomic DNA. This provokes the substitution of a conserved proline residue at the second (M2) and third (M3) transmembrane domain loop into a serine. The strain CB1072 *unc-29 (e1072)* contains a G to A single point mutation identified in the splicing acceptor of intron 8 in the genomic DNA. This caused the formation of a new splicing site utilizing the first G in exon 9 (E9). B) RNA organization of *unc-29* indicating the position of the single point mutation in *e193* and *e1072* alleles. The mutation of *e1072* allele triggers a frameshift and a premature stop codon at the end of the first (M1) and second (M2) transmembrane domain loop. Black arrow represents 100 pb and the sense of transcription. Black triangles in the genomic and cDNA represents the position of the four transmembrane domains. The position indicated in each chromatogram corresponds to the position of the respective base from the ATG starting codon in the genomic and cDNA of N2 wild type.

If we hypothesise that *lev-1 (e211)* and *unc-29 (e193)* genes harbouring non-null mutations encode for subunits that could be incorporated into the mature L-type, our data suggest that the resulting receptor might be altered in its sensitivity and/or function. This modification could be

involved in the sustained recovery of the pharyngeal function after initial paraoxon-induced inhibition occurred. The fact that the paraoxon-induced plasticity in the pharyngeal phenotype observed in *lev-1 (e211)* and *unc-29 (e193)* mutant strains phenocopy the paraoxon response observed in the mutant strain *molo-1 (kr100)* supports the hypothesis (Figure 4.9). Since MOLO-1 is an auxiliary protein that acts as positive modulator of the L-type receptor [317], the data suggest that the *lev-1 (e211)* and *unc-29 (e193)* mutations might confer different sensitivity to the L-type receptor at the body wall muscles of *C. elegans*.

To further investigate this hypothesis, the L-type of *C. elegans* was expressed in *Xenopus* oocytes by co-injecting cRNAs of the five subunits generating the ion channel (UNC-63, UNC-38, UNC-29, LEV-1 and LEV-8) along with the three ancillary proteins (UNC-50, RIC-3 and UNC-74) as previously reported [265]. The wild type version of either LEV-1 or UNC-29 was replaced by the mutated version corresponding to the genes *e211* and *e193*, respectively, and the current amplitude to 300 µM acetylcholine was compared between the different population of receptors (Figure 4.12). The co-expression of any of the mutations described along with the wild type cRNAs of the other components significantly dropped the amplitude of the current being the *e193* mutation in *unc-29* the most restrictive for the L-type receptor function (Figure 4.12). However, the fact that the current amplitude is not abolished in these two subtypes of L-type receptors supports the hypothesis of the insertion of the mutated subunits in the functional ion channel. Indeed, omission to add either LEV-1 or UNC-29 cRNA in combination with the other *C. elegans* L-type receptor subunits failed to give rise to functional channels when expressed in the *Xenopus* oocyte [265] . Subsequently, cRNAs of the mutated subunits, either *lev-1 (e211)* or *unc-29 (e193)*, were co-injected with the five wild type subunits in a 1:1 ratio. Interestingly, the co-expression of any of the mutations described in either *lev-1* or *unc-29* with their respective wild type cRNA significantly reduce the amplitude of the acetylcholine-elicited currents (Figure 4.12). This indicates that the wild type and the mutated version of the protein compete for the formation of the mature ion channel. Such a result strongly supports a dominant-negative effect of the mutated subunit on the L-type receptor function.

Overall, the data indicate that *lev-1 (e211)* and *unc-29 (e193)* encode for functional subunit proteins that can be inserted into the mature receptor, modifying its sensitivity to the neurotransmitter.

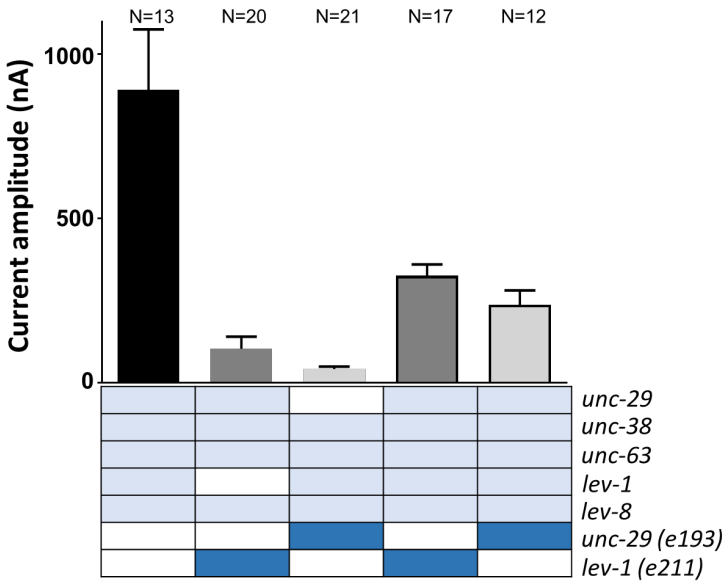

Figure 4.12. *lev-1 (e211)* and *unc-29 (e193)* encode for functional subunits that modify the signalling property of the L-type receptor. Current amplitude to 300 µM of acetylcholine was quantified in different populations of L-type receptors expressed in *Xenopus oocytes* containing either *lev-1 (e211)* or *unc-29 (e193)* mutations (dark blue). The substitution of the wild type subunits *lev-1* or *unc-29* for their respective *lev-1 (e211)* or *unc-29 (e193)* alleles reduced the current amplitude of the L-type receptor. The co-expression of wild type and mutant genes in a 1:1 ratio causes a reduction of the amplitude to acetylcholine-evoked currents, indicating the competitivity of both subunits in being incorporated into the mature ion channel. Data are shown as the mean ± SEM. Numbers above bars indicate the number of oocytes recorded for each condition. The experiment was performed by Claude L. Charvet at the French National Institute for Agricultural Research.

4.4.8. The location of the L-type receptor at the body wall neuromuscular junction might be involved in the spontaneous recovery of the pharyngeal pumping in the presence of paraoxon-ethyl

Prompted by the important modulatory role of the L-type receptor in allowing the expression of mitigating plasticity to paraoxon-ethyl exposure, we tested the pharyngeal pattern to paraoxon intoxication in different auxiliary proteins of the receptor function. RSU-1 and OIG-4 are neuromuscular junction proteins that play an important role in organizing the L-type receptor within the body wall neuromuscular junction [314,322]. These mutants exhibited wild type sensitivity to paraoxon-ethyl exposure (Figure 4.13). The pharyngeal function was completely inhibited after 3 hours of incubation with the drug. However, they did not show the spontaneous recovery of the pumping rate in the presence of paraoxon as the wild type strain (Figure 4.13), being both deficient in the paraoxon-induced mitigating plasticity.

Overall, the data identify tuneable plasticity with respect to organophosphate intoxication which has the potential to mitigate or aggravate paraoxon-ethyl toxicity. This plasticity is driven from the function of the L-type receptor at the body wall muscle. However, distinct molecular determinants interfering in its function and/or sensitivity are additionally involved in the process.

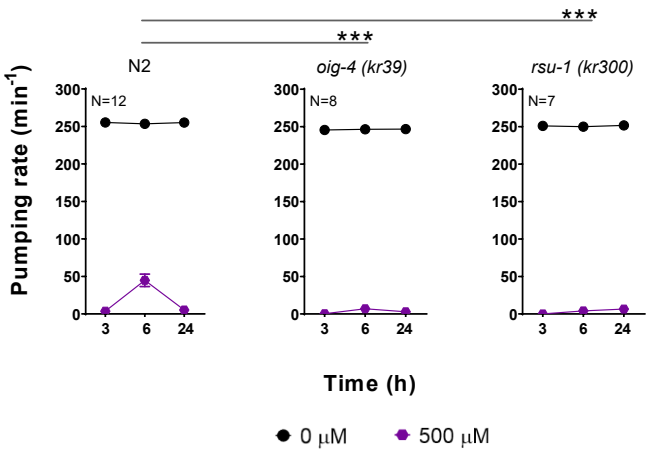

Figure 4.13. The synaptic organization of the L-type receptors underpins spontaneous recovery of the pharyngeal function observed in nematodes exposed to paraoxon-ethyl. The pharyngeal function of wild type nematodes exposed to paraoxon-ethyl exhibited drug induced plasticity. Data are shown as mean ± SEM of 12 worms in at least 6 independent experiments. OIG-4 is a muscle-secreted protein involved in the location of the L-type receptor at the body wall neuromuscular junction [314]. *oig-4* lacking nematodes are deficient in the spontaneous recovery of the pharyngeal pumping in the presence of paraoxon-ethyl observed in the wild type worms. Data are shown as mean ± SEM of 8 worms in at least 4 independent experiments. RSU-1 is a cytosolic muscle protein involved in maintaining the equilibrium between synaptic and extra-synaptic nicotinic receptors [322]. *rsu-1* lacking nematodes exposed to paraoxon-ethyl are deficient in the spontaneously recovery of the pharyngeal function in the presence of paraoxon-ethyl. Data are shown as mean ± SEM of 7 worms in at least 4 independent experiments. Statistical significance was calculated by two-way ANOVA test followed by Bonferroni corrections. ***p≤0.001.

4.5. Discussion

Organophosphates are environmental biohazards that cause at least two million of poisoning cases and lead to an estimated 200,000 deaths annually [11-13]. The nature of this intoxication is the impediment of ending the acetylcholine signal by the binding and inhibition of acetylcholinesterases in the synaptic cleft [88,367]. The overstimulation of the cholinergic transmission at the central and peripheral nervous system triggers a wide range of clinical manifestations [42,367]. However, the pharmacological treatment to mitigate the symptoms of the cholinergic syndrome is restricted to two main mechanisms, the inhibition of muscarinic receptors by atropine and the reactivation of organophosphate-bond acetylcholinesterase by oximes. Benzodiazepines are additionally used to treat seizures during the first stage of intoxication [162]. Since the efficiency of these medications is limited in many aspects [89,162,186,187], we propose here the investigation of plasticity-promoting mechanisms in order to develop alternative pathways to mitigate against the effects of anti-cholinesterase poisoning (Figure 4.14). The model organism *C. elegans* was utilized for this purpose. This free-living nematode has neuromuscular organs led by a highly conserved cholinergic pathway, compared with mammals, that triggers easy quantifiable phenotypes [250,251,261]. However, these phenotypes can be modulated according present or past experiences generating homeostatic responses and plasticity [448,449]. In previous investigations, we highlighted the quantification of pharyngeal pumping movements as the most suitable cholinergic-dependent phenotype to investigate acetylcholinesterase intoxication and recovery

[415]. Here, we demonstrated that *C. elegans* nematodes are able to develop cholinergic plasticity in two different contexts, preconditioning with low doses of the drug and chronic exposure to large concentrations. However, the behavioural consequences of these two paradigms are opposite for organophosphate intoxication.

The preconditioning effect with lower doses of paraoxon-ethyl aggravated the pharyngeal inhibition in nematodes post-exposed to a larger concentration of the same drug (Figure 4.3). Surprisingly, this plasticity effect with the organophosphate paraoxon-ethyl was completely opposite to the effect observed with the carbamate aldicarb in the same experiment (Figure 4.2). Organophosphates and carbamates are equivalent drugs with identical mode of action [88]. However, our data indicate that the intoxication consequences beyond the inhibition of acetylcholinesterase are different for both chemicals. This should avoid the use of one of them as model to research the other.

In the context of chronic exposure to a high concentration of the organophosphate paraoxon-ethyl, nematodes developed mitigating plasticity in the presence of the drug. This was observed by a spontaneous recovery of about 20% of the pharyngeal and body wall phenotypes after their complete initial inhibition by paraoxon-ethyl intoxication. The spontaneous recovery of the pumping rate and body length was not sustained over the time, being entirely abolished at 24 hours of exposure (Figure 4.5). This indicates three phases of intoxication when nematodes are exposed to paraoxon-ethyl, the initial inhibition, the spontaneous recovery and the subsequent inhibition of pharyngeal pumping and body length.

In order to identify molecular components of this mitigating plasticity, we systematically investigated the ability to express these three phases of paraoxon-ethyl intoxication in the pharyngeal pumping of mutants involved in the cholinergic pathway. We demonstrated that cholinergic components of the pharyngeal neuromuscular junction had little effect on the expression or modulation of the plasticity observed in the wild type nematodes (Figure 4.6). This builds on previous observations indicating that the *per se* inhibition of the pumping rate in the presence of the anti-cholinesterase aldicarb is mediated by determinants executing their function outside the pharyngeal system [454]. Indeed, the investigation with mutants in molecular components of the body wall neuromuscular junction highlighted the pivotal role of the L-type receptor signalling to induce the paraoxon-ethyl mitigating plasticity of the pharyngeal pumping (Figure 4.14). This acetylcholine-gated cation channel is composed by the alpha subunits UNC-63, UNC-38 and LEV-8 and the non-alpha subunits UNC-29 and LEV-1 [265]. Auxiliary and ancillary proteins have been linked with the function of the receptor by controlling trafficking, sensitivity, expression or clustering [265,313-315,317,321,322,333]. We observed that *oig-4 (kr39)* and *rsu-1 (kr300)* deficient nematodes lack the spontaneous recovery of the pharyngeal pumping in the presence of

paraoxon-ethyl compared with wild type worms (Figure 4.13). OIG-4 is a muscle secreted protein that interacts with the complex formed by L-type receptor, LEV-9 and LEV-10 at the neuromuscular junction stabilizing the clusters [314]. Neither *lev-9* nor *lev-10* phenocopied the paraoxon-ethyl induced plasticity observed in *oig-4* deficient animals (data not shown). However, OIG-4 remains partially localized independently of LEV-9 and LEV-10, possibly by its interaction with UNC-29, explaining the difference observed in their phenotype [314]. RSU-1 is a protein expressed in the cytoplasm of the muscle cells and is required for the proper balance of the L-type receptor distribution between synaptic and extra synaptic regions [322]. The fact that these two proteins are involved in the location of the muscle receptor indicate that the position of the receptor during organophosphate intoxication might be altered to modulate the excess of cholinergic signal (Figure 4.14). This alteration could be necessary for the expression of paraoxon-induced mitigating plasticity of the pharyngeal pumping. These data are consistent with previous observations where the distribution of nicotinic receptors at the mammalian neuromuscular junction of skeletal muscle is altered in acetylcholinesterase knockout mice to compensate the chronic absence of enzyme activity [464].

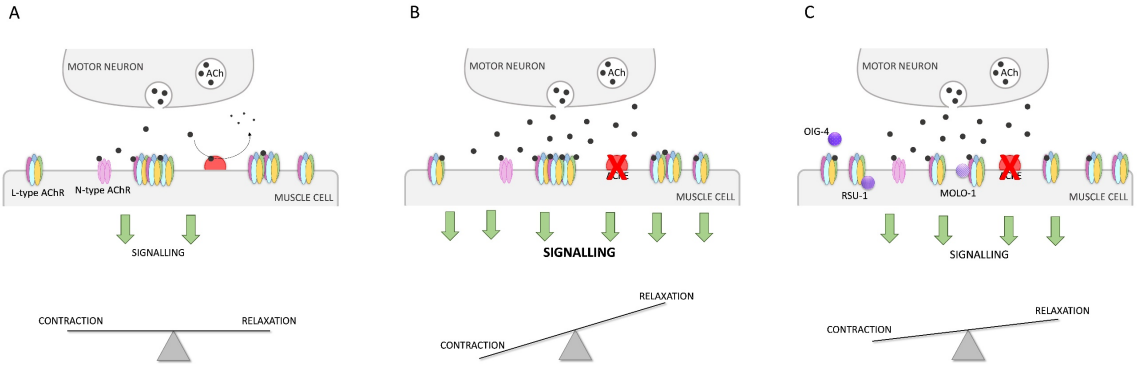

Figure 4.14. Hypothesised mechanism underpinning paraoxon-induced plasticity in nematodes exposed to 500 µM paraoxon-ethyl. A) The body wall motor neuron releases acetylcholine to the neuromuscular junction that activates L-type and N-type nicotinic receptors causing the muscle contraction. Acetylcholinesterases catalyse the breakdown of acetylcholine ending the signalling. This causes a cholinergic transmission from the motor neuron that allows the proper balance between contraction and relaxation of the muscle fibres, and therefore, the normal feeding and locomotion of animals. B) The inhibition of the acetylcholinesterase function by the presence of paraoxon-ethyl causes an increase of acetylcholine at the neuromuscular junction. This leads to the hyperstimulation of the cholinergic receptors expressed in the muscle fibres and, therefore the overstimulation of the cholinergic transmission. This overstimulation triggers the hypercontraction of the muscle cells causing the paralysis of the underpinned phenotypes, feeding and locomotion. C) The location of the L-type receptors at the body wall neuromuscular junction is altered in an OIG-4 and/or RSU-1 dependent mechanism. The sensitivity this L-type receptor is additionally modified in a mechanism dependent of the auxiliary protein MOLO-1. These two pathways contribute to the modulation of the cholinergic signal in the presence of paraoxon-ethyl, allowing an improvement in the contraction-relaxation balance of the muscle fibres and, therefore the spontaneous recovery of the phenotypes involved. These pathways underpinning the paraoxon-induced mitigating plasticity in nematodes could bring light to alternative pharmacological treatments in order to palliate against the effects of organophosphate poisoning.

The two non-alpha subunits, UNC-29 and LEV-1, of the L-type receptor were previously pointed as molecular determinants of the aldicarb sensitivity in the pharyngeal pumping of nematodes exposed to the carbamate [454]. Here, we observed that mutant nematodes *unc-29 (e193)* and *lev-1 (e211)* displayed a paraoxon-induced plasticity response in the pharyngeal pumping characterized by only two phases: the initial inhibition and spontaneous recovery. This spontaneous recovery is sustained over the time, lacking the subsequent inhibition observed in wild type worms (Figure 4.7). Interestingly, this phenotype is not conserved in null mutant strains of *unc-29 (e1072)* or *lev-1 (x427)* but phenocopy the response observed in *molo-1 (kr100)* deficient nematodes (Figure 4.9). Since MOLO-1 is an auxiliary protein involved in the sensitivity of the L-type acetylcholine receptor [317], the data indicate that the *e193* mutation of *unc-29* and the *e211* mutation of *lev-1* might affect the L-type receptor sensitivity or shifting at the body wall muscles influencing in its potency and/or efficiency. In addition, we demonstrated that LEV-1 and UNC-29 subunits harbouring the *e211* and *e193* mutations, respectively, are able to assemble with the alpha subunits UNC-38, UNC-63 and LEV-8, and reconstitute functional L-type receptors when expressed in *Xenopus* oocytes. The resulting L-type receptor displayed reduced response to a high concentration of acetylcholine (Figure 4.12) suggesting a role of the mutated subunits as modulators of the L-type receptor activity. The fact that the *e193* mutation in UNC-29 exhibited a stronger dominant negative effect compared to *e211* in LEV-1 lays an explanation for the partial rescue of the phenotype observed in transgenic lines expressing wild type UNC-29 into the body wall muscle of a *unc-29 (e193)* mutant strain (Figure 4.8B).

The *e211* mutation consists in a glycine to glutamic acid substitution at the fourth transmembrane domain of the LEV-1 subunit (Figure 4.10). This domain of the acetylcholine receptor subunits mediates the interaction of the receptor with the phospholipid bilayer and contributes to the kinetic of activation of the receptor. Several studies revealed that mutations in the fourth transmembrane domain of the nicotinic receptor subunits alter the channel opening and closing more than the trafficking or expression of the receptor [465-469]. In fact, the equivalent mutation within the transmembrane domain of a non-alpha subunit in *Torpedo californica* reduced the potency of the receptor to high concentrations of acetylcholine but has no effect at low doses [466]. This could explain why nematodes harbouring this change exhibit wild type phenotype for locomotion and pumping but strong resistance to inhibition of these two behaviours in the presence of anti-cholinesterases [454].

The *e193* mutation of *unc-29* consists of a proline to serine substitution at the loop connecting the second and third transmembrane domain (Figure 4.11). This proline is highly conserved in all the subunits of the Cys-loop receptor superfamily of the ligand-gated ion channels [470,471]. The coupling

of this proline with extra cellular domains in the mammalian muscle-type receptor is essential for the gating of the channel without affecting the trafficking or expression [470,472-475].

Four strains were identified by exhibiting a sustained recovery of the pharyngeal function in the presence of paraoxon-ethyl, *ric-3 (hm9)*, *lev-1 (e211)*, *unc-29 (e193)* and *molo-1 (kr100)*. RIC-3 is an ancillary protein responsible of the maturation of different types of acetylcholine receptors (L-type, N-type and ACR-2R) [265,476]. However, the *e211* mutation of LEV-1, the *e193* mutation of UNC-29 and MOLO-1 affect the sensitivity of the L-type receptor by decreasing the channel gating. This points that the disruption of the L-type receptor function during organophosphate intoxication might be an interesting route to mitigate the symptoms of the cholinergic syndrome (Figure 4.14). The use of nicotinic receptor antagonists has been previously proposed in the treatment of organophosphate intoxication [207,213,477,478]. However, this medication causes a significant hypotension due to the blockage of the cholinergic signal at the parasympathetic ganglia [213,478]. A more specific antagonist of the nicotinic receptor at the skeletal muscle has been also considered. In fact, there are strong evidences supporting that some oximes have a beneficial effect in the recovery from nicotinic overstimulation symptoms due to the blockage of the nicotinic receptors at the skeletal muscle [173,178,226]. However, the allosteric modulation of the nicotinic receptor sensitivity could represent the most attractive option [207,213,477,478]. Negative allosteric modulators could block the nicotinic receptor activation greater as the stimulation by acetylcholine increases. Non-competitive antagonist drugs have been demonstrated to block the open of the channel *in vivo* and *in vitro* organophosphate poisoning models with beneficial effects in the recovery from intoxication [183,207,209,210].

Although further investigations will be required in order to identify pharmacological treatments to modulate the cholinergic signalling during organophosphate intoxication, our research open new insights into the mechanisms that induce cholinergic plasticity in this context (Figure 4.14). To achieve this, the nematode *C. elegans* might provide an attractive *in vivo* model for screening of non-competitive nicotinic receptor antagonist with potential effects against organophosphate poisoning.

4.6. Conclusion

In the present work, we demonstrated that cholinergic plasticity as consequence of anti-cholinesterase poisoning is readily expressed in the model organism *C. elegans*. This can be observed as clear effects on the pharyngeal phenotype, previously highlighted as bio-assay for investigating anti-cholinesterase poisoning [415]. The pre-exposure of nematodes to low doses of either aldicarb or paraoxon-ethyl modifies the pumping rate when nematodes are exposed to higher doses of the same drug. This effect was opposite for aldicarb and paraoxon-ethyl indicating

a drug-dependent mechanism. However, the chronic exposure to high doses of paraoxon-ethyl triggers a spontaneous recovery of the pharyngeal and body wall phenotypes in wild type nematodes in the presence of the drug. Our results are consistent with previous observations where the cholinergic activity can be partially restored independently of acetylcholinesterase reactivation or *de novo* synthesis [479-483]. This might indicate the potential of plasticity-promoting treatments as an alternative option against anti-cholinesterase poisoning symptoms.

4.7. Acknowledgements

We thank Dr Jean-Louis Bessereau, Dr Denise Walker and Dr William Schafer for sharing strains; Dr Antonio Miranda-Vizuete for sharing *Punc-122::gfp* marker plasmid.

Additional *C. elegans* strains were provided by the CGC, which is funded by NIH Office of Research Infrastructure Programs (P40 OD010440).

4.8. Author contributions

Patricia G. Izquierdo: Conceptualization, Data curation, Formal analysis, Investigation, Methodology, Validation, Visualization, Roles/Writing - original draft, review & editing. **Claude L. Charvet**: Data curation, Formal analysis, Investigation, Methodology, Writing – review & editing. **Cedric Neveu:** Funding acquisition, Writing - review & editing. **Vincent O'Connor**: Conceptualization, Funding acquisition, Methodology, Supervision, Writing - review & editing. **Christopher Green**: Conceptualization, Funding acquisition, Methodology, Supervision, Writing - review & editing. **Lindy Holden-Dye**: Conceptualization, Funding acquisition, Methodology, Supervision, Writing - review & editing. **John Tattersall**: Conceptualization, Funding acquisition, Methodology, Supervision, Writing - review & editing.

4.9. Funding

This work was funded by the University of Southampton (United Kingdom), The Gerald Kerkut Charitable Trust (United Kingdom) and the Defence Science and Technology Laboratory, Porton Down, Wiltshire (United Kingdom). Support was received by the Institut National de Recherche pour l'Agriculture, l'Alimentation et l'Environnement (INRAE) to CLC and CN.

The funders had no role in study design, data collection and analysis, decision to publish, or preparation of the manuscript.

4.10. Conflict of interest

The authors declare that they have no conflicts of interest with the contents of this article.

Chapter 5

General discussion

Organophosphates are potent neurotoxins used as pesticides in agriculture and nerve agents in warfare and terrorism [367,371]. The associated human toxicity is not only a public health issue but also a national security concern [11-13]. Current pharmacological countermeasures against organophosphate poisoning have limited efficacy [186,373] and the research of alternative antidotes relies on the use of model organisms [236].

A suitable model organism for organophosphate research needs to replicate the human toxicity developed by these neurotoxins. Furthermore, these signs of poisoning need to be correlated with organophosphate mode of action during intoxication and recovery [236].

Mammalian model organisms exhibit a faithful manifestation of human organophosphate signs and symptoms that are well-correlated with acetylcholinesterase activity [236]. However, invertebrate models might offer other advantages without sacrificing the molecular basis of organophosphate toxicity (see section 1.3.4.2) [246,247,251]. These models also exhibit impairments of neuromuscular-controlled phenotypes [249,334,353,360].

In this thesis, I have introduced the quantification of pharyngeal pumping in *C. elegans* as a bio-assay to research organophosphate intoxication and recovery [415]. This set the basis to dig into the molecular consequences of the cholinergic transmission during the overstimulation caused by organophosphate exposure. I observed that nematodes respond to this stress condition by developing behavioural plasticity that mitigates the toxicity of the neurotoxin. The molecular mechanism underpinning this response was investigated and highlighted the modulation of the acetylcholine signalling by adjusting the response of nicotinic receptors. This level of regulation could be achieved by either targeting the receptor or the auxiliary proteins that support its function. Specifically, proteins involved in the clustering and sensitivity of nicotinic receptors were identified potential therapeutic targets to develop antidotes against organophosphate poisoning.

5.1. *C. elegans* pharyngeal pumping as platform to investigate organophosphate toxicity

Among the phenotypes impaired by organophosphate exposure in *C. elegans* [249,334,353,360], I have defined the inhibition of pharyngeal pumping on food as a particularly appropriate bio-assay to research organophosphate intoxication and antidotes (chapter 2) [415]. The dose- and time-dependent inhibition of pumping phenotype was consistent with the residual acetylcholinesterase

activity in nematodes exposed to either aldicarb or organophosphates. This fulfils the criteria to consider *C. elegans* a suitable model for organophosphate toxicity.

Beyond this, the pharyngeal phenotype of nematodes exposed to anti-cholinesterases exhibited the best correlation between the behavioural output and the enzyme function compared to paralysis and body length (Figure 2.6 and Figure 2.8). This implied that the pharyngeal neuromuscular junction is more directly linked to acetylcholinesterase inhibition. Furthermore, nematodes pump about 250 times per minute on food and this could offer a better dynamic scale to discriminate incremental effects of the drug action compared to the binary quantification of paralysis and the limited range of decrease in the body length (chapter 2). In this sense, pharyngeal pumping provides a whole organism bio-assay to investigate organophosphate toxicity.

5.2. *C. elegans* pharyngeal pumping as bio-assay to research recovery from intoxication and antidotes

I have demonstrated the potential of the nematode as platform to research recovery from intoxication as well as antidotes (chapter 2) [415]. This was evidenced by the organophosphate-dependent pattern of restoration of the pharyngeal function observed when nematodes are removed from the intoxicating compound. This aligns with the processes of spontaneous reactivation and irreversible inhibitions observed in mammalian models. Further biochemical *in vitro* analysis of the acetylcholinesterase activity confirmed the correlation between phenotype recovery and enzyme activity restoration.

Overall, I concluded that the quantification of pumping rate provides an excellent bio-assay to research organophosphate toxicity as well as a potential improved throughput screening platform to assess the efficiency of new antidotes [415]. This approach could replace some of the experimental model animals currently used for this purpose, aligning with the 3R principles of animal experimental techniques (replacement, reduction and refinement).

5.3. Organophosphate-induce plasticity as alternative approach to mitigate poisoning

Having established a baseline for utilizing pumping phenotype to investigate toxicity, the worm exposure to toxicants was manipulated to probe if *C. elegans* develop organophosphate-induced plasticity. I hypothesised that molecular pathways underpinning the plasticity in this context might modulate the strength of the acetylcholine signalling with potential benefits to develop alternative pathways to mitigate organophosphate toxicity. Two classical experimental protocols were used to induce behavioural plasticity in *C. elegans*: the preconditioning with sublethal doses

prior exposure to higher concentrations and the chronic exposure to high intoxicating doses [448,449]. Both paradigms, precondition and protracted drug exposure, induced pharyngeal plasticity in *C. elegans* (chapter 4). The preconditioning paradigm resulted in the aggravation of the organophosphate signs in *C. elegans* behaviour, contrary what I was pursuing (Figure 4.3). Interestingly, nematodes continuously exposed to 25-fold higher concentration than the IC_{50} value for paraoxon-ethyl displayed an intoxication pattern of the pumping rate characterized by three phases: an initial inhibition, a spontaneous recovery and a subsequent inhibition after 3, 6 and 24 hours of exposure, respectively (Figure 4.5). Furthermore, this plasticity effect was conserved for both pumping rate and body length, supporting the notion of a common mechanism developing behavioural plasticity in nematodes exposed to this neurotoxin. To my knowledge, this is the first evidence of organophosphate-induced plasticity during high dose exposure with potential benefits for poisoning mitigation. Hence, understanding the molecular mechanism underpinning this could bring to light new alternative targets in the development of antidotes against organophosphate poisoning.

5.4. Molecular determinants of the paraoxon-ethyl mitigating plasticity at the pharynx are located at the body wall neuromuscular junction

The screening of mutant nematodes against absence and/or potentiation of this pharyngeal plasticity suggested that the molecular determinants of this paradigm exert their action from the body wall neuromuscular junction. Thus, this highlights two levels of regulation of feeding in nematodes (Figure 3.7). Under physiological cholinergic stimulation, the pharyngeal function is governed by molecular determinants at the pharynx. However, under pharmacological overstimulation of the body wall muscle, determinants at the body wall neuromuscular junction can additionally modulate the rate of food intake [454]. These conclusions about the distal modulation of the pharynx by the body wall neuromuscular junction add value to the use of pharyngeal pumping as bio-assay to investigate intoxication and recovery. In this sense, the pharyngeal function allows a readout of the stage of two neuromuscular junctions during organophosphate intoxication. This paradigm additionally offers an opportunity to investigate mechanisms of inter-tissue communication in the nematode.

5.5. Modulation of L-type receptor signalling as mechanism triggering organophosphate-induced behavioural plasticity

5.5.1. Modulation by targeting the receptor

Three mutant strains were identified to exhibit an enhanced and sustained recovery of the pharyngeal pumping after the spontaneous recovery when intoxicated with paraoxon-ethyl.

These strains carried different mutations involved in the gating of the L-type receptor without affecting the level, clustering or trafficking to the receptors into the membrane surface. This function is consistent with the mode of action of allosteric modulators. In the case of MOLO-1 deficient strains, it is noteworthy that it is the absence of positive modulator that triggers the sustained recovery of the pharyngeal function. Thus, negative allosteric modulators are proposed as potential antidotes against organophosphate poisoning. This approach aligns with the previous hypothesis about the potential benefits of nicotinic receptor antagonists as antidotes for organophosphate intoxication (reviewed in section 1.3.3.3 and discussed in section 4.5).

The reason why MOLO-1 does not exert any function at the two first phases of intoxication (initial inhibition and spontaneous recovery) is still unclear. A hypothesis would suggest a different expression profile of *molo-1* between first and late stages of the paraoxon-ethyl intoxication. If the transcription of the gene was upregulated at 24 hours of intoxication this could result in an increase of acetylcholine receptor signalling and therefore a stronger inhibition of the pumping rate. Further transcriptomic analysis at the different steps of intoxication would be required to either confirm this hypothesis or propose new ones.

5.5.2. Modulation by targeting auxiliary proteins

Two mutant strains were identified to lack the spontaneous recovery of the pharyngeal pumping characterized in wild type nematodes exposed to paraoxon-ethyl. These strains carried mutations in two neuromuscular junction proteins involved in the clustering of the L-type receptor at the body wall muscle (Figure 4.13). As mentioned above, the absence of MOLO-1 triggered the opposite effect, viz, an enhanced and sustained recovery after the spontaneous recovery (Figure 4.9). These results indicate that paraoxon-ethyl induced plasticity is underpinned by auxiliary proteins that support acetylcholine signalling via L-type receptor. While the plasticity involved in the spontaneous recovery might be caused by dynamic changes in receptor clustering, the subsequent inhibition might be triggered by a differential sensitivity of the receptor to acetylcholine during organophosphate intoxication (chapter 4).

These proteins allow a fine tune adjustment of the receptor kinetics under overstimulation conditions, leading to a better adjustment of the contraction relaxation balance at the body wall muscle (chapter 4). This indicates that different levels of nicotinic receptor modulation could be achieved by altering the interaction of these receptors with endogenous auxiliary proteins that support its proper function (Figure 4.14).

5.5.3. Potential alternative pathways to treat organophosphate poisoning

Among the auxiliary proteins that orchestrate the formation of a mature functional nicotinic receptor at the synapse (Figure 1.19), I identified three that underpin the drug-induced plasticity, OIG-4 and RSU-1 are involved in clustering and MOLO-1 alters sensitivity of the L-type receptor.

5.5.3.1. Targeting the clustering pathway of nicotinic receptors

OIG-4 is a single immunoglobulin domain protein secreted by the muscle and required for the synaptic organization of the L-type receptor at the body wall neuromuscular junction [314]. RSU-1 is a cytoplasmic protein containing seven leucine-rich repeats evolutionarily conserved to mammals. OIG-4 orthologue has not been identified in vertebrates. RSU-1 exists in mammals but has not been linked with the clustering of nicotinic receptors. However, the mammalian genome encodes for other auxiliary proteins that mimic the function of OIG-4 and RSU-1 in *C. elegans* (Figure 5.1).

The balance of synaptic and extra synaptic receptors at the neuromuscular junction of mammals implicates a complex machinery of proteins (recently reviewed by Cruz, P.M.R. et al [484]) (Figure 5.1). Mutations in some proteins of this machinery or abnormal expression of antibodies against them have been implicated in myasthenia syndromes, disorders of the neuromuscular transmission characterized by muscle weakness and fatigue [485-487]. In fact, pharmacological targeting of the agrin-LRP4-MuSK signalling pathway has been hypothesised to have potential benefits in the treatment of myasthenia gravis and other neuromuscular disorders [488]. I have demonstrated that this approach could be extended for the treatment of organophosphate poisoning.

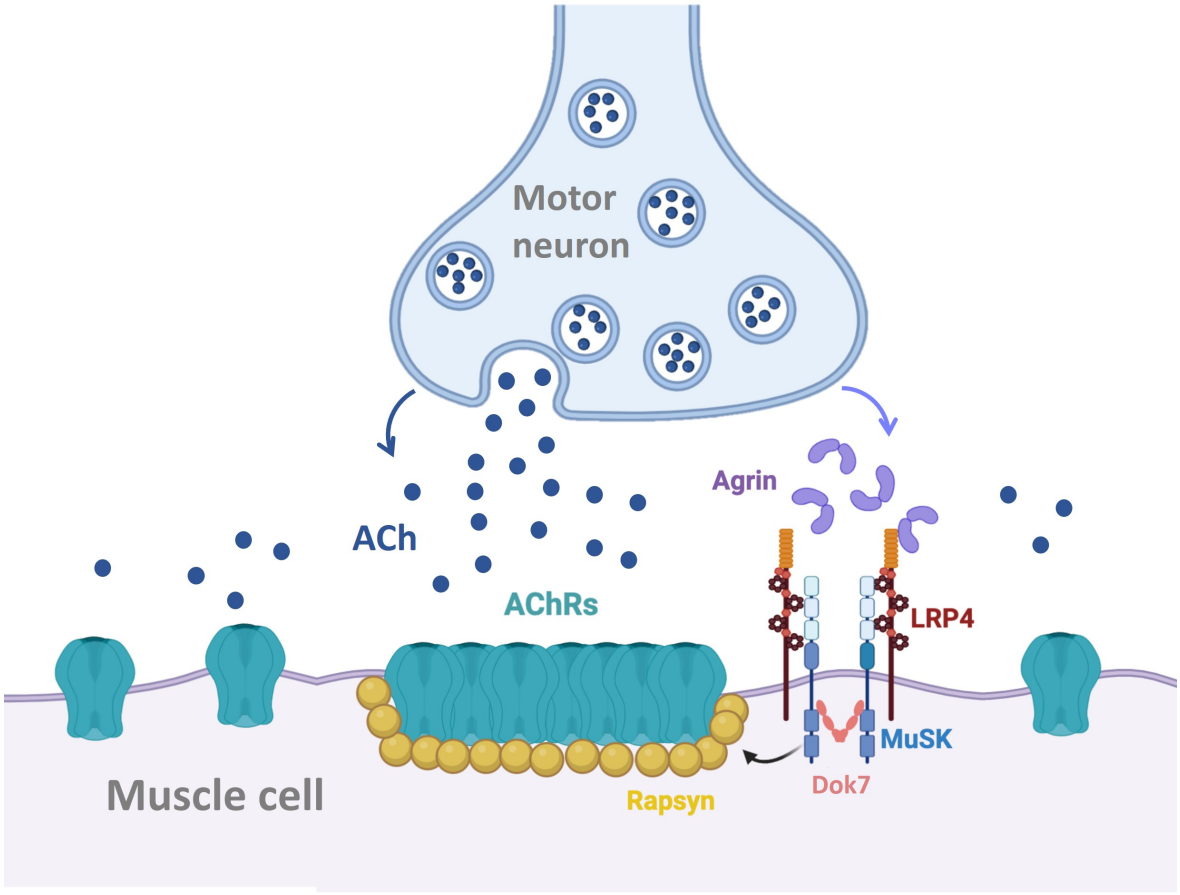

Figure 5.1. Schematic representation of the acetylcholine receptor clustering at mammalian neuromuscular junction. The glycoprotein agrin is released by the motor neuron and binds to the low-density lipoprotein receptor LRP4 at the membrane of the muscle, triggering its dimerization [489]. This is essential for the activation of MuSK [490]. This activation is sustained by the cytoplasmic protein Dok-7 [491]. MuSK is a protein tyrosine kinase that auto phosphorylates upon activation inducing a complex signalling cascade that results in the clustering of nicotinic receptors by the cytoplasmic anchoring protein rapsyn [492]. Figure adapted from [484] and created with BioRender.com.

5.5.3.2. Targeting the sensitivity of nicotinic receptors

MOLO-1 consists of a single transmembrane protein that interacts with the subunits of the L-type receptor early in the secretory pathway and traffics with it to the plasma membrane [317]. Since this interaction promotes the channel opening conformation, MOLO-1 is considered a positive allosteric modulator of the L-type receptor [317]. This principle of auxiliary proteins acting to modulate receptor function beyond the process of trafficking and clustering is well established in glutamate receptors in mammals but is less well articulated in the context of nicotinic acetylcholine receptors [493].

MOLO-1 orthologue proteins have not been identified in vertebrates. However, prototoxins are endogenous toxin-like proteins which show similar functionality to MOLO-1 modulating the gating of nicotinic receptors in mammals (Figure 5.2) [444].

Prototoxins are members of the ly6/uPAR superfamily. This is characterized by the presence of highly conserved cysteine residues to create a three-finger toxin fold, a highly effective receptor

binding motif [494,495]. The different proteins composing this family have distinct expression profiles and nicotinic receptor subtype selectivity [495,496]. These features open a wide range of opportunity in the fine tune modulation of the cholinergic signalling. Although some authors have hypothesised their potential benefit in the treatment of developmental disorders such as Alzheimer's and nicotine addiction [444,496,497], it is surprising that their potential has not been uncovered to address the organophosphate intoxication issue.

The outcome of this thesis encourages the characterization of prototoxins as promising pharmaceutical targets against organophosphate poisoning.

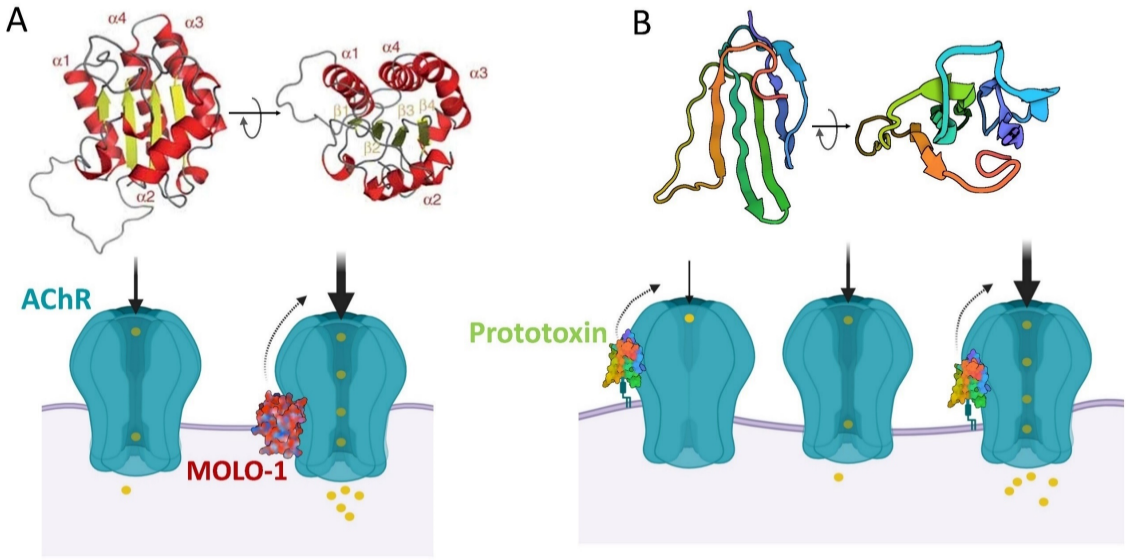

Figure 5.2. MOLO-1 and prototoxins are structurally different proteins with similar function in *C. elegans* and mammals, respectively. A) Front and top view of MOLO-1 protein structure modelled on the basis of homology with the bacterial 2KW7 structure. Figure taken from [317]. Co-expression of MOLO-1 along with L-type receptor subunits (UNC-63, UNC-38, UNC-29, LEV-1 and LEV-8) increases the sensitivity of the receptor. B) Front and top view of Lynx-1 (PDB accession number 2L03) as general model for prototoxin structure. These auxiliary proteins can be found soluble or GPI anchor to the membrane interacting with the receptor at the extracellular domain. Different prototoxins exhibit subtype specificity functioning either as positive or a negative allosteric modulator of nicotinic receptors in mammals [444]. Yellow circles represent cations. Figure created with BioRender.com.

5.6. Conclusion and future perspectives

Three main points can be extracted from this thesis that lay the background for future research.

Firstly, I have demonstrated the suitability of *C. elegans* pharyngeal pumping as a bio-assay to investigate organophosphate toxicity and antidotes. However, this platform could be improved by the transgenic expression of human acetylcholinesterase. In these transgenic lines, the control of the neuromuscular-dependent behavioural output will be performed by the human enzyme. This might allow a better refinement of the antidotes tested before moving to mammalian models.

Secondly, I have observed that the overstimulation of the cholinergic transmission at the body wall muscle that control locomotion imposes an indirect control of feeding. This highlights an interesting inter-tissue communication paradigm that has parallels with systemic signalling observed in cachexia. Discovering the molecular mechanisms behind this might be crucial to understanding how tissues communicate with each other during stress.

Finally, I have discovered a drug-induced plasticity paradigm that is enhanced or abolished in different mutants involved in the sensitivity or clustering of the L-type receptor at the body wall muscle, respectively. On the one hand, this provokes investigations of the structural organization of cholinergic synapses as well as the transcription profile of nematodes during intoxication to understand the principles of mitigating plasticity. On the other hand, this inspires the characterization of the role of prototoxins and proteins involved in the clustering of the receptors in mammalian models during organophosphate poisoning. This might be a first step in the development of alternative and more efficient antidotes.

List of references

1 Goulding, R. Organophosphorus Insecticides - a General Introduction - Who. *J. R. Soc. Health* **107**, 159-159, doi:Doi 10.1177/146642408710700420 (1987).

2 FAO. *Food and Agriculture Organization of the United Nations. FAOSTAT Pesticides Use*, <http://www.fao.org/faostat/en/#data/RP> (2017).

3 Szinicz, L. History of chemical and biological warfare agents. *Toxicology* **214**, 167-181, doi:10.1016/j.tox.2005.06.011 (2005).

4 Johnson, N. H., Larsen, J. C. & Meek, E. in *Handbook of Toxicology of Chemical Warfare Agents (Second Edition)* (ed Ramesh C. Gupta) 7-15 (Academic Press, 2015).

5 Chai, P. R., Hayes, B. D., Erickson, T. B. & Boyer, E. W. Novichok agents: a historical, current, and toxicological perspective. *Toxicology Communications* **2**, 45-48, doi:10.1080/24734306.2018.1475151 (2018).

6 Nepovimova, E. & Kuca, K. Chemical warfare agent NOVICHOK - mini-review of available data. *Food Chem Toxicol* **121**, 343-350, doi:10.1016/j.fct.2018.09.015 (2018).

7 Morris, J. C. *et al.* Metrifonate benefits cognitive, behavioral, and global function in patients with Alzheimer's disease. *Neurology* **50**, 1222-1230, doi:10.1212/wnl.50.5.1222 (1998).

8 Scali, C. *et al.* Effect of metrifonate on extracellular brain acetylcholine and object recognition in aged rats. *Eur. J. Pharmacol.* **325**, 173-180, doi:10.1016/s0014-2999(97)00128-3 (1997).

9 Raskind, M. A., Cyrus, P. A., Ruzicka, B. B., Gulanski, B. I. & Metrifonate Study, G. The effects of metrifonate on the cognitive, behavioral, and functional performance of Alzheimer's disease patients. *J. Clin. Psychiatry* **60**, 318-325, doi:10.4088/JCP.v60n0510 (1999).

10 Cholkar, K., Trinh, H. M., Pal, D. & Mitra, A. K. Discovery of novel inhibitors for the treatment of glaucoma. *Expert Opin Drug Discov* **10**, 293-313, doi:10.1517/17460441.2015.1000857 (2015).

11 Jeyaratnam, J. Acute pesticide poisoning: a major global health problem. *World Health Statistics Quarterly* **43**, 6 (1990).

12 Eddleston, M. & Phillips, M. R. Self poisoning with pesticides. *Bmj-Brit Med J* **328**, 42-44, doi:DOI 10.1136/bmj.328.7430.42 (2004).

13 Gunnell, D., Eddleston, M., Phillips, M. R. & Konradsen, F. The global distribution of fatal pesticide self-poisoning: Systematic review. *Bmc Public Health* **7**, doi:Artn 357

10.1186/1471-2458-7-357 (2007).

14 Bajgar, J., Fusek, J., Kassa, J., Kuca, K. & Jun, D. *Global Impact of Chemical Warfare Agents Used Before and After 1945*. (Academic Press Ltd-Elsevier Science Ltd, 2015).

15 Nagao, M. *et al.* Definitive evidence for the acute sarin poisoning diagnosis in the Tokyo subway. *Toxicology and Applied Pharmacology* **144**, 198-203, doi:DOI 10.1006/taap.1997.8110 (1997).

16 John, H. *et al.* Fatal sarin poisoning in Syria 2013: forensic verification within an international laboratory network. *Forensic Toxicol* **36**, 61-71, doi:10.1007/s11419-017-0376-7 (2018).

17 Chai, P. R., Boyer, E. W., Al-Nahhas, H. & Erickson, T. B. Toxic chemical weapons of assassination and warfare: nerve agents VX and sarin. *Toxicol Commun* **1**, 21-23, doi:10.1080/24734306.2017.1373503 (2017).

18 Vale, J. A., Marrs, T. O. & Maynard, R. C. Novichok: a murderous nerve agent attack in the UK. *Clin Toxicol (Phila)* **56**, 1093-1097, doi:10.1080/15563650.2018.1469759 (2018).

19 Steindl, D. *et al.* Novichok nerve agent poisoning. *Lancet* **397**, 249-252, doi:10.1016/S0140-6736(20)32644-1 (2021).

20 John, H., Balszuweit, F., Kai, K. H., Worek, F. & Thiermann, H. *Toxicokinetic Aspects of Nerve Agents and Vesicants*. (Academic Press Ltd-Elsevier Science Ltd, 2015).

21 Kim, S. *et al.* PubChem 2019 update: improved access to chemical data. *Nucleic Acids Res.* **47**, D1102-D1109, doi:10.1093/nar/gky1033 (2019).

22 Niven, A. S. & Roop, S. A. Inhalational exposure to nerve agents. *Respir Care Clin N Am* **10**, 59-74, doi:10.1016/S1078-5337(03)00049-2 (2004).

23 Kim, K. H., Kabir, E. & Jahan, S. A. Exposure to pesticides and the associated human health effects. *Sci Total Environ* **575**, 525-535, doi:10.1016/j.scitotenv.2016.09.009 (2017).

24 John, H., Breyer, F., Thumfart, J. O., Hochstetter, H. & Thiermann, H. Matrix-assisted laser desorption/ionization time-of-flight mass spectrometry (MALDI-TOF MS) for detection and identification of albumin phosphylation by organophosphorus pesticides and G- and V-type nerve agents. *Anal Bioanal Chem* **398**, 2677-2691, doi:10.1007/s00216-010-4076-y (2010).

25 Sun, J. C. & Lynn, B. C. Development of a MALDI-TOF-MS method to identify and quantify butyrylcholinesterase inhibition resulting from exposure to organophosphate and carbamate pesticides. *J Am Soc Mass Spectr* **18**, 698-706, doi:10.1016/j.jasms.2006.11.009 (2007).

26 Sweeney, R. E., Langenberg, J. P. & Maxwell, D. M. A physiologically based pharmacokinetic (PB/PK) model for multiple exposure routes of soman in multiple species. *Arch Toxicol* **80**, 719-731, doi:10.1007/s00204-006-0114-0 (2006).

27 Chilcott, R. P. *et al.* In vivo skin absorption and distribution of the nerve agent VX (O-ethyl-S-[2(diisopropylamino)ethyl] methylphosphonothioate) in the domestic white pig. *Hum Exp Toxicol* **24**, 347-352, doi:10.1191/0960327105ht537oa (2005).

28 Vilanova, E. & Sogorb, M. A. The role of phosphotriesterases in the detoxication of organophosphorus compounds. *Crit Rev Toxicol* **29**, 21-57, doi:Doi 10.1080/10408449991349177 (1999).

29 Mackness, M. I. A-Esterases - Enzymes Looking for a Role. *Biochem. Pharmacol.* **38**, 385-390, doi:Doi 10.1016/0006-2952(89)90376-6 (1989).

30 Brealey, C. J., Walker, C. H. & Baldwin, B. C. A-Esterase Activities in Relation to the Differential Toxicity of Pirimiphos-Methyl to Birds and Mammals. *Pestic Sci* **11**, 546-554, doi:DOI 10.1002/ps.2780110512 (1980).

31 Walker, C. H., Brealey, C. J., Mackness, M. I. & Johnston, G. Toxicity of Pesticides to Birds - the Enzymatic Factor. *Biochem Soc T* **19**, 741-745, doi:DOI 10.1042/bst0190741 (1991).

32 Rice, H. *et al.* The potential role of bioscavenger in the medical management of nerve-agent poisoned casualties. *Chem-Biol Interact* **259**, 175-181, doi:10.1016/j.cbi.2016.04.038 (2016).

33 Butler, A. M. & Murray, M. Biotransformation of Parathion in Human Liver: Participation of CYP3A4 and its Inactivation during Microsomal Parathion Oxidation. *J Pharmacol Exp Ther* **280**, 966-973 (1997).

34 Kasagami, T., Miyamoto, T. & Yamamoto, I. Activated transformations of organophosphorus insecticides in the case of non-AChE inhibitory oxons. *Pest Management Science* **58**, 1107-1117, doi:10.1002/ps.546 (2002).

35 Li, B., Schopfer, L. M., Hinrichs, S. H., Masson, P. & Lockridge, O. Matrix-assisted laser desorption/ionization time-of-flight mass spectrometry assay for organophosphorus toxicants bound to human albumin at Tyr411. *Anal Biochem* **361**, 263-272, doi:10.1016/j.ab.2006.11.018 (2007).

36 Li, B. *et al.* Binding and hydrolysis of soman by human serum albumin. *Chemical Research in Toxicology* **21**, 421-431, doi:10.1021/tx700339m (2008).

37 Pope, C. N. Organophosphorus pesticides: Do they all have the same mechanism of toxicity? *J Toxicol Env Heal B* **2**, 161-181, doi:Doi 10.1080/109374099281205 (1999).

38 Silveira, C. L. P., Eldefrawi, A. T. & Elderfrawi, M. E. Putative M2 Muscarinic Receptors of Rat-Heart Have High-Affinity for Organophosphorus Anticholinesterases. *Toxicology and Applied Pharmacology* **103**, 474-481, doi:Doi 10.1016/0041-008x(90)90320-T (1990).

39 Bakry, N. M., el-Rashidy, A. H., Eldefrawi, A. T. & Eldefrawi, M. E. Direct actions of organophosphate anticholinesterases on nicotinic and muscarinic acetylcholine receptors. *J Biochem Toxicol* **3**, 235-259, doi:10.1002/jbt.2570030404 (1988).

40 Casida, J. E. & Quistad, G. B. Serine hydrolase targets of organophosphorus toxicants. *Chem-Biol Interact* **157**, 277-283, doi:10.1016/j.cbi.2005.10.036 (2005).

41 Lotti, M. The pathogenesis of organophosphate delayed polyneuropathy. *Crit Rev Toxicol* **21**, 465-487, doi:10.3109/10408449209089884 (1992).

42 Jokanovic, M. & Kosanovic, M. Neurotoxic effects in patients poisoned with organophosphorus pesticides. *Environ. Toxicol. Pharmacol.* **29**, 195-201, doi:10.1016/j.etap.2010.01.006 (2010).

43 Richardson, R. J. *et al.* Neuropathy target esterase (NTE/PNPLA6) and organophosphorus compound-induced delayed neurotoxicity (OPIDN). *Adv Neurotoxicol* **4**, 1-78, doi:10.1016/bs.ant.2020.01.001 (2020).

44 Jokanovic, M., Stukalov, P. V. & Kosanovic, M. Organophosphate Induced Delayed Polyneuropathy. *CNS Neurol. Disord.-Drug Targets* **1**, 593-602, doi:10.2174/1568007023338879 (2002).

45 Greiner, A. J., Richardson, R. J., Worden, R. M. & Ofoli, R. Y. Influence of lysophospholipid hydrolysis by the catalytic domain of neuropathy target esterase on the fluidity of bilayer lipid membranes. *Biochim Biophys Acta* **1798**, 1533-1539, doi:10.1016/j.bbamem.2010.03.015 (2010).

46 Zaccheo, O., Dinsdale, D., Meacock, P. A. & Glynn, P. Neuropathy target esterase and its yeast homologue degrade phosphatidylcholine to glycerophosphocholine in living cells. *J Biol Chem* **279**, 24024-24033, doi:10.1074/jbc.M400830200 (2004).

47 Ray, D. E. & Richards, P. G. The potential for toxic effects of chronic, low-dose exposure to organophosphates. *Toxicol Lett* **120**, 343-351, doi:10.1016/s0378-4274(01)00266-1 (2001).

48 Singh, S. & Sharma, N. Neurological syndromes following organophosphate poisoning. *Neurol India* **48**, 308-313 (2000).

49 M, A. & D. R. Davies, G. Chronic Organophosphate Exposure: Towards the Definition of a Neuropsychiatric Syndrome. *Journal of Nutritional & Environmental Medicine* **7**, 169-176, doi:10.1080/13590849762583 (1997).

50 Misik, J., Pavlikova, R., Cabal, J. & Kuca, K. Acute toxicity of some nerve agents and pesticides in rats. *Drug and Chemical Toxicology* **38**, 32-36, doi:10.3109/01480545.2014.900070 (2015).

51 Tan, D. H. *et al.* Chronic organophosphate (OP)-induced neuropsychiatric disorder is a withdrawal syndrome. *Med Hypotheses* **72**, 405-406, doi:10.1016/j.mehy.2008.11.026 (2009).

52 Koehn, G. L., Henderson, G. & Karczmar, A. G. Di-Isopropyl Phosphofluoridate-Induced Antinociception - Possible Role of Endogenous Opioids. *Eur. J. Pharmacol.* **61**, 167-173, doi:Doi 10.1016/0014-2999(80)90159-4 (1980).

53 Kubek, M. J., Shih, T. M. & Meyerhoff, J. L. Thyrotropin-releasing hormone (TRH) is markedly increased in the rat brain following soman-induced convulsions. *Brain Res* **747**, 328-331, doi:Doi 10.1016/S0006-8993(96)01315-7 (1997).

54 London, L., Flisher, A. J., Wesseling, C., Mergler, D. & Kromhout, H. Suicide and exposure to organophosphate insecticides: Cause or effect? *Am J Ind Med* **47**, 308-321, doi:10.1002/ajim.20147 (2005).

55 Abdollahi, M., Ranjbar, A., Shadnia, S., Nikfar, S. & Rezaie, A. Pesticides and oxidative stress: a review. *Med Sci Monitor* **10**, Ra141-Ra147 (2004).

56 Maxwell, D. M., Brecht, K. M., Koplovitz, I. & Sweeney, R. E. Acetylcholinesterase inhibition: does it explain the toxicity of organophosphorus compounds? *Arch Toxicol* **80**, 756-760, doi:10.1007/s00204-006-0120-2 (2006).

57 Wecker, L., Pollock, V. V., Pacheco, M. A. & Pastoor, T. NICOTINE-INDUCED UP REGULATION OF alpha 4 beta 2 NEURONAL NICOTINIC RECEPTORS IS MEDIATED BY THE PROTEIN KINASE C-DEPENDENT PHOSPHORYLATION OF alpha 4 SUBUNITS. *Neuroscience* **171**, 12-22, doi:10.1016/j.neuroscience.2010.09.005 (2010).

58 Meshorer, E. & Soreq, H. Virtues and woes of AChE alternative splicing in stress-related neuropathologies. *Trends Neurosci* **29**, 216-224, doi:10.1016/j.tins.2006.02.005 (2006).

59 Selkirk, M. E., Lazari, O. & Matthews, J. B. Functional genomics of nematode acetylcholinesterases. *Parasitology* **131**, S3-S18 (2005).

60 Massoulie, J. *et al.* The polymorphism of acetylcholinesterase: post-translational processing, quaternary associations and localization. *Chem Biol Interact* **119-120**, 29-42 (1999).

61 Massoulie, J. *et al.* Acetylcholinesterase: C-terminal domains, molecular forms and functional localization. *J Physiology-Paris* **92**, 183-190, doi:Doi 10.1016/S0928-4257(98)80007-7 (1998).

62 Futerman, A. H., Fiorini, R. M., Roth, E., Low, M. G. & Silman, I. Physicochemical Behavior and Structural Characteristics of Membrane-Bound Acetylcholinesterase from Torpedo Electric Organ - Effect of Phosphatidylinositol-Specific Phospholipase-C. *Biochem J* **226**, 369-377 (1985).

63 Futerman, A. H., Low, M. G., Ackermann, K. E., Sherman, W. R. & Silman, I. Identification of Covalently Bound Inositol in the Hydrophobic Membrane-Anchoring Domain of Torpedo Acetylcholinesterase. *Biochem Bioph Res Co* **129**, 312-317, doi:Doi 10.1016/0006-291x(85)91439-1 (1985).

64 Futerman, A. H., Low, M. G., Michaelson, D. M. & Silman, I. Solubilization of Membrane-Bound Acetylcholinesterase by a Phosphatidylinositol-Specific Phospholipase-C. *Journal of Neurochemistry* **45**, 1487-1494, doi:DOI 10.1111/j.1471-4159.1985.tb07217.x (1985).

65 Low, M. G., Futerman, A. H., Ackermann, K. E., Sherman, W. R. & Silman, I. Removal of Covalently Bound Inositol from Torpedo Acetylcholinesterase and Mammalian Alkaline-

Phosphatases by Deamination with Nitrous-Acid - Evidence for a Common Membrane-Anchoring Structure. *Biochem J* **241**, 615-619 (1987).

66 Silman, I. & Futerman, A. H. Modes of Attachment of Acetylcholinesterase to the Surface-Membrane. *Eur J Biochem* **170**, 11-22, doi:DOI 10.1111/j.1432-1033.1987.tb13662.x (1987).

67 Selkirk, M. E., Lazari, O., Hussein, A. S. & Matthews, J. B. Nematode acetylcholinesterases are encoded by multiple genes and perform non-overlapping functions. *Chem-Biol Interact* **157**, 263-268, doi:10.1016/j.cbi.2005.10.039 (2005).

68 Massoulie, J. The origin of the molecular diversity and functional anchoring of cholinesterases. *Neurosignals* **11**, 130-143, doi:Doi 10.1159/000065054 (2002).

69 Meshorer, E. *et al.* Alternative splicing and neuritic mRNA translocation under long-term neuronal hypersensitivity. *Science* **295**, 508-512, doi:DOI 10.1126/science.1066752 (2002).

70 Kaufer, D., Friedman, A., Seidman, S. & Soreq, H. Acute stress facilitates long-lasting changes in cholinergic gene expression (vol 393, pg 373, 1998). *Nature* **531** (2016).

71 Kaufer, D., Friedman, A., Seidman, S. & Soreq, H. Acute stress facilitates long-lasting changes in cholinergic gene expression. *Nature* **393**, 373-377 (1998).

72 Rotundo, R. L. Biogenesis, assembly and trafficking of acetylcholinesterase. *J Neurochem* **142 Suppl 2**, 52-58, doi:10.1111/jnc.13982 (2017).

73 Marrero, E., Rossi, S. G., Darr, A., Tsoulfas, P. & Rotundo, R. L. Translational regulation of acetylcholinesterase by the RNA-binding protein Pumilio-2 at the neuromuscular synapse. *J. Biol. Chem.* **286**, 36492-36499 (2011).

74 Rotundo, R. L. Asymmetric acetylcholinesterase is assembled in the Golgi apparatus. *Proceedings of the National Academy of Sciences* **81**, 479-483 (1984).

75 Rotundo, R. *et al.* Intracellular Transport, Sorting, and Turnover of Acetylcholinesterase: Evidence for an endoglycosidase H-sensitive form in Golgi apparatus, sarcoplasmic reticulum, and clathrin-coated vesicles and its rapid degradation by a non-lysosomal mechanism. *J. Biol. Chem.* **264**, 3146-3152 (1989).

76 Kasprzak, H. & Salpeter, M. M. Recovery of acetylcholinesterase at intact neuromuscular junctions after in vivo inactivation with di-isopropylfluorophosphate. *Journal of Neuroscience* **5**, 951-955 (1985).

77 Krejci, E., y Valenzuela, I. M.-P., Ameziane, R. & Akaaboune, M. Acetylcholinesterase dynamics at the neuromuscular junction of live animals. *J. Biol. Chem.* **281**, 10347-10354 (2006).

78 y Valenzuela, I. & Akaaboune, M. Acetylcholinesterase mobility and stability at the neuromuscular junction of living mice. *Mol Biol Cell* **18**, 2904 (2007).

79 y Valenzuela, I. M.-P., Hume, R. I., Krejci, E. & Akaaboune, M. In vivo regulation of acetylcholinesterase insertion at the neuromuscular junction. *J. Biol. Chem.* **280**, 31801-31808 (2005).

80 Rotundo, R. L. & Fambrough, D. M. Synthesis, transport and fate of acetylcholinesterase in cultured chick embryo muscle cells. *Cell* **22**, 583-594 (1980).

81 Dvir, H., Silman, I., Harel, M., Rosenberry, T. L. & Sussman, J. L. Acetylcholinesterase: from 3D structure to function. *Chem Biol Interact* **187**, 10-22, doi:10.1016/j.cbi.2010.01.042 (2010).

82 Harel, M. *et al.* Three-dimensional structures of Drosophila melanogaster acetylcholinesterase and of its complexes with two potent inhibitors. *Protein Sci* **9**, 1063-1072 (2000).

83 Hornberg, A., Tunemalm, A. K. & Ekstrom, F. Crystal structures of acetylcholinesterase in complex with organophosphorus compounds suggest that the acyl pocket modulates the aging reaction by precluding the formation of the trigonal bipyramidal transition state. *Biochemistry* **46**, 4815-4825, doi:10.1021/bi0621361 (2007).

84 Quinn, D. M. Acetylcholinesterase - Enzyme Structure, Reaction Dynamics, and Virtual Transition-States. *Chem Rev* **87**, 955-979, doi:DOI 10.1021/cr00081a005 (1987).

85 Wiesner, J., Kriz, Z., Kuca, K., Jun, D. & Koca, J. Acetylcholinesterases - the structural similarities and differences. *J Enzym Inhib Med Ch* **22**, 417-424, doi:10.1080/14756360701421294 (2007).

86 Soreq, H. & Seidman, S. Acetylcholinesterase - new roles for an old actor. *Nat Rev Neurosci* **2**, 294-302, doi:Doi 10.1038/35067589 (2001).

87 Nachmansohn, D. & Wilson, I. B. The enzymic hydrolysis and synthesis of acetylcholine. *Adv Enzymol Relat Subj Biochem* **12**, 259-339, doi:10.1002/9780470122570.ch5 (1951).

88 Colovic, M. B., Krstic, D. Z., Lazarevic-Pasti, T. D., Bondzic, A. M. & Vasic, V. M. Acetylcholinesterase Inhibitors: Pharmacology and Toxicology. *Curr. Neuropharmacol.* **11**, 315-335 (2013).

89 Worek, F., Thiermann, H., Szinicz, L. & Eyer, P. Kinetic analysis of interactions between human acetylcholinesterase, structurally different organophosphorus compounds and oximes. *Biochem. Pharmacol.* **68**, 2237-2248, doi:10.1016/j.bcp.2004.07.038 (2004).

90 Wiener, S. W. & Hoffman, R. S. Nerve agents: a comprehensive review. *J Intensive Care Med* **19**, 22-37, doi:10.1177/0885066603258659 (2004).

91 Li, H. *et al.* Aging pathways for organophosphate-inhibited human butyrylcholinesterase, including novel pathways for isomalathion, resolved by mass spectrometry. *Toxicol Sci* **100**, 136-145, doi:10.1093/toxsci/kfm215 (2007).

92 Adams, G. K., 3rd, Yamamura, H. I. & O'Leary, J. F. Recovery of central respiratory function following anticholinesterase intoxication. *Eur J Pharmacol* **38**, 101-112 (1976).

93 LeBouef, T., Yaker, Z. & Whited, L. in *StatPearls* (2020).

94 Mesulam, M. M., Mufson, E. J., Levey, A. I. & Wainer, B. H. Cholinergic innervation of cortex by the basal forebrain: cytochemistry and cortical connections of the septal area, diagonal band nuclei, nucleus basalis (substantia innominata), and hypothalamus in the rhesus monkey. *J Comp Neurol* **214**, 170-197, doi:10.1002/cne.902140206 (1983).

95 Woolf, N. J. Cholinergic systems in mammalian brain and spinal cord. *Prog Neurobiol* **37**, 475-524, doi:10.1016/0301-0082(91)90006-m (1991).

96 Kawai, H., Lazar, R. & Metherate, R. Nicotinic control of axon excitability regulates thalamocortical transmission. *Nat Neurosci* **10**, 1168-1175, doi:10.1038/nn1956 (2007).

97 Rice, M. E. & Cragg, S. J. Nicotine amplifies reward-related dopamine signals in striatum. *Nat Neurosci* **7**, 583-584, doi:10.1038/nn1244 (2004).

98 Wonnacott, S. Presynaptic nicotinic ACh receptors. *Trends Neurosci* **20**, 92-98, doi:10.1016/s0166-2236(96)10073-4 (1997).

99 Goutier, W., Lowry, J. P., McCreary, A. C. & O'Connor, J. J. Frequency-Dependent Modulation of Dopamine Release by Nicotine and Dopamine D1 Receptor Ligands: An In Vitro Fast Cyclic Voltammetry Study in Rat Striatum. *Neurochem Res* **41**, 945-950, doi:10.1007/s11064-015-1786-8 (2016).

100 Zhang, H. & Sulzer, D. Frequency-dependent modulation of dopamine release by nicotine. *Nat Neurosci* **7**, 581-582, doi:10.1038/nn1243 (2004).

101 Furness, J. B. The organisation of the autonomic nervous system: peripheral connections. *Auton Neurosci* **130**, 1-5, doi:10.1016/j.autneu.2006.05.003 (2006).

102 Li, Z. & Vance, D. E. Phosphatidylcholine and choline homeostasis. *J Lipid Res* **49**, 1187-1194, doi:10.1194/jlr.R700019-JLR200 (2008).

103 Prado, V. F., Roy, A., Kolisnyk, B., Gros, R. & Prado, M. A. Regulation of cholinergic activity by the vesicular acetylcholine transporter. *Biochem J* **450**, 265-274, doi:10.1042/BJ20121662 (2013).

104 Ribeiro, J. A., Cunha, R. A., Correia-de-Sá, P. & Sebastião, A. M. Purinergic regulation of acetylcholine release. *Prog Brain Res* **109**, 231-241 (1996).

105 Aidoo, A. Y. & Ward, K. Spatio-temporal concentration of acetylcholine in vertebrate synaptic cleft. *Math Comput Model* **44**, 952-962, doi:10.1016/j.mcm.2006.03.003 (2006).

106 Tougu, V. Acetylcholinesterase: mechanism of catalysis and inhibition. *Current Medicinal Chemistry-Central Nervous System Agents* **1**, 155-170 (2001).

107 Shen, T., Tai, K., Henchman, R. H. & McCammon, J. A. Molecular dynamics of acetylcholinesterase. *Accounts of Chemical Research* **35**, 332-340 (2002).

108 Eglen, R. M. Muscarinic receptor subtype pharmacology and physiology. *Prog Med Chem* **43**, 105-136, doi:10.1016/S0079-6468(05)43004-0 (2005).

109 Morales-Perez, C. L., Noviello, C. M. & Hibbs, R. E. X-ray structure of the human α4β2 nicotinic receptor. *Nature* **538**, 411-415 (2016).

110 Unwin, N. Refined structure of the nicotinic acetylcholine receptor at 4 angstrom resolution. *J Mol Biol* **346**, 967-989, doi:10.1016/j.jmb.2004.12.031 (2005).

111 Albuquerque, E. X., Pereira, E. F., Alkondon, M. & Rogers, S. W. Mammalian nicotinic acetylcholine receptors: from structure to function. *Physiol Rev* **89**, 73-120, doi:10.1152/physrev.00015.2008 (2009).

112 Miyazawa, A., Fujiyoshi, Y. & Unwin, N. Structure and gating mechanism of the acetylcholine receptor pore. *Nature* **423**, 949-955 (2003).

113 Jones, A. K. & Sattelle, D. B. Functional genomics of the nicotinic acetylcholine receptor gene family of the nematode, Caenorhabditis elegans. *Bioessays* **26**, 39-49, doi:10.1002/bies.10377 (2004).

114 Karlin, A. Emerging structure of the nicotinic acetylcholine receptors. *Nat Rev Neurosci* **3**, 102-114, doi:DOI 10.1038/nrn731 (2002).

115 Mongan, N. P. *et al.* An extensive and diverse gene family of nicotinic acetylcholine receptor alpha subunits in Caenorhabditis elegans. *Receptor Channel* **6**, 213-+ (1998).

116 Towers, P. R., Edwards, B., Richmond, J. E. & Sattelle, D. B. The Caenorhabditis elegans lev-8 gene encodes a novel type of nicotinic acetylcholine receptor alpha subunit. *Journal of Neurochemistry* **93**, 1-9, doi:10.1111/j.1471-4159.2004.02951.x (2005).

117 Changeux, J. P. & Edelstein, S. J. Allosteric receptors after 30 years. *Neuron* **21**, 959-980, doi:Doi 10.1016/S0896-6273(00)80616-9 (1998).

118 Gao, F. *et al.* Agonist-mediated conformational changes in acetylcholine-binding protein revealed by simulation and intrinsic tryptophan fluorescence. *J. Biol. Chem.* **280**, 8443-8451 (2005).

119 Fagerlund, M. J. & Eriksson, L. I. Current concepts in neuromuscular transmission. *Brit J Anaesth* **103**, 108-114, doi:10.1093/bja/aep150 (2009).

120 Kalamida, D. *et al.* Muscle and neuronal nicotinic acetylcholine receptors - Structure, function and pathogenicity. *Febs J* **274**, 3799-3845, doi:10.1111/j.1742-4658.2007.05935.x (2007).

121 Gerzanich, V., Wang, F., Kuryatov, A. & Lindstrom, J. alpha 5 subunit alters desensitization, pharmacology, Ca++ permeability and Ca++ modulation of human neuronal alpha 3 nicotinic receptors. *J Pharmacol Exp Ther* **286**, 311-320 (1998).

122 Papke, R. L., Dwoskin, L. P. & Crooks, P. A. The pharmacological activity of nicotine and nornicotine on nAChRs subtypes: relevance to nicotine dependence and drug discovery. *Journal of neurochemistry* **101**, 160-167 (2007).

123 Bertrand, S., Weiland, S., Berkovic, S. F., Steinlein, O. K. & Bertrand, D. Properties of neuronal nicotinic acetylcholine receptor mutants from humans suffering from autosomal dominant nocturnal frontal lobe epilepsy. *Br J Pharmacol* **125**, 751-760, doi:10.1038/sj.bjp.0702154 (1998).

124 Liang, Y. *et al.* Functional polymorphisms in the human beta4 subunit of nicotinic acetylcholine receptors. *Neurogenetics* **6**, 37-44, doi:10.1007/s10048-004-0199-7 (2005).

125 Briggs, C. A. & McKenna, D. G. Activation and inhibition of the human α7 nicotinic acetylcholine receptor by agonists. *Neuropharmacology* **37**, 1095-1102 (1998).

126 Sgard, F. *et al.* A novel human nicotinic receptor subunit, α10, that confers functionality to the α9-subunit. *Molecular pharmacology* **61**, 150-159 (2002).

127 Millar, N. S. & Gotti, C. Diversity of vertebrate nicotinic acetylcholine receptors. *Neuropharmacology* **56**, 237-246, doi:10.1016/j.neuropharm.2008.07.041 (2009).

128 Gotti, C., Zoli, M. & Clementi, F. Brain nicotinic acetylcholine receptors: native subtypes and their relevance. *Trends Pharmacol Sci* **27**, 482-491, doi:10.1016/j.tips.2006.07.004 (2006).

129 Hurst, R., Rollema, H. & Bertrand, D. Nicotinic acetylcholine receptors: From basic science to therapeutics. *Pharmacol Therapeut* **137**, 22-54, doi:10.1016/j.pharmthera.2012.08.012 (2013).

130 Fraterman, S., Khurana, T. S. & Rubinstein, N. A. Identification of acetylcholine receptor subunits differentially expressed in singly and multiply innervated fibers of extraocular muscles. *Invest Ophth Vis Sci* **47**, 3828-3834, doi:10.1167/iovs.06-0073 (2006).

131 Missias, A. C., Chu, G. C., Klocke, B. J., Sanes, J. R. & Merlie, J. P. Maturation of the acetylcholine receptor in skeletal muscle: Regulation of the AChR gamma-to-epsilon switch. *Dev Biol* **179**, 223-238, doi:DOI 10.1006/dbio.1996.0253 (1996).

132 Corriveau, R. A., Romano, S. J., Conroy, W. G., Oliva, L. & Berg, D. K. Expression of Neuronal Acetylcholine-Receptor Genes in Vertebrate Skeletal-Muscle during Development. *Journal of Neuroscience* **15**, 1372-1383 (1995).

133 Fischer, U., Reinhardt, S., Albuquerque, E. X. & Maelicke, A. Expression of functional alpha 7 nicotinic acetylcholine receptor during mammalian muscle development and denervation. *Eur J Neurosci* **11**, 2856-2864, doi:DOI 10.1046/j.1460-9568.1999.00703.x (1999).

134 Romano, S. J., Pugh, P. C., McIntosh, J. M. & Berg, D. K. Neuronal-type acetylcholine receptors and regulation of alpha 7 gene expression in vertebrate skeletal muscle. *J Neurobiol* **32**, 69-80, doi:Doi 10.1002/(Sici)1097-4695(199701)32:1<69::Aid-Neu7>3.0.Co;2-C (1997).

135 Wessler, I. & Kirkpatrick, C. Acetylcholine beyond neurons: the non-neuronal cholinergic system in humans. *Brit J Pharmacol* **154**, 1558-1571 (2008).

136 Haga, T. Molecular properties of muscarinic acetylcholine receptors. *Proc Jpn Acad Ser B Phys Biol Sci* **89**, 226-256 (2013).

137 Bonner, T. I., Buckley, N. J., Young, A. C. & Brann, M. R. Identification of a Family of Muscarinic Acetylcholine-Receptor Genes. *Science* **237**, 527-532, doi:DOI 10.1126/science.3037705 (1987).

138 Bonner, T. I., Young, A. C., Brann, M. R. & Buckley, N. J. Cloning and Expression of the Human and Rat M5 Muscarinic Acetylcholine-Receptor Genes. *Neuron* **1**, 403-410, doi:Doi 10.1016/0896-6273(88)90190-0 (1988).

139 Martens, G. J. M. Molecular-Biology of G-Protein-Coupled Receptors. *Peptidergic Neuron* **92**, 201-214, doi:Doi 10.1016/S0079-6123(08)61176-0 (1992).

140 Peralta, E. G., Ashkenazi, A., Winslow, J. W., Ramachandran, J. & Capon, D. J. Differential Regulation of Pi Hydrolysis and Adenylyl Cyclase by Muscarinic Receptor Subtypes. *Nature* **334**, 434-437, doi:DOI 10.1038/334434a0 (1988).

141 Kruse, A. C. *et al.* Structure and dynamics of the M3 muscarinic acetylcholine receptor. *Nature* **482**, 552-556 (2012).

142 Conn, P. J., Jones, C. K. & Lindsley, C. W. Subtype-selective allosteric modulators of muscarinic receptors for the treatment of CNS disorders. *Trends Pharmacol Sci* **30**, 148-155 (2009).

143 Bock, A., Schrage, R. & Mohr, K. Allosteric modulators targeting CNS muscarinic receptors. *Neuropharmacology* **136**, 427-437 (2018).

144 Bymaster, F. P. *et al.* Role of specific muscarinic receptor subtypes in cholinergic parasympathomimetic responses, in vivo phosphoinositide hydrolysis, and pilocarpine-induced seizure activity. *Eur J Neurosci* **17**, 1403-1410, doi:10.1046/j.1460-9568.2003.02588.x (2003).

145 Terry Jr, A. V., Callahan, P. M. & Hernandez, C. M. Nicotinic ligands as multifunctional agents for the treatment of neuropsychiatric disorders. *Biochem. Pharmacol.* **97**, 388-398 (2015).

146 Gosens, R., Zaagsma, J., Meurs, H. & Halayko, A. J. Muscarinic receptor signaling in the pathophysiology of asthma and COPD. *Respir Res* **7**, 73, doi:10.1186/1465-9921-7-73 (2006).

147 Hegde, S. S. Muscarinic receptors in the bladder: from basic research to therapeutics. *Br J Pharmacol* **147 Suppl 2**, S80-87, doi:10.1038/sj.bjp.0706560 (2006).

148 Rahman, S. Nicotinic receptors as therapeutic targets for drug addictive disorders. *CNS & Neurological Disorders-Drug Targets (Formerly Current Drug Targets-CNS & Neurological Disorders)* **12**, 633-640 (2013).

149 Tattersall, J. in *Chemical Warfare Toxicology, Vol 2: Management of Poisoning* Vol. 27 *Issues in Toxicology* (eds F. Worek, J. Jenner, & H. Thiermann) 82-119 (Royal Soc Chemistry, 2016).

150 Wanamaker, C. P. & Green, W. N. Endoplasmic reticulum chaperones stabilize nicotinic receptor subunits and regulate receptor assembly. *J Biol Chem* **282**, 31113-31123, doi:10.1074/jbc.M705369200 (2007).

151 Ben-David, Y. *et al.* RIC-3 expression and splicing regulate nAChR functional expression. *Mol Brain* **9**, 47, doi:10.1186/s13041-016-0231-5 (2016).

152 Jakubik, J. & El-Fakahany, E. E. Current Advances in Allosteric Modulation of Muscarinic Receptors. *Biomolecules* **10**, doi:10.3390/biom10020325 (2020).

153 Crespi, A., Colombo, S. F. & Gotti, C. Proteins and chemical chaperones involved in neuronal nicotinic receptor expression and function: an update. *Br J Pharmacol* **175**, 1869-1879, doi:10.1111/bph.13777 (2018).

154 Brown, M. A. & Brix, K. A. Review of health consequences from high-, intermediate- and low-level exposure to organophosphorus nerve agents. *J Appl Toxicol* **18**, 393-408, doi:10.1002/(sici)1099-1263(199811/12)18:6<393::aid-jat528>3.0.co;2-0 (1998).

155 O'Malley, M. Clinical evaluation of pesticide exposure and poisonings. *Lancet* **349**, 1161-1166, doi:10.1016/S0140-6736(96)07222-4 (1997).

156 Pope, C. N. in *Toxicology of Organophosphate & Carbamate Compounds* 271-291 (Elsevier, 2006).

157 Senanayake, N. & Karalliedde, L. Neurotoxic effects of organophosphorus insecticides. An intermediate syndrome. *N Engl J Med* **316**, 761-763, doi:10.1056/nejm198703263161301 (1987).

158 Shailesh, K. K., Pais, P., Vengamma, B. & Muthane, U. Clinical and electrophysiological study of intermediate syndrome in patients with organophosphorous poisoning. *J Assoc Physicians India* **42**, 451-453 (1994).

159 Eddleston, M., Buckley, N. A., Eyer, P. & Dawson, A. H. Management of acute organophosphorus pesticide poisoning. *Lancet* **371**, 597-607, doi:10.1016/S0140-6736(07)61202-1 (2008).

160 Eddleston, M. *et al.* Early management after self-poisoning with an organophosphorus or carbamate pesticide - a treatment protocol for junior doctors. *Crit Care* **8**, R391-397, doi:10.1186/cc2953 (2004).

161 Alozi, M. & Rawas-Qalaji, M. Treating organophosphates poisoning: management challenges and potential solutions. *Crit Rev Toxicol*, 1-16, doi:10.1080/10408444.2020.1837069 (2020).

162 Eddleston, M. & Chowdhury, F. R. Pharmacological treatment of organophosphorus insecticide poisoning: the old and the (possible) new. *Br J Clin Pharmacol* **81**, 462-470, doi:10.1111/bcp.12784 (2016).

163 Jiang, S. Z., Ma, B. E., Liu, C. & Wang, R. Clinical efficacy of intravenous infusion of atropine with micropump in combination with hemoperfusion on organophosphorus poisoning. *Saudi J Biol Sci* **26**, 2018-2021, doi:10.1016/j.sjbs.2019.08.010 (2019).

164 Peng, A., Meng, F. Q., Sun, L. F., Ji, Z. S. & Li, Y. H. Therapeutic efficacy of charcoal hemoperfusion in patients with acute severe dichlorvos poisoning. *Acta Pharmacol Sin* **25**, 15-21 (2004).

165 Marrs, T. C. Diazepam in the treatment of organophosphorus ester pesticide poisoning. *Toxicol Rev* **22**, 75-81, doi:10.2165/00139709-200322020-00002 (2003).

166 Sanderson, D. M. Treatment of poisoning by anticholinesterase insecticides in the rat. *J Pharm Pharmacol* **13**, 435-442, doi:10.1111/j.2042-7158.1961.tb11849.x (1961).

167 Broadley, K. J. & Kelly, D. R. Muscarinic receptor agonists and antagonists. *Molecules* **6**, 142-193, doi:Doi 10.3390/60300142 (2001).

168 Wilson, I. B. & Ginsburg, S. A powerful reactivator of alkylphosphate-inhibited acetylcholinesterase. *Biochim Biophys Acta* **18**, 3 (1955).

169 Ekstrom, F. *et al.* Structure of HI-6 center dot Sarin-Acetylcholinesterase Determined by X-Ray Crystallography and Molecular Dynamics Simulation: Reactivator Mechanism and Design. *Plos One* **4**, 19, doi:10.1371/journal.pone.0005957 (2009).

170 Artursson, E., Akfur, C., Hornberg, A., Worek, F. & Ekstrom, F. Reactivation of tabun-hAChE investigated by structurally analogous oximes and mutagenesis. *Toxicology* **265**, 108-114, doi:10.1016/j.tox.2009.09.002 (2009).

171 Sanson, B. *et al.* Crystallographic snapshots of nonaged and aged conjugates of soman with acetylcholinesterase, and of a ternary complex of the aged conjugate with pralidoxime. *J Med Chem* **52**, 7593-7603, doi:10.1021/jm900433t (2009).

172 Worek, F. & Thiermann, H. The value of novel oximes for treatment of poisoning by organophosphorus compounds. *Pharmacol Ther* **139**, 249-259, doi:10.1016/j.pharmthera.2013.04.009 (2013).

173 Alkondon, M., Rao, K. S. & Albuquerque, E. X. Acetylcholinesterase reactivators modify the functional properties of the nicotinic acetylcholine receptor ion channel. *J Pharmacol Exp Ther* **245**, 543-556 (1988).

174 Amitai, G., Kloog, Y., Balderman, D. & Sokolovsky, M. INTERACTION OF BIS-PYRIDINIUM OXIMES WITH MOUSE-BRAIN MUSCARINIC RECEPTOR. *Biochem. Pharmacol.* **29**, 483-488, doi:10.1016/0006-2952(80)90366-4 (1980).

175 Kloog, Y., Galron, R. & Sokolovsky, M. Bisquaternary pyridinium oximes as presynaptic agonists and postsynaptic antagonists of muscarinic receptors. *J Neurochem* **46**, 767-772 (1986).

176 Kloog, Y. & Sokolovsky, M. Bisquaternary pyridinium oximes as allosteric inhibitors of rat brain muscarinic receptors. *Mol Pharmacol* **27**, 418-428 (1985).

177 Kuhnen-Clausen, D., Hagedorn, I., Gross, G., Bayer, H. & Hucho, F. Interactions of bisquaternary pyridine salts (H-oximes) with cholinergic receptors. *Arch Toxicol* **54**, 171-179 (1983).

178 Tattersall, J. E. Ion channel blockade by oximes and recovery of diaphragm muscle from soman poisoning in vitro. *Br J Pharmacol* **108**, 1006-1015 (1993).

179 Busker, R. W., Zijlstra, J. J., van der Wiel, H. J., Melchers, B. P. & van Helden, H. P. Organophosphate poisoning: a method to test therapeutic effects of oximes other than acetylcholinesterase reactivation in the rat. *Toxicology* **69**, 331-344 (1991).

180 Seeger, T. *et al.* Restoration of nerve agent inhibited muscle force production in human intercostal muscle strips with HI 6. *Toxicol Lett* **206**, 72-76, doi:10.1016/j.toxlet.2011.07.016 (2011).

181 Tattersall, J. E. H., Smith, A. P., Waters, K., Mistry, R. & Weeden, D. Therapeutic action of HI-6 against soman poisoning in vitro: An interspecies comparison. *Brit J Pharmacol* **125**, U5-U5 (1998).

182 van Helden, H. P., de Lange, J., Busker, R. W. & Melchers, B. P. Therapy of organophosphate poisoning in the rat by direct effects of oximes unrelated to ChE reactivation. *Arch Toxicol* **65**, 586-593 (1991).

183 Seeger, T. *et al.* Restoration of soman-blocked neuromuscular transmission in human and rat muscle by the bispyridinium non-oxime MB327 in vitro. *Toxicology* **294**, 80-84, doi:10.1016/j.tox.2012.02.002 (2012).

184 Diamantis, W. & Kletzkin, M. Evaluation of muscle relaxant drugs by head-drop and by decerebrate rigidity. *Int J Neuropharmacol* **5**, 305-310, doi:10.1016/0028-3908(66)90039-6 (1966).

185 Murphy, M. R., Blick, D. W., Dunn, M. A., Fanton, J. W. & Hartgraves, S. L. Diazepam as a Treatment for Nerve Agent Poisoning in Primates. *Aviat Space Envir Md* **64**, 110-115 (1993).

186 Buckley, N. A., Karalliedde, L., Dawson, A., Senanayake, N. & Eddleston, M. Where is the evidence for treatments used in pesticide poisoning? Is clinical toxicology fiddling while the developing world burns? *J Toxicol Clin Toxicol* **42**, 113-116, doi:10.1081/clt-120028756 (2004).

187 Eddleston, M. *et al.* Speed of initial atropinisation in significant organophosphorus pesticide poisoning--a systematic comparison of recommended regimens. *J Toxicol Clin Toxicol* **42**, 865-875, doi:10.1081/clt-200035223 (2004).

188 Eddleston, M., Szinicz, L., Eyer, P. & Buckley, N. Oximes in acute organophosphorus pesticide poisoning: a systematic review of clinical trials. *QJM* **95**, 275-283 (2002).

189 Worek, F., Thiermann, H. & Wille, T. Organophosphorus compounds and oximes: a critical review. *Arch Toxicol* **94**, 2275-2292, doi:10.1007/s00204-020-02797-0 (2020).

190 Worek, F., Thiermann, H. & Wille, T. Oximes in organophosphate poisoning: 60 years of hope and despair. *Chem Biol Interact* **259**, 93-98, doi:10.1016/j.cbi.2016.04.032 (2016).

191 Kuca, K. *et al.* Universality of Oxime K203 for Reactivation of Nerve Agent-Inhibited AChE. *Med Chem* **11**, 683-686, doi:10.2174/1573406411666150407154204 (2015).

192 Kassa, J., Misik, J. & Karasova, J. Z. A Comparison of the Potency of a Novel Bispyridinium Oxime K203 and currently available Oximes (Obidoxime, HI-6) to Counteract the Acute Neurotoxicity of Sarin in Rats. *Basic Clin Pharmacol* **111**, 333-338, doi:10.1111/j.1742-7843.2012.00897.x (2012).

193 Rosenberg, Y. J. *et al.* Post-exposure treatment with the oxime RS194B rapidly reverses early and advanced symptoms in macaques exposed to sarin vapor. *Chem Biol Interact* **274**, 50-57, doi:10.1016/j.cbi.2017.07.003 (2017).

194 Radic, Z. *et al.* Refinement of structural leads for centrally acting oxime reactivators of phosphylated cholinesterases. *J Biol Chem* **287**, 11798-11809, doi:10.1074/jbc.M111.333732 (2012).

195 Katz, F. S. *et al.* Discovery of New Classes of Compounds that Reactivate Acetylcholinesterase Inhibited by Organophosphates. *Chembiochem* **16**, 2205-2215, doi:10.1002/cbic.201500348 (2015).

196 Bierwisch, A., Wille, T., Thiermann, H. & Worek, F. Kinetic analysis of interactions of amodiaquine with human cholinesterases and organophosphorus compounds. *Toxicol Lett* **246**, 49-56, doi:10.1016/j.toxlet.2016.02.004 (2016).

197 Nachon, F., Brazzolotto, X., Trovaslet, M. & Masson, P. Progress in the development of enzyme-based nerve agent bioscavengers. *Chem Biol Interact* **206**, 536-544, doi:10.1016/j.cbi.2013.06.012 (2013).

198 Lushchekina, S. V. *et al.* Optimization of Cholinesterase-Based Catalytic Bioscavengers Against Organophosphorus Agents. *Front Pharmacol* **9**, 211, doi:10.3389/fphar.2018.00211 (2018).

199 Lockridge, O. Review of human butyrylcholinesterase structure, function, genetic variants, history of use in the clinic, and potential therapeutic uses. *Pharmacol Therapeut* **148**, 34-46, doi:10.1016/j.pharmthera.2014.11.011 (2015).

200 Ashani, Y. *et al.* In vitro evaluation of the catalytic activity of paraoxonases and phosphotriesterases predicts the enzyme circulatory levels required for in vivo protection against organophosphate intoxications. *Chem Biol Interact* **259**, 252-256, doi:10.1016/j.cbi.2016.04.039 (2016).

201 Wille, T. *et al.* Single treatment of VX poisoned guinea pigs with the phosphotriesterase mutant C23AL: Intraosseous versus intravenous injection. *Toxicol Lett* **258**, 198-206, doi:10.1016/j.toxlet.2016.07.004 (2016).

202 Betapudi, V., Goswami, R., Silayeva, L., Doctor, D. M. & Chilukuri, N. Gene therapy delivering a paraoxonase 1 variant offers long-term prophylactic protection against nerve agents in mice. *Sci Transl Med* **12**, doi:10.1126/scitranslmed.aay0356 (2020).

203 Kassa, J., Karasova, J. Z., Musilek, K. & Kuca, K. A comparison of reactivating and therapeutic efficacy of newly-developed oximes (K156, K203) and commonly used oximes (obidoxime, HI-6) in cyclosarin-poisoned rats and mice. *Toxicol Mech Method* **19**, 346-350, doi:10.1080/15376510903019307 (2009).

204 Broomfield, C. A. *et al.* Protection by Butyrylcholinesterase against Organophosphorus Poisoning in Nonhuman-Primates. *J Pharmacol Exp Ther* **259**, 633-638 (1991).

205 Raveh, L., Grauer, E., Grunwald, J., Cohen, E. & Ashani, Y. The stoichiometry of protection against soman and VX toxicity in monkeys pretreated with human butyrylcholinesterase. *Toxicology and applied pharmacology* **145**, 43-53 (1997).

206 Saxena, A. *et al.* Bioscavenger for protection from toxicity of organophosphorus compounds. *J Mol Neurosci* **30**, 145-147, doi:10.1385/Jmn:30:1:145 (2006).

207 Turner, S. R. *et al.* Protection against nerve agent poisoning by a noncompetitive nicotinic antagonist. *Toxicol Lett* **206**, 105-111, doi:10.1016/j.toxlet.2011.05.1035 (2011).

208 Price, M. E., Whitmore, C. L., Tattersall, J. E. H., Green, A. C. & Rice, H. Efficacy of the antinicotinic compound MB327 against soman poisoning - Importance of experimental end point. *Toxicol Lett* **293**, 167-171, doi:10.1016/j.toxlet.2017.11.006 (2018).

209 Price, M. E. *et al.* Pharmacokinetic profile and quantitation of protection against soman poisoning by the antinicotinic compound MB327 in the guinea-pig. *Toxicol Lett* **244**, 154-160, doi:10.1016/j.toxlet.2015.08.013 (2016).

210 Timperley, C. M. *et al.* 1,1 '-(Propane-1,3-diyl)bis(4-tert-butylpyridinium) di(methanesulfonate) protects guinea pigs from soman poisoning when used as part of a combined therapy. *Medchemcomm* **3**, 352-356, doi:10.1039/c2md00258b (2012).

211 Whitmore, C. *et al.* Assessment of false transmitters as treatments for nerve agent poisoning. *Toxicol Lett* **321**, 21-31, doi:10.1016/j.toxlet.2019.12.010 (2020).

212 Patterson, T. A., Terry, A. V., Jr. & Kosh, J. W. Prevention of physostigmine-, DFP-, and diazinon-induced acute toxicity by monoethylcholine and N-aminodeanol. *Br J Pharmacol* **97**, 451-460, doi:10.1111/j.1476-5381.1989.tb11972.x (1989).

213 Sheridan, R. D., Smith, A. P., Turner, S. R. & Tattersall, J. E. Nicotinic antagonists in the treatment of nerve agent intoxication. *J R Soc Med* **98**, 114-115, doi:10.1258/jrsm.98.3.114 (2005).

214 Smythies, J. & Golomb, B. Nerve gas antidotes. *J R Soc Med* **97**, 32, doi:10.1258/jrsm.97.1.32 (2004).

215 Aronstam, R. S., Marshall, D. C. & Buccafusco, J. J. Cholinergic false transmitters: physiological and biochemical actions in central and peripheral systems. *Neuropharmacology* **27**, 217-225, doi:10.1016/0028-3908(88)90037-8 (1988).

216 Boksa, P. & Collier, B. N-Ethyl analogues of choline as precursors to cholinergic false transmitters. *J Neurochem* **35**, 1099-1104, doi:10.1111/j.1471-4159.1980.tb07864.x (1980).

217 Worek, F., Eyer, P. & Thiermann, H. Determination of acetylcholinesterase activity by the Ellman assay: a versatile tool for in vitro research on medical countermeasures against organophosphate poisoning. *Drug Test Anal* **4**, 282-291, doi:10.1002/dta.337 (2012).

218 Louhimies, S. Revised Eu Legislation on the Protection of Animals Used for Scientific Purposes Directive 2010/63/Eu. *J Shellfish Res* **30**, 1011-1011 (2011).

219 Ellman, G. L., Courtney, K. D., Andres, V., Jr. & Feather-Stone, R. M. A new and rapid colorimetric determination of acetylcholinesterase activity. *Biochem Pharmacol* **7**, 88-95 (1961).

220 Wilson, B. W. & Henderson, J. D. Blood Esterase Determinations as Markers of Exposure. *Rev Environ Contam T* **128**, 55-69 (1992).

221 Worek, F., Koller, M., Thiermann, H. & Szinicz, L. Diagnostic aspects of organophosphate poisoning. *Toxicology* **214**, 182-189, doi:10.1016/j.tox.2005.06.012 (2005).

222 Forsberg, A. & Puu, G. Kinetics for the Inhibition of Acetylcholinesterase from the Electric-Eel by Some Organophosphates and Carbamates. *Eur J Biochem* **140**, 153-156, doi:DOI 10.1111/j.1432-1033.1984.tb08079.x (1984).

223 Costa, M. D., Freitas, M. L., Soares, F. A. A., Carratu, V. S. & Brandao, R. Potential of two new oximes in reactivate human acetylcholinesterase and butyrylcholinesterase inhibited by organophosphate compounds: An in vitro study. *Toxicol in Vitro* **25**, 2120-2123, doi:10.1016/j.tiv.2011.09.018 (2011).

224 Scheffel, C. *et al.* Electrophysiological investigation of the effect of structurally different bispyridinium non-oxime compounds on human α7-nicotinic acetylcholine receptor activity-An in vitro structure-activity analysis. *Toxicol Lett* **293**, 157-166, doi:10.1016/j.toxlet.2017.11.025 (2018).

225 Scheffel, C. *et al.* Counteracting desensitization of human α7-nicotinic acetylcholine receptors with bispyridinium compounds as an approach against organophosphorus poisoning. *Toxicol Lett* **293**, 149-156, doi:10.1016/j.toxlet.2017.12.005 (2018).

226 Ring, A. *et al.* Bispyridinium Compounds Inhibit Both Muscle and Neuronal Nicotinic Acetylcholine Receptors in Human Cell Lines. *Plos One* **10**, doi:ARTN e0135811

10.1371/journal.pone.0135811 (2015).

227 Timperley, C. M. *et al.* 3-Quinuclidinyl-α-methoxydiphenylacetate: A multi-targeted ligand with antimuscarinic and antinicotinic effects designed for the treatment of anticholinesterase poisoning. *Toxicol Lett* **325**, 67-76, doi:10.1016/j.toxlet.2020.01.027 (2020).

228 Beeson, D., Amar, M., Bermudez, I., Vincent, A. & Newsom-Davis, J. Stable functional expression of the adult subtype of human muscle acetylcholine receptor following transfection of the human rhabdomyosarcoma cell line TE671 with cDNA encoding the epsilon subunit. *Neurosci Lett* **207**, 57-60, doi:10.1016/0304-3940(96)12488-5 (1996).

229 Bencherif, M. & Lukas, R. J. Ligand binding and functional characterization of muscarinic acetylcholine receptors on the TE671/RD human cell line. *J Pharmacol Exp Ther* **257**, 946-953 (1991).

230 Lukas, R. J., Norman, S. A. & Lucero, L. Characterization of Nicotinic Acetylcholine Receptors Expressed by Cells of the SH-SY5Y Human Neuroblastoma Clonal Line. *Mol Cell Neurosci* **4**, 1-12, doi:10.1006/mcne.1993.1001 (1993).

231 Gould, J., Reeve, H. L., Vaughan, P. F. & Peers, C. Nicotinic acetylcholine receptors in human neuroblastoma (SH-SY5Y) cells. *Neurosci Lett* **145**, 201-204, doi:10.1016/0304-3940(92)90022-γ (1992).

232 Adem, A., Mattsson, M. E., Nordberg, A. & Pahlman, S. Muscarinic receptors in human SH-SY5Y neuroblastoma cell line: regulation by phorbol ester and retinoic acid-induced differentiation. *Brain Res* **430**, 235-242, doi:10.1016/0165-3806(87)90156-8 (1987).

233 Schucht, R. *et al.* A new generation of retroviral producer cells: predictable and stable virus production by Flp-mediated site-specific integration of retroviral vectors. *Mol Ther* **14**, 285-292, doi:10.1016/j.ymthe.2005.12.003 (2006).

234 Soukup, O. *et al.* Oxime reactivators and their in vivo and in vitro effects on nicotinic receptors. *Physiol Res* **60**, 679-686, doi:10.33549/physiolres.932105 (2011).

235 Hsu, F. L. *et al.* Synthesis and Molecular Properties of Nerve Agent Reactivator HLo-7 Dimethanesulfonate. *Acs Med Chem Lett* **10**, 761-766, doi:10.1021/acsmedchemlett.9b00021 (2019).

236 Pereira, E. F. R. *et al.* Animal Models That Best Reproduce the Clinical Manifestations of Human Intoxication with Organophosphorus Compounds. *J Pharmacol Exp Ther* **350**, 313-321, doi:10.1124/jpet.114.214932 (2014).

237 Fawcett, W. P., Aracava, Y., Adler, M., Pereira, E. F. R. & Albuquerque, E. X. Acute Toxicity of Organophosphorus Compounds in Guinea Pigs Is Sex- and Age-Dependent and Cannot Be Solely Accounted for by Acetylcholinesterase Inhibition. *J Pharmacol Exp Ther* **328**, 516-524, doi:10.1124/jpet.108.146639 (2009).

238 Sivam, S. P., Hoskins, B. & Ho, I. K. An assessment of comparative acute toxicity of diisopropyl-fluorophosphate, tabun, sarin, and soman in relation to cholinergic and GABAergic enzyme activities in rats. *Fundam Appl Toxicol* **4**, 531-538, doi:10.1016/0272-0590(84)90042-3 (1984).

239 Kassa, J. *et al.* Some benefit from non-oximes MB408, MB442 and MB444 in combination with the oximes HI-6 or obidoxime and atropine in antidoting sarin or cyclosarin poisoned mice. *Toxicology* **408**, 95-100, doi:10.1016/j.tox.2018.07.008 (2018).

240 Kayouka, M., Houze, P., Lejay, M., Baud, F. J. & Kuca, K. Safety and Efficacy of New Oximes to Reverse Low Dose Diethyl-Paraoxon-Induced Ventilatory Effects in Rats. *Molecules* **25**, doi:10.3390/molecules25133056 (2020).

241 Bruun, D. A., Guignet, M., Harvey, D. J. & Lein, P. J. Pretreatment with pyridostigmine bromide has no effect on seizure behavior or 24 hour survival in the rat model of acute diisopropylfluorophosphate intoxication. *Neurotoxicology* **73**, 81-84, doi:10.1016/j.neuro.2019.03.001 (2019).

242 Jacevic, V., Nepovimova, E. & Kuca, K. Toxic Injury to Muscle Tissue of Rats Following Acute Oximes Exposure. *Sci Rep* **9**, 1457, doi:10.1038/s41598-018-37837-4 (2019).

243 Kaplan, E. L. & Meier, P. Nonparametric estimation from incomplete observations. *J Am Stat Assoc* **53**, 457-481 (1958).

244 Petroianu, G. A., Nurulain, S. M., Arafat, K., Rajan, S. & Hasan, M. Y. Effect of pyridostigmine, pralidoxime and their combination on survival and cholinesterase activity in rats exposed to the organophosphate paraoxon. *Arch Toxicol* **80**, 777-784, doi:10.1007/s00204-006-0098-9 (2006).

245 Rahman, M. S., Islam, S. M. M., Haque, A. & Shahjahan, M. Toxicity of the organophosphate insecticide sumithion to embryo and larvae of zebrafish. *Toxicol Rep* **7**, 317-323, doi:10.1016/j.toxrep.2020.02.004 (2020).

246 Faria, M. *et al.* Zebrafish Models for Human Acute Organophosphorus Poisoning. *Sci Rep* **5**, 15591, doi:10.1038/srep15591 (2015).

247 Hagstrom, D. *et al.* Planarian cholinesterase: molecular and functional characterization of an evolutionarily ancient enzyme to study organophosphorus pesticide toxicity. *Arch Toxicol* **92**, 1161-1176, doi:10.1007/s00204-017-2130-7 (2018).

248 Poirier, L. *et al.* Enzymatic degradation of organophosphorus insecticides decreases toxicity in planarians and enhances survival. *Sci Rep* **7**, 15194, doi:10.1038/s41598-017-15209-8 (2017).

249 Cole, R. D., Anderson, G. L. & Williams, P. L. The nematode Caenorhabditis elegans as a model of organophosphate-induced mammalian neurotoxicity. *Toxicology and Applied Pharmacology* **194**, 248-256, doi:10.1016/j.taap.2003.09.013 (2004).

250 McVey, K. *et al.* Caenorhabditis elegans: an emerging model system for pesticide neurotoxicity. *J Environ Anal Toxicol S* **4**, S4-003 (2012).

251 Rand, J. B. Acetylcholine. *WormBook*, 1-21, doi:10.1895/wormbook.1.131.1 (2007).

252 d'Amora, M. & Giordani, S. The utility of zebrafish as a model for screening developmental neurotoxicity. *Frontiers in neuroscience* **12**, 976 (2018).

253 Hagstrom, D., Cochet-Escartin, O., Zhang, S., Khuu, C. & Collins, E.-M. S. Freshwater planarians as an alternative animal model for neurotoxicology. *Toxicol. Sci.* **147**, 270-285 (2015).

254 Kinser, H. E. & Pincus, Z. High-throughput screening in the C. elegans nervous system. *Mol Cell Neurosci* **80**, 192-197, doi:10.1016/j.mcn.2016.06.001 (2017).

255 Russell, W. M. S. & Burch, R. L. *The principles of humane experimental technique*. (Methuen, 1959).

256 Zhang, Z.-Y., Yu, X.-Y., Wang, D.-L., Yan, H.-J. & Liu, X.-J. Acute toxicity to zebrafish of two organophosphates and four pyrethroids and their binary mixtures. *Pest Management Science* **66**, 84-89, doi:https://doi.org/10.1002/ps.1834 (2010).

257 Poirier, L., Plener, L., Daude, D. & Chabriere, E. Enzymatic decontamination of paraoxon-ethyl limits long-term effects in planarians. *Sci Rep* **10**, 3843, doi:10.1038/s41598-020-60846-1 (2020).

258 Brenner, S. The genetics of Caenorhabditis elegans. *Genetics* **77**, 71-94 (1974).

259 White, J. G., Southgate, E., Thomson, J. N. & Brenner, S. The structure of the nervous system of the nematode Caenorhabditis elegans. *Philos Trans R Soc Lond B Biol Sci* **314**, 1-340, doi:10.1098/rstb.1986.0056 (1986).

260 Hall, D. H. & Russell, R. L. The posterior nervous system of the nematode Caenorhabditis elegans: serial reconstruction of identified neurons and complete pattern of synaptic interactions. *J Neurosci* **11**, 1-22 (1991).

261 Pereira, L. *et al.* A cellular and regulatory map of the cholinergic nervous system of C. elegans. *Elife* **4**, doi:10.7554/eLife.12432 (2015).

262 Ranganathan, R., Sawin, E. R., Trent, C. & Horvitz, H. R. Mutations in the Caenorhabditis elegans serotonin reuptake transporter MOD-5 reveal serotonin-dependent and -independent activities of fluoxetine. *J Neurosci* **21**, 5871-5884 (2001).

263 Duerr, J. S. *et al.* The cat-1 gene of Caenorhabditis elegans encodes a vesicular monoamine transporter required for specific monoamine-dependent behaviors. *J Neurosci* **19**, 72-84 (1999).

264 Combes, D., Fedon, Y., Grauso, M., Toutant, J. P. & Arpagaus, M. Four genes encode acetylcholinesterases in the nematodes Caenorhabditis elegans and Caenorhabditis briggsae. cDNA sequences, Genomic structures, mutations and in vivo expression. *J Mol Biol* **300**, 727-742, doi:DOI 10.1006/jmbi.2000.3917 (2000).

265 Boulin, T. *et al.* Eight genes are required for functional reconstitution of the Caenorhabditis elegans levamisole-sensitive acetylcholine receptor. *Proc Natl Acad Sci U S A* **105**, 18590-18595, doi:10.1073/pnas.0806933105 (2008).

266 Brownlee, D. J. & Fairweather, I. Exploring the neurotransmitter labyrinth in nematodes. *Trends Neurosci* **22**, 16-24, doi:10.1016/s0166-2236(98)01281-8 (1999).

267 Calahorro, F. & Izquierdo, P. G. The presynaptic machinery at the synapse of C. elegans. *Invertebr Neurosci* **18**, doi:ARTN 4

10.1007/s10158-018-0207-5 (2018).

268 Safran, M. *et al.* GeneCards Version 3: the human gene integrator. *Database* **2010** (2010).

269 Harris, T. W. *et al.* WormBase: a modern model organism information resource. *Nucleic Acids Res.* **48**, D762-D767 (2020).

270 Mullen, G. P. *et al.* Choline transport and de novo choline synthesis support acetylcholine biosynthesis in Caenorhabditis elegans cholinergic neurons. *Genetics* **177**, 195-204, doi:10.1534/genetics.107.074120 (2007).

271 Combes, D., Fedon, Y., Toutant, J. P. & Arpagaus, M. Multiple ace genes encoding acetylcholinesterases of Caenorhabditis elegans have distinct tissue expression. *Eur J Neurosci* **18**, 497-512, doi:10.1046/j.1460-9568.2003.02749.x (2003).

272 Culotti, J. G., Vonehrenstein, G., Culotti, M. R. & Russell, R. L. A 2nd Class of Acetylcholinesterase-Deficient Mutants of the Nematode Caenorhabditis-Elegans. *Genetics* **97**, 281-305 (1981).

273 Johnson, C. D. *et al.* An Acetylcholinesterase-Deficient Mutant of the Nematode Caenorhabditis-Elegans. *Genetics* **97**, 261-279 (1981).

274 Johnson, C. D., Rand, J. B., Herman, R. K., Stern, B. D. & Russell, R. L. The Acetylcholinesterase Genes of C-Elegans - Identification of a 3rd Gene (Ace-3) and Mosaic Mapping of a Synthetic Lethal Phenotype. *Neuron* **1**, 165-173, doi:Doi 10.1016/0896-6273(88)90201-2 (1988).

275 Culetto, E. *et al.* Structure and promoter activity of the 5 ' flanking region of ace-1, the gene encoding acetylcholinesterase of class a in Caenorhabditis elegans. *J Mol Biol* **290**, 951-966, doi:DOI 10.1006/jmbi.1999.2937 (1999).

276 Giles, K. Interactions underlying subunit association in cholinesterases. *Protein Eng* **10**, 677-685, doi:DOI 10.1093/protein/10.6.677 (1997).

277 Simon, S., Krejci, E. & Massoulie, J. A four-to-one association between peptide motifs: four C-terminal domains from cholinesterase assemble with one proline-rich attachment domain (PRAD) in the secretory pathway. *Embo J* **17**, 6178-6187, doi:DOI 10.1093/emboj/17.21.6178 (1998).

278 Kolson, D. L. & Russell, R. L. A novel class of acetylcholinesterase, revealed by mutations, in the nematode Caenorhabditis elegans. *J Neurogenet* **2**, 93-110 (1985).

279 Han, Y., Song, S., Guo, Y., Zhang, J. & Ma, E. ace-3 plays an important role in phoxim resistance in Caenorhabditis elegans. *Ecotoxicology* **25**, 835-844, doi:10.1007/s10646-016-1640-z (2016).

280 Altun, Z. *et al.*

281 Gibney, G., Camp, S., Dionne, M., MacPhee-Quigley, K. & Taylor, P. Mutagenesis of essential functional residues in acetylcholinesterase. *Proc Natl Acad Sci U S A* **87**, 7546-7550 (1990).

282 Blumenthal, T. & Steward, K. in *C. elegans II* (eds D. L. Riddle, T. Blumenthal, B. J. Meyer, & J. R. Priess) (1997).

283 Fleming, J. T. *et al.* Caenorhabditis elegans levamisole resistance genes lev-1, unc-29, and unc-38 encode functional nicotinic acetylcholine receptor subunits. *Journal of Neuroscience* **17**, 5843-5857 (1997).

284 Kim, S., Shin, Y., Shin, Y., Park, Y. S. & Cho, J. Regulation of ERK1/2 by the C-elegans muscarinic acetylcholine receptor GAR-3 in Chinese hamster ovary cells. *Mol Cells* **25**, 504-509 (2008).

285 Liu, Y. S., LeBoeuf, B. & Garcia, L. R. G alpha(q)-coupled muscarinic acetylcholine receptors enhance nicotinic acetylcholine receptor signaling in Caenorhabditis elegans mating behavior. *Journal of Neuroscience* **27**, 1411-1421, doi:10.1523/Jneurosci.4320-06.2007 (2007).

286 Park, Y. S., Kim, S., Shin, Y., Choi, B. & Cho, N. J. Alternative splicing of the muscarinic acetylcholine receptor GAR-3 in Caenorhabditis elegans. *Biochem Bioph Res Co* **308**, 961-965, doi:10.1016/S0006-291x(03)01508-0 (2003).

287 Sattelle, D. B. Invertebrate nicotinic acetylcholine receptors-targets for chemicals and drugs important in agriculture, veterinary medicine and human health. *J Pestic Sci* **34**, 233-240, doi:10.1584/jpestics.R09-02 (2009).

288 Steger, K. A. & Avery, L. The GAR-3 muscarinic receptor cooperates with calcium signals to regulate muscle contraction in the Caenorhabditis elegans pharynx. *Genetics* **167**, 633-643, doi:DOI 10.1534/genetics.103.020230 (2004).

289 Culetto, E. *et al.* The Caenorhabditis elegans unc-63 gene encodes a levamisole-sensitive nicotinic acetylcholine receptor alpha subunit. *J Biol Chem* **279**, 42476-42483, doi:10.1074/jbc.M404370200 (2004).

290 Caulfield, M. P. & Birdsall, N. J. M. International Union of Pharmacology. XVII. Classification of muscarinic acetylcholine receptors. *Pharmacological Reviews* **50**, 279-290 (1998).

291 Langmead, C. J., Watson, J. & Reavill, C. Muscarinic acetylcholine receptors as CNS drug targets. *Pharmacol Therapeut* **117**, 232-243, doi:10.1016/j.pharmthera.2007.09.009 (2008).

292 Lanzafame, A. A., Christopoulos, A. & Mitchelson, F. Cellular signaling mechanisms for muscarinic acetylcholine receptors. *Receptor Channel* **9**, 241-260, doi:10.1080/10606820390217078 (2003).

293 Hobert, O. Neurogenesis in the Nematode Caenorhabditis elegans. *Comprehensive Developmental Neuroscience: Patterning and Cell Type Specification in the Developing Cns and Pns*, 609-626, doi:10.1016/B978-0-12-397265-1.00115-5 (2013).

294 Putrenko, I., Zakikhani, M. & Dent, J. A. A family of acetylcholine-gated chloride channel subunits in Caenorhabditis elegans. *J. Biol. Chem.* **280**, 6392-6398, doi:10.1074/jbc.M412644200 (2005).

295 Jospin, M. *et al.* A Neuronal Acetylcholine Receptor Regulates the Balance of Muscle Excitation and Inhibition in Caenorhabditis elegans. *Plos Biol* **7**, doi:ARTN e1000265

10.1371/journal.pbio.1000265 (2009).

296 Choudhary, S. *et al.* EAT-18 is an essential auxiliary protein interacting with the non-alpha nAChR subunit EAT-2 to form a functional receptor. *Plos Pathogens* **16**, doi:ARTN e1008396

10.1371/journal.ppat.1008396 (2020).

297 Yassin, L. *et al.* Characterization of the DEG-3/DES-2 receptor: A nicotinic acetylcholine receptor that mutates to cause neuronal degeneration. *Mol Cell Neurosci* **17**, 589-599, doi:10.1006/mcne.2000.0944 (2001).

298 Squire, M. D. *et al.* Molecular-Cloning and Functional Coexpression of a Caenorhabditis-Elegans Nicotinic Acetylcholine-Receptor Subunit (Acr-2). *Receptor Channel* **3**, 107-115 (1995).

299 Holden-Dye, L., Joyner, M., O'Connor, V. & Walker, R. J. Nicotinic acetylcholine receptors: A comparison of the nAChRs of Caenorhabditis elegans and parasitic nematodes. *Parasitol Int* **62**, 606-615, doi:10.1016/j.parint.2013.03.004 (2013).

300 Lee, Y. S. *et al.* Cloning and expression of a G protein-linked acetylcholine receptor from Caenorhabditis elegans. *Journal of Neurochemistry* **72**, 58-65, doi:DOI 10.1046/j.1471-4159.1999.0720058.x (1999).

301 Park, Y. S., Lee, Y. S., Cho, N. J. & Kaang, B. K. Alternative splicing of gar-1, a Caenorhabditis elegans G-protein-linked acetylcholine receptor gene. *Biochem Bioph Res Co* **268**, 354-358, doi:DOI 10.1006/bbrc.2000.2108 (2000).

302 Suh, S. *et al.* Three functional isoforms of GAR-2, a Caenorhabditis elegans G-protein-linked acetylcholine receptor, are produced by alternative splicing. *Biochem Bioph Res Co* **288**, 1238-1243, doi:DOI 10.1006/bbrc.2001.5909 (2001).

303 Hwang, J. M. *et al.* Cloning and functional characterization of a Caenorhabditis elegans muscarinic acetylcholine receptor. *Receptor Channel* **6**, 415-424 (1999).

304 Park, Y. S., Cho, T. J. & Cho, N. J. Stimulation of cyclic AMP production by the Caenorhabditis elegans muscarinic acetylcholine receptor GAR-3 in Chinese hamster ovary cells. *Arch Biochem Biophys* **450**, 203-207, doi:10.1016/j.abb.2006.03.022 (2006).

305 Lee, Y. S. *et al.* Characterization of GAR-2, a novel G protein-linked acetylcholine receptor from Caenorhabditis elegans. *Journal of Neurochemistry* **75**, 1800-1809, doi:DOI 10.1046/j.1471-4159.2000.0751800.x (2000).

306 Thapliyal, S. & Babu, K. C. elegans Locomotion: Finding Balance in Imbalance. *Biochemical and Biophysical Roles of Cell Surface Molecules* **1112**, 185-196, doi:10.1007/978-981-13-3065-0_14 (2018).

307 McKay, J. P., Raizen, D. M., Gottschalk, A., Schafer, W. R. & Avery, L. eat-2 and eat-18 are required for nicotinic neurotransmission in the Caenorhabditis elegans pharynx. *Genetics* **166**, 161-169, doi:DOI 10.1534/genetics.166.1.161 (2004).

308 Alexander, J. K. *et al.* Ric-3 promotes alpha7 nicotinic receptor assembly and trafficking through the ER subcompartment of dendrites. *J Neurosci* **30**, 10112-10126, doi:10.1523/JNEUROSCI.6344-09.2010 (2010).

309 Halevi, S. *et al.* The C-elegans ric-3 gene is required for maturation of nicotinic acetylcholine receptors. *Embo J* **21**, 1012-1020, doi:10.1093/emboj/21.5.1012 (2002).

310 d'Alessandro, M. *et al.* CRELD1 is an evolutionarily-conserved maturational enhancer of ionotropic acetylcholine receptors. *Elife* **7**, e39649 (2018).

311 Gottschalk, A. *et al.* Identification and characterization of novel nicotinic receptor-associated proteins in Caenorhabditis elegans. *Embo J* **24**, 2566-2578, doi:10.1038/sj.emboj.7600741 (2005).

312 Richard, M., Boulin, T., Robert, V. J., Richmond, J. E. & Bessereau, J. L. Biosynthesis of ionotropic acetylcholine receptors requires the evolutionarily conserved ER membrane complex. *Proc Natl Acad Sci U S A* **110**, E1055-1063, doi:10.1073/pnas.1216154110 (2013).

313 Gendrel, M., Rapti, G., Richmond, J. E. & Bessereau, J. L. A secreted complement-control-related protein ensures acetylcholine receptor clustering. *Nature* **461**, 992-U258, doi:10.1038/nature08430 (2009).

314 Rapti, G., Richmond, J. & Bessereau, J. L. A single immunoglobulin-domain protein required for clustering acetylcholine receptors in C. elegans. *Embo J* **30**, 706-718, doi:10.1038/emboj.2010.355 (2011).

315 Gally, C., Eimer, S., Richmond, J. E. & Bessereau, J. L. A transmembrane protein required for acetylcholine receptor clustering in Caenorhabditis elegans. *Nature* **431**, 578-582, doi:10.1038/nature02893 (2004).

316 Pinan-Lucarre, B. *et al.* C. elegans Punctin specifies cholinergic versus GABAergic identity of postsynaptic domains. *Nature* **511**, 466-+, doi:10.1038/nature13313 (2014).

317 Boulin, T. *et al.* Positive modulation of a Cys-loop acetylcholine receptor by an auxiliary transmembrane subunit. *Nature Neuroscience* **15**, 1374-1381, doi:10.1038/nn.3197 (2012).

318 Almedom, R. B. *et al.* An ER-resident membrane protein complex regulates nicotinic acetylcholine receptor subunit composition at the synapse. *Embo J* **28**, 2636-2649, doi:10.1038/emboj.2009.204 (2009).

319 Shteingauz, A., Cohen, E., Biala, Y. & Treinin, M. The BTB-MATH protein BATH-42 interacts with RIC-3 to regulate maturation of nicotinic acetylcholine receptors. *J Cell Sci* **122**, 807-812, doi:10.1242/jcs.036343 (2009).

320 Nam, S. *et al.* Control of Rapsyn Stability by the CUL-3-containing E3 Ligase Complex. *J. Biol. Chem.* **284**, 8192-8206, doi:10.1074/jbc.M808230200 (2009).

321 Ramarao, M. K. & Cohen, J. B. Mechanism of nicotinic acetylcholine receptor clustering by rapsyn. *Journal of Neurochemistry* **70**, S2-S2 (1998).

322 Pierron, M., Pinan-Lucarre, B. & Bessereau, J. L. Preventing Illegitimate Extrasynaptic Acetylcholine Receptor Clustering Requires the RSU-1 Protein. *Journal of Neuroscience* **36**, 6525-6537, doi:10.1523/Jneurosci.3733-15.2016 (2016).

323 Waggoner, L. E. *et al.* Long-term nicotine adaptation in Caenorhabditis elegans involves PKC-dependent changes in nicotinic receptor abundance. *Journal of Neuroscience* **20**, 8802-8811 (2000).

324 Eimer, S. *et al.* Regulation of nicotinic receptor trafficking by the transmembrane Golgi protein UNC-50. *Embo J* **26**, 4313-4323, doi:10.1038/sj.emboj.7601858 (2007).

325 Nagy, S., Huang, Y.-C., Alkema, M. J. & Biron, D. Caenorhabditis elegans exhibit a coupling between the defecation motor program and directed locomotion. *Sci Rep-Uk* **5**, 1-13 (2015).

326 Hardaker, L. A., Singer, E., Kerr, R., Zhou, G. & Schafer, W. R. Serotonin modulates locomotory behavior and coordinates egg-laying and movement in Caenorhabditis elegans. *J Neurobiol* **49**, 303-313, doi:10.1002/neu.10014 (2001).

327 Takahashi, M. & Takagi, S. Optical silencing of body wall muscles induces pumping inhibition in Caenorhabditis elegans. *Plos Genet* **13**, doi:ARTN e1007134

10.1371/journal.pgen.1007134 (2017).

328 Zhen, M. & Samuel, A. D. C. elegans locomotion: small circuits, complex functions. *Curr Opin Neurobiol* **33**, 117-126, doi:10.1016/j.conb.2015.03.009 (2015).

329 Nawa, M. & Matsuoka, M. The method of the body bending assay using Caenorhabditis elegans. *Bio-Protocol* **2**, e253-e253 (2012).

330 Mulcahy, B., Holden-Dye, L. & O'Connor, V. Pharmacological assays reveal age-related changes in synaptic transmission at the Caenorhabditis elegans neuromuscular junction that are modified by reduced insulin signalling. *J Exp Biol* **216**, 492-501, doi:10.1242/jeb.068734 (2013).

331 Mahoney, T. R., Luo, S. & Nonet, M. L. Analysis of synaptic transmission in Caenorhabditis elegans using an aldicarb-sensitivity assay. *Nat Protoc* **1**, 1772-1777, doi:10.1038/nprot.2006.281 (2006).

332 Oh, K. H. & Kim, H. Aldicarb-induced Paralysis Assay to Determine Defects in Synaptic Transmission in Caenorhabditis elegans. *Bio Protoc* **7**, doi:10.21769/BioProtoc.2400 (2017).

333 Briseno-Roa, L. & Bessereau, J. L. Proteolytic Processing of the Extracellular Scaffolding Protein LEV-9 Is Required for Clustering Acetylcholine Receptors. *J. Biol. Chem.* **289**, 10967-10974, doi:10.1074/jbc.C113.534677 (2014).

334 Rajini, P. S., Melstrom, P. & Williams, P. L. A comparative study on the relationship between various toxicological endpoints in Caenorhabditis elegans exposed to organophosphorus insecticides. *J Toxicol Environ Health A* **71**, 1043-1050, doi:10.1080/15287390801989002 (2008).

335 Melstrom, P. C. & Williams, P. L. Reversible AChE inhibitors in C. elegans vs. rats, mice. *Biochem Biophys Res Commun* **357**, 200-205, doi:10.1016/j.bbrc.2007.03.122 (2007).

336 Albertson, D. G. & Thomson, J. N. The pharynx of Caenorhabditis elegans. *Philos Trans R Soc Lond B Biol Sci* **275**, 299-325 (1976).

337 Avery, L. & Horvitz, H. R. A Cell That Dies during Wild-Type C-Elegans Development Can Function as a Neuron in a Ced-3 Mutant. *Cell* **51**, 1071-1078, doi:Doi 10.1016/0092-8674(87)90593-9 (1987).

338 Avery, L. & Horvitz, R. Pharyngeal Pumping Continues after Laser Killing of the Pharyngeal Nervous-System of C-Elegans. *Neuron* **3**, 473-485, doi:Doi 10.1016/0896-6273(89)90206-7 (1989).

339 Avery, L. The genetics of feeding in Caenorhabditis elegans. *Genetics* **133**, 897-917 (1993).

340 Avery, L. Motor-Neuron M3 Controls Pharyngeal Muscle-Relaxation Timing in Caenorhabditis-Elegans. *J Exp Biol* **175**, 283-297 (1993).

341 Trojanowski, N. F., Padovan-Merhar, O., Raizen, D. M. & Fang-Yen, C. Neural and genetic degeneracy underlies Caenorhabditis elegans feeding behavior. *J Neurophysiol* **112**, 951-961, doi:10.1152/jn.00150.2014 (2014).

342 Song, B. M., Faumont, S., Lockery, S. & Avery, L. Recognition of familiar food activates feeding via an endocrine serotonin signal in Caenorhabditis elegans. *Elife* **2**, doi:ARTN e00329

10.7554/eLife.00329 (2013).

343 Li, Z. Y. *et al.* Dissecting a central flip-flop circuit that integrates contradictory sensory cues in C. elegans feeding regulation. *Nat Commun* **3**, doi:ARTN 776

10.1038/ncomms1780 (2012).

344 Hobson, R. J. *et al.* SER-7, a Caenorhabditis elegans 5-HT7-like receptor, is essential for the 5-HT stimulation of pharyngeal pumping and egg laying. *Genetics* **172**, 159-169, doi:10.1534/genetics.105.044495 (2006).

345 Song, B. M. & Avery, L. Serotonin Activates Overall Feeding by Activating Two Separate Neural Pathways in Caenorhabditis elegans. *Journal of Neuroscience* **32**, 1920-1931, doi:10.1523/Jneurosci.2064-11.2012 (2012).

346 Dent, J. A., Davis, M. W. & Avery, L. avr-15 encodes a chloride channel subunit that mediates inhibitory glutamatergic neurotransmission and ivermectin sensitivity in Caenorhabditis elegans. *Embo J* **16**, 5867-5879, doi:DOI 10.1093/emboj/16.19.5867 (1997).

347 Fu, J. *et al.* AIM interneurons mediate feeding suppression through the TYRA-2 receptor in C. elegans. *Biophysics reports* **4**, 17-24 (2018).

348 Seymour, M. K., Wright, K. A. & Doncaster, C. C. The Action of the Anterior Feeding Apparatus of Caenorhabditis-Elegans (Nematoda, Rhabditida). *J Zool* **201**, 527-539 (1983).

349 Holden-Dye, L. & Walker, R. Caenorhabditis elegans feeding behaviours. *Oxford Research Encyclopedia of Neuroscience* (2017).

350 Raizen, D., Song, B.-m., Trojanowski, N. & You, Y.-J. Methods for measuring pharyngeal behaviors. *WormBook: The Online Review of C. elegans Biology [Internet]* (2018).

351 Scholz, M., Lynch, D. J., Lee, K. S., Levine, E. & Biron, D. A scalable method for automatically measuring pharyngeal pumping in C. elegans. *J Neurosci Methods* **274**, 172-178, doi:10.1016/j.jneumeth.2016.07.016 (2016).

352 Rodriguez-Palero, M. J. *et al.* An automated method for the analysis of food intake behaviour in Caenorhabditis elegans. *Sci Rep* **8**, 3633, doi:10.1038/s41598-018-21964-z (2018).

353 Jadhav, K. B. & Rajini, P. S. Evaluation of Sublethal Effects of Dichlorvos upon Caenorhabditis elegans Based on a Set of End Points of Toxicity. *J Biochem Mol Toxic* **23**, 9-17, doi:10.1002/jbt.20258 (2009).

354 Schafer, W. R. Genetics of egg-laying in worms. *Annu. Rev. Genet.* **40**, 487-509 (2006).

355 Sloan, M. A., Reaves, B. J., Maclean, M. J., Storey, B. E. & Wolstenholme, A. J. Expression of nicotinic acetylcholine receptor subunits from parasitic nematodes in Caenorhabditis elegans. *Mol Biochem Parasitol* **204**, 44-50, doi:10.1016/j.molbiopara.2015.12.006 (2015).

356 Weinshenker, D., Garriga, G. & Thomas, J. H. Genetic and pharmacological analysis of neurotransmitters controlling egg laying in C. elegans. *J Neurosci* **15**, 6975-6985 (1995).

357 Bany, I. A., Dong, M. Q. & Koelle, M. R. Genetic and cellular basis for acetylcholine inhibition of Caenorhabditis elegans egg-laying behavior. *J Neurosci* **23**, 8060-8069 (2003).

358 Collins, K. M. *et al.* Activity of the C. elegans egg-laying behavior circuit is controlled by competing activation and feedback inhibition. *Elife* **5**, e21126 (2016).

359 Waggoner, L. E., Zhou, G. T., Schafer, R. W. & Schafer, W. R. Control of alternative behavioral states by serotonin in Caenorhabditis elegans. *Neuron* **21**, 203-214, doi:10.1016/s0896-6273(00)80527-9 (1998).

360 Leelaja, B. C. & Rajini, P. S. Biochemical and physiological responses in Caenorhabditis elegans exposed to sublethal concentrations of the organophosphorus insecticide, monocrotophos. *Ecotoxicol Environ Saf* **94**, 8-13, doi:10.1016/j.ecoenv.2013.04.015 (2013).

361 Branicky, R. & Hekimi, S. What keeps C-elegans regular: the genetics of defecation. *Trends Genet* **22**, 571-579, doi:10.1016/j.tig.2006.08.006 (2006).

362 Thomas, J. H. Genetic-Analysis of Defecation in Caenorhabditis-Elegans. *Genetics* **124**, 855-872 (1990).

363 Lewis, J. A., Gehman, E. A., Baer, C. E. & Jackson, D. A. Alterations in gene expression in Caenorhabditis elegans associated with organophosphate pesticide intoxication and recovery. *BMC Genomics* **14**, 291, doi:10.1186/1471-2164-14-291 (2013).

364 Lewis, J. A., Szilagyi, M., Gehman, E., Dennis, W. E. & Jackson, D. A. Distinct patterns of gene and protein expression elicited by organophosphorus pesticides in Caenorhabditis elegans. *BMC Genomics* **10**, 202, doi:10.1186/1471-2164-10-202 (2009).

365 Vinuela, A., Snoek, L. B., Riksen, J. A. & Kammenga, J. E. Genome-wide gene expression analysis in response to organophosphorus pesticide chlorpyrifos and diazinon in C. elegans. *Plos One* **5**, e12145, doi:10.1371/journal.pone.0012145 (2010).

366 Chan, J. Y. *et al.* Cholinergic receptor-independent dysfunction of mitochondrial respiratory chain enzymes, reduced mitochondrial transmembrane potential and ATP depletion underlie necrotic cell death induced by the organophosphate poison mevinphos. *Neuropharmacology* **51**, 1109-1119 (2006).

367 Tattersall, J. E. H. Anticholinesterase toxicity. *Curr Opin Physiol* **4**, 49-56, doi:10.1016/j.cophys.2018.05.005 (2018).

368 Koelle, G. B. The histochemical localization of cholinesterases in the central nervous system of the rat. *J Comp Neurol* **100**, 211-235 (1954).

369 Massoulie, J., Pezzementi, L., Bon, S., Krejci, E. & Vallette, F. M. Molecular and cellular biology of cholinesterases. *Prog Neurobiol* **41**, 31-91 (1993).

370 Takahashi, N. & Hashizume, M. A systematic review of the influence of occupational organophosphate pesticides exposure on neurological impairment. *Bmj Open* **4**, doi:ARTN e004798

10.1136/bmjopen-2014-004798 (2014).

371 Worek, F., Wille, T., Koller, M. & Thiermann, H. Toxicology of organophosphorus compounds in view of an increasing terrorist threat. *Arch Toxicol* **90**, 2131-2145, doi:10.1007/s00204-016-1772-1 (2016).

372 Albuquerque, E. X. *et al.* Multiple actions of anticholinesterase agents on chemosensitive synapses: molecular basis for prophylaxis and treatment of organophosphate poisoning. *Fundam Appl Toxicol* **5**, S182-203, doi:10.1016/0272-0590(85)90129-0 (1985).

373 Konradsen, F. Acute pesticide poisoning - a global public health problem - secondary publication. *Dan. Med. Bull.* **54**, 58-59 (2007).

374 Balls, M. & Combes, R. D. Alternative Methods in Toxicity Testing in the UK. *Hist Toxicol Envir*, 17-22, doi:10.1016/B978-0-12-813697-3.00004-4 (2019).

375 Prescott, M. J. & Lidster, K. Improving quality of science through better animal welfare: the NC3Rs strategy. *Lab Animal* **46**, 152-156 (2017).

376 Arpagaus, M. *et al.* Four acetylcholinesterase genes in the nematode Caenorhabditis elegans. *J Physiol Paris* **92**, 363-367, doi:10.1016/S0928-4257(99)80006-0 (1998).

377 Edgar, R. S., Cox, G. N., Kusch, M. & Politz, J. C. The Cuticle of Caenorhabditis elegans. *J Nematol* **14**, 248-258 (1982).

378 Peixoto, C. A., Kramer, J. M. & de Souza, W. Caenorhabditis elegans cuticle: a description of new elements of the fibrous layer. *J Parasitol* **83**, 368-372 (1997).

379 Avery, L. & Shtonda, B. B. Food transport in the C-elegans pharynx. *J Exp Biol* **206**, 2441-2457, doi:10.1242/jeb.00433 (2003).

380 Niacaris, T. & Avery, L. Serotonin regulates repolarization of the C-elegans pharyngeal muscle. *J Exp Biol* **206**, 223-231, doi:10.1242/jeb.00101 (2003).

381 Dalliere, N. *et al.* Multiple excitatory and inhibitory neural signals converge to fine-tune Caenorhabditis elegans feeding to food availability. *FASEB J* **30**, 836-848, doi:10.1096/fj.15-279257 (2016).

382 Kudelska, M. M. *et al.* Investigation of feeding behaviour in C. elegans reveals distinct pharmacological and antibacterial effects of nicotine. *Invert Neurosci* **18**, 14, doi:10.1007/s10158-018-0219-1 (2018).

383 Franks, C. J., Murray, C., Ogden, D., O'Connor, V. & Holden-Dye, L. A comparison of electrically evoked and channel rhodopsin-evoked postsynaptic potentials in the pharyngeal system of Caenorhabditis elegans. *Invertebr Neurosci* **9**, 43-56, doi:10.1007/s10158-009-0088-8 (2009).

384 Blaxter, M. L. Cuticle surface proteins of wild type and mutant Caenorhabditis elegans. *J Biol Chem* **268**, 6600-6609 (1993).

385 Bradford, M. M. A rapid and sensitive method for the quantitation of microgram quantities of protein utilizing the principle of protein-dye binding. *Anal Biochem* **72**, 248-254, doi:10.1006/abio.1976.9999 (1976).

386 Kardos, S. A. & Sultatos, L. G. Interactions of the organophosphates paraoxon and methyl paraoxon with mouse brain acetylcholinesterase. *Toxicol Sci* **58**, 118-126 (2000).

387 Wolthuis, O. L., Groen, B., Busker, R. W. & van Helden, H. P. Effects of low doses of cholinesterase inhibitors on behavioral performance of robot-tested marmosets. *Pharmacol Biochem Behav* **51**, 443-456 (1995).

388 Boyd, W. A., McBride, S. J. & Freedman, J. H. Effects of genetic mutations and chemical exposures on Caenorhabditis elegans feeding: evaluation of a novel, high-throughput screening assay. *Plos One* **2**, e1259, doi:10.1371/journal.pone.0001259 (2007).

389 Boyd, W. A., Smith, M. V., Kissling, G. E. & Freedman, J. H. Medium- and high-throughput screening of neurotoxicants using C. elegans. *Neurotoxicol Teratol* **32**, 68-73, doi:10.1016/j.ntt.2008.12.004 (2010).

390 Trojanowski, N. F., Raizen, D. M. & Fang-Yen, C. Pharyngeal pumping in Caenorhabditis elegans depends on tonic and phasic signaling from the nervous system. *Sci Rep* **6**, 22940, doi:10.1038/srep22940 (2016).

391 Johnson, J. A. & Wallace, K. B. Species-related differences in the inhibition of brain acetylcholinesterase by paraoxon and malaoxon. *Toxicol Appl Pharmacol* **88**, 234-241, doi:10.1016/0041-008x(87)90009-3 (1987).

392 Gearhart, J. M., Jepson, G. W., Clewell, H. J., 3rd, Andersen, M. E. & Conolly, R. B. Physiologically based pharmacokinetic and pharmacodynamic model for the inhibition of acetylcholinesterase by diisopropylfluorophosphate. *Toxicol Appl Pharmacol* **106**, 295-310, doi:10.1016/0041-008x(90)90249-t (1990).

393 Coban, A., Carr, R. L., Chambers, H. W., Willeford, K. O. & Chambers, J. E. Comparison of inhibition kinetics of several organophosphates, including some nerve agent surrogates, using human erythrocyte and rat and mouse brain acetylcholinesterase. *Toxicol Lett* **248**, 39-45, doi:10.1016/j.toxlet.2016.03.002 (2016).

394 Worek, F. *et al.* Inhibition, reactivation and aging kinetics of highly toxic organophosphorus compounds: pig versus minipig acetylcholinesterase. *Toxicology* **244**, 35-41, doi:10.1016/j.tox.2007.10.021 (2008).

395 Bajgar, J. Biological Monitoring of Exposure to Nerve Agents. *Brit J Ind Med* **49**, 648-653 (1992).

396 Maxwell, D. M., Brecht, K. M. & Oneill, B. L. The Effect of Carboxylesterase Inhibition on Interspecies Differences in Soman Toxicity. *Toxicol Lett* **39**, 35-42, doi:Doi 10.1016/0378-4274(87)90254-2 (1987).

397 Tripathi, H. L. & Dewey, W. L. Comparison of the Effects of Diisopropylfluorophosphate, Sarin, Soman, and Tabun on Toxicity and Brain Acetylcholinesterase Activity in Mice. *J Toxicol Env Health* **26**, 437-446, doi:Doi 10.1080/15287398909531267 (1989).

398 Karsenty, G. & Olson, E. N. Bone and Muscle Endocrine Functions: Unexpected Paradigms of Inter-organ Communication. *Cell* **164**, 1248-1256, doi:10.1016/j.cell.2016.02.043 (2016).

399 Rai, M. & Demontis, F. Systemic Nutrient and Stress Signaling via Myokines and Myometabolites. *Annual Review of Physiology, Vol 78* **78**, 85-107, doi:10.1146/annurev-physiol-021115-105305 (2016).

400 Egan, B. & Zierath, J. R. Exercise Metabolism and the Molecular Regulation of Skeletal Muscle Adaptation. *Cell Metab* **17**, 162-184, doi:10.1016/j.cmet.2012.12.012 (2013).

401 Argiles, J. M., Stemmler, B., Lopez-Soriano, F. J. & Busquets, S. Inter-tissue communication in cancer cachexia. *Nat Rev Endocrinol* **15**, 9-20, doi:10.1038/s41574-018-0123-0 (2018).

402 Delanoue, R., Slaidina, M. & Leopold, P. The steroid hormone ecdysone controls systemic growth by repressing dMyc function in Drosophila fat cells. *Dev Cell* **18**, 1012-1021, doi:10.1016/j.devcel.2010.05.007 (2010).

403 Demontis, F. & Perrimon, N. Integration of Insulin receptor/Foxo signaling and dMyc activity during muscle growth regulates body size in Drosophila. *Development* **136**, 983-993, doi:10.1242/dev.027466 (2009).

404 Rajan, A. & Perrimon, N. Drosophila as a model for interorgan communication: lessons from studies on energy homeostasis. *Dev Cell* **21**, 29-31, doi:10.1016/j.devcel.2011.06.034 (2011).

405 Avery, L. & Horvitz, H. R. Effects of Starvation and Neuroactive Drugs on Feeding in Caenorhabditis-Elegans. *J Exp Zool* **253**, 263-270, doi:DOI 10.1002/jez.1402530305 (1990).

406 Sawin, E. R., Ranganathan, R. & Horvitz, H. R. C-elegans locomotory rate is modulated by the environment through a dopaminergic pathway and by experience through a serotonergic pathway. *Neuron* **26**, 619-631, doi:Doi 10.1016/S0896-6273(00)81199-X (2000).

407 Ben Arous, J., Laffont, S. & Chatenay, D. Molecular and sensory basis of a food related two-state behavior in C. elegans. *Plos One* **4**, e7584, doi:10.1371/journal.pone.0007584 (2009).

408 Shtonda, B. B. & Avery, L. Dietary choice behavior in Caenorhabditis elegans. *J Exp Biol* **209**, 89-102, doi:10.1242/jeb.01955 (2006).

409 Chalfie, M. *et al.* The Neural Circuit for Touch Sensitivity in Caenorhabditis-Elegans. *Journal of Neuroscience* **5**, 956-964 (1985).

410 Keane, J. & Avery, L. Mechanosensory inputs influence Caenorhabditis elegans pharyngeal activity via ivermectin sensitivity genes. *Genetics* **164**, 153-162 (2003).

411 Avery, L. & Thomas, J. H. in *C. elegans II* (eds nd *et al.*) (1997).

412 Miyabayashi, T., Palfreyman, M. T., Sluder, A. E., Slack, F. & Sengupta, P. Expression and function of members of a divergent nuclear receptor family in Caenorhabditis elegans. *Dev Biol* **215**, 314-331, doi:DOI 10.1006/dbio.1999.9470 (1999).

413 Mello, C. C., Kramer, J. M., Stinchcomb, D. & Ambros, V. Efficient gene transfer in C.elegans: extrachromosomal maintenance and integration of transforming sequences. *Embo J* **10**, 3959-3970 (1991).

414 Ly, K., Reid, S. J. & Snell, R. G. Rapid RNA analysis of individual Caenorhabditis elegans. *MethodsX* **2**, 59-63, doi:10.1016/j.mex.2015.02.002 (2015).

415 Izquierdo, P. G., O'Connor, V., Green, A. C., Holden-Dye, L. & Tattersall, J. E. H. C. elegans pharyngeal pumping provides a whole organism bio-assay to investigate anti-cholinesterase intoxication and antidotes. *Neurotoxicology* **82**, 50-62, doi:10.1016/j.neuro.2020.11.001 (2020).

416 Culotti, J. G. & Klein, W. L. Occurrence of muscarinic acetylcholine receptors in wild type and cholinergic mutants of Caenorhabditis elegans. *J Neurosci* **3**, 359-368 (1983).

417 Bandyopadhyay, J. *et al.* Calcineurin, a calcium/calmodulin-dependent protein phosphatase, is involved in movement, fertility, egg laying, and growth in Caenorhabditis elegans. *Mol Biol Cell* **13**, 3281-3293, doi:10.1091/mbc.E02-01-0005 (2002).

418 Maryon, E. B., Coronado, R. & Anderson, P. unc-68 encodes a ryanodine receptor involved in regulating C-elegans body-wall muscle contraction. *J Cell Biol* **134**, 885-893, doi:DOI 10.1083/jcb.134.4.885 (1996).

419 Hernando, G., Berge, I., Rayes, D. & Bouzat, C. Contribution of Subunits to Caenorhabditis elegans Levamisole-Sensitive Nicotinic Receptor Function. *Molecular Pharmacology* **82**, 550-560, doi:10.1124/mol.112.079962 (2012).

420 Lewis, J. A., Wu, C. H., Berg, H. & Levine, J. H. The Genetics of Levamisole Resistance in the Nematode Caenorhabditis-Elegans. *Genetics* **95**, 905-928 (1980).

421 Lewis, J. A., Wu, C. H., Levine, J. H. & Berg, H. Levamisole-Resistant Mutants of the Nematode Caenorhabditis-Elegans Appear to Lack Pharmacological Acetylcholine-Receptors. *Neuroscience* **5**, 967-989, doi:Doi 10.1016/0306-4522(80)90180-3 (1980).

422 Gottschalk, A. & Schafer, W. R. Visualization of integral and peripheral cell surface proteins in live Caenorhabditis elegans. *J Neurosci Meth* **154**, 68-79, doi:10.1016/j.jneumeth.2005.11.016 (2006).

423 Dalliere, N. *Delineation of a gut brain axis that regulates context-dependent feeding behaviour of the nematode Caenorhabditis elegans* Doctoral Thesis thesis, University of Southampton (UK), (2015).

424 Raizen, D. M., Lee, R. Y. N. & Avery, L. Interacting Genes Required for Pharyngeal Excitation by Motor-Neuron Mc in Caenorhabditis-Elegans. *Genetics* **141**, 1365-1382 (1995).

425 Evans, W. J. *et al.* Cachexia: a new definition. *Clin Nutr* **27**, 793-799, doi:10.1016/j.clnu.2008.06.013 (2008).

426 Mateos-Aparicio, P. & Rodriguez-Moreno, A. The Impact of Studying Brain Plasticity. *Front Cell Neurosci* **13**, 66, doi:10.3389/fncel.2019.00066 (2019).

427 Citri, A. & Malenka, R. C. Synaptic plasticity: multiple forms, functions, and mechanisms. *Neuropsychopharmacol* **33**, 18-41, doi:10.1038/sj.npp.1301559 (2008).

428 Markram, H., Gerstner, W. & Sjostrom, P. J. A history of spike-timing-dependent plasticity. *Front Synaptic Neurosci* **3**, 4, doi:10.3389/fnsyn.2011.00004 (2011).

429 Byrne, J. H., LaBar, K. S., LeDoux, J. E., Schafe, G. E. & Thompson, R. F. in *From Molecules to Networks. An Introduction to Cellular and Molecular Neuroscience* (eds John H. Byrne, Ruth Heidelberger, & M. Neal Waxham) (2014).

430 Okano, H., Hirano, T. & Balaban, E. Learning and memory. *Proc Natl Acad Sci U S A* **97**, 12403-12404, doi:10.1073/pnas.210381897 (2000).

431 Thompson, R. F. The neurobiology of learning and memory. *Science* **233**, 941-947, doi:10.1126/science.3738519 (1986).

432 Jokanovic, M. & Petrovic, R. S. Pyridinium Oximes as Cholinesterase Reactivators. An Update of the Structure-Activity Relationship and Efficacy in the Treatment of Poisoning with Organophosphorus Compounds. *Front Med Chem* **8**, 171-205 (2016).

433 Jokanovic, M. & Prostran, M. Pyridinium Oximes as Cholinesterase Reactivators. Structure-Activity Relationship and Efficacy in the Treatment of Poisoning with Organophosphorus Compounds. *Curr Med Chem* **16**, 2177-2188, doi:Doi 10.2174/092986709788612729 (2009).

434 Wang, L., Conner, J. M., Nagahara, A. H. & Tuszynski, M. H. Rehabilitation drives enhancement of neuronal structure in functionally relevant neuronal subsets. *Proc Natl Acad Sci U S A* **113**, 2750-2755, doi:10.1073/pnas.1514682113 (2016).

435 Starke, K., Gothert, M. & Kilbinger, H. Modulation of neurotransmitter release by presynaptic autoreceptors. *Physiol Rev* **69**, 864-989, doi:10.1152/physrev.1989.69.3.864 (1989).

436 Albrecht, C., Bloss, H. G., Jackisch, R. & Feuerstein, T. J. Evaluation of autoreceptor-mediated control of [(3)H]acetylcholine release in rat and human neocortex. *Exp Brain Res* **128**, 383-389, doi:10.1007/s002210050858 (1999).

437 Muramatsu, I. *et al.* Novel regulatory systems for acetylcholine release in rat striatum and anti-Alzheimer's disease drugs. *J Neurochem* **149**, 605-623, doi:10.1111/jnc.14701 (2019).

438 Gotti, C., Fornasari, D. & Clementi, F. Human neuronal nicotinic receptors. *Prog Neurobiol* **53**, 199-237, doi:10.1016/s0301-0082(97)00034-8 (1997).

439 Schwartz, R. D. & Kellar, K. J. Nicotinic cholinergic receptor binding sites in the brain: regulation in vivo. *Science* **220**, 214-216, doi:10.1126/science.6828889 (1983).

440 Nashmi, R. *et al.* Chronic nicotine cell specifically upregulates functional alpha 4*nicotinic receptors: Basis for both tolerance in midbrain and enhanced long-term potentiation in perforant path. *Journal of Neuroscience* **27**, 8202-8218, doi:10.1523/Jneurosci.2199-07.2007 (2007).

441 Marks, M. J., Burch, J. B. & Collins, A. C. Effects of Chronic Nicotine Infusion on Tolerance Development and Nicotinic Receptors. *J Pharmacol Exp Ther* **226**, 817-825 (1983).

442 Fenster, C. P., Whitworth, T. L., Sheffield, E. B., Quick, M. W. & Lester, R. A. J. Upregulation of surface alpha 4 beta 2 nicotinic receptors is initiated by receptor desensitization after chronic exposure to nicotine. *Journal of Neuroscience* **19**, 4804-4814 (1999).

443 Lansdell, S. J. *et al.* RIC-3 enhances functional expression of multiple nicotinic acetylcholine receptor subtypes in mammalian cells. *Mol Pharmacol* **68**, 1431-1438, doi:10.1124/mol.105.017459 (2005).

444 Miwa, J. M., Anderson, K. R. & Hoffman, K. M. Lynx Prototoxins: Roles of Endogenous Mammalian Neurotoxin-Like Proteins in Modulating Nicotinic Acetylcholine Receptor Function to Influence Complex Biological Processes. *Frontiers in Pharmacology* **10**, doi:ARTN 343

10.3389/fphar.2019.00343 (2019).

445 Jeanclos, E. M. *et al.* The chaperone protein 14-3-3eta interacts with the nicotinic acetylcholine receptor alpha 4 subunit. Evidence for a dynamic role in subunit stabilization. *J Biol Chem* **276**, 28281-28290, doi:10.1074/jbc.M011549200 (2001).

446 Lin, L. *et al.* The calcium sensor protein visinin-like protein-1 modulates the surface expression and agonist sensitivity of the alpha 4beta 2 nicotinic acetylcholine receptor. *J Biol Chem* **277**, 41872-41878, doi:10.1074/jbc.M206857200 (2002).

447 Sanes, J. R. & Lichtman, J. W. Induction, assembly, maturation and maintenance of a postsynaptic apparatus. *Nat Rev Neurosci* **2**, 791-805, doi:10.1038/35097557 (2001).

448 Hobert, O. Behavioral plasticity in C-elegans: Paradigms, circuits, genes. *J Neurobiol* **54**, 203-223, doi:10.1002/neu.10168 (2003).

449 Ardiel, E. L. & Rankin, C. H. An elegant mind: learning and memory in Caenorhabditis elegans. *Learn Mem* **17**, 191-201, doi:10.1101/lm.960510 (2010).

450 Hedgecock, E. M. & Russell, R. L. Normal and mutant thermotaxis in the nematode Caenorhabditis elegans. *Proc Natl Acad Sci U S A* **72**, 4061-4065, doi:10.1073/pnas.72.10.4061 (1975).

451 Mori, I. Genetics of chemotaxis and thermotaxis in the nematode Caenorhabditis elegans. *Annu Rev Genet* **33**, 399-422, doi:DOI 10.1146/annurev.genet.33.1.399 (1999).

452 Feng, Z. *et al.* A C. elegans model of nicotine-dependent behavior: regulation by TRP-family channels. *Cell* **127**, 621-633, doi:10.1016/j.cell.2006.09.035 (2006).

453 Colbert, H. A. & Bargmann, C. I. Odorant-Specific Adaptation Pathways Generate Olfactory Plasticity in C-Elegans. *Neuron* **14**, 803-812, doi:Doi 10.1016/0896-6273(95)90224-4 (1995).

454 Izquierdo, P. G. *et al.* Cholinergic signalling at the body wall neuromuscular junction couples to distal inhibition of feeding in *C. elegans*. *bioRxiv*, 2021.2002.2012.430967, doi:10.1101/2021.02.12.430967 (2021).

455 Blanchard, A. *et al.* Deciphering the molecular determinants of cholinergic anthelmintic sensitivity in nematodes: When novel functional validation approaches highlight major differences between the model Caenorhabditis elegans and parasitic species. *PLoS Pathogens* **14**, e1006996 (2018).

456 Kunitomo, H. *et al.* Concentration memory-dependent synaptic plasticity of a taste circuit regulates salt concentration chemotaxis in Caenorhabditis elegans. *Nat Commun* **4**, doi:ARTN 2210

10.1038/ncomms3210 (2013).

457 Bernhard, N. & van der Kooy, D. A behavioral and genetic dissection of two forms of olfactory plasticity in Caenorhabditis elegans: Adaptation and habituation. *Learn Memory* **7**, 199-212, doi:DOI 10.1101/lm.7.4.199 (2000).

458 Opperman, C. H. & Chang, S. Effects of Aldicarb and Fenamiphos on Acetylcholinesterase and Motility of Caenorhabditis-Elegans. *J Nematol* **23**, 20-27 (1991).

459 Kozlova, A. A., Lotfi, M. & Okkema, P. G. Cross Talk with the GAR-3 Receptor Contributes to Feeding Defects in Caenorhabditis elegans eat-2 Mutants. *Genetics* **212**, 231-243, doi:10.1534/genetics.119.302053 (2019).

460 Weise, C. *et al.* Functional Domains of the Nicotinic Acetylcholine-Receptor. *Biol Chem H-S* **372**, 911-912 (1991).

461 Lummis, S. C. R. *et al.* Cis-trans isomerization at a proline opens the pore of a neurotransmitter-gated ion channel. *Nature* **438**, 248-252, doi:10.1038/nature04130 (2005).

462 Connolly, C. N. & Wafford, K. A. The Cys-loop superfamily of ligand-gated ion channels: the impact of receptor structure on function. *Biochem Soc T* **32**, 529-534, doi:Doi 10.1042/Bst0320529 (2004).

463 Richmond, J. E. & Jorgensen, E. M. One GABA and two acetylcholine receptors function at the C-elegans neuromuscular junction. *Nature Neuroscience* **2**, 791-797, doi:Doi 10.1038/12160 (1999).

464 Girard, E., Barbier, J., Chatonnet, A., Krejci, E. & Molgo, J. Synaptic remodeling at the skeletal neuromuscular junction of acetylcholinesterase knockout mice and its physiological relevance. *Chem-Biol Interact* **157**, 87-96, doi:10.1016/j.cbi.2005.10.010 (2005).

465 Li, L., Lee, Y. H., Pappone, P., Palma, A. & Mcnamee, M. G. Site-Specific Mutations of Nicotinic Acetylcholine-Receptor at the Lipid-Protein Interface Dramatically Alter Ion Channel Gating. *Biophys J* **62**, 61-63, doi:Doi 10.1016/S0006-3495(92)81779-4 (1992).

466 Lasalde, J. A. *et al.* Tryptophan substitutions at the lipid-exposed transmembrane segment M4 of Torpedo californica acetylcholine receptor govern channel gating. *Biochemistry* **35**, 14139-14148, doi:DOI 10.1021/bi961583l (1996).

467 Bouzat, C., Roccamo, A. M., Garbus, I. & Barrantes, F. J. Mutations at lipid-exposed residues of the acetylcholine receptor affect its gating kinetics. *Molecular Pharmacology* **54**, 146-153 (1998).

468 Lee, Y. H. *et al.* Mutations in the M4 Domain of Torpedo-Californica Acetylcholine-Receptor Dramatically Alter Ion-Channel Function. *Biophys J* **66**, 646-653, doi:Doi 10.1016/S0006-3495(94)80838-0 (1994).

469 OrtizMiranda, S. I., Lasalde, J. A., Pappone, P. A. & McNamee, M. G. Mutations in the M4 domain of the Torpedo californica nicotinic acetylcholine receptor alter channel opening and closing. *J Membrane Biol* **158**, 17-30, doi:DOI 10.1007/s002329900240 (1997).

470 Mosesso, R., Dougherty, D. A. & Lummis, S. C. R. Proline Residues in the Transmembrane/Extracellular Domain Interface Loops Have Different Behaviors in 5-HT3 and nACh Receptors. *Acs Chem Neurosci* **10**, 3327-3333, doi:10.1021/acschemneuro.9b00315 (2019).

471 Deane, C. M. & Lummis, S. C. The role and predicted propensity of conserved proline residues in the 5-HT3 receptor. *J Biol Chem* **276**, 37962-37966, doi:10.1074/jbc.M104569200 (2001).

472 Jha, A., Cadugan, D. J., Purohit, P. & Auerbach, A. Acetylcholine receptor gating at extracellular transmembrane domain interface: the Cys-loop and M2-M3 linker. *J Gen Physiol* **130**, 547-558, doi:10.1085/jgp.200709856 (2007).

473 Lee, W. Y. & Sine, S. M. Principal pathway coupling agonist binding to channel gating in nicotinic receptors. *Nature* **438**, 243-247, doi:10.1038/nature04156 (2005).

474 Lee, W. Y., Free, C. R. & Sine, S. M. Binding to Gating Transduction in Nicotinic Receptors: Cys-Loop Energetically Couples to Pre-M1 and M2-M3 Regions. *Journal of Neuroscience* **29**, 3189-3199, doi:10.1523/Jneurosci.6185-08.2009 (2009).

475 Hanek, A. P., Lester, H. A. & Dougherty, D. A. A stereochemical test of a proposed structural feature of the nicotinic acetylcholine receptor. *Journal of the American Chemical Society* **130**, 13216-13218 (2008).

476 Petrash, H. A., Philbrook, A., Haburcak, M., Barbagallo, B. & Francis, M. M. ACR-12 Ionotropic Acetylcholine Receptor Complexes Regulate Inhibitory Motor Neuron Activity in Caenorhabditis elegans. *Journal of Neuroscience* **33**, 5524-5532, doi:10.1523/Jneurosci.4384-12.2013 (2013).

477 Amend, N. *et al.* Diagnostics and treatment of nerve agent poisoning-current status and future developments. *Ann N Y Acad Sci* **1479**, 13-28, doi:10.1111/nyas.14336 (2020).

478 Rosenbaum, C. & Bird, S. B. Non-muscarinic therapeutic targets for acute organophosphorus poisoning. *J Med Toxicol* **6**, 408-412, doi:10.1007/s13181-010-0093-7 (2010).

479 Meeter, E. & Wolthuis, O. L. The spontaneous recovery of respiration and neuromuscular transmission in the rat after anticholinesterase poisoning. *Eur J Pharmacol* **2**, 377-386 (1968).

480 Blaber, L. C. & Creasey, N. H. The mode of recovery of cholinesterase activity in vivo after organophosphorus poisoning. 2. Brain cholinesterase. *Biochem J* **77**, 597-604 (1960).

481 Melchers, B. P. & Van der Laaken, A. L. On the mechanism of spontaneous recovery of neuromuscular transmission after acetylcholinesterase inhibition in the rat neuromuscular junction. *Brain Res* **563**, 49-56 (1991).

482 Kim, K. C. & Karczmar, A. G. Adaptation of the neuromuscular junction to constant concentration of ACh. *Int J Neuropharmacol* **6**, 51-61 (1967).

483 Gissen, A. J. & Nastuk, W. L. The mechanisms underlying neuromuscular block following prolonged exposure to depolarizing agents. *Ann N Y Acad Sci* **135**, 184-194 (1966).

484 Cruz, P. M. R., Cossins, J., Beeson, D. & Vincent, A. The Neuromuscular Junction in Health and Disease: Molecular Mechanisms Governing Synaptic Formation and Homeostasis. *Front Mol Neurosci* **13**, doi:ARTN 610964

10.3389/fnmol.2020.610964 (2020).

485 Vincent, A. & Newsomdavis, J. Acetylcholine-Receptor Antibody as a Diagnostic-Test for Myasthenia-Gravis - Results in 153 Validated Cases and 2967 Diagnostic Assays. *J Neurol Neurosur Ps* **48**, 1246-1252, doi:DOI 10.1136/jnnp.48.12.1246 (1985).

486 Lindstrom, J. M., Seybold, M. E., Lennon, V. A., Whittingham, S. & Duane, D. D. Antibody to Acetylcholine-Receptor in Myasthenia-Gravis - Prevalence, Clinical Correlates, and Diagnostic Value. *Neurology* **26**, 1054-1059, doi:Doi 10.1212/Wnl.26.11.1054 (1976).

487 Cruz, P. M. R., Palace, J. & Beeson, D. The Neuromuscular Junction and Wide Heterogeneity of Congenital Myasthenic Syndromes. *Int J Mol Sci* **19**, doi:ARTN 1677

10.3390/ijms19061677 (2018).

488 Ohno, K., Ohkawara, B. & Ito, M. Agrin-LRP4-MuSK signaling as a therapeutic target for myasthenia gravis and other neuromuscular disorders. *Expert Opin Ther Tar* **21**, 949-958, doi:10.1080/14728222.2017.1369960 (2017).

489 Weatherbee, S. D., Anderson, K. V. & Niswander, L. A. LDL-receptor-related protein 4 is crucial for formation of the neuromuscular junction. *Development* **133**, 4993-5000, doi:10.1242/dev.02696 (2006).

490 Zong, Y. N. *et al.* Structural basis of agrin-LRP4-MuSK signaling. *Gene Dev* **26**, 247-258, doi:10.1101/gad.180885.111 (2012).

491 Yamanashi, Y., Higuch, O. & Beeson, D. Dok-7/MuSK signaling and a congenital myasthenic syndrome. *Acta Myol* **27**, 25-29 (2008).

492 Gautam, M. *et al.* Failure of Postsynaptic Specialization to Develop at Neuromuscular-Junctions of Rapsyn-Deficient Mice. *Nature* **377**, 232-236, doi:DOI 10.1038/377232a0 (1995).

493 Tomita, S. Regulation of Ionotropic Glutamate Receptors by Their Auxiliary Subunits. *Physiology* **25**, 41-49, doi:10.1152/physiol.00033.2009 (2010).

494 Lyukmanova, E. N. *et al.* NMR Structure and Action on Nicotinic Acetylcholine Receptors of Water-soluble Domain of Human LYNX1. *J. Biol. Chem.* **286**, 10618-10627, doi:10.1074/jbc.M110.189100 (2011).

495 Vasilyeva, N. A., Loktyushov, E. V., Bychkov, M. L., Shenkarev, Z. O. & Lyukmanova, E. N. Three-Finger Proteins from the Ly6/uPAR Family: Functional Diversity within One Structural Motif. *Biochemistry-Moscow+* **82**, 1702-1715, doi:10.1134/S0006297917130090 (2017).

496 Tsetlin, V. I. Three-finger snake neurotoxins and Ly6 proteins targeting nicotinic acetylcholine receptors: pharmacological tools and endogenous modulators. *Trends Pharmacol Sci* **36**, 109-123, doi:10.1016/j.tips.2014.11.003 (2015).

497 Miwa, J. M., Lester, H. A. & Walz, A. Optimizing Cholinergic Tone Through Lynx Modulators of Nicotinic Receptors: Implications for Plasticity and Nicotine Addiction. *Physiology* **27**, 187-199, doi:10.1152/physiol.00002.2012 (2012).